



University  
of Glasgow

Thomson, Katrina (2011) *Investigating and detecting biomarkers for oxidative stress*. PhD thesis.

<http://theses.gla.ac.uk/2408/>

Copyright and moral rights for this thesis are retained by the author

A copy can be downloaded for personal non-commercial research or study, without prior permission or charge

This thesis cannot be reproduced or quoted extensively from without first obtaining permission in writing from the Author

The content must not be changed in any way or sold commercially in any format or medium without the formal permission of the Author

When referring to this work, full bibliographic details including the author, title, awarding institution and date of the thesis must be given

PRESENTED BY KATRINA THOMSON B.Sc. (Hons), M.Res.  
TO THE UNIVERSITY OF GLASGOW FOR THE DEGREE OF DOCTOR OF PHILOSOPHY

# Investigating and detecting biomarkers for oxidative stress

---

## Acknowledgements

*If you want something bad enough, you will work for it.*

There are too many people to thank and I am not able to mention them all here, but you know who you are.

Firstly I'd like to thank Dr Andy Pitt for his supervision, wisdom and never-ending patience and also for taking a chance and offering me a place at the doctoral training centre. Thanks to Professor Chick Wilson who always believed I could do a PhD and to Dr Corinne Spickett, who has always offered help and advice.

Thank you to Dr Laetitia Mouls for helping me to start this project. I have made many good friends here in the last four years; Heather Allingham, Kit-Yee Tan, Emma Carrick, Scott Heron, Anne-Marie Reid, Becky Warren, Chris Hinds and Michael Lang. You lot made the sometimes unbearable bearable. I cannot forget the post-docs that pushed, teased, terrorised, mocked and tormented me either; Karl Burgess for his guidance and coffee and Richard Goodwin for his helpful but always blunt advice.

I'd also like to thank my family and my Sensei Tony Leith. My father who is an academic inspiration to me, my mother who would never let me give up and who would always have a word of encouragement for me when I needed it the most and to my twin sister Fiona, who always pushed me to do well by just being herself. I am also very appreciative of my Sensei Tony Leith who is the embodiment of *go ju ittai*. Thank you Tony for keeping me sane and teaching me mental and physical toughness to be the best I can be. I owe these people everything.

Thank you to the friends who put up with me and the men who have loved me, what can I say guys? It's been emotional and I am finally beginning to understand the meaning of True Strength.

*"arigato goza-imashita"* - Thank you for teaching me.

## **Declaration**

I hereby declare that the thesis that follows is my own composition, that it is a record of the work done by myself, and that it has not been presented in any previous application for a higher degree.

Katrina Thomson

## Abstract

It is widely reported that during periods of inflammation the heme enzyme, myeloperoxidase is generated by macrophages producing reactive oxidative species. Oxidative stress is the imbalance of these oxidative species which will lead to the post translational modification of proteins. Some biomarkers are proteins or post translational modifications that can be used to indicate disease and are becoming increasingly important particularly for the study of progressive diseases. Analysis of biomarkers in bodily fluids will not only be faster and less invasive than a biopsy but will also diagnose disease at an earlier stage and allow disease treatment and progression to be monitored. Known biomarkers for the production of myeloperoxidase are chlorotyrosine and nitrotyrosine. Elevated levels of chlorotyrosine and nitrotyrosine are indicative of atherosclerosis. The early diagnosis of atherosclerosis is important as the onset of this disease can occur at a young age and be asymptomatic until later, more developed stages.

Here I aim to develop sensitive methods of detection for these biomarkers in a hope that they can be used to classify disease. A Qtrap mass spectrometer is employed with precursor scan for the selective and sensitive detection of chlorotyrosine modifications in *in vitro* HOCl modified 9 protein mix samples. Compared to a conventional MSMS experiment the precursor scan detects more chlorotyrosine modifications suggesting it is a better method for the detection of post translational modifications. Additionally the precursor scan can be used when there is no prior knowledge of the modification sites.

A multiple reaction monitoring method was developed from the MSMS analysis of *in vitro* chemical modification of human serum albumin and plasma samples. Observations from the MSMS analysis were employed to write the multiple reaction monitoring method to target for chloro- and nitrotyrosine modified peptides of the human serum albumin protein in plasma samples. Detection of these modified peptides was indicated by the common elution of three transitions specific to the peptides precursor mass. Where anomalous peaks of one transition were seen it was known that this was not the elution of the targeted peptide. The use of three transition masses instead of one reduces the generation of false positives. Where more than one peak for the common elution

time was seen for a targeted peptide in the chromatography gradient the retention times were used for identification. Peptides are separated by liquid chromatography prior to their analysis on the Qtrap by their hydrophobicity or their polarity. When a peptide becomes chloro- or nitrotyrosine modified the peptide becomes less polar and therefore is seen later in the gradient than in the unmodified state. The observation of more than one peak where the three transitions are seen to be commonly eluted was caused by break-through of signal from poor selection of a  $m/z$  value in Q1.

The multiple reaction method developed from the analysis of *in vitro* chemically modified human serum albumin and plasma was then applied for the analysis of clinical samples in the hope that the chloro- and nitrotyrosine modified peptides targeted for in the samples could be used to classify disease. The clinical plasma samples were sourced from 12 healthy volunteers and 12 diseased cardiovascular patients. The multiple reaction monitoring method indicated the modification of peptides and the presence of these modified peptides was confirmed using targeted MSMS. Classification of these samples was not successful and it was thought that a combination of biomarkers is required for the classification of disease.

## Abbreviations

Apo	Apolipoprotein
AQUA	Absolute quantification
CPS	Counts per second
CVD	Cardiovascular disease
CSF	Colony stimulating factor
ClTyr	Chlorotyrosine
CID	Collision induced dissociation
CAD	Collision activated dissociation
DTP	Direct tissue proteomics
ER	Enhanced resolution
EPI	Enhanced product ion
ESI	Electrospray ionisation
ETD	Electron transfer dissociation
GPF	Gas phase fractionation
HDL	High density lipoprotein
HSA	Human serum albumin
HRP	Horse radish peroxidase
HPLC	High performance liquid chromatography
IDL	Intermediate density lipoprotein
IEM	Inborn error metabolite
IEX	Ion exchange chromatography
LC	Liquid chromatography
LDL	Low density lipoprotein
LIT	Linear ion trap
LPL	Lipoprotein lipase
MRM	Multiple reaction monitoring
MOWSE	Molecular weight search
MS	Mass spectrometry
MPO	Myeloperoxidase
NiTyr	Nitrotyrosine
Ox-LDL	Oxidised low density lipoprotein
ROS	Reactive oxygen species
RCT	Reverse cholesterol transport
SID	Surface induced ionisation
SRM	Single reaction monitoring
SMC	Smooth muscle cell
SIN-1	3-morpholinopyrrolidine
TOF	Time of flight
TIC	Total ion count
TLC	Thin layer chromatography
XIC	Extracted ion chromatogram
VLDL	Very low density lipoprotein

## Contents

Acknowledgements .....	2
Declaration .....	3
Abstract.....	4
Abbreviations .....	6
<b>1 Introduction .....</b>	<b>12</b>
1.1 Atherosclerosis .....	12
1.1.1 The composition and development of the atherosclerotic plaque .....	13
1.1.2 Classification of lipoproteins .....	18
1.1.3 The LDL particle .....	14
1.2 A defence against atherosclerosis .....	21
1.2.1 Genetic disorders leading to high levels of LDL .....	23
1.3 Oxidative stress and the production of reactive species .....	23
1.3.1 Hypochlorite-induced damage to proteins .....	25
1.3.2 Myeloperoxidase-generated reactive nitrogen species .....	27
1.3.3 Stable markers of oxidant damage to proteins.....	27
1.4 Detecting Biomarkers for Disease .....	30
1.4.1 Stable Isotope dilution for the detection and quantification of proteins and or post translational modifications.....	32
1.4.2 Western Blotting.....	32
1.5 Mass spectrometry for the analysis of the proteome.....	34
1.5.1 The quadrupole mass filter.....	35
1.5.2 The quadrupole ion trap .....	36
1.5.3 The Qtrap.....	39
1.6 The capabilities and modes of operation of the Qtrap.....	39
1.6.1 Q3 quadrupole and trap mode (enhanced MS) .....	40
1.6.2 Enhanced Resolution (ER) mode.....	40
1.6.3 Enhanced Product Ion (EPI) mode .....	40
1.6.4 The ionisation and fragmentation of peptides in a mass spectrometer .....	41
1.6.5 Alternative Dissociation Methods .....	44
1.7 Sensitive and selective triple quadrupole mass spectrometry methods for the discovery of post translational modifications.....	46
1.7.1 The Precursor Scan.....	47
1.7.2 The Neutral Loss scan .....	48
1.7.3 Multiple Reaction Monitoring.....	48
1.8 Search engines and databases to analyse mass spectrum data	50
1.8.1 The MOWSE (Molecular Weight Search) Algorithm .....	52
1.9 Conclusions .....	53
1.10 Aims.....	53
<b>2 Chapter – Precursor Scanning for the Sensitive and Selective Detection of Chlorotyrosine Modified Peptides in a 9-Protein Mix .....</b>	<b>56</b>

2.1	The chlorotyrosine modification.....	56
2.2	Introducing the Qtrap and the various scanning techniques and their uses.....	57
2.2.1	Conventional ion-traps and the QTrap.....	58
2.3	Aims.....	59
2.3.1	Materials and Methods.....	59
2.4	Results and Discussion – The Precursor Scan.....	63
2.4.1	Assignment of the ClTyr modification by Mascot and manual validation.....	63
2.4.2	Reviewing the sensitivity of the precursor scan for the detection of chlorotyrosine in the HOCl modified 9 protein mix.....	65
2.4.3	Investigating the potential ClTyr modifications in a 15mM HOCl and 60mM HOCl modified 9 protein mix samples.....	67
2.4.4	Investigating modifications by HOCl in a 9 protein mix at higher HOCl concentrations.....	68
2.5	Optimising the precursor scan for the detection of chlorotyrosine in complex samples.....	70
2.5.1	Improving sensitivity - dynamic exclusion.....	71
2.5.2	Improving sensitivity – the gas phase fractionation experiment.....	72
2.5.3	Optimising the Gas Phase Fractionation Experiment.....	74
2.5.4	Discussion - the advantages and disadvantages of the precursor scan method and GPF method.....	79

<b>3</b>	<b>Chapter</b> – Developing a MRM method to detect nitrotyrosine and chlorotyrosine modifications in human serum albumin and real biological Samples.....	82
3.1	Sensitive techniques for the validation and verification of biomarkers.....	82
3.1.1	Multiple reaction monitoring (MRM) for validation of biomarkers.....	84
3.2	Materials and Methods.....	86
3.2.1	Chlorination of HSA and Plasma.....	86
3.2.2	Nitration of HSA and plasma.....	87
3.2.3	Enzymatic Digestion.....	88
3.2.4	MIDAS workflow designer.....	89
3.3	Results and Discussion – detecting chlorotyrosine in HSA.....	90
3.3.1	Orthogonal digestion for the detection of ClTyr modified peptides in HSA.....	92
3.4	Development of an MRM method to target ClTyr modifications in the HSA protein.....	94
3.4.1	MRM analysis of a 30mM HOCl HSA sample targeting the unmodified and ClTyr modified RHPDYSVLLLLR peptide.....	95
3.4.2	MRM detection of ClTyr modified peptides in HOCl modified HSA samples.....	97
3.4.3	The investigation of the RHPYFYAPPELLFFAK peptide - determination of ClTyr Modification.....	105
3.4.4	The investigation of the DVFLGMFLYEYAR peptide's Modification states in various HOCl in vitro Modified HSA samples.....	107
3.5	The application of the ClTyr MRM acquisition method for the analysis of plasma.....	110

3.5.1 Comparing the XICs of the unmodified and CiTyr modified RHPYFYAPELLFFAK peptide in the 10mM HOCl plasma sample.....	112
3.5.2 The relative percentage modification in the 10mM HOCl modified plasma sample for the RHPDYSVLLLLR peptide.....	113
3.5.3 The relative percentage modification in the 0.25mM HOCl modified plasma sample for the RHPDYSVLLLLR.....	115
3.5.4 Conclusion of the development of the CiTyr MRM acquisition method.....	117
3.6 Nitration of HSA.....	117
3.6.1 Results and Discussion – Detecting Nitrotyrosine in HSA.....	118
3.6.2 The analysis of an unmodified HSA sample in comparison to a 2.5mM SIN-1 in vitro modified HSA and plasma sample by the NiTyr MRM acquisition method.....	121
3.6.3 Optimising the NiTyr MRM method by increasing the scan time	122
3.6.4 Searching for the YLY <sup>2</sup> EIAR + NiTyr modified peptide by MSMS and the omission of the dynamic exclusion parameter.....	124
3.7 Optimisation of the NiTyr MRM method to target all possible modified states of the peptides.....	128
3.7.1 The extraction of XIC's to investigate the most abundant modified state of targeted peptides.....	131
3.8 The comparison of the automated generation of an MRM acquisition method to the manual generation by MSMS observations	133
3.9 Discussion.....	138
3.9.1 The presence of lysine leading to specific oxidative products	138
3.9.2 The effect of methionine and the modification of a tyrosine residue.....	139
3.10 Conclusion.....	140

<b>4 Chapter - The Application of MRM (Multiple Reaction Monitoring) Methods for the Detection of Nitrotyrosine and Chlorotyrosine in Clinical Samples.....</b>	<b>142</b>
4.1.1 MRM methods used to classify disease in biological samples	142
4.1.2 Using MRMs to detect targeted NiTyr and CiTyr modified peptides in clinical samples.....	144
4.2 Aims.....	145
4.3 Materials and Methods.....	145
4.3.1 Mass Spectrometry Methods.....	145
4.4 Results and Discussion.....	146
4.4.1 MSMS Analysis of the 24 Clinical Samples.....	146
4.4.2 Random analysis of the 24 Clinical Samples by the MRM Method.....	147
4.4.3 Confirmation of the modified peptides detected.....	151
4.5 Summary and comparison of the clinical samples 1- 24.....	159
4.5.1 The clinical samples "un-blinded".....	162
4.6 Comparison of conventional MSMS with the MRM.....	166
4.7 Oxidative modification seen in healthy samples.....	167
4.7.1 The initial development of atherosclerosis by the heme enzyme, myeloperoxidase (MPO).....	167

4.7.2	Development of atherosclerotic lesions.....	168
4.7.3	Challenges when choosing targeted modified peptides specific to disease .....	169
4.8	Conclusion and further work.....	170
4.8.1	False Positives .....	171
4.8.2	Improving the MRM method to detect disease specific Ni- and CITyr modifications .....	171
<b>5</b>	<b>Chapter – Investigating the post-translational modification of the low density lipoprotein (LDL) protein moiety, apolipoprotein B-100 (Apo B100), caused by oxidative Stress.....</b>	<b>174</b>
5.1	Aims.....	175
5.2	Materials and Methods .....	175
5.2.1	Preparation of LDL from Plasma.....	175
5.2.2	Assay of Cholesterol.....	176
5.2.3	Chemical <i>in vitro</i> modification of the LDL.....	177
5.2.4	Trichloroacetic Acid (TCA) Delipidation .....	178
5.2.5	Mass Spectrometry methods .....	179
5.2.6	Detecting CITyr by Western Blotting .....	179
5.3	Results and Discussion.....	180
5.3.1	Analysis of HOCl modified LDL and lysozyme samples .....	180
5.3.2	Detecting CITyr in LDL.....	182
5.3.3	An alternative oxidization product - Hydroxytryptophan .....	187
5.3.4	Using the precursor scan for the detection of CITyr modifications on the apo B-100 protein.....	188
5.3.5	Further work to investigate CITyr modifications on the Apo B100 protein.....	189
5.4	The detection of specific nitration sites on the Apo B100 protein	190
5.4.1	Detecting nitrotyrosine modifications on the Apo B100 protein	193
5.5	An MRM acquisition method.....	193
5.5.1	Analysing SIN-1 modified LDL by the MRM acquisition method	194
5.5.2	Critical evaluation of the MRM acquisition method.....	204
5.6	Conclusion and Further work on the Detection of NiTyr modifications on the Apo B100 protein .....	205
<b>6</b>	<b>General Discussion.....</b>	<b>206</b>
6.1	A summary of the findings from this study .....	206
6.2	The limitations and advantages.....	207
6.2.1	The Precursor Scan.....	207
6.2.2	The MRM method –developing and applying a targeted approach for the classification of disease in clinical samples .....	207
6.2.3	The MRM method and precursor scan – NiTyr detection in the Apo B100 protein.....	209

UNIVERSITY OF GLASGOW

# Chapter 1

# Introduction

---

Detecting Biomarkers of Disease

# **1 Introduction**

The Human Genome Project was completed in 2001 <sup>[1]</sup>. It was predicted that this would lead to the development of many prognostic and diagnostic tests that would be specific to the human subject within the following 5-10 years <sup>[2]</sup>.

However, this prediction has not been fulfilled because in some diseases, those resulting from oxidative stress in particular, there is no causal relationship found between genetic information and the sudden occurrence of acute disease. To overcome this problem the study of proteomics representing the link between genes, proteins and diseases was developed <sup>[3, 4]</sup>. Proteomics aims to look at the “Big Picture”, characterising the behaviour of systems rather than the behaviour of a single protein or component and can be used to investigate progressive disease states such as atherosclerosis.

Here I discuss the need for the early diagnosis of diseases, focussing on cardiovascular disease and the techniques used to detect the proteins and post translational modifications related to disease.

## **1.1 Atherosclerosis**

The main cause of death and disability in the Western world is the progressive development of cardiovascular disease <sup>[5]</sup>. The onset of cardiovascular disease is gradual and the chances of suffering from it are increased by environmental factors such as smoking, obesity, lack of exercise and the regular consumption of fatty foods. Atherosclerosis is the thickening of the arterial wall due to the formation of a fibrous plaque [Figure 1]. The term “*Atherosclerosis*” comes from “*Atheromatous*” - referring to the soft, lipid-rich ‘gruel’ within a mature plaque and “*Sclerosis*” - referring to the collagen-rich hardness <sup>[6]</sup>.

The formation of the atherosclerotic plaque decreases the space in the arterial lumen causing an increase in blood pressure which can further lead to cardiovascular diseases (CVD) as a result including, coronary artery diseases and in more severe cases cause congestive heart failure and strokes <sup>[7, 8]</sup>.

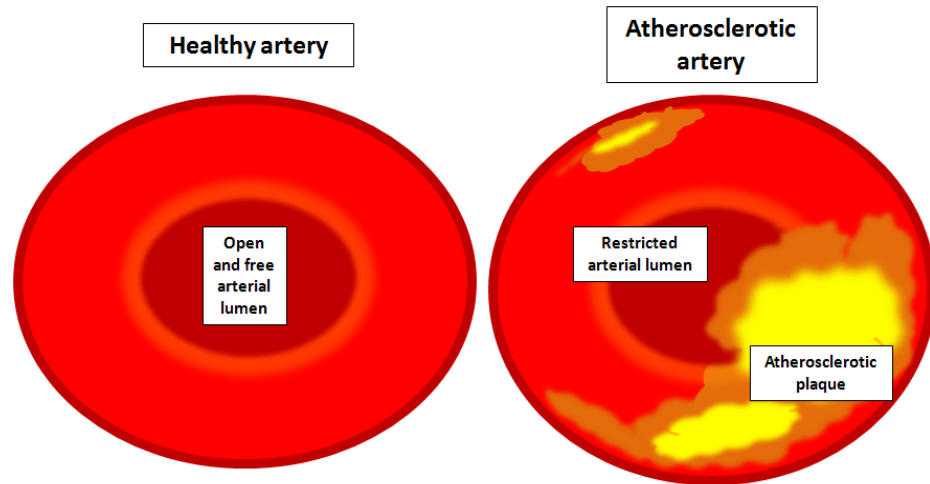


Figure 1: Atherosclerotic plaque formation. The left-hand side of the figure illustrates a healthy artery free from obstruction. The right-hand side of the figure illustrates the atherosclerotic plaque extending into the arterial lumen.

### 1.1.1 The composition of the atherosclerotic plaque

The core of atherosclerotic plaques is characterised principally by profuse lipid deposition and the disappearance of endothelial cells and fibrous tissue elements<sup>[9]</sup>. The composition of the atherosclerotic plaque was first investigated by carrying out studies on arteries from individuals that had suffered atherosclerosis at a very developed stage. Restrepo et al<sup>[10]</sup> found that the foci of cell necrosis in human aortic fatty streaks was associated with the development and initiation of fibrous plaque followed by Katz et al<sup>[11]</sup> who then later identified cholesterol crystals in a subset of human aortic lesions within these fatty streaks. Brooks et al<sup>[12]</sup> later identified oxidised cholesterol and cholesterol ester derivatives using solvent extraction techniques to characterise the lipids. Ylaherttuala et al<sup>[13]</sup> then went on to identify oxidised low density lipoproteins (LDL) within these lesions and myeloperoxidase (MPO), a haeme oxidative enzyme, was then found to be present in and around the core of the atherosclerotic plaque<sup>[14]</sup>. Structures resembling lipoprotein aggregates have been observed with the aid of an electron microscope within the arterial intima<sup>[15]</sup> and ApoB-100<sup>[16]</sup>, has also been successfully isolated from lipid aggregates<sup>[17 9;18]</sup>. These observations were then linked when oxidised LDL (Ox-LDL) was found to promote aggregation of macrophages<sup>[19]</sup>.

### 1.1.2 The LDL particle

The LDL particles are approximately spherical in shape with a diameter of about 22 nm (Figure 2). The core of the LDL particle consists of a high proportion of cholesteryl ester and the remainder of tri-glycerides. The LDL coat consists of phospholipids, free cholesterol and a large single protein, apolipoprotein B-100. The fatty acids in LDL phospholipids are the main fatty acids consumed in the diet, the most abundant being the polyunsaturated fatty acid, linoleate. The LDL particle is adhesive in nature due to the high lipid content present and during extraction from plasma can denature due to slight changes in pH, oxidation or excessive agitation so therefore must be treated with care.

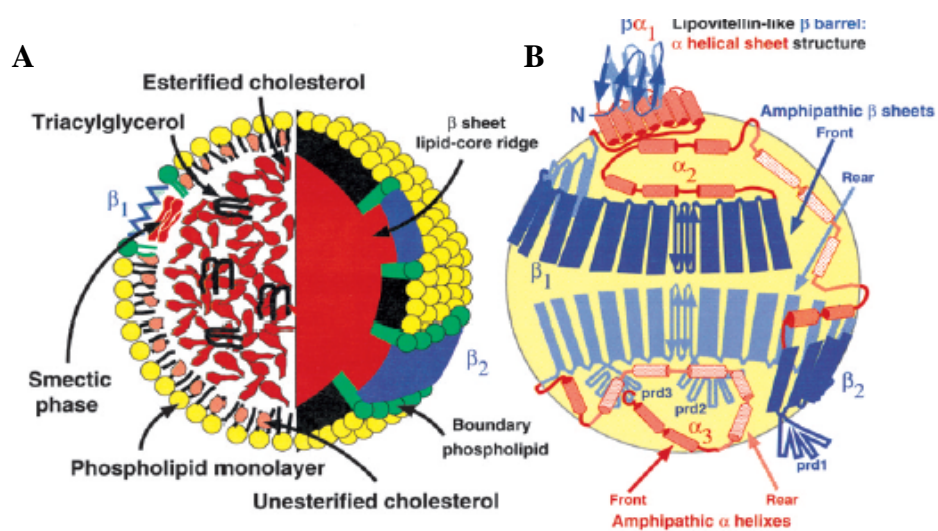


Figure 2: Schematic diagram of an LDL particle (reproduced from [20]). “A” summarises the organization of the lipid. The surface phospholipids and triglyceride lipid core is shown as well as the amphipathic  $\beta$ -sheet-induced lipid core ridges and the boundary phospholipids  $\beta$ -sheets. “B” summarises the organisation of ApoB-100 on the LDL surface. The coloured regions indicate where the ApoB-100 differs in structure.

The protein moiety, ApoB-100 is 4,536 amino acids in length and circumnavigates the LDL particle. The apolipoprotein is hydrophobic in segments which “dive” in and out of the neutral lipid core of the particle. The apoB-100 protein is both hydrophilic and hydrophobic and classed as amphipathic. This means that apoB-100 can not only interact with the lipids on the lipoprotein but will also interact with the surrounding aqueous environment [20]. Due to the amphipathic nature of the LDL particle, post translational modifications will be difficult to predict during disease states. The size of the protein will also mean that any post translational modifications present will be challenging to detect due to their low

abundance in comparison to the rest of the protein. These challenges will be dealt with during our study.

The hydrophilic regions of the apoB-100 are the most likely portions of the protein to be modified during disease states as the side chains are exposed to the LDL's surrounding environment. The apoB-100 acts as a ligand for the uptake of LDL by cells and as a mediator for binding. Yang et al <sup>[23]</sup> were able to map lipid-associating regions of apoB-100 using trypsin-treated intact LDL particles. The trypsin-releasable regions of the apoB-100 protein were determined and those that were not were assumed to be lipid associated (Figure 3) <sup>[21-23]</sup>. Any modification of the apoB-100 protein during our study will be performed on intact, native LDL particles to mimic post translational modification *in vivo*.

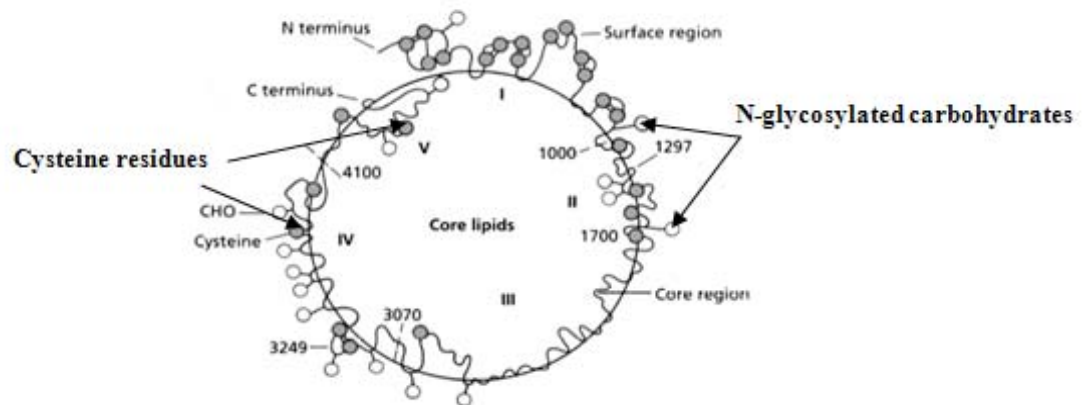


Figure 3: Structure of ApolipoproteinB-100 in Low-density Lipoproteins (reproduced from <sup>[20]</sup>). Trypsin-releasable regions are on the outside of the particle and non-trypsin releasable regions on the inside.

### 1.1.3 Initiation of atherosclerosis

An initiating event for atherosclerosis is the transportation of circulating oxidised low-density lipoproteins (Ox-LDL) across the endothelial cell layer of the artery wall. Transportation of Ox-LDL is most likely where there is already damage to the endothelial layer caused by either Ox-LDL itself or physical or chemical forces or infection <sup>[7]</sup>. Extra-cellular Ox-LDL can damage endothelial cells and smooth muscle cells (SMCs) by inducing the expression of adhesion molecules and chemotactic factors. Chemotactic factors such as monocyte chemoattractant peptide 1 (MCP-1) and macrophage colony stimulating factor (CSF) will help lead to the formation of fatty streaks or fibrous plaque and

lesions in the artery. The oxidation of LDL causes aggregation which leads to foam cell formation by macrophage cells.

Atherosclerosis is an inflammatory response of macrophages and lymphocytes in the blood to 'invading' pathogenic lipoproteins in the arterial wall <sup>[24]</sup>. Invading pathogens or molecules unknown to the body can be destroyed by phagocytosis. So although able to defend the body, macrophages are also one of the central mechanisms contributing to the development of atherosclerosis <sup>[25]</sup>. The formation of foam cells occurs by macrophage ingestion of LDL by endocytosis and the macrophage scavenger receptor CD36 is found to play an important role in lesion development and therefore the binding and uptake of the Ox-LDL <sup>[26]</sup>. Podrez et al <sup>[26]</sup> demonstrated that changes in the LDL caused by oxidation such as phospholipid oxidation, increased overall electronegativity of the particle and the unfolding of the apolipoprotein for example, promotes CD36- dependent recognition. When present at only a few modifications per particle, this results in increased macrophage binding, uptake of Ox-LDL, metabolism, cholesterol accumulation and foam cell formation. The increased uptake is due to the LDL receptor no longer recognising the LDL particle (see also 1.2.1)

The fatty streaks are in fact aggregated macrophages that have phagocytosed the Ox-LDL to become foam cells. The monocytes adhere to the activated endothelial cells before moving into the subendothelial space in response to the chemoattractant molecule, 'monocyte chemoattractant peptide 1' where they will proliferate in response to CSF (Figure 4).

In the subendothelial space, the monocytes ingest the lipoproteins which causes them to differentiate into macrophages. The macrophages then generate the reactive oxygen species (ROS) that convert Ox-LDL into highly oxidised LDL. The highly oxidised LDL is also consumed by the macrophages, thus taking up cholesterol, continuing to increase the formation of foam cells. Yoshida et al <sup>[27]</sup> have demonstrated that as LDL becomes increasingly oxidised the lipoproteins electrophoretic mobility also increases. Oxidised LDL will therefore run further on an agarose gel than LDL that has not been oxidised and the degree of oxidation of the lipoproteins can be visualised this way <sup>[27;28]</sup>.

The foam cells combine with the leukocytes to become the fatty streak and the process continues. Proliferation of the smooth muscle cells coupled with the

continuous differentiation of monocytes to macrophages inside the subendothelial space will convert the fatty streaks to more advanced lesions and finally a fibrous plaque that protrudes into the arterial lumen. A fibrous cap consisting of SMCs and macrophages can develop over the lesion which will surround a high lipid core. This fibrous cap can be vulnerable to rupturing and in extreme cardiovascular disease cases will result in the formation and release of thrombi into the bloodstream, which can lead to a blockage of a blood vessel [29]. Over time the atherosclerotic lesion can stabilise becoming tougher forming a cap consisting of connective tissue and a higher SMC content than a more vulnerable cap. The cap can be further strengthened and become even more resistant to rupturing by calcification [30-32].

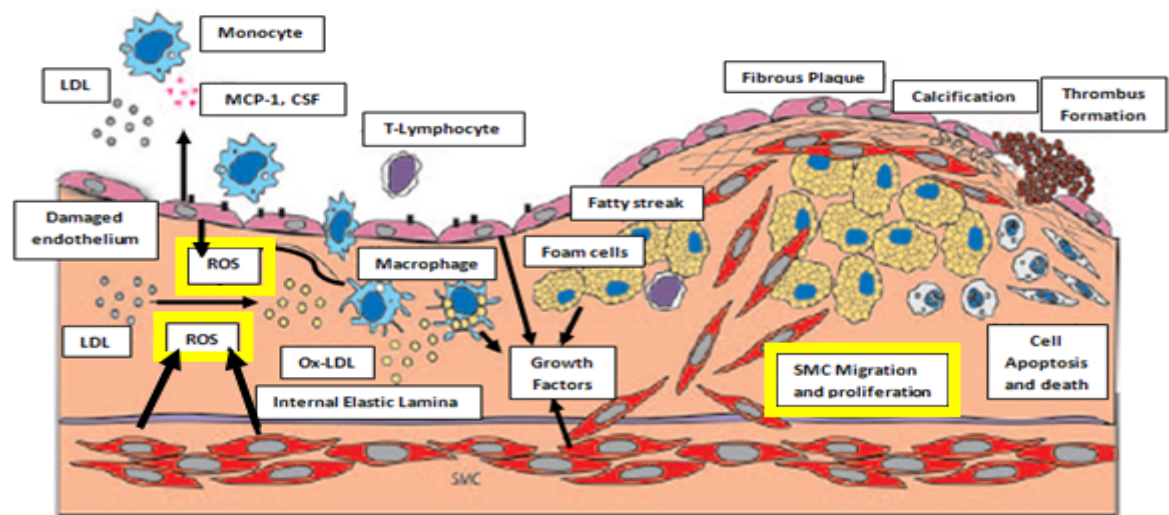


Figure 4: The development of atherosclerosis (adapted from [7]). The reactive oxygen species (ROS) that oxidise LDL are produced in endothelial cells, smooth muscle cells (SMCs) and macrophages in the subendothelial space. The resulting build up of macrophage foam cells leads to fatty streaks that form a fibrous plaque which can calcify and lead to thrombus formation.

### 1.1.3.1 The unfolding of the apolipoprotein B100

The secondary sequence and conformation of the LDLs protein moiety, Apo B100, is influenced by lipid-protein interactions and dynamics so will be affected by the introduction or removal of lipids during the metabolism of the lipoprotein particle [33]. The oxidation of lipids on the LDL will alter the water-lipid interface leading to the destabilising of the Apo B100 protein causing it to unfold and denature. Ursini et al states the unfolding of the Apo B100 protein has been observed in *in vivo* oxidatively modified LDL particles and that atherosclerotic

progression is due to the effect of the protein unfolding. This initiating event leading to protein misfolding may differ from disease to disease but the general pattern where loss of protein stability is seen is during destabilisation when what is usually an  $\alpha$ -helix misfolds, leading to a relative increase in  $\beta$ -sheet structure.

#### 1.1.4 Classification of lipoproteins

Cholesterol and triglyceride are insoluble, essential lipids that are packaged into lipoproteins to allow circulation within human blood plasma from sites of absorption or synthesis to areas of use. Each lipoprotein consists of a non-polar, hydrophobic cholesterol ester and triglycerol core. The outer layer of the lipoproteins consists of free cholesterol, phospholipids and specific apolipoproteins. The outer layer is polar permitting transportation of the lipoproteins within the plasma. The surrounding apolipoproteins (apo) such as apoB, apoC and apoE, coat the lipoprotein and serve a number of different functions including lipid transport and lipoprotein particle recognition by enzymes allowing the removal of lipids from the particle <sup>[21]</sup>. Apo-CII, for example, activates the lipoprotein lipase (LPL) which removes triglyceride from chylomicrons and very-low density lipoproteins (VLDL).

There are five different classes of lipoproteins which includes: high-density lipoproteins (HDL), chylomicrons, very low-density (VLDL), intermediate-density lipoproteins (IDL) and low-density lipoproteins (LDL) <sup>[34]</sup>. The source, composition and density of each class of lipoprotein is described in more detail (Table 1).

**Table 1: The source and composition of lipoproteins.**

	Chylomicrons	VLDL	IDL	LDL	HDL
Density (g/ml)	<0.95	<0.95 - 1.006	1.006 - 1.019	1.019 - 1.063	1.063 - 1.210
Diameter (nm)	75 - 1200nm	30 - 80nm	25 - 35nm	18 - 25nm	5 - 12nm
Components (% dry weight) protein	1 - 2%	10%	18%	25%	33%
Triglycerol (%)	83	50	31	10	8
Cholesterol and Cholesterol esters (%)	8	22	29	46	30
Phospholipids (%)	7	18	22	22	29
Apoprotein composition	A-I, A-II, B-48, C-I C-II, C-III	B-100, C-I, C-II C-III, E	B-100, C-I, C-II C-III, E	B-100	A-I, A-II, C-I, C-II, C-III, D, E
Source	Intestine	Liver	Catabolism of VLDL	Catabolism of IDL	Liver, intestine

The source, size, density, and composition of each lipoprotein <sup>[34]</sup>.

#### 1.1.4.1 High-Density Lipoproteins (HDLs)

HDLs are generated in the liver and small intestine <sup>[34, 35]</sup>. When first excreted from the liver into the plasma, the HDL particles are mainly protein with very little cholesterol. The enzyme, lecithin:cholesterol acyltransferase, promotes the HDL uptake of free cholesterol in the bloodstream by esterification. By esterifying the free cholesterol into cholesterol esters, the hydrophobicity of the lipoprotein core will increase, making the particle denser. HDL levels are known to be inversely proportional to the risk of cardiovascular disease <sup>[35;36]</sup> as the HDL particles return to the liver from where the excess cholesterol can be excreted from the body in bile. HDL therefore plays a cardioprotective role by removing excess cholesterol from the tissues. This transfer process of cholesterol from extrahepatic tissues to the liver is called reverse cholesterol transport <sup>[36]</sup>.

#### 1.1.4.2 Chylomicrons

Chylomicrons are assembled and formed in the intestinal mucosa to immobilize dietary (exogenous) lipids. Chylomicrons are the largest class of lipoprotein and are assembled in order to transport dietary cholesterol and triacylglycerols to the rest of the body <sup>[37]</sup>. They leave the intestine via the lymphatic system and enter the bloodstream where apoC-II and apoE are acquired from HDL in the plasma. In the capillaries apoC-II activates lipoprotein lipase (LPL) which is found on the surface of endothelial cells. The LPL acts by removing the fatty acids from the triglycerols on the chylomicrons <sup>[38]</sup>. The free fatty acids are then absorbed by tissues and the triglycerol decomposites returned via the bloodstream to the liver and kidneys. During the fatty acid removal by the enzymatic action of LPL from the chylomicrons, a large proportion of phospholipid, apoA and apoC is relocated to the HDLs. Losing apoC-II prevents further degradation of the chylomicrons by lipoprotein lipase.

#### 1.1.4.3 Very low-density lipoproteins (VLDLs), intermediate-density lipoproteins (IDLs) and low-density lipoproteins (LDLs)

Excess dietary fat and carbohydrate are converted to triacylglycerols in the liver. The triacylglycerols are packaged into very low-density lipoproteins (VLDLs) for distribution and delivery to various tissues for storage or use. The triglycerol portion of VLDLs is hydrolysed in the capillary by LPL to provide fatty acids for storage or use by muscle tissue. The apoCs that are also lost are transferred to the HDLs. The predominant remaining proteins are apoE and

apoB-100 and the remaining lipid portion is called VLDL remnants or intermediate-density lipoproteins (IDLs). The remnant VLDL is metabolised in the circulation to a smaller, denser, cholesteryl ester-rich particle which is closer in density to LDLs. The final processing stage of VLDL transformation to LDL involves another lipolytic enzyme, hepatic lipase. If the LDL is not oxidised, it will reside in the circulation for approximately 2-3 days before being taken up into the liver or extrahepatic tissues <sup>[17]</sup>.

Therefore, further loss of triacylglycerols converts the IDLs to Low Density-Lipoproteins (LDL) (Figure 5). Low-density lipoproteins or LDL carry cholesterol in the human plasma. Large quantities of LDL-associated cholesterol in the bloodstream will lead to heart disease <sup>[5;17;21]</sup>. Studies have shown that there is a link between elevated levels of LDL in the bloodstream and the eventual progression of atherosclerosis. Young et al <sup>[39]</sup> hypothesised that the first stage of atherosclerosis is the oxidation of LDL within the arterial wall followed by the uptake of the oxidized LDL by macrophages that leads to the formation of foam cells in the early stages of the formation of arterial lesions <sup>[21;40]</sup>.

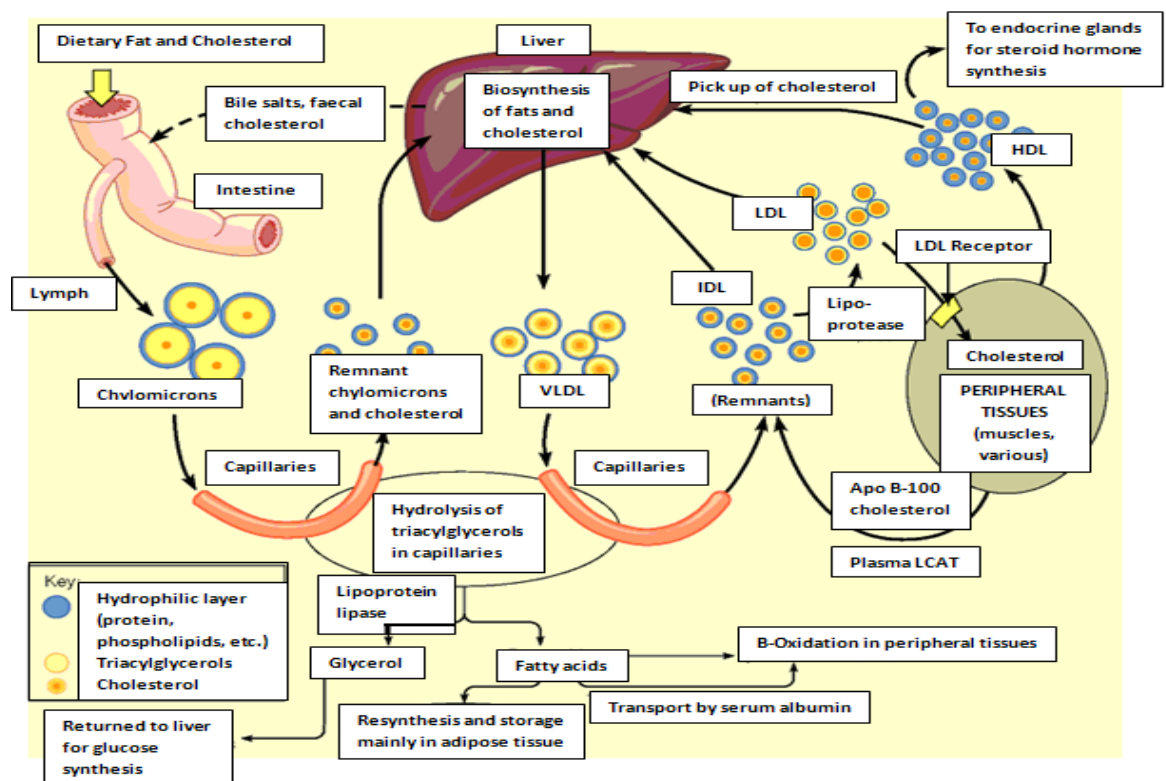


Figure 5: An overview of lipoprotein pathways and fates (adapted from <sup>[41]</sup>). The above figure illustrates where and how chylomicrons, VLDL, LDL and HDL are generated and their fate in the system. Chylomicrons are produced in the intestine before being hydrolysed in the capillaries. VLDL is also hydrolysed in capillaries and the remnants (IDL) are utilised for LDL

formation. HDL is shown to pick up free cholesterol in extrahepatic tissue before returning to the liver where cholesterol is metabolised and excreted from the body in bile.

## 1.2 A defence against atherosclerosis

The required cholesterol for vital structural and metabolic roles in the cell is gained due to the domains called rafts and caveolae <sup>[42]</sup> distributed along the plasma membrane of cells. The caveolae along the plasma membrane are invaginations of the cell plasma membrane able to transport molecules, in this case cholesterol, by endocytosis into the cell <sup>[43]</sup>. Caveolae systems are sensitive to oxidised cholesterol and contain receptors that recognise and bind to HDL, LDL and oxidised lipoproteins. Caveolae contain various signalling molecules that depend on a maintained 'normal' cholesterol content in the body for activity. The natural internal defence mechanism against atherosclerosis leads to the excretion of excess cholesterol in the faeces when the cholesterol content is too high but if there is too much cholesterol in cells, particularly those in the arterial wall, the accumulation will initiate atherosclerotic cardiovascular disease. HDL will also act to remove excess cholesterol from foam cells, transporting a variety of lipids and lipophilic molecules between tissues and other lipoproteins. The transportation of cholesterol from peripheral tissues to the liver and then bile followed by excretion in the faeces, is called reverse cholesterol transport (RCT) <sup>[44]</sup>.

The feedback system, RCT pathway (Figure 6), opposes atherosclerosis by taking accumulated cholesterol from the vessel wall to the liver for excretion. Macrophages ingest cholesterol by endocytotic and phagocytotic means. These cholesterol-ingestion processes are not regulated by the feedback system so the macrophages must therefore store or secrete the engulfed cholesterol. ApoA-I is secreted from the liver and intestine and loaded with cholesterol and phospholipids by ATP-Binding Cassette Transporter A1 (ABCA1). Pre-B-HDL picks up cholesterol and phospholipids from ABCA1 in macrophages and peripheral cells and converts to HDL<sub>2</sub>. HDL<sub>2</sub> can be further loaded with cholesterol by ABCG1 and possibly scavenger receptor B1 (SR-B1), in macrophages. ABCG1 has recently been identified as a facilitator of cholesterol and phospholipid efflux from macrophages to HDL <sup>[45]</sup>. The cholesterol cargo is unloaded to SR-B1 in liver. Cholesterol can be secreted into bile either in the free form or after

conversion as bile salt. After transportation into the intestine, cholesterol and bile salt are reabsorbed or excreted in faeces.

Phospholipids, and other metabolites as well as accumulated cholesterol in macrophages, are removed by the ATP-binding Cassette Transporter A1 (ABCA1), a cell membrane protein, to lipid-depleted HDL apolipoproteins. Liver ABCA1 initiates HDL particle formation and macrophage ABCA1 protects the arteries from atherosclerosis. Esterified HDL is then delivered to the liver for excretion. High levels of HDL are therefore inversely proportional to the risk of cardiovascular disease <sup>[46]</sup>. Other mechanisms such as passive diffusion, SR-B1, caveolins and sterol 27-hydroxylase and the collection of apoA-I can also take part in this process. Additionally HDL phospholipids absorb cholesterol that has passively diffused from the plasma membrane into the aqueous phase facilitated by the interaction with the scavenger receptor B1 (SR-B1) <sup>[46-48]</sup>.

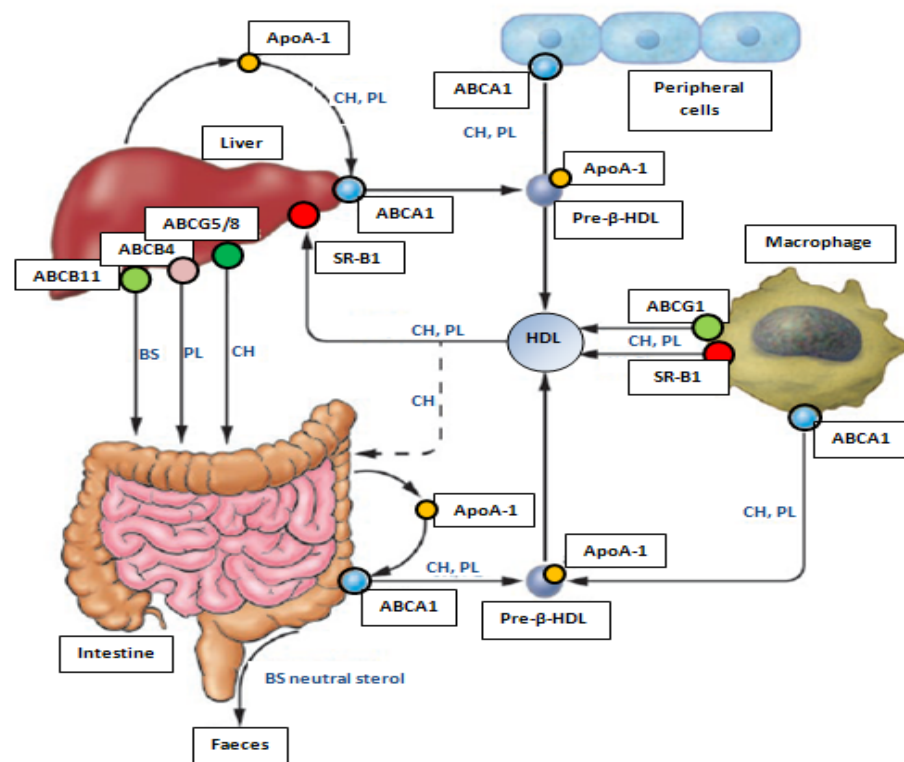


Figure 6: Liver SR-B1 drives reverse cholesterol transport in macrophages (adapted from <sup>[44]</sup>). Illustration of the major pathways involved in Reverse Cholesterol Transport (RCT) from peripheral tissues and cholesterol ingested macrophages also referred to as foam cells.

CH = Cholesterol, PL = Phospholipids BS = Bile Salt

### 1.2.1 Genetic disorders leading to high levels of LDL

Atherosclerosis can be caused by not only environmental factors but also by underlying genetic defects which will lead to an increased cholesterol level regardless of cholesterol intake. The reverse cholesterol transport (RCT) pathway naturally protects against atherosclerosis but if there is a mutation in the ABCA1 genes the feedback pathway and cholesterol efflux will be hindered which, regardless of diet and life style factors, will lead to higher levels of cholesterol in the body thus increasing the risk of atherosclerosis. This genetic disorder may be treated by supplementing the HDL and/or the ApoA-I levels which will reverse atherosclerotic development by the acceleration of RCT and cholesterol efflux<sup>[47]</sup>. Also, if the LDL receptor in cells is absent or damaged LDL cannot bind at a normal rate which leads to a build up or accumulation of LDL in the plasma. If the apoB-100 is defective with a substituted amino acid for example this may also hinder or prevent binding to the LDL receptor thus leading to the same accumulative build-up<sup>[47]</sup>.

### 1.3 Oxidative stress and the production of reactive species

The presence of reactive species or oxidants in a biological system will produce oxidised macromolecules (e.g. Ox-LDL) if the reactive species are in sufficiently reactive, in sufficient quantity or concentration. The imbalance of oxidants in the body leading to oxidised macromolecules under these conditions is called “oxidative stress” and has been linked to the mechanism of atherosclerosis.

These reactive species or oxidants are radicals which are atoms or molecules with at least one unpaired electron. They are highly reactive allowing protein side-chains, lipids and DNA to be easily modified without the aid or presence of catalytic enzymes<sup>[40]</sup>. Some small molecules that are radicals or are easily converted into radicals are shown in Table 2. In our bodies one of the most abundant radicals is oxygen and is not as reactive as would be expected due to the unpaired electrons being situated in different molecular orbitals and therefore possessing parallel spins. Enzymes, such as nicotinamide adenine dinucleotide (phosphate) (NADH/NAD(P)H) oxidases and xanthine oxidases (XO) are therefore required to convert the relatively stable O<sub>2</sub> molecule into superoxide, O<sup>2•-</sup>, by univalent reduction. Superoxide, (O<sup>2•-</sup>), can also be formed non-enzymatically by reacting oxygen with redox active compound, semiubiquinone of the mitochondrial electron transport chain<sup>[49]</sup> (Figure 7).

Table 2: Reactive species and radicals [40].

•NO	Nitric Oxide
•NO <sub>2</sub>	Nitrogen dioxide
ONOO <sup>-</sup>	Peroxynitrite
O <sub>2</sub> • <sup>-</sup>	Superoxide
•OH	Hydroxyl radical
H <sub>2</sub> O <sub>2</sub>	Hydrogen peroxide
ROO•	Peroxy radical
HOCl	Hypochlorous acid

Examples of reactive species categorised by their primary atom, oxygen or nitrogen. They are small molecules easily able to modify protein side chains without the aid of catalytic enzymes.

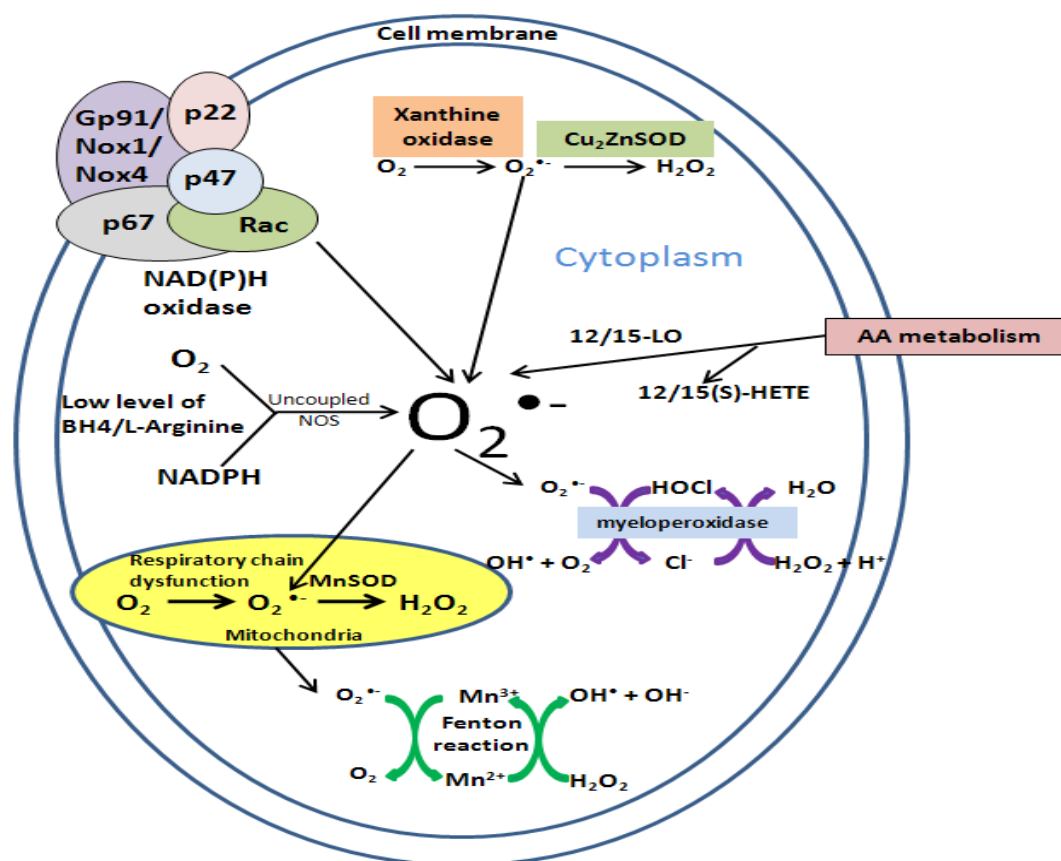


Figure 7: The production of reactive species (adapted from [7]). Activated NAD(P)H oxidase, 12/15-LO (Leukocyte-type 12/15-Lipoxygenase) and XO (Xanthine oxidase) generate superoxide. Nitric oxide synthases (NOS) switches from a coupled state to a non-coupled state to generate superoxide when BH<sub>4</sub> (5,6,7,8-tetrahydrobiopterin) or L-arginine levels are low. Membrane-bound sub-units; Gp91, Nox1 and Nox4, cytosolic components; p22phox, p47phox, p67phox, and G-proteins Rac1 and Rac2 are the catalytic site of the NAD(P)H derived O<sub>2</sub>•<sup>-</sup>. If the mitochondrial respiratory chain is dysfunctional SOD isoforms are produced which will dismutate superoxidase to hydrogen peroxidase. Myeloperoxidase will generate hypochlorous acid from hydrogen peroxide in the presence of chloride ions. Hydrogen peroxide reacts with various transition metals (mainly iron) to produce hydroxyl radicals.

Hydrogen peroxide ( $\text{H}_2\text{O}_2$ ) can be produced from the superoxide anion by superoxide dismutases (SODs) such as manganese SOD and copper-zinc SOD. Hydrogen peroxide ( $\text{H}_2\text{O}_2$ ) can go on to react with other radicals and transition metals such as  $\text{Fe}^{2+}$  to produce highly reactive hydroxyl radicals ( $\text{OH}^\cdot$ ). This is called the Fenton reaction (Equation 1) [50].



The superoxide anion reacts with the transition metal,  $\text{Fe}^{3+}$ , producing molecular oxygen and regenerating  $\text{Fe}^{2+}$  (Equation 2). The  $\text{Fe}^{2+}$  will then go on to produce the hydroxide anion and the hydroxyl radical from reaction with hydrogen peroxide. This regenerates  $\text{Fe}^{3+}$  which will then react again with any remaining superoxide, perpetuating the production of the hydroxyl radical.

Stimulated monocytes and neutrophils will generate hypochlorite ( $\text{HOCl}$ ), via the action of the enzyme, myeloperoxidase on hydrogen peroxide,  $\text{H}_2\text{O}_2$ , which is known to damage proteins by reacting with their sidechains. Myeloperoxidase, a heme protein secreted by phagocytes, and hydrogen peroxide are produced during inflammatory conditions, including atherosclerosis [51] (Figure 8). The MPO catalyses the reaction of the  $\text{Cl}^-$  with hydrogen peroxide to generate  $\text{HOCl}$ .

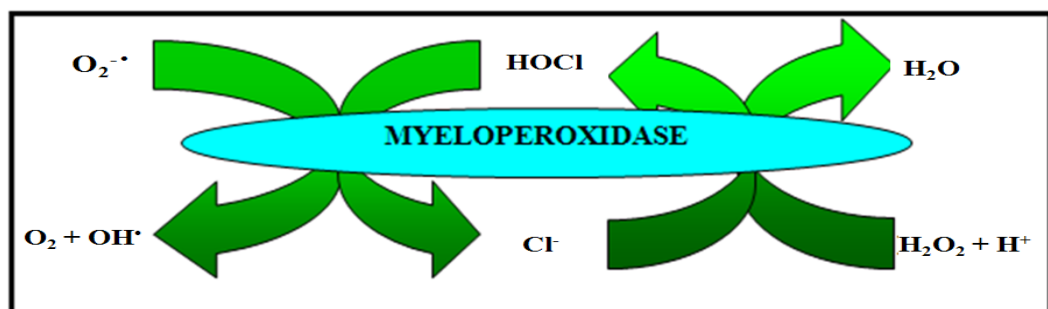
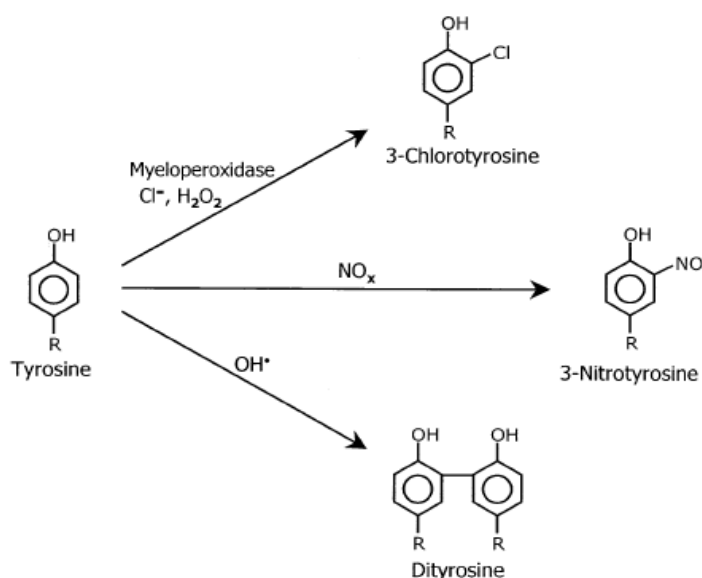


Figure 8: Hypochlorous acid is produced by the reaction of hydrogen peroxide with the chlorite anion.  $\text{HOCl}$  will then reduce the superoxide anion to molecular oxygen and the hydroxide radical.

### 1.3.1 Hypochlorite-induced damage to proteins

Hypochlorous acid ( $\text{HOCl}$ ) is a potent bactericide known to defend against invading bacteria, pathogens and fungi in the body.  $\text{HOCl}$  and other oxidising intermediates generated by myeloperoxidase can react with a wide variety of

biological molecules and is known to cause tissue damage [52, 53]. When hypochlorite reacts with peptides and proteins the amino acid sidechains can become modified resulting in the formation of chlorotyrosine for example. This process can indicate the initiation atherosclerosis. Treatment of proteins with HOCl is found to cause direct oxidative damage. When a protein becomes damaged in this way, it becomes vulnerable to degradation by proteolytic enzymes. In fibronectin, for example, exposure to HOCl alters the protein's primary and tertiary structures which will then in turn render the protein more susceptible to elastase [54]. Certain amino acids are more susceptible to modification by HOCl than others. The ease of oxidation of the aromatic side chains, tyrosine and tryptophan, is due to the reactivity of the aromatic ring present. This means that tyrosine and tryptophan can undergo reactions resulting in ring oxidation and can therefore be employed as biomarkers for HOCl-damage. Studies carried out by Heinecke et al, confirm 3-chlorotyrosine is present in oxidised LDL on the arterial wall at atherosclerotic lesions [55]. The oxidation of tyrosine can lead to many end products that are specific for myeloperoxidase-catalysed reaction pathways, free radical pathways and reactive nitrogen species pathways [56] (Figure 9).



**Figure 9:** The reaction of tyrosine [56]. Tyrosine is oxidised by myeloperoxidase in the presence of hydrogen peroxide and hypochlorous acid (HOCl) to form 3-chlorotyrosine. When tyrosine is oxidised by reactive nitrogen species, 3-nitrotyrosine is formed instead. When oxidised via a free radical pathway, a dimer of tyrosine, dityrosine is produced.

### 1.3.2 Myeloperoxidase-generated reactive nitrogen species

As discussed, the expression of the myeloperoxidase enzyme during inflammatory conditions such as atherosclerosis, lung disease and sepsis for example, leads to the formation of chlorotyrosine (ClTyr) and nitrotyrosine (NiTyr). When these inflammatory diseases are treated the levels of ClTyr and NiTyr which were determined by isotope dilution LC-MS (discussed further in 1.4.1), were seen to deplete<sup>[57]</sup>. Stable isotope dilution is performed by adding a known concentration of isotope to label the sample being studied and internal standards are used to quantify.

Souza et al<sup>[58]</sup> employed stable isotope dilution LC-MS to study the levels of protein bound NiTyr in plasma proteins and in LDL found in atherosclerotic plaques. Using the technique Souza reported that approximately 1 to 10 tyrosine residues per 100,000 (10-100 $\mu$ mol NiTyr/mol tyrosine) were found nitrated in plasma proteins under inflammatory conditions like cardiovascular disease<sup>[59]</sup>. Although NiTyr was found to be protein-bound in the plasma proteins, up to 10 times more NiTyr was detected in tissues. In the case of LDL it was found that 9 $\mu$ mol NiTyr/mol tyrosine was found in healthy subjects but in LDL extracted from atherosclerotic plaques 840 $\mu$ mol NiTyr/mol tyrosine was found representing a 90-fold increase<sup>[60]</sup>. The problem with the stable isotope dilution method is that isotopes are very expensive to buy. Unfortunately in the study Souza does not differentiate between the NiTyr in free LDL in the plasma of atherosclerotic patients and only investigates the NiTyr in LDL found in the lesions.

It is known that the production of reactive nitrogen species is as important as a biomarker for oxidative stress along with chlorotyrosine. Nitrotyrosine has also been found to be enriched in atherosclerotic aorta. Podrez et al<sup>[61]</sup> reports that reactive nitrogen species are formed from the MPO-H<sub>2</sub>O<sub>2</sub>-NO<sub>2</sub><sup>-</sup> pathway converting LDL into NO<sub>2</sub>-LDL that is then taken up and degraded by macrophages leading to deposition of cholesterol, foam cell formation and the beginnings of lesion development.

### 1.3.3 Stable markers of oxidant damage to proteins

Protein oxidation products are sensitive markers of oxidative damage and therefore the pattern of oxidation products can yield information as to the nature of the original oxidative insult to the protein<sup>[62]</sup>. The reaction of radicals

with proteins or peptides in the presence of  $O_2$  will give rise to an altered backbone and side chains. Studying the protein's oxidised fragmented backbone from clinical samples has its limitations: problems arise during the investigation of the altered backbone due to the quantity and abundance of any other proteins and the activity of any proteases that are/may be present. Backbone fragmentation therefore is rarely used to quantify protein oxidation in complex systems and the study of oxidised peptides with altered side chains is investigated instead.

Due to their chemical differences (e.g. electronegativity, conjugation etc.) aliphatic sidechains, those containing a hetero-atom (a non-carbon or non-hydrogen atom on a cyclic ring) and aromatic sidechains react differently with reactive oxidative species (ROS) (Table 3).

Most oxidative products of side chains that are aliphatic (glutamic acid, valine and leucine) or those containing a heteroatom (arginine, lysine and methionine) are shown to be unstable or generated enzymatically. Oxidation products of aliphatic sidechains can also be found naturally in the cell which makes it difficult to specifically determine if oxidative stress has occurred or not. The most stable and therefore the best oxidative biomarkers appear to be produced by the aromatic sidechains: tyrosine, phenylalanine, tryptophan, and histidine.

Table 3: Stable markers of oxidant damage to proteins [62].

Substrate and oxidative insult	Product	Potential as marker
Tyr plus HO <sup>•</sup> or reactive nitrogen species	DOPA	Yes, but susceptible to further oxidation
Tyr plus HOCl	3-Chlorotyrosine	Yes
	3,5-Dichlorotyrosine	
Tyr plus reactive nitrogen species	3-Nitrotyrosine	Yes
	3,5-Dinitrotyrosine	
Tyr plus HO <sup>•</sup> , one electron oxidants, or HOCl, followed by radical-radical combination	Di-tyrosine	Yes, but yield dependent on radical flux as a result of radical-radical reactions
Tyr plus <sup>1</sup> O <sub>2</sub>	Tyr endoperoxide	No, unstable
Phe plus HO <sup>•</sup> , one electron oxidants or, reactive nitrogen species	<i>o</i> -, <i>m</i> -Tyrosine	Yes
Phe plus HO <sup>•</sup> before or after dimerization	Dimers of hydroxylated species	Possible, but complex mixture
Trp plus HO <sup>•</sup> , or one electron oxidants	N-Formylkynurenine 3-Hydroxykynurenine Kynurenine	} Can be generated enzymatically, and hence not advised
	2-, 4-, 5-, 6-, or 7-Hydroxytryptophans	
Trp plus <sup>1</sup> O <sub>2</sub>	Trp hydro-/endo-peroxide	No, unstable
His plus HO <sup>•</sup> , or one electron oxidants	2-Oxo-histidine	Possible
His plus <sup>1</sup> O <sub>2</sub>	His hydro-/endo-peroxide	No, unstable
Glu plus HO <sup>•</sup> in presence of O <sub>2</sub>	Glutamic acid hydroperoxides	No, unstable
Leu plus HO <sup>•</sup> in presence of O <sub>2</sub>	4-Hydroxyglutamic acid	Possible
	4- and 5-Hydroperoxy-leucines	No, unstable species
	4-Hydroxy-leucine	Possible, but co-elutes with other products
	5-Hydroxy-leucine	Yes
	$\alpha$ -Ketoisocaproic acid, Isovaleric acid, Isovaleraldehyde, Isovaleraldehyde oxime	} Can be generated by other reactions
	3- and 4-Hydroperoxyvalines	
Val plus HO <sup>•</sup> in presence of O <sub>2</sub>	3-Hydroxyvaline	Yes
	4-Hydroxyvaline	Possible, but coelutes with other products
Lys plus HO <sup>•</sup> in presence of O <sub>2</sub>	Lysine hydroperoxides	No, unstable species
	3-Hydroxylysine	Yes
	4- and 5-Hydroxylysines	No, can be generated enzymatically
Pro plus HO <sup>•</sup> in presence of O <sub>2</sub>	Proline hydroperoxides	No, unstable species
	3-Hydroxyproline	Possible
	4-Hydroxyproline	No, can be generated enzymatically
	5-hydroxy-2-aminovaleric acid	Yes, but also from other amino acids
Arg plus HO <sup>•</sup> in presence of O <sub>2</sub>	5-hydroxy-2-aminovaleric acid	Yes, but also from other amino acids
Ile plus HO <sup>•</sup> in presence of O <sub>2</sub>	Isoleucine hydroperoxides	No, unstable species
	Hydroxyisoleucines	Possible, but not fully characterized
Gly: hydrogen atom abstraction from $\alpha$ -carbon followed by reaction with CO <sub>2</sub> <sup>•-</sup> radicals	Aminomalonic acid	Yes, but may arise via successive oxidations of other amino acids (e.g., Ser)
Met plus HO <sup>•</sup> or one-electron oxidation	Methionine sulfoxide	Yes, but can be enzymatically reduced, and levels may be misleading
Cys plus HO <sup>•</sup> , or other hydrogen atom abstracting species	Cystine, Oxy acids	No, natural product Possible

The table displays the compounds found as oxidative-lesions on radical- and oxidant-damaged proteins and their potential use as biomarkers for oxidative damage. The oxidative products, 3-chlorotyrosine (red boxed) and 3-nitrotyrosine (blue-boxed) are highlighted and discussed further in the thesis.

## 1.4 Detecting biomarkers for disease

The development of atherosclerosis is difficult to track as there are no imaging techniques that are available to monitor the changes of inflammation in the arteries. An arterial biopsy is currently the best way to assess the disease but it is invasive and therefore not practical or efficient <sup>[63]</sup>. Current research is now trying to find ways where disease can not only be detected earlier and faster, but also in ways which are less invasive and more convenient for the patient.

Bodily fluids are easier to obtain and assay when compared with invasive techniques which require tissue samples for biopsies. Blood can be easily withdrawn from subjects and is an obvious choice for biomarker discovery. Plasma is a frequently sampled proteome for medical diagnosis and contains other tissue proteomes from which disease may be suspected <sup>[64]</sup>. Enzyme assays can be exploited to assay plasma and the advantages are that the level of function rather than the amount of a molecule is measured. Plasma may represent the deepest portrayal of the human proteome as it circulates the entire body and will not only contain plasma proteins but also all cell proteins as leakage markers <sup>[65;66]</sup>. Enzyme assays of plasma will therefore give a full picture of the levels of disease within the body. The disadvantages of enzyme assays and other biochemical assays are that only a single protein activity can be assayed per experiment. Both proteomics and protein chemistry involve protein identification but proteomics takes multi-protein systems into consideration and looks at possible interactions within a larger network.

Specific proteins or post translational modifications of proteins related to disease are known as biomarkers. The need for biomarker discovery is important for drug development and the early diagnosis of disease. Biomarkers are becoming more important particularly for the study of progressive diseases such as Alzheimer's disease <sup>[67, 68]</sup>, rheumatoid arthritis <sup>[69]</sup> and cardiovascular disease which are initially asymptomatic <sup>[70]</sup>. Biomarkers for disease are screened for by gauging deviations from normal states in the human body <sup>[71]</sup> allowing for the diagnosis of high-risk individuals early. Some disease processes can first occur in the proteins so they therefore show the most potential as "patient-tailored" drug targets <sup>[72]</sup>.

Frank et al <sup>[73]</sup> and Shishehbor <sup>[74]</sup> report how biomarkers can be employed to quantify and monitor the therapeutic effect of drugs. Tsimikas <sup>[75]</sup> discusses how the studies of oxidation-related molecules are not only helping define atherosclerotic mechanisms but can also be used to improve cardiovascular risk assessment by measurement of the circulating levels of specific oxidant compounds. Oxidation is recognised to be involved in all stages of atherosclerosis from the initiation of fatty streaks in the arteries to the more advanced stage of the disease when the plaque ruptures. Myeloperoxidase (MPO) is an enzyme released by white blood cells during inflammation that will generate oxidants. Products of MPO include: hypochlorous acid, tyrosyl radical and nitrogen dioxide and are mediated through a reaction with hydrogen peroxide contributing to oxidative damage to host lipids and proteins leading to atherosclerosis. MPO levels and the enzyme's oxidative products have been found to be elevated in association with coronary artery disease. Response to treatment with the drug, Atorvastatin which is prescribed to lower blood cholesterol <sup>[76;77]</sup>, stabilizing the atherosclerotic plaque and preventing strokes, can be monitored by determining levels of oxidative products including those from MPO-mediated oxidation. The study <sup>[75]</sup> produced data that suggested statins reduce MPO expression and therefore damage by oxidation providing a method for the observation of the progression and treatment of atherosclerosis.

The search for biomarkers however is challenging as the proteome is varied and complicated by the various extent and variety of post-translational modifications that can occur on an individual protein. The biomarkers indicative of disease found within these complex fluids are usually small in quantity and masked by more abundant proteins such as albumin in the case of human blood plasma, making their detection problematic <sup>[78]</sup>. Pre-fractionation techniques using IgY immunoaffinity spin columns have been used to deplete albumin from plasma but this technique proves problematic as the results are not reproducible <sup>[79]</sup>. Reproducible analytical methods for detecting and quantifying protein biomarkers in their modified and unmodified states are therefore required and examples of these are discussed (1.4.1 and 1.4.2).

### **1.4.1 Stable isotope dilution for the detection and quantification of proteins and or post translational modifications**

Stable isotope dilution LC-MS as briefly discussed in 1.3.2 can be used for the detection and quantification of proteins and post translational modifications. Quantification can be performed when the results are compared with internal standards. Shishehbor et al <sup>[74]</sup> detected and compared levels of NiTyr levels in atherosclerotic patients before and after statin therapy. The study was performed by adding synthetic 3-nitro-<sup>[13C<sub>6</sub>]</sup> tyrosine and <sup>[13C<sub>9</sub> 15N<sub>1</sub>]</sup>tyrosine to plasma protein both as an internal standard and to simultaneously monitor nitrotyrosine, tyrosine, and potential formation of nitrotyrosine during analysis. Patients with coronary artery disease plus peripheral arterial disease were shown to demonstrate an increase in the prevalence of atherosclerosis with increasing levels of nitrotyrosine.

### **1.4.2 Western Blotting**

Western blotting (or immuno-blotting) was introduced by Towbin et al in 1979 <sup>[80;81]</sup> and was developed as a sensitive visualisation assay for the detection of proteins by employing SDS-PAGE and the transfer of the separated proteins from a gel onto an unmodified nitro-cellulose sheet before being probed using antibodies. Western blotting for known biomarkers in a protein sample is an inexpensive conventional method for the detection of post translational modifications such as ClTyr and NiTyr. The technique relies on the specific binding interaction of a protein-antigen allowing the targeted protein of interest to be identified amidst a number of more abundant proteins in a complex sample. Qualitative and semi-quantitative data can be produced for the proteins detected. Target proteins in a complex sample can be detected using western blotting in a number of ways; two of which are discussed here.

#### **1.4.2.1 Indirect detection of a protein or posttranslational modification**

For detection using a primary and secondary antibody the first antibody or “probe” is used to initially identify or recognise the protein of interest. The second antibody is then used to detect and bind to the primary antibody. The secondary antibody to be used depends on either the animal species in which the primary antibody was raised (i.e. if the primary was raised in a mouse monoclonal the secondary must be anti-mouse or from a non-mouse host) or dependant on the tag of that anti body (e.g. biotin). Enzymes are commonly

conjugated to the secondary antibody, the most popular being horseradish peroxidase (HRP), to visualise the protein of interest. A chemiluminescent substrate is employed and the signal is detected by either x-ray film or digital imaging equipment. Using an indirect detection method for the targeting of a protein using a western blot has its advantages and disadvantages. For example, one secondary antibody can be used for the detection of a variety of primary antibodies and although there are additional steps involved leading to a longer protocol, the signal from the antibody-antigen interaction can be amplified by use of the second antibody. The amplification of the signal by the secondary antibody is an invaluable advantage of the technique especially for the detection of very low abundance proteins but use of the secondary antibody can lead to non-specific staining.

Khan et al <sup>[82]</sup> compared the presence of NiTyr in the plasma of healthy non-smoking volunteers and those suffering from the inflammatory disease, systemic sclerosis. During the study they were able to visualise and compare NiTyr levels in plasma from the patients and of the healthy subjects. They found that those suffering from systemic sclerosis possessed higher levels of NiTyr in plasma than present in the healthy controls.

#### **1.4.2.2 Direct detection of a protein or post translational modification**

Direct detection fluorescently tagged antibodies can be used for the identification and visualisation of post translational modifications in systems. Spickett et al <sup>[83]</sup> investigated cysteine oxidation by employing modification-specific fluorescent chromophores to effectively target the modified cysteines. The technique can be utilised to compare two samples which are labelled with two different chromophores before being mixed and run on the same gel. Running the two samples on the same gel removes the variation between gels and also allows both targeted modifications in each sample to be analysed and their abundance compared using differential colour scanning.

Whichever method of the technique is applied, direct or indirect detection, the intensity of the signal will correlate with the abundance of the protein targeted. There are advantages and disadvantages to both techniques. Direct detection with fluorescent tagging is a quicker method requiring fewer steps as a primary antibody is not required. The equipment required for the detection of the

fluorophore-conjugated antibodies, however is more expensive and specialised as the fluorescent signal must be detected and documented and a light source is required for the excitation of the fluorophore. Although fluorophore detection is a more expensive technique, chemical waste is reduced in comparison to other western blot methods.

Although very sensitive the biggest drawback of the western blot technique for the detection of proteins and post translational modifications is that there is no sequence information gained. The presence of the protein or modification can be confirmed but there is not “site-specific” information. When studying the proteome for biomarkers knowing which peptides from which protein that have been modified is important. If the targeted site of modification is known drug therapy can be monitored and new, more site-specific drugs can be developed.

## **1.5 Mass spectrometry for the analysis of the proteome**

The Edman degradation technique has traditionally been employed to sequence peptides <sup>[84]</sup>. Sample quantities required for the technique is between 1-10pmol <sup>[85]</sup> and the automated process employs chemical reagents to remove one amino acid at a time from the terminus of an intact peptide. The amino acid derivative generated is then purified and identified by HPLC and the amino acid was then identified by the retention time in comparison to those of standard amino acids.

The Edman technique can be problematic. Firstly, an amino acids retention time is altered by the presence of a post translational modification which can subsequently lead to the mis-identification of a peptide sequence and secondly the technique is also very time consuming. For the identification of a peptide using HPLC, cycle times are ~30min/amino acid meaning that sequencing a peptide containing 8 amino acids would take 4 hours. The Edman technique is therefore not suitable for biomarker discovery and the investigation of disease as the validation of post translational modifications are of extreme importance <sup>[86]</sup> and due to the time constraints is not suitable for identifying proteins and peptides in very complex samples.

In comparison to the Edman degradation technique, analysis by mass spectrometry is a high-sensitivity, high-throughput technique capable of acquiring both the molecular weight and sequence information of proteins and

peptides. Less sample is required in comparison to the Edman degradation technique and typical sample quantities required for analysis by mass spectrometry are from the low to mid femtomole level <sup>[87]</sup>. Information about the amino acid sequence for peptides can be found through the use of collision aided dissociation (CAD), otherwise known as collision induced dissociation (CID), by tandem mass spectrometers. As well as sequence information, the presence of post translational modifications can also be determined <sup>[88]</sup>. Hybrid mass spectrometers (the quadrupole time-of-flight (QToF) and the quadrupole ion-trap (Qtrap) for example) consist of more than one mass/charge ( $m/z$ ) separation device to allow for tandem mass spectrometry. Tandem mass spectrometry allows for MSMS to be performed which can involve multiple steps of selection by  $m/z$  with some form of fragmentation occurring in between stages. Examples of the various modes of operation for a tandem mass spectrometer are the product ion scan and the precursor ion scan which are discussed further in 1.6.

### **1.5.1 The quadrupole mass filter**

In a quadrupole mass spectrometer the quadrupole mass filter is used to separate molecules by their mass/charge ( $m/z$ ) ratios. The quadrupole mass filter (Figure 10) consists of four parallel rods. The ions are separated based on the stability of their trajectories through the field which is determined by their mass-to-charge ratios ( $m/z$ ). The electric field is created by placing a dc voltage and an rf voltage on the four quadrupole rods. The adjacent rods have opposite polarities. Ions enter the mass analyzer and by increasing the magnitude of the dc and ac voltages stable trajectories are created for ions of increasing  $m/z$ . Mass resolution is dependent on the number of ac cycles and how long the ion spends in the field.

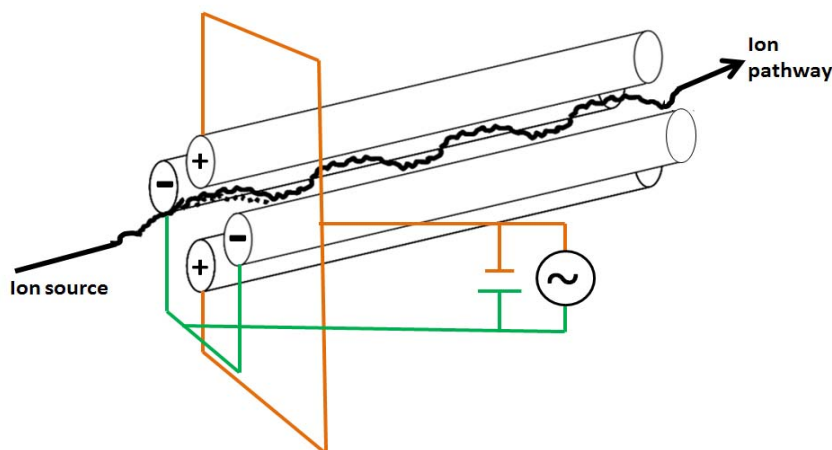


Figure 10: Quadrupole mass filter. The figure illustrates how ions from a source enter the quadrupole mass filter. An electric field is applied to the rods and the ions are separated based on the stability of their trajectories through the field which is determined by their  $m/z$  ratios.

Mass filtering of ions can be seen as a separation process. If quadrupoles are coupled together this will create a powerful approach for the analysis of complex protein mixtures <sup>[88]</sup>. For triple quadrupole mass spectrometers a reaction region such as a collision cell is situated between two quadrupoles. In the collision cell gas pressure is raised to allow multiple low-energy collisions in a short time frame to fragment masses. The main benefit of a quadrupole collision cell is the ability to refocus the ions that become scattered by collision with the neutral gas. The  $m/z$  values of the dissociation or fragment products are then measured in the second mass analyzer, for example, the third quadrupole before being allowed through to the detector. Collision induced dissociation experiments allow the structure or sequence of peptides to be determined by fragmentation of the labile peptide bonds. CID primarily cleaves at the amide bonds generating sequence-specific fragmentation (further discussed in 1.6.4.4).

### 1.5.2 The quadrupole ion trap

Quadrupoles can be used to guide ions from a source to an analyser as an ion guide or as a collision cell when ions are deliberately injected into the quadrupole with sufficient energy leading to the collision with gas and ending in fragmentation. The ions from the source are focussed into the trap by a lens before the quadrupole is converted to an ion trap (known as a 2D trap) <sup>[89]</sup> by applying stopping potentials to the electrodes or electrostatic mirrors at both

the entrance and exit of the quadrupole (Figure 11). The four poles or electrodes of the linear ion trap stabilise the ions in 2D by dc and rf. The four poles (1, 2, 3 and 4 [Figure 12]) have opposing charges ([A]: poles 1 and 3 possess a positive charge, poles 2 and 4 possess a negative charge) and when a positive ion is present it experiences repulsion from the positive electrodes ([B]: 1 and 3) and attraction and therefore acceleration towards the negative electrode ([B]: either 2 or 4). The potentials on the electrodes switch before the positive ion can reach the negative electrodes ([C]) resulting in the trapping of the ion in a quadrupolar electric field.

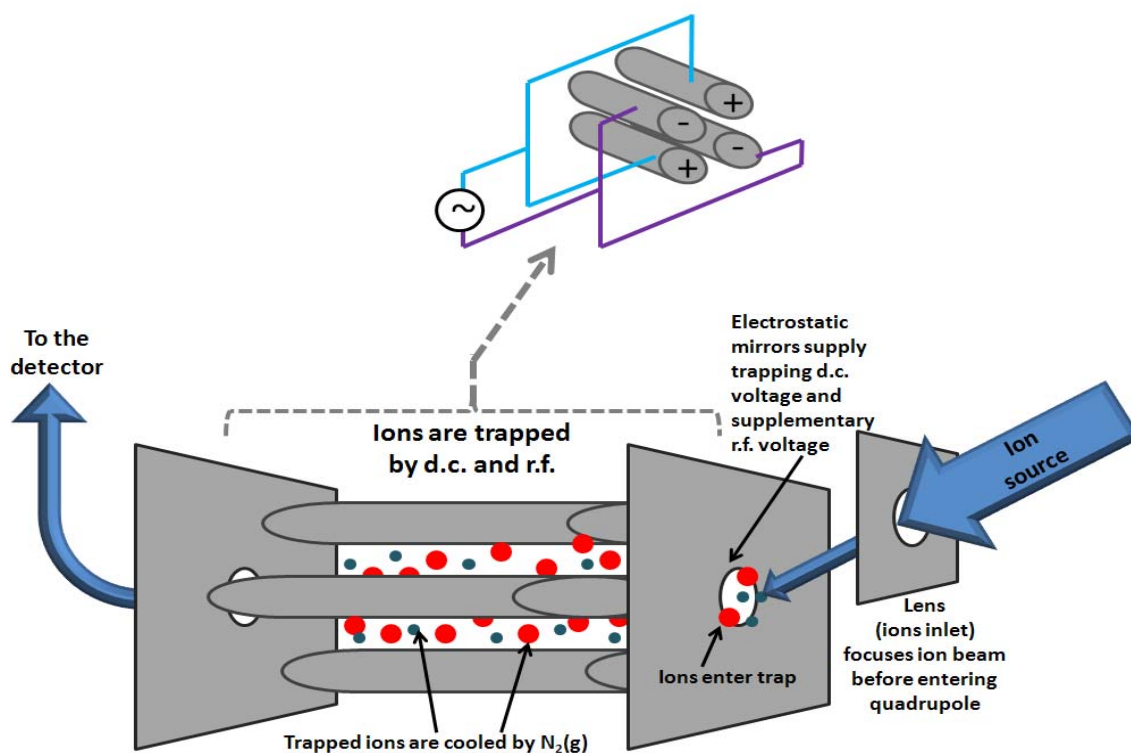


**Figure 11: The quadrupole ion trap.** The figure displays the ion trap. In trap mode ions are stored and selected due to the combined action of a static dc and a rf electric field. Confinement of the ions radially is achieved by the rf fields and axially by the stopping potentials (Figure 12).

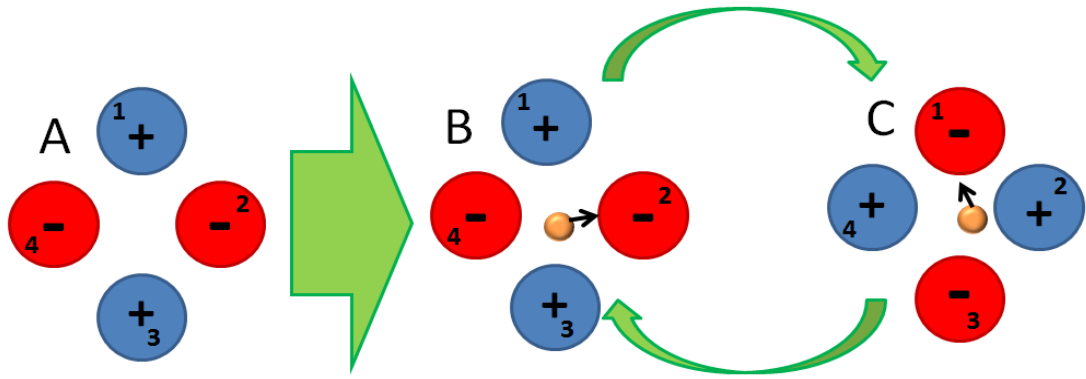


Figure 12: Trapping the ions in a quadrupole. The polarity of the electrodes switch resulting in trapping an ion or ions in a quadrupolar electric field.

In 1989 Wolfgang Paul invented the 3D quadrupole ion trap (Figure 13) which consisted of two hyperbolic electrodes and a ring electrode. This trap is filled with ions by means of a gate voltage which opens allowing ions to enter the trap and then closes when the trap is filled preventing over-filling and space charging effects which will cause disproportionate ion density. Ions are trapped between the electrodes by using rf and dc frequencies producing a 3D quadrupolar electric field. The rf and dc potentials alter to destabilise the ion motions resulting in the ejection of the ions through the exit endcap to the detector. Trapping is enhanced by a gas, often helium, to cool the ions helping to prevent their escape. Ions are ejected by application of an rf voltage to the ends of the trap <sup>[90]</sup>.

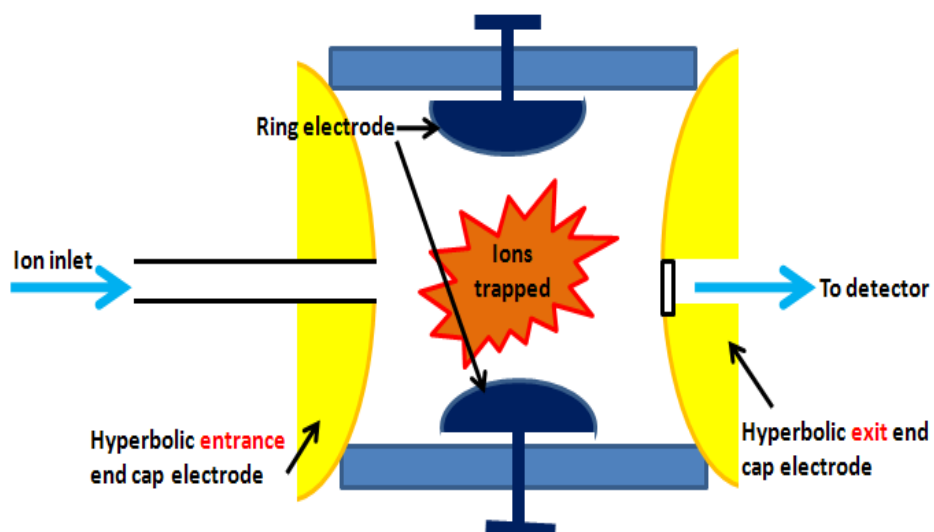


Figure 13: The 3D ion trap invented by Wolfgang Paul consists of two hyperbolic electrodes and a ring electrode. The ions are trapped in a quadrupolar electric field.

### 1.5.3 The Qtrap

The Qtrap (Applied Biosystems) used in this research thesis is a hybrid mass spectrometer and is a 2D ion trap instrument consisting of four quadrupoles ( $Q_0$ ,  $Q_1$ ,  $Q_2$  and  $Q_3$ ) where the second quadrupole ( $Q_1$ ) acts as a mass filter (1.5.1) and the fourth ( $Q_3$ ) will perform in quadrupole mode or trap mode. A collision cell, ( $Q_2$ ), is situated between the second and third quadrupoles (Figure 14).

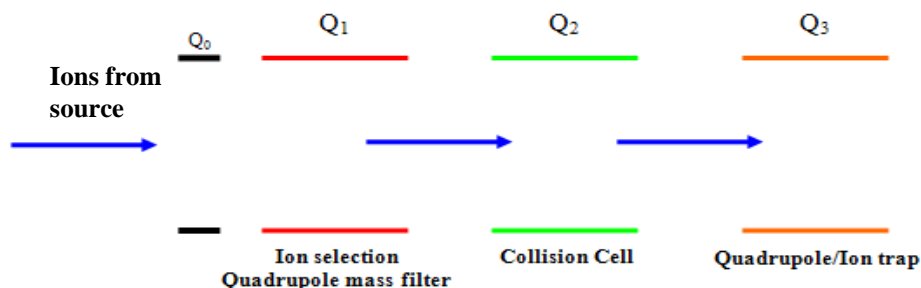


Figure 14: The triple quadrupole mass spectrometer. The above figure shows the schematic internal set up of the Qtrap.

For a conventional MSMS experiment the peptides are in most cases separated of using reverse-phase liquid chromatography (LC) before entry into the mass spectrometer. The reverse-phase LC column is packed with an inert non-polar material typically carbon bonded silica and peptides are loaded onto the column to be eluted with respect to their polarity (the most polar first). The mobile phase which is typically a mixture of water or aqueous solvents and organic solvents washes the peptides from the column resulting in their separation. The length of time a peptide takes to elute off the column is called the retention time. The separated peptides are then ionised before entry into  $Q_1$  where the precursor of interest is selected to be fragmented. The chosen ion or ions are then allowed to enter  $Q_2$  where they are fragmented by the collision gas. The Qtrap fragmented ions are then trapped cooled and scanned in  $Q_3$ .  $Q_0$  is a potential ion trap that is used to increase the sensitivity of the technology, and for focussing the ion beam before the ions reach  $Q_1$ .  $Q_0$  can also trap ions produced in the source while  $Q_3$  is scanning.

### 1.6 The capabilities and modes of operation of the Qtrap

The hybrid mass spectrometer, the Qtrap, can perform various modes of tandem mass spectrometry. The third quadrupole ( $Q_3$ ) can perform multiple stages of fragmentation<sup>[91]</sup> allowing for functions such as product ion (PI), neutral loss

(NL) and precursor ion (PC) scanning while still retaining sensitivity due to the presence of the ion trap <sup>[92,93, 94 95]</sup> (Table 4).

Table 4: Triple quadrupole ion trap MS modes of operation <sup>[94]</sup>.

Mode of operation	Q1	q2	Q3
Q1 Scan	Resolving (Scan)	RF-only	RF-only
Q3 Scan	RF-only	RF-only	Resolving (Scan)
Product Ion Scan (PI)	Resolving (Fixed)	Fragment	Resolving (Scan)
Precursor Ion Scan (PC)	Resolving (Scan)	Fragment	Resolving (Fixed)
Neutral Loss Scan (NL)	Resolving (Scan)	Fragment	Resolving (Scan Offset)
Selected Reaction Monitoring mode (SRM)	Resolving (Fixed)	Fragment	Resolving (Fixed)

Enhanced Q3 Single MS (EMS)	RF-only	No frag	Trap/scan
Enhanced Product Ion (EPI)	Resolving (Fixed)	Fragment	Trap/scan
MS <sup>3</sup>	Resolving (Fixed)	Fragment	Isolation/frag trap/scan
Time delayed fragmentation (TDF)	Resolving (Fixed)	Trap/No frag	Frag/trap/scan
Enhanced Resolution Q3 Single MS (ER)	RF-only	No frag	Trap/scan
Enhanced Multiply Charged (EMC)	RF-only	No frag	Trap/scan

The above displays the various triple quadrupole mass spectrometer modes of operation and the abilities of Q1, q2 and Q3. When in resolving mode the quadrupole will only scan.

### 1.6.1 Q3 quadrupole and trap mode (enhanced MS)

For quadrupole scans, Q1 or Q3 are operated in the rf/dc mode (resonance frequency/direct current). In trap mode an rf potential is applied to the quadrupole. Ions are trapped in Q3 by the radial directed rf voltage and the dc axial operated aperture plates. In Q3 the trapped ions are cooled typically for 10-30ms, and the fill times usually vary in the range of 1-500ms. Trapped ions are mass selectively ejected from the quadrupole trap by fringe fields caused by the lenses at either end. The Q3 can act as a quadrupole or trap and can switch between these modes in milliseconds.

### 1.6.2 Enhanced Resolution (ER) mode

When the linear ion trap (LIT) scan rate is slowed, resolution is increased but sensitivity decreases. The ER scan is usually performed after the enhanced MS mode and before the enhanced product ion scan.

### 1.6.3 Enhanced Product Ion (EPI) mode

The precursor ion is selected in Q1, collision-induced dissociation occurs in the collision cell (q2) and the fragmented ions are trapped in Q3 which is operating in the LIT mode where the quadrupole acts as a trap and ejects ions axially by

mass selection to the detector. In a quadrupole collision cell, ions will undergo many collisions and the resulting fragment ions are reactivated and fragmented further. Product ions are usually too cool to fragment further and so therefore require specific excitation which is completed in  $MS^3$  and  $MS^4$  experiments. Ion traps have low mass cut-offs when fragmentation is performed “in-trap” as it is difficult to excite the parent to be fragmented without exciting the trapped fragment ions <sup>[93]</sup>. When in the enhanced product ion mode, the precursor ion selected in Q1 is fragmented in the quadrupole collision cell q2 and the mass fragments are used to obtain a complete collision-induced dissociation (CID) spectrum down to  $m/z$  50.

#### **1.6.4 The ionisation and fragmentation of peptides in a mass spectrometer**

To identify proteins in a sample or post translational modifications on a protein, the sample is usually enzymatically digested by a sequence-specific protease. The protease trypsin which cleaves at amino acids; arginine and lysine except after proline, is a popular choice. The reason for protein digestion and the analysis of peptides and not intact proteins is that proteins can be challenging; they can be insoluble and the use of detergents will interfere and affect MS due to their high ionisation efficiencies <sup>[96]</sup>.

##### **1.6.4.1 Electrospray Ionisation**

Protein digest samples are commonly separated on a chromatography column before being introduced into the mass spectrometer by electrospray ionisation (ESI) <sup>[97]</sup>. The development of ESI began in 1914 when Zeleny et al <sup>[98]</sup> reported that a liquid could be dispersed from the end of a capillary by applying a high electrical potential across its exit. Dole and Fenn <sup>[99-101]</sup> then went on to report that ESI could be used as an ionisation method for large biological molecules and polymers.

Gaseous ionised molecules are produced from solution by the generation of a fine spray of droplets in the presence of a strong electric field (Figure 15). The droplets are driven by the electric field toward the mass spectrometer. The charge density increases towards the Rayleigh limit until the Coulomb repulsion becomes of the same order as the surface tension. The resulting instability or “coulomb explosion” disperses the droplet; generating charged smaller progeny droplets that also go onto evaporate and perpetuate the process. The process

continues until the resulting droplet becomes so small in size that the electric field, due to the surface charge density, is strong enough to desorb ions from the droplet (the charge from the droplets surface is removed onto the peptide or biomolecule). The charged peptides then go on into the mass spectrometer for analysis <sup>[97]</sup>.

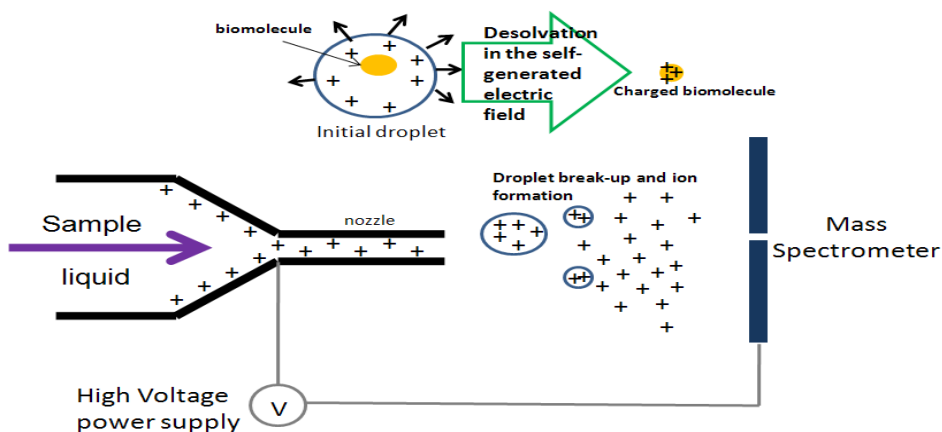


Figure 15: Electro spray ionisation into a mass spectrometer. The above figure illustrates the electro spray ionisation of biomolecules in a solution.

#### 1.6.4.2 The Rayleigh Limit - the stability of a charged droplet

During electro spray ionisation, the charge density of a droplet arrives at a threshold where the repulsive electrostatic force equals or surpasses the cohesive force due to surface tension, the droplet will become unstable.

Rayleigh <sup>[102]</sup> reported the earliest analysis on the stability of a charged droplet. His analysis showed that a macroscopic, incompressible droplet of an inviscid and perfectly conducting liquid, will become unstable when a critical value (or charge limit) is reached. The critical value is given by Equation 3

$$\text{Equation 3} \quad q_R = 8\pi\sqrt{\epsilon_0\gamma\alpha^3} \quad [102]$$

Where  $\epsilon_0$  is the variable permittivity constant,  $\gamma$  is the surface tension of the droplet and  $\alpha$  is the droplet radius. At the critical value (i.e.  $q \geq q_R$ ) the disturbances due to the change in shape lead to the fission of the droplet.

#### 1.6.4.3 Nanoelectrospray Ionisation - comparison in droplet size

The nanoelectrospray source (nanoES) is different from conventional electro spray sources <sup>[103]</sup>. It is miniaturised, runs at a lower flow rate and

generates smaller sized droplets. Juraschek et al <sup>[104]</sup> investigated the difference between electrospray ionisation and ionisation from a miniaturised nanoES source. Both the electrospray source and nanoES generate droplet sizes in the  $\mu\text{m}$  range for ion spray but the nanoES produces droplets thought to be one order of magnitude smaller. In the context of the “un-even fission” model (the Rayleigh critical charge limit), nanospray would enter one fission generation later due to the smaller size of the droplets. The smaller droplets would also mean that the initial charge density of the droplets is higher which results in earlier fissions without extensive evaporation leading to the increase in sample concentration. Another benefit that nanoES provides is the ability to run at very low flow rates ( $\sim 200\text{nL}/\text{min}$ ) therefore increasing sensitivity and limit of detection. Abian et al <sup>[105]</sup> investigated and compared flow rates and confirmed that lower flow rates (comparing  $100\mu\text{L}/\text{min}$  and  $0.5\mu\text{L}/\text{min}$ ) increased the sensitivity (from  $50\text{fmol}$  to  $1.5\text{fmol}$  respectively).

#### 1.6.4.4 Collision induced dissociation (CID)

The fragmentation of peptides by CID (or collisionally activated dissociation, CAD) in the collisional cell occurs by the peptide first becoming multiply charged by ionization. A proton will then migrate along the peptide backbone, pausing at the peptide bonds  $-\text{NH}-\text{CO}-$ . The charged peptide then collides with the gas in the collision cell and fragmentation occurs at the peptide bond due to the increased labiality by the presence of the extra proton (Figure 16).

Multiple collisions of the peptide with the inert gas ions lead to the rapid vibrational re-distribution of the internal energy causing a “heating” of the precursor ions. When the internal fragmentation energy reaches a threshold, the weakest bonds are cleaved preferentially <sup>[106]</sup>. There is one bond fragmentation for every one of an approximate 500 precursors and an average of these fragmentations is the mass spectrum. Depending on which terminus (N or C) the protein fragments from determines if it will form part of the *y* or *b-ion* series (Figure 17). At low energy CID conditions *b-ions*, *y-ions* and neutral losses of water and ammonia dominate the mass spectrum. There are other methods of dissociation for example, photo dissociation and electron transfer dissociation (ETD). Gas phase CID dissociation is the most widely used method of dissociation in commercial tandem mass spectrometers <sup>[107]</sup>.

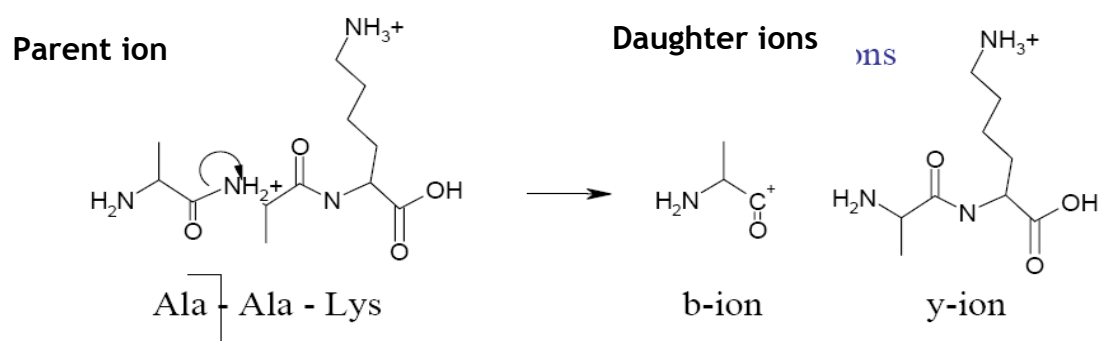


Figure 16: Collision induced fragmentation. The figure displays the migration of the proton down the peptide backbone. Fragmentation is then caused by collision with inert gas to produce two daughter ions.

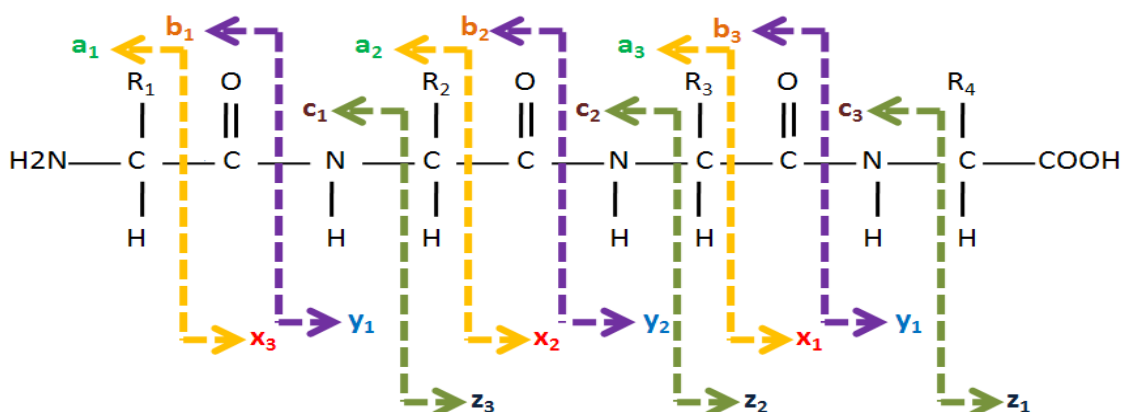


Figure 17: Various fragmentation patterns of a peptide. The above figure illustrates the fragmentation pattern of *a*-, *x*-, *b*-, *y*-, *c*- and *z*-ions.

## 1.6.5 Alternative dissociation methods

### 1.6.5.1 Electron transfer dissociation

Electron transfer dissociation (ETD) provides an alternative fragmentation pattern. Fragmentation by ETD rather than CID can preserve more labile modifications such as phosphorylation, methylation and glycosylation.

Sobott et al <sup>[106]</sup> demonstrated the preservation of the ubiquitination modification on proteins using ETD. The ubiquitination modification is unstable due to the iso peptide bond linkage between the C-terminal glycine and the N( $\epsilon$ ) lysyl chain. The alternative fragmentation ETD method was found to allow for

the detection of gly-gly-modified lysyl sidechains on DNA polymerase B1 that were not easily observed using CID.

ETD fragments peptides using ion/ion chemistry<sup>[108;109]</sup>. ETD fragments peptides by transferring an electron from a radical anion to a protonated peptide, inducing fragmentation of the peptide backbone by causing cleavage of the C $\alpha$ -N bond. This generates a series of *c* and *z*-ions instead of the *b* and *y*-ions observed after CID (see Figure 17).

### 1.6.5.2 Photo dissociation

Thompson et al<sup>[110]</sup> report fragmentation of peptides using a 157nm light excitation to induce backbone cleavage in singly protonated peptide ions. Peptides and or proteins are protonated by atmospheric ion sources. Photo dissociation with 157nm light will generate *x*-, *v*- and *w*-type fragments. The *x*-ion corresponds to the cleavage of the backbone bond between the  $\alpha$ -carbon and the carbonyl carbon with the charge remaining on the C-terminal fragment (Figure 17). The *v*-ions are high energy C-terminal fragments that have completely lost an adjacent amino acid side chain. Certain amino acids produce *w*-ions from partial, incomplete side-chain loss with the cleavage occurring between the  $\beta$  and  $\gamma$  carbon atoms. The *w*-ions are commonly observed at leucine (molecular weight = 131Da) residues rendering them distinguishable from isoleucine (molecular weight = 131Da) amino acids (Figure 18).

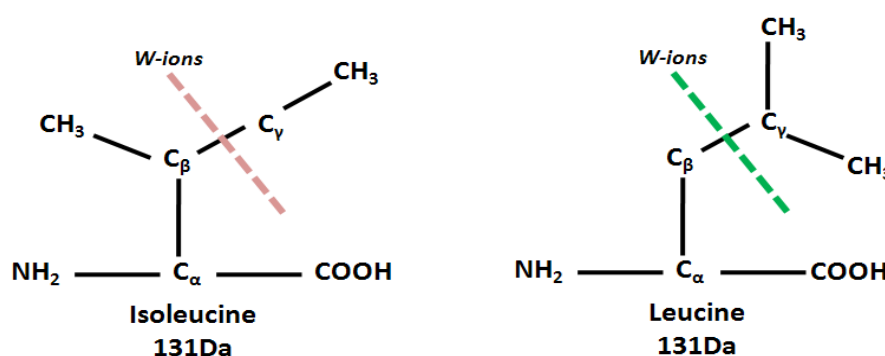


Figure 18: The *w*-ions. Partial, incomplete side-chain loss cleaving between  $\beta$  the  $\gamma$  and carbons allow for the distinguishing between leucine and isoleucine.

Thompson et al demonstrated a number of peptides dissociated by photo dissociation illustrating that the spectrum is indeed dominated by *x*-, *v*- and *w*-type fragments. Light is not affected by electric or magnetic fields so photo

fragmentation of singly and multiply protonated peptides and protein ions should be compatible with various mass analyzers.

### 1.6.5.3 Surface induced dissociation (SID)

Surface induced dissociation (SID) is used to activate ions stored in a quadrupole ion trap mass spectrometer. A short ( $<5\mu\text{s}$ ), fast rising ( $<20\text{ns}$  rise time), high voltage (dc) current pulse is applied to the ends of the quadrupole ion trap. This is comparable to the CID method of fragmentation where an alternating (ac) current is used to excite and dissociate ions. The effect of the dc pulse causes the ions to become unstable in the radial direction and consequently collide with the ring electrode in the 3D Paul trap. During SID a significant amount of precursor ion translational energy is converted into internal energy causing fragmentation. This fragmentation is high energy and the resulting fragments are then scanned out of the ion trap using the conventional mass-selective instability scan mode<sup>[111;112]</sup>. The higher energy is explained by the effective mass of the surface compared to the effective mass of the CID gas. The high energy collisions associated with SID make it possible for very large molecules to be dissociated. SID also has the potential advantage of improved ion collection in comparison to CID where multiple collisions may cause scattering of the ion beam. The internal energy distributions show the SID method of fragmentation to be narrower than the sum of multiple collisions during CID. In conclusion, SID can dissociate precursors of higher  $m/z$  in comparison to CID but their product ion spectrums are similar in resolution. The mass spectrum for SID fragmentation is dominated by *a-*, *b-* and *y-ions* (see Figure 17) although there were a greater ratio of *a-* to *b-ions* and an enhancement in immonium ions in SID than the CID<sup>[113]</sup>.

## 1.7 Sensitive and selective triple quadrupole mass spectrometry methods for the discovery of post translational modifications

Mass spectrometry has become the method of choice for the analysis of complex protein samples<sup>[114]</sup>. Compared to Time-of-flight (TOF) mass spectrometers, LITs are higher in sensitivity although lower in resolution meaning that co-eluting peptides with similar  $m/z$  ratio's will frequently overlap preventing accurate mass analysis and charge state determination<sup>[115]</sup>.

The mass spectrum of an unknown protein digested with a specific enzyme will produce a specific series of specific peptides. This series of peptides is the

protein's peptide-mass 'fingerprint'. This information alone can be used to identify the protein in question. By obtaining these fingerprints by digestion and screening against a database of known proteins, post-translational modifications can be characterised <sup>[116]</sup>.

### 1.7.1 The precursor scan

A sensitive and selective technique for the discovery and detection of modification sites in complex protein samples which has been used in many studies is the precursor scan<sup>[94;117-121]</sup>. The precursor scan (discussed in more detail in Chapter 2) can be performed on tandem mass spectrometers where the second analyzer is set or fixed to detect a reporter ion while the first mass analyzer scans through the mass range <sup>[122]</sup>. Only peptides or "precursors" that fragment to generate or give the reporter ion are registered in the final mass spectrum. This allows modified peptides to be identified when in very low abundance or in an excess of background ions. Precursor scanning has been a popular method to detect and identify post translational modifications for example the phosphorylation modification sites in protein kinases <sup>[123]</sup>.

Phosphorylation is the addition of a phosphate ( $\text{PO}_4$ ) group onto a protein which can activate or deactivate enzymes leading to the initiation or prevention of diseases such as cancer and diabetes. Reversible phosphorylation is an important regulatory mechanism involving kinases (phosphorylation) and phosphatases (dephosphorylation) <sup>[124;125]</sup>. Williamson et al, applied a precursor scan for  $m/z$  - 79 (due to loss of  $\text{PO}_3^-$ ) in the negative ion mode, followed by an enhanced resolution and enhanced product ion scan in positive mode to effectively identify phosphorylation sites in low abundance (femtomole level) proteins. Another way of detecting the phosphorylation modification is to perform a precursor ion scan using the immonium ion of the phosphotyrosine, 216.043 $m/z$ , in positive ion mode. The benefits of using the 216.043 $m/z$  immonium ion as the "reporter" instead of the -79 $m/z$   $\text{PO}_3^-$ , is that the precursor ion scan can be performed in positive mode making the need for polarity switching or the changing of the pH of the spraying solvent redundant <sup>[122;126]</sup>. By applying the triple quadrupole precursor and neutral loss scan mode, free phosphopeptides were detected in biological fluids, serum, saliva and urine showing high sensitivity and selectivity even in low concentrations <sup>[127]</sup>. Cirulli et al, used the precursor -79 $m/z$  for the  $\text{PO}_3^-$  <sup>[128-131]</sup>, and the constant neutral loss scan was offset by the 49Da

corresponding to the loss of neutral phosphoric acid from doubly charged peptides.

The precursor scan is a selective scan and can be used to detect post-translational modifications where there is no previous knowledge of the modification sites.

### 1.7.2 The neutral loss scan

Post translational ion signatures (specific as an indicator of modification) are monitored during mass spectrometry and neutral loss has been used to detect phosphorylation events in proteins <sup>[132]</sup>. Protein phosphorylation modifications are detected by mass shifts in fragment ions. Neutral loss detection is the measured loss of a neutral species yielding a product with a lowered mass. For example a -98Da mass loss from a peptide is from the cleavage of the phosphoester bond and the loss of H<sub>3</sub>PO<sub>4</sub>.

In tandem mass spectrometers for a neutral loss scan both the first and second mass analysers are set to scan simultaneously but with a mass offset <sup>[133]</sup>. In respect to the detection of phosphorylation the mass offset would be -98Da. The first mass analyser scans all masses and the second mass analyser scans but is offset by the mass loss commonly seen for the modification. In the neutral loss scan all precursors that undergo the loss of a specified common neutral mass are monitored. As with the precursor scan the neutral loss scan is a sensitive and selective method for the detection of post translational modifications, requiring no prior information, in a complex mixture <sup>[134]</sup>.

### 1.7.3 Multiple reaction monitoring

The mass-spectrometry based methods, precursor scanning and neutral loss scanning are sensitive and selective methods used to detect post translational modifications but they do not take advantage of any prior knowledge known about the protein being studied. Prior knowledge may include the primary sequence of the protein and the potential modification sites. This information can be used and then applied for the detection of post translational modifications. The precursor ion and fragment m/z values resulting from CID can be predicted for a multiple reaction monitoring (MRM) experiment <sup>[135]</sup>. The MRM technique has been used to quantify and monitor the progression of drug therapy

[136] and disease [137-142] (further discussed in Chapter 3). I am interested in oxidative stress and there have been studies measuring the oxidative stress parameters in biological samples e.g. blood, serum and urine etc using MRM methods [138]. In a review Winnik et al [138] discusses the oxidative stress parameters isoprostanes, thiol markers, 8-OHdG (8-hydroxydeoxyguanosine) and the oxidation products of aromatic side chains. Isoprostanes can be detected using a malondialdehyde-based thiobarbituric (TBARS) acid reacting substance for a quantitative, spectrophotometric assay. Morrow et al [143] has also employed a gas chromatography mass spectrometry method to quantify isoprostanes. Isoprostanes are used as a biomarker for oxidative stress as they are related to the peroxidation of lipids. The TBARS assay has been used before but, as discussed by Winnik, can lack specificity and lead to false positives. Thiol markers indicating the reduced and oxidized levels of antioxidant glutathione (GSH, a tripeptide consisting of the linking between the amine group of cysteine and the carboxyl group of the glutamate side chain) can be detected using LC-MSMS and SIM (selective ion monitoring). The 8-OHdG product is an oxidised product of the DNA nucleoside or base, guanine. Upon DNA repair this molecule will be excreted in the urine as a waste product. Detection of 8-OHdG can be performed using LC-MSMS or antibody-based methods but can be problematic due to the oxidation of guanine during sample preparation. The presence of oxidized aromatic side chains (NiTyr and ClTyr for example) are usually detected by isotope dilution LC-MSMS.

The MRM experiment (commonly referred to as a selective ion monitoring (SIM)) focuses the specific precursor ions and fragment ions that have been targeted for. Although the precursor and neutral loss scans are sensitive by taking full advantage of any biological knowledge surrounding the protein of interest even higher sensitivity can be achieved. This targeted approach is suited for the investigation and quantification of a specific protein or post translational modification in a complex sample.

#### **1.7.3.1 MIDAS (monitoring-initiated detection and sequence) software to design an MRM assay**

The MIDAS workflow designer software is used to automatically build an MRM assay. MIDAS can be used to detect and target for post translational modifications such as phosphorylation [144;145]. Mollah et al [146] applied the MIDAS

workflow to design a MRM assay to target and detect ubiquitination sites the substrate protein and receptor interacting protein. The information required for the MIDAS designer workflow is the sequence of the protein that is to be targeted, the enzyme employed and the variable post translational modification; in this case, ubiquitin. For each peptide generated by the *in silico* digestion an MRM transition is produced whereby both the precursor and fragment ion are to be monitored during the assay. The MIDAS program will typically produce two charge states for two fragment ions per peptide (precursor) for confirmation. Ions from the first quadrupole were accelerated into the collision cell where they undergo collision-activated dissociation (CAD) and the resultant fragments accelerated to the third quadrupole which is scanned for the selected, targeted fragment ions. A signal is detected when the selected precursor in the first quadrupole generates the targeted fragment ion in the third quadrupole. When an MRM has been detected the third quadrupole can switch to linear ion trap mode to obtain MSMS verification for the precursor-fragment ion pair.

## **1.8 Search engines and databases to analyse mass spectrum data**

Mass spectrum data is produced during a proteomic study. These spectrum can be analysed manually or by using a search engine to match the spectra to sequence information contained in proteomic databases <sup>[147;148]</sup>.

Using MSMS data and database searching has become a valuable technology for rapidly analysing, detecting and identifying proteins and their post translational modifications. Protein databases (MSDB, NCBIInr, Swissprot for example) are created by in-silico digestions of the proteins contained in them. Post translational modifications can be added to these databases by adding the complete set of in-silico modified fragments to each protein for each incorporated post translational modification. The search engine Mascot is probability based and is a commonly used tool to correlate tandem MS data (resulting peak list) with the peptides in a database. Identification of proteins using Mascot is based on the characteristic amino acid sequence of the peptides, although partial information of the amino acid sequence of a protein can still be used to search for and identify the protein <sup>[149]</sup>.

A possible method of identification is to sequence the MSMS spectrum by *de novo* sequencing (predictions are made using only a computational model without comparison to existing data) to give a complete sequence of the peptide and the presence and location of any existing post translational modifications. The peptide sequence is then searched against a protein database to identify the protein. Another possible method of identification is to use software algorithms to directly match the MSMS data collected experimentally with theoretical MSMS data generated from a peptide in a protein database. Mascot uses a scoring algorithm to provide a probability-based model for peptide identification. Brent Weatherly et al <sup>[150]</sup> describes a proteomic study using LC MSMS and Mascot. Proteins are first extracted from biological material followed by an enzymatic digestion to produce peptides. The next stage is to separate the peptides by liquid chromatography before MSMS analysis. To correlate an MSMS spectrum to a peptide and therefore the protein it originated from the MSMS data is submitted to Mascot in the form of peak lists. The lists consist of centroided mass values and their intensity, the peaks detected and their retention time. Multiple spectra from one peptide can therefore be summed together and spectra from the chromatographic baseline can be discarded <sup>[151]</sup>. The peptide masses detected experimentally are first compared with the theoretical peptide masses generated from *in silico* enzymatic digestions of proteins in the database. Theoretical peptides with similar masses (a mass tolerance is set by the user) are fragmented *in silico* following specific cleavage rules and these theoretical fragment ion masses are compared with the fragment ion masses collected experimentally. Search engines match theoretical peptide sequences to experimental MSMS data but not every match is statistically significant. The protein score in the Peptide Summary is derived from the ion scores and reports protein hits in a logical order. Peptide matches are grouped to protein hits. Red and bold text is used to highlight the most logical assignments of peptides to proteins. When a peptide is reported in a bold text or typeface it means it is the first time this peptide has been matched to a query and when shown in red it means that that peptide is the top ranking peptide match. Peptides with protein hits reported in a bold, red typeface are therefore the statistically most likely assignments (reference [www.matrixscience.com](http://www.matrixscience.com)).

To combat any confusion the search algorithms score each match indicating how close the relationship between the experimental and the theoretical MSMS

spectra are. The scoring algorithms are probability based reflecting the probability of a match being random.

### **1.8.1 The MOWSE (molecular weight search) algorithm**

The Mascot probability model is based on the MOWSE (molecular weight search) algorithm. Pearson et al <sup>[152]</sup> reports that the performance of algorithms for the identification of proteins based on MS data should be judged on sensitivity i.e. the ability to make a correct identification using weak or noisy data and selectivity; the ability to calculate low-ranking scores for false, random matches. The MOWSE algorithm was generated from a composite protein sequence database comprising of calculated molecular weights of all peptide fragments derived from a specific enzyme or by reagent cleavage rules. Scoring algorithms were developed from the observed distribution of the frequency of peptides in the source database.

Distribution is dependent on the protein's size (number of amino acids in the primary sequence) smaller proteins generally yield fewer peptide fragments. Pappin et al <sup>[153]</sup> reported that for all proteins 30kDa and above, 1 in 8 or 13% of peptide fragments were required to be generated by MSMS before the protein could be identified. The experimentally derived peptide masses were screened against a peptide fragment database derived from approximately 50,000 proteins. For proteins 40kDa and above fewer than 1 in 10 or 10% of peptide fragments were required for protein identification.

Mascot reports an ion score for each peptide-match indicating the statistical significance of the MSMS assignment. Peptides and their ion score are grouped according to their protein of origin and the protein is then assigned a cumulative protein score (a total of all the peptides identified and their ion scores). Generally a protein will be reported if one peptide from that protein is matched at or above the threshold ion score. If a number of proteins are assigned present in a sample Mascot will report them ranked in order of their protein scores.

#### **1.8.1.1 Peptide identification from a database**

To identify peptides from a protein database MOWSE does not just count the number of matching peptides but empirically determines factors to assign a statistical weight for each peptide match. The matrix of weighting factors is

calculated during the database build stage. A frequency factor matrix,  $F$ , is created in which each row represents an interval of 100Da in peptide mass and each column an interval of 10Da in intact protein match. The appropriate matrix elements are incremented to accumulate statistics on the size distribution of peptide masses as a function of protein mass as each sequence entry is processed. After searching experimental mass values against a database the ion score for each entry is calculated according to the Equation 4;

$$\text{Equation 4} \quad \text{Score} = 50,000 / (M_{\text{prot}} \times \prod_n m_{i,j}) \quad [65;153]$$

The score is normalised for 50kDa where  $M_{\text{prot}}$  is the mass of the intact protein,  $n$  is the number of matched peptides and  $m_{i,j}$  is the matrix elements.

### 1.8.1.2 Significance level of a peptide match

The significance level is the commonly accepted threshold that an event is significant if it would be expected to occur at random with a frequency of less than 5% (for example, scores greater than 67 are significant ( $p < 0.05$ )).

Significance is a function of data quality so if a peptide is a *significant* match it may not always be the *best* match.

## 1.9 Conclusions

There is a need for biomarkers to diagnose and determine the progression of disease. This is especially important for the development of atherosclerosis where the early stages of the disease are asymptomatic. Tandem mass spectrometers have been continually used for the high throughput identification of post translational modifications and therefore could be useful for detecting and identifying biomarkers.

### 1.10 Aims

Hybrid mass spectrometry instruments are optimal for the high-throughput analysis of protein samples. In my study to identify and detect cardiovascular biomarkers I have chosen to use the triple quadrupole linear ion trap mass spectrometer, the Qtrap 2000 (*Applied Biosystems*, Warrington, UK). The triple quadrupole linear ion trap is superior for biomarker analysis due to its sensitivity and selectivity owing to its ability to perform precursor scans and targeted MRM scans. I hypothesise that it is possible to classify diseased samples from those

from healthy individuals by the presence of oxidatively modified peptides. I will focus on the post translational modifications chloro- and nitrotyrosine as these are specific and stable biomarkers for cardiovascular disease as previously discussed.

- My primary aim is to successfully modify purified proteins and native LDL *in vitro* and detect ClTyr and NiTyr modifications in these samples.
- Analysis of *in vitro* modified purified proteins and LDL will be performed on a high-throughput hybrid MS.
- Modes of operation used and compared will be a conventional MSMS experiment, precursor ion scans and multiple reaction monitoring experiments.
- Sensitive methods for the detection of NiTyr and ClTyr biomarkers for cardiovascular disease will be developed by the analysis of the modified purified proteins before being applied to clinical samples.
- Mascot will be employed to search the mass spectrometry data produced to assign and verify protein and post translational modifications. As discussed in the Introduction there is sometimes a need for manual confirmation of these results so a targeted MSMS experiment will also be performed.

UNIVERSITY OF GLASGOW

# Chapter 2

---

Precursor scanning for the sensitive and selective detection of chlorotyrosine modified peptides in a 9-protein mix

## **2 Chapter – Precursor scanning for the sensitive and selective detection of chlorotyrosine modified peptides in a 9-protein mix**

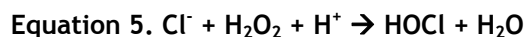
### **2.1 The chlorotyrosine modification**

In response to inflammation, stimulated neutrophils release the heme enzyme myeloperoxidase (MPO) <sup>[154]</sup> which is the only human enzyme known to generate hypochlorous acid, HOCl <sup>[155]</sup>. Hypochlorous acid (HOCl) is a highly reactive species and will oxidise many biological targets including proteins and lipids <sup>[156]</sup>. Examples of biological chlorination reactions within the body are the reaction with amine groups giving chloramines <sup>[156;157]</sup>, the reaction with tyrosyl residues giving chlorotyrosine products <sup>[156;158]</sup> and the reaction with unsaturated lipids and cholesterol to give chlorohydrins <sup>[159]</sup>.

Levels of 3-chlorotyrosine have been found to be elevated in human atherosclerotic tissue obtained during surgery and in LDL isolated from vascular lesions <sup>[155]</sup>. An increased level of LDL is thought to be a major risk factor in the development of atherosclerosis and evidence suggests that LDL must be oxidised to trigger these pathological events which leads to the development of the disease. Myeloperoxidase (MPO) employs hydrogen peroxidase (H<sub>2</sub>O<sub>2</sub>) generated by activated microbial oxidants which triggers the modification of LDL by oxidation. Most oxidation products generated by HOCl are non-specific or unstable but the post translational ClTyr is not (as discussed in 1.3.3) <sup>[14;56;160]</sup>. When tyrosine reacts with a HO<sup>•</sup> radical DOPA (dihydroxyphenylalanine) is produced but is susceptible to further oxidations. DOPA is a reducing agent, becoming further oxidised itself and is also naturally occurring and therefore not a stable or specific biomarker. The formation of N-Formylkynurenine by oxidation of a tryptophan side chain is stable but also not specific as this product can be generated enzymatically and not specifically by MPO. The generation of methionine sulfoxide by oxidative damage to the methionine side chain by a HO<sup>•</sup> can be enzymatically reduced and the products levels therefore may be misleading.

As discussed (in 1.3.3) there are many substrates or sites for oxidation; we focus mainly on chlorotyrosine as it is a stable and specific biomarker. ClTyr is not naturally occurring, acid stable, not susceptible to further oxidation and is specific to the activity of MPO so is the favoured biomarker to indicate for oxidative stress <sup>[62]</sup>.

The following equation (equation 5) explains the generation of HOCl by the catalysis of MPO;



Here I aim to design a precursor scan mass spectrometry method for the detection of ClTyr modification in a model sample (9 protein mix - see 2.4).

## **2.2 The Qtrap and the various scanning techniques and their uses**

The Qtrap™ (*Applied Biosystems*, Warrington, UK) combines the capabilities of a triple quadrupole mass spectrometer and ion trap technology on a single platform. Triple quadrupole instruments are referred to as “tandem-in-space” devices allowing for each stage of an MSMS experiment to be performed at a spatially distinct location in the instrument <sup>[119]</sup>. Triple quadrupoles have two selective MSMS scans; the precursor ion scan and the constant neutral loss scan (that are ideal for the detection and identification of analytes in complex samples). Triple quadrupole instruments are capable of performing scans where both Q1 and Q3 can be simultaneously scanned in unison or fixed to scan for a specific mass which is unique to this design of instrument (Figure 19). Although this means that the duty cycles are low the scans are extremely selective therefore increasing resolution making the triple quadrupole ideal for the analysis of posttranslational modifications of proteins <sup>[161]</sup>.

Product ion scanning is used with a purpose to collect a fragment ion spectrum for the identification of the amino acid sequence of specific peptides. The first analyzer (MS1) is set to select one precursor ion at a time. The chosen precursor is fragmented by CID (collision induced dissociation) in the collision cell and the resulting fragments are analyzed by the second analyzer (MS2). In this scan the

MS2, or Q3 (quadrupole 3) is in quadrupole mode. This process is repeated for different precursors.

The precursor scan has been used as a sensitive and selective technique to identify and detect many posttranslational modifications in different studies<sup>[94;117-120;162;163]</sup> and is performed by setting or fixing the second mass analyzer (MS2) to scan for a specific mass (Q3 in trap mode) to transmit only one specific fragment ion to the detector. The first mass analyzer (MS1) scans to detect all precursor ions that generate the set  $m/z$  of the fragment which MS2 is fixed for (MS2 or Q3 switches to quadrupole mode). This method is usually used to detect for a known functional group or modification on an amino acid. Neutral loss scanning is where both analyzers (MS1 and MS2) scan in a synchronized manner so that the mass difference passing through MS1 and MS2 remains constant. In this scan both MS1 and MS2 (Q1 and Q3 are in quadrupole mode). The mass difference between ions corresponds to a neutral fragment that is lost from the peptide in the collisions cell (by CID).

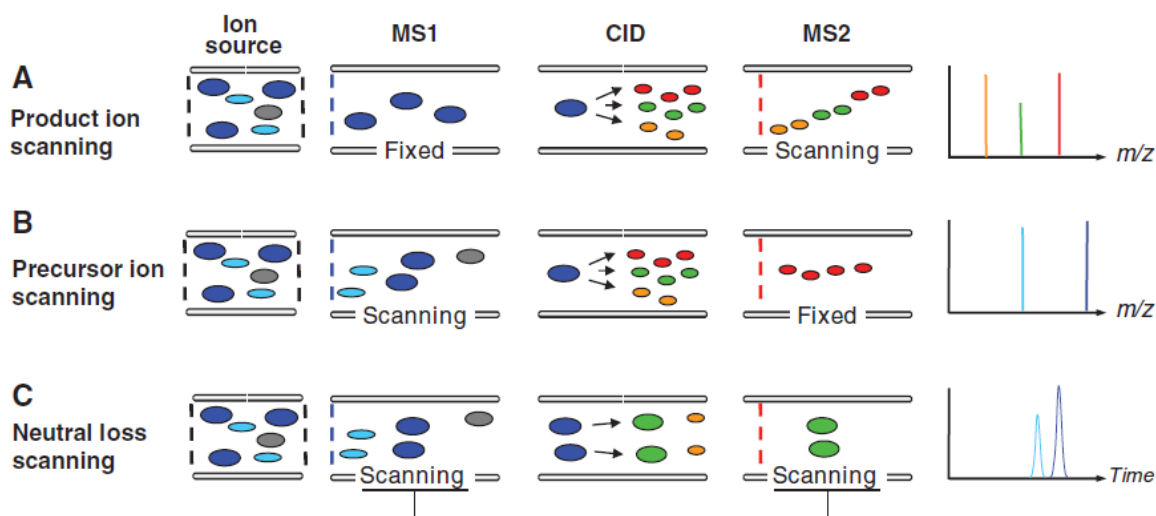


Figure 19: Various types of tandem MS experiments <sup>[161]</sup>. The figure illustrates various mass spectrometry experiments. “A” is product ion scanning, “B” is precursor ion scanning and “C” is the neutral loss scanning experiments.

### 2.2.1 Conventional ion-traps and the QTrap

The conventional ion-trap mass spectrometers perform MSMS experiments in a “tandem-in-time” fashion rather than a “tandem-in-space” manner meaning that once the ions are introduced into the ion trap the numerous steps of ion manipulation are performed in the same volume but at different times <sup>[119]</sup>. This

“tandem-in-time” is advantageous as a complete mass spectrum can be collected during each pulse of ions introduced into the ion trap. However, although the “tandem-in-time” conventional ion-traps lead to faster duty cycles and increased scanning sensitivity in relation to triple quadrupoles and the “tandem-in-space” method, very selective precursor ion scans and constant neutral loss scans are not possible <sup>[164]</sup>.

## 2.3 Aims

Here I use the Qtrap 2000 (*Applied Biosystems*, Warrington, UK) precursor scan to detect chlorotyrosine modifications in varying concentrations of HOCl modified 9-protein mixes as a model sample.

## 2.4 Materials and Methods

### 2.4.1.1 The 9 Protein Mix (9PM)

The 9 protein mix was modified using varying concentrations of HOCl (from Sigma Aldrich) in Tris Buffer (pH7, 50mM concentration) at 37°C for 4hours. The modified 9 protein mix was then dried down using the centrifugal evaporator (Eppendorf concentrator 5301) before being trypsin digested.

To generate the 9 protein mix, 10mg/ml solutions were made up of each of the proteins (from Sigma Aldrich) in Eppendorf tubes, then aliquots of each were added in the following volumes to a fresh 1.5ml Eppendorf:

1. BSA (300µl)
2. Cytochrome C (50.5µl)
3. Carbonic Anhydrase (125µl)
4. Alpha Casein (106µl)
5. Alpha Lactalbumin (70µl)
6. Myoglobin (73µl)
7. Ovalbumin (184.5µl)
8. Beta Lactoglobulin (85.5µl)
9. Lysozyme (70µl)

The above gives a total concentration of 41pmoles/µl for each protein. The total protein concentration is 10mg/ml.

## Samples

Sample	Protein	HOCl	Tris Buffer
Unmodified 9PM	2 $\mu$ l (20 $\mu$ g)	X	198 $\mu$ l
60mM HOCl Modified 9PM	2 $\mu$ l (20 $\mu$ g)	80 $\mu$ l HOCl, 150ML	118 $\mu$ l
30mM HOCl Modified 9PM	2 $\mu$ l (20 $\mu$ g)	40 $\mu$ l HOCl, 150ML	158 $\mu$ l
15mM HOCl Modified 9PM	2 $\mu$ l (20 $\mu$ g)	20 $\mu$ l HOCl, 150ML	178 $\mu$ l
3mM HOCl Modified 9PM	2 $\mu$ l (20 $\mu$ g)	40 $\mu$ l HOCl, 15ML	158 $\mu$ l
1.5mM HOCl Modified 9PM	2 $\mu$ l (20 $\mu$ g)	20 $\mu$ l HOCl, 15ML	178 $\mu$ l

### 2.4.1.2 Trypsin Digestion

- Tris Buffer 50mM pH 8.4 - The tris buffer is at pH 8.4 as this is the optimum pH for trypsin activity. A tris buffer solution was made by using deionised water and tris base. The pH was varied using 10M HCl or 10M NaOH.
- 6M Urea - 2g of Urea in 1.25ml Tris Buffer and 3.75ml water. Urea will denature and unfold the protein for digestion.
- 184mM Iodoacetamide (alkylating agent) - 34mg Iodoacetamide in 250 $\mu$ l Tris and 750 $\mu$ l water. The alkylating agent will alkylate the -SH groups in the cysteine amino acid side chains.
- 194mM Dithiothreitol (DTT) (reducing agent) - 30mg DTT in 250 $\mu$ l Tris and 750 $\mu$ l water. The reducing agent will reduce any disulfide bonds that have formed or are present between cysteine residues in the protein.
- Trypsin solution 0.2 $\mu$ g/ $\mu$ l - 100 $\mu$ l of 25mM ammonium bicarbonate solution is added to 20 $\mu$ g of porcine trypsin.

100 $\mu$ l 6M Urea and 5 $\mu$ l DTT are added to the dry 9 protein mix in the eppendorf tube. The protein is resuspended by vortexing and incubated at room temperature for one hour. 20 $\mu$ l iodoacetamide is added and vortexed. The solution is incubated at room temperature for an hour. 20 $\mu$ l DTT is added to react with any unreacted iodoacetamide and to prevent further alkylation of nucleophilic residues such as lysine. The solution is mixed by vortex and left at room temperature. 775 $\mu$ l water is finally added to the protein solution to reduce the urea concentration from 6M to 0.6M where trypsin activity is not inhibited.

An aliquot of 184 $\mu$ l of this solution is taken and 3 $\mu$ l (0.6 $\mu$ g) trypsin solution is added. The final digestion solution was mixed and left at 37C overnight.

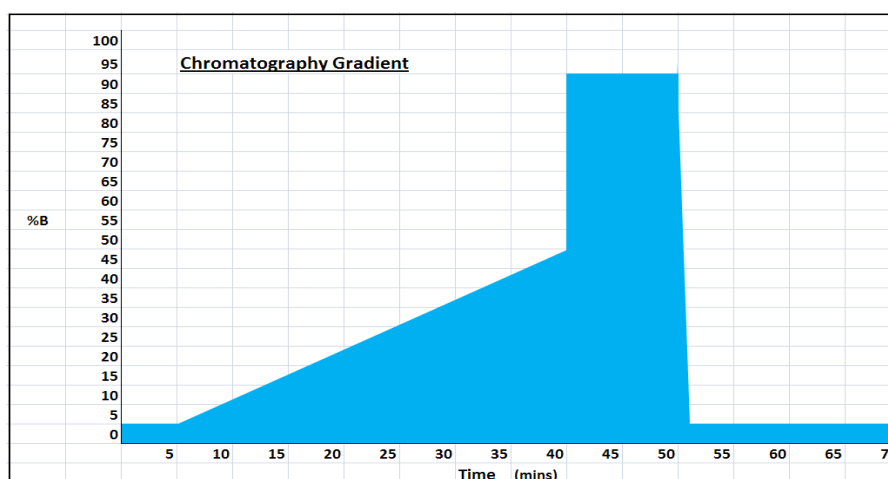
### 2.4.1.3 Chromatography method

Buffer A (loading buffer) - 2% acetonitrile, 0.1% trifluoroacetic acid

Buffer B - 80% acetonitrile, 0.5% formic acid

Buffer C - 2% acetonitrile, 0.5% formic acid

10 $\mu$ l of 9 protein mix sample (2 $\mu$ g protein) was made up to 20 $\mu$ l with loading buffer and injected into the LC (Ultimate 3000, *Dionex*). The flow rate of the loading pump was 20 $\mu$ l/min. The micro-pump flow rate was 300nl/min. The chromatography gradient used was from 5% buffer B at 0-5minutes rising to 50% buffer B at 40minutes to 90% buffer B at 41minutes to 51minutes followed by a decrease in buffer B to 5% between 52 and 70minutes. The mass spectrometry instrument collects data between 5 and 70minutes during the chromatography gradient. Peptides were separated on a C18 (150mm in length, 75 $\mu$ m I.D) column from Alltech Associates.



### 2.4.1.4 Mass spectrometry analysis

The mass spectrometry experiments were run to collect data for 65minutes.

*The conventional MSMS Experiment* - All mass spectrometry experiments were performed in positive ion mode. The enhanced MS collected between a mass range of 400 and 1500amu, the step size was 0.06amu and the scan rate was 1000amu/s. The enhanced resolution scan followed before the information

dependant acquisition experiment where 1 to 2 of the most intense precursors with charge states from 2<sup>+</sup> to 4<sup>+</sup> were chosen to be fragmented for ions greater than 400m/z and less than 1500m/z. The collisional energy was rolling and former target ions were excluded for 300seconds after two occurrences. Two enhanced product ion scans followed. Q1 is set to low resolution to increase sensitivity, the step size was 0.12amu and the scan rate was 4000amu/s scanning between 50 and 1500amu.

*The Precursor Scan Experiment* - The precursor scan mass spectrometry experiment was performed by setting the following parameters. All mass spectrometry experiments were performed in positive ion mode.

The precursor scan scanned between a mass range of 400 to 1000amu for precursors of 170m/z. The total scan time was 5seconds, the step size 1amu and the scan rate 1000amu/s. The collisional energy used was 80eV with the resolution of Q1 and Q3 set to low. The information-dependant acquisition method is set to choose the top most intense precursor exceeding a threshold of 200cps. The dynamic exclusion parameter was turned on to always exclude former target ions. In the enhanced product ion scan the mass range scanned was between 50 and 1500amu, step size was 0.12amu, the scan rate 4000amu/s, the resolution in Q1 set to low and the collisional energy employed was 45eV.

#### **2.4.1.5 Data analysis by Mascot 1.4 version 1.6b9**

The MSMS ion searches carried out on the data collected by the mass spectrometer in this study were set to the following parameters; the enzyme was “trypsin”, the fixed modifications were “carbamidomethyl (C), the variable modifications were chlorotyrosine (ClTyr (Y)) and oxidation (M) and the mass values were monoisotopic. The peptide mass tolerance was  $\pm 2\text{Da}$ , the fragment mass tolerance was  $\pm 1\text{Da}$  and the maximum missed cleavages were set to 1. The sequence database searched against was SwissProt (release 56.6).

The Mascot Search Options - The default precursor charge states are to be 1+ to 4+ and ions with a 5+ charge or higher were to be discarded. The MSMS averaging of IDA dependents were set; the precursor mass tolerance for grouping was 0.2, maximum cycles between groups were 10 and the minimum number of cycles between groups was 1. For MSMS filtering, spectra were rejected if less than 10

peaks or a precursor was below 50 or above 10,000. The MSMS data centroid and threshold parameter was set to centroid all data and to remove peaks with less than 0% of the highest peaks.

## 2.5 Results and Discussion – The Precursor Scan

The 3, 15 and 30mM HOCl modified, trypsin digested, 9 protein mix samples were analyzed by the precursor scan (see 2.4 Mass Spectrometry Analysis in Materials and Methods) on the Qtrap 2000 (*Applied Biosystems*, Warrington, UK) then searched with Mascot, a MS data searching algorithm, version 1.6b9.

### 2.5.1 Assignment of the ClTyr modification by Mascot and manual validation

The precursor scan method was used to analyse the 3, 15 and 30mM HOCl modified 9 protein mix samples and the number of chlorotyrosine (ClTyr) modifications detected were then assigned by Mascot and compared (Figure 20). The precursor scan analysis led to Mascot identifying 3ClTyr modifications in the 3mM HOCl 9 protein mix sample, and 7ClTyr modifications in the 15mM and 30mM HOCl modified 9 protein mix samples. Mascot identifies modifications statistically and the ClTyr modification of the peptides identified were then manually validated. To be a true positive the peptide had a good statistical score (above the significance threshold set by Mascot) and has a good *y-ion* series (Figure 21). The statistical score for the LGEYGFQNALIVR + ClTyr peptide (shown boxed in Figure 20 and Figure 21) is 87 and the significance threshold was calculated to be 48. The ion-match table (Figure 22) displays 11 of the 12 possible *y-ions*. The ClTyr modified LGEYGFQNALIVR peptide identified by Mascot was manually confirmed as a true positive as the *y-ion* series has been detected and these can be seen in the mass spectrometry data collected by the Qtrap using the EPI experiment in the method.

Sample	Protein with modification	Modification	Peptide
3mM HOCl Mod 9Protein Mix	Lysozyme (LYSC CHICK)	CITyr	R.HGLDNYR.G
	Ovalbumin (OVAL CHICK)	HOTrp	R.ELINSWVESQTNGIIR.N
	Myoglobin (MYG EQUBU)	CITyr	K.YKELGFGG
		Ox(HW)	M.GLSDGGEWQVNLVWVK.V
	$\beta$ -lactoglobulin (LACB BOVIN)	CITyr	K.VLVLDTDYKK.Y
		HOTyr	K.VAGTWYSLAMAASDISLLDAQSAPLR.V
15mM HOCl Mod 9Protein Mix	Ovalbumin (OVAL CHICK)	HOTrp	K.LTEWTSNFMEEER.K
		Ox(HW)	R.ELINSWVESQTNGIIR.N
		CITyr + 2Ox(M)	R.VTEQESKFPVQMYQIGLFR.V
	BSA (ALBU BOVIN)	CITyr	K.LGEYGFQNALIVR.Y
	Carbonic anhydrase (CAH2 SHEEP)	CITyr	K.YAABLHLVHWNTK.Y
	Myoglobin (MYG EQUBU)	CITyr	K.YKELGFGG
	Cytochrome C (CYC HORSE)	CITyr	K.TEREDLIAYLK.K
	CITyr	K.TGQAPGFTYTDANK.N	
	CITyr	K.TGQAPGFTYTDANKNK.G	
30mM HOCl Mod 9Protein Mix	BSA (ALBU BOVIN)	CITyr	K.YLYEIAR.R
		CITyr	R.RHPEYAVSVLLR.L
		CITyr	K.LGEYGFQNALIVR.Y
	Myoglobin (MYG EQUBU)	CITyr	K.YKELGFGG
	Carbonic anhydrase (CAH2 BOVIN)	CITyr	K.YAABLHLVHWNTK.Y
	Lysozyme (LYSC CHICK)	CITyr	R.HGLDNYR.G
	Ovalbumin (OVAL CHICK)	HOTrp	R.ELINSWVESQTNGIIR.N
	CITyr	R.VTEQESKFPVQMYQIGLFR.V	

Figure 20: Precursor scan analysis of the 3mM, 15mM and 30mM HOCl modified 9 protein mix samples. The above figure displays and compares the protein modifications assigned by Mascot for the 3mM, 15mM and 30mM 9 protein mix samples. The 3mM HOCl modified 9 protein mix sample is assigned 3CITyr modifications, the 15mM HOCl modified 9 protein mix sample is assigned 7CITyr modifications and the 30mM HOCl is also assigned 7CITyr modifications.

1. [ALBU\\_BOVIN](#) Mass: 71244 Score: 380 Queries matched: 20 emPAI: 0.84  
Serum albumin precursor - Bos taurus (Bovine)

Check to include this hit in error tolerant search or archive report

Query	Observed	Mr (expt)	Mr (calc)	Delta	Miss	Score	Expect	Rank	Peptide
<a href="#">161</a>	424.2500	846.4854	846.4963	-0.0109	1	36	1.2	1	R.LSQKFPK.A
<a href="#">168</a>	443.6900	885.3654	885.4080	-0.0425	0	33	2.6	1	K.DDSPDLPK.L
<a href="#">182</a>	461.7200	921.4254	921.4807	-0.0553	0	50	0.041	1	K.AEFVEVTK.L
<a href="#">187</a>	464.2900	926.5654	926.4861	0.0793	0	37	0.91	1	K.YLYEIAR.R
<a href="#">221</a>	501.8900	1001.7654	1001.5757	0.1897	0	46	0.11	1	K.LVSTQTALA.-
<a href="#">224</a>	507.7800	1013.5454	1013.6121	-0.0666	0	53	0.022	1	K.QTALVELLK.H
<a href="#">225</a>	508.2700	1014.5254	1013.6121	0.9134	0	(48)	0.083	1	K.QTALVELLK.H
<a href="#">246</a>	571.8700	1141.7254	1141.7070	0.0184	1	48	0.078	1	K.KQTALVELLK.H
<a href="#">248</a>	582.2700	1162.5254	1162.6234	-0.0979	0	60	0.0042	1	K.LVNELTEPAK.T
<a href="#">262</a>	625.3300	1248.6454	1248.6139	0.0316	1	35	1.5	7	R.FRDLGEEHFK.G
<a href="#">277</a>	653.3600	1304.7054	1304.7088	-0.0034	0	66	0.0011	1	K.HLVDEPQNLIK.Q
<a href="#">303</a>	708.3300	1414.6454	1414.6803	-0.0348	0	99	5.2e-07	1	K.TVMENFVAFVVK.C + Oxidation (M)
<a href="#">313</a>	720.3000	1438.5854	1438.8045	-0.2190	1	53	0.022	1	R.RHPEYAVSVLLR.L
<a href="#">326</a>	740.2900	1478.5654	1478.7881	-0.2227	0	(55)	0.014	1	K.LGEYGFQNALIVR.Y
<a href="#">327</a>	740.3900	1478.7654	1478.7881	-0.0227	0	107	8.8e-08	1	K.LGEYGFQNALIVR.Y
<a href="#">339</a>	758.2500	1514.4854	1512.7492	1.7363	0	(87)	9.4e-06	1	K.LGEYGFQNALIVR.Y + ChloroTyr (Y)
<a href="#">367</a>	784.2600	1566.5054	1566.7354	-0.2300	0	(34)	1.6	1	K.DAFLGSLYEYSR.R
<a href="#">368</a>	784.3100	1566.6054	1566.7354	-0.1300	0	95	1.4e-06	1	K.DAFLGSLYEYSR.R
<a href="#">382</a>	801.7500	1601.4854	1600.6965	0.7890	0	(75)	0.00012	1	K.DAFLGSLYEYSR.R + ChloroTyr (Y)
<a href="#">392</a>	821.0400	1640.0654	1638.9305	1.1350	1	76	0.00011	1	R.KVPQVSTPTLVEYSR.S

Figure 21: Mascot search results from the analysis of the 30mM HOCl modified 9 protein mix sample. The above figure displays the Mascot search results for the analysis of the 30mM HOCl modified 9 protein mix sample. The LGEYGFQNALIVR peptide is assigned a CITyr modification. The statistical score is 87.

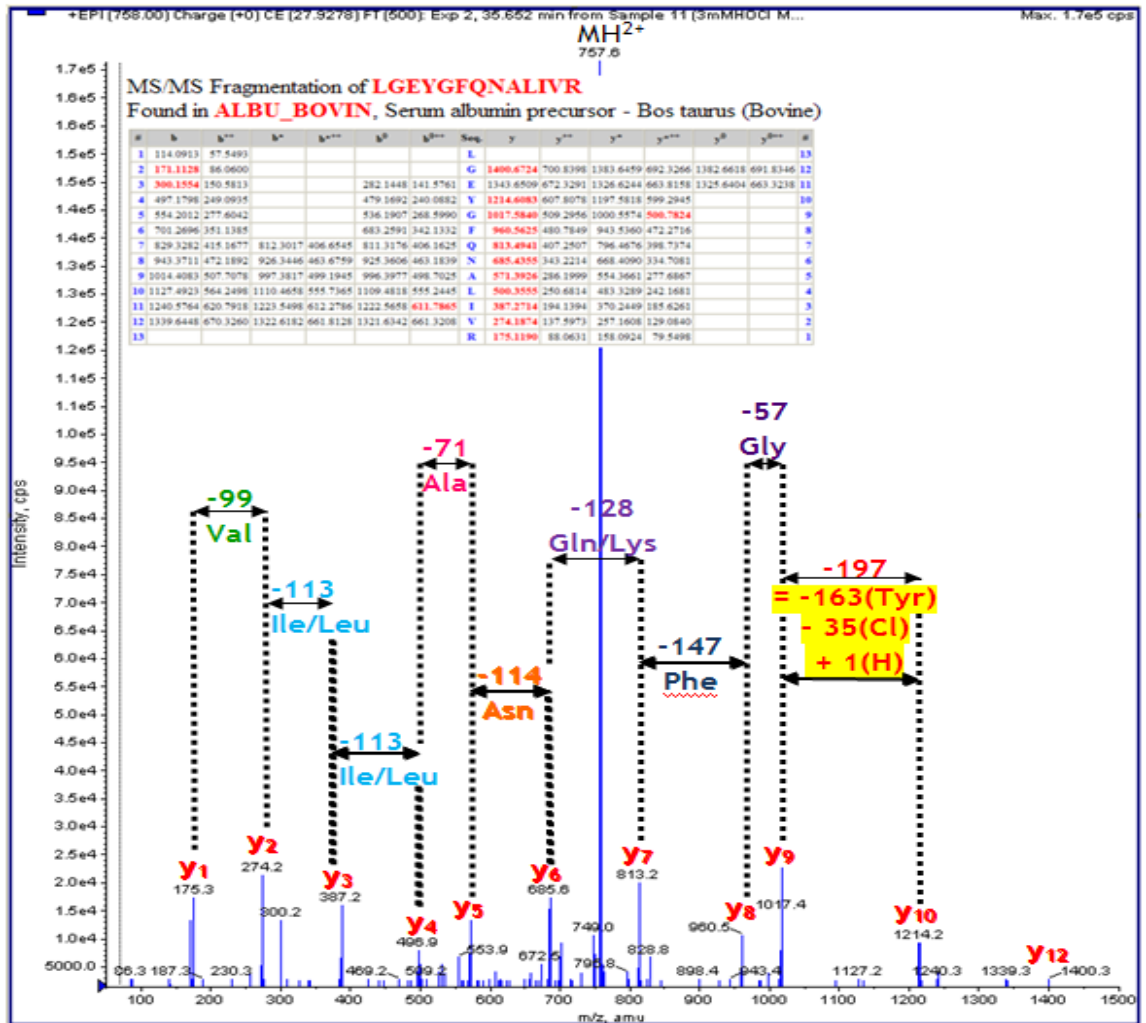


Figure 22: Ion-match table and mass spectrum for the LGEYGFQNALIVR + ClTyr peptide detected in the 30mM HOCl modified 9 protein mix sample. The above figure illustrates the mass spectrum data collected for the LGEYGFQNALIVR + ClTyr peptide detected in the 30mM HOCl modified 9 protein mix sample by the precursor scan. The ion-match table displays that an almost complete *y-ion* series has been detected and assigned by Mascot. The *y-ions* have been labelled and highlighted in yellow is the ClTyr modified ion-fragment.

### 2.5.2 Reviewing the sensitivity of the precursor scan for the detection of chlorotyrosine in the HOCl modified 9 protein mix

Not all potential tyrosine sites in each of the 9 proteins in the mix were seen to be modified so it is possible that there were perhaps more ClTyr modifications present in the HOCl modified samples that had not been detected. The number of tyrosine residues that had been found to be ClTyr modified (in a 3mM HOCl modified 9PM sample) were compared with the number of tyrosines available in each protein (Table5).

Table 5: Number of tyrosines in protein compared with the number of tyrosines found to be ClTyr modified by Qtrap.

Protein	No. of Tyr (Y) present in Protein	No. of Tyr (Y) ClTyr detected
Lysozyme	3	1
Bovine Serum Albumin	20	3
Carbonic Anhydrase	8	1
$\alpha$ -Caesin	10	none seen
$\alpha$ -Lactalbumin	4	none seen
Myoglobin	2	2
Ovalbumin	10	3
$\beta$ -Lactoglobulin	4	2
Cytochrome C	4	3

From left to right the first column displays the protein in the 9 protein mix sample, the second column displays the number of tyrosines present in the protein and the third column displays the number of ClTyr modifications detected.

When analysed with the precursor scan method on the Qtrap the 15mM HOCl modified 9 protein mix sample was identified by Mascot to have 7ClTyr modifications present compared to the 3mM HOCl modified 9 protein mix sample which was identified as having 3ClTyr modifications present. The ClTyr modified peptides were manually validated as before (see 2.5.1). The 30mM HOCl modified sample however did not yield any more ClTyr modifications than the 15mM HOCl modified sample. It was expected that a 9 protein mix sample modified with 30mM HOCl when analysed by the precursor scan would lead to a greater number of ClTyr-modified peptides being detected than a 9 protein mix sample modified at 15mM HOCl. ClTyr modified peptides in the protein mix detected at a lower HOCl concentration would also be expected to be detected in a sample modified at a higher HOCl concentration. At a higher HOCl concentration this unexpected result may be caused by the aggregation of the proteins which would lead to poor sampling.

Winter et al, demonstrated that at low molar ratios (10-fold molar excess) HOCl can cause oxidative protein unfolding or the aggregation of proteins *in vitro* <sup>[165]</sup>. HOCl is a well known effective antimicrobial produced by mammalian host defences to kill invading microorganisms. From the study it is now suggested that the anti-microbial effects of household bleach (HOCl is the active ingredient) could be largely based on HOCl's ability to cause aggregation of

essential bacterial proteins. At the high HOCl concentrations used in this study it is possible that the protein can precipitate out of solution. There was no pellet or an increase in the cloudiness of the sample in the eppendorf tube after modification or prior to loading onto the mass spectrometer that was visible to the eye which would suggest no aggregation.

### 2.5.3 Investigating the potential ClTyr modifications in a 15mM HOCl and 60mM HOCl modified 9 protein mix samples

The precursor scan is selective but not very sensitive due to its long scan time (5 secs). To increase the sensitivity and detection of all potential ClTyr modifications of the peptides in the 9 protein mix samples, we performed the precursor scan alone. The precursor scan will only select the ions that give the 170m/z fragment-ion which is the *potential* chlorotyrosine immonium ion. The tryptic digests of a 15mM and 60mM HOCl modified protein mix were separated on the LC before being analyzed on the QTrap. The Total Ion Counts (TICs) for each sample were compared (Figure 23). The 15mM HOCl modified sample has a greater intensity,  $4.4 \times 10^4$  cps, than the 60mM HOCl sample,  $1.0 \times 10^4$  cps. The TIC traces suggest that there are potentially more ClTyr modifications in the lower HOCl concentration modified sample than in the higher, 60mM HOCl modified sample. There appears to be more peaks in the 15mM HOCl modified sample than the number of ClTyr modifications identified. In the protein summary there are many peptides that are identified as being ClTyr modified but Mascot does not assign these to a protein hit so are likely false positives.

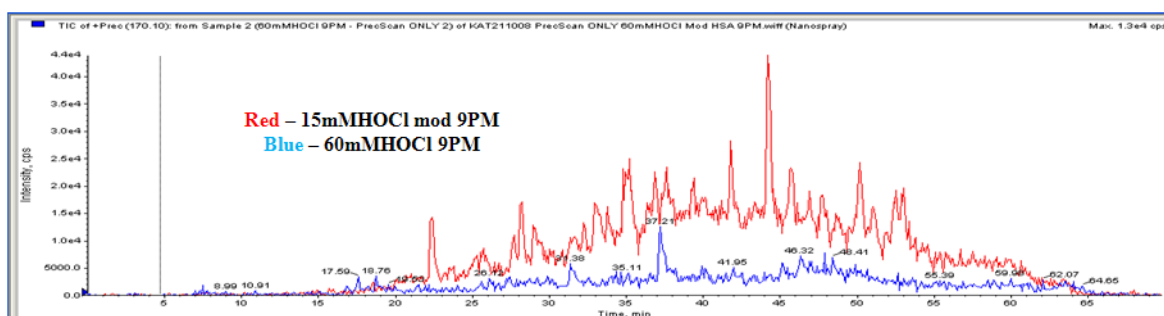


Figure 23: Investigating and comparing the potential abundance of chlorotyrosine in 15mM and 60mM HOCl modified 9 protein mix samples. The figure illustrates the over-laid TIC's (total ion chromatograph's) of the potential ClTyr modified peptides in a 15mM (red trace) and 60mM (blue) HOCl modified 9 protein samples after analysis by the precursor scan only.

## 2.5.4 Investigating modifications by HOCl in a 9 protein mix at higher HOCl concentrations

Another possibility for the observed “decrease” in 170m/z precursors at higher [HOCl] is the formation of di-chlorotyrosine (di-ClTyr). When the HOCl concentration is increased to a critical level, the formation of di-chlorotyrosine (Figure 24) begins to increase. Chapman et al <sup>[166]</sup> reported that at low HOCl concentrations (50nmol per milligram of protein), ClTyr levels ranged from 1 per 835 tyrosines and di-ClTyr levels ranged from 1 per 12,000 tyrosines. At this HOCl concentration ClTyr is formed at an order of magnitude greater in comparison to di-ClTyr. At higher HOCl concentrations (200nmol per milligram of protein) ClTyr and di-ClTyr formation was increased by 3- and 10-fold respectively. Di-chlorotyrosine requires a larger HOCl concentration to form as the addition of a secondary chlorine atom onto tyrosine’s aromatic ring is less favourable than the addition of the first chlorine to form mono-chlorotyrosine. This could be the reasoning behind a 60mMHOCl sample apparently showing less chlorotyrosine modification than a 15mMHOCl sample.

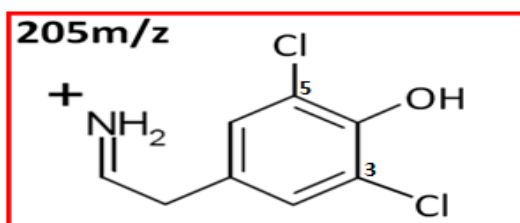


Figure 24: The di-chlorotyrosine immonium ion. The above figure displays the di-chlorotyrosine immonium ion (205m/z). The chlorine atom is shown at positions 3 and 5 of the tyrosine ring.

### 2.5.4.1 The formation of mono- and di-chlorinated tyrosines in HOCl modified proteins

Drabik et al <sup>[167]</sup> discovered how the molar ratio between the number of exposed tyrosine residues in proteins and the OCl<sup>-</sup> ion in a system affected the predominant chloro-derivative product. They studied the chlorination of the N-acetyl-L-tyrosine (N-acTyr) residue at positions 3 and 5 in reactions with NaOCl. The N-acTyr, with the alpha amine residue blocked by acetylation, mimicked the reactivity of exposed tyrosyl residues in polypeptides or proteins. The reaction of HOCl/OCl<sup>-</sup> with N-acTyr was dependant on the reactant concentration ratio employed. When the reactant ratio, OCl<sup>-</sup>/N-acTyr, was 1:4 the predominant

reaction product was 3-chlorotyrosine. When the reactant molar ratio was 1:1.1 protein to HOCl, both 3-chlorotyrosine and 3,5-dichlorotyrosine was produced. They also found that the pH affected the yield of tyrosine chlorination between N-acTyr and OCl<sup>-</sup> where at pH5.5 it was 100% and 91% at pH4.5 and 66% at pH3.

The 15mM HOCl and 60mM HOCl modified 9 protein mix samples were also analysed using a precursor scan alone to select only for precursor masses which give the 205m/z fragment-ion, the potential di-ClTyr immonium ion. It is not likely due to favourability that there are a greater number of di-ClTyr modifications than ClTyr modifications in higher HOCl modified 9 protein mix samples (Figure 25). The intensity of the 15mM HOCl modified sample with the precursor scan is <4800cps and the intensity of the 60mM HOCl modified sample with the precursor scan is <2800cps. The maximum intensity of both HOCl modified samples is seen at 60minutes into the chromatography gradient.

The TIC for the potential precursors possessing the di-ClTyr 205m/z immonium ion is low in intensity (<4800cps for the 15mM HOCl modified and <2800cps for the 60mM HOCl modified 9 protein mix sample) compared to the TIC for the potential precursors possessing the ClTyr 170m/z immonium ion (<4.4 x 10<sup>4</sup>cps for the 15mM HOCl modified and <1.0 x 10<sup>4</sup>cps for the 60mM HOCl modified 9 protein mix sample). It is likely that any di-ClTyr modifications that are present in the HOCl modified 9 protein mix samples are very low in abundance in comparison to ClTyr modifications. From these 170m/z and 205m/z precursor scan experiments detecting for potential ClTyr and di-ClTyr modifications it can be assumed that when the HOCl concentration reaches a certain level aggregation of the protein, (although not visible to the eye), occurs. The aggregation of protein and not the formation of di-chlorotyrosine may explain the reasoning between the same number of ClTyr modification seen in a 15mM HOCl and a 30mM HOCl modified 9 protein mix sample <sup>[165]</sup> (see 2.5.2).

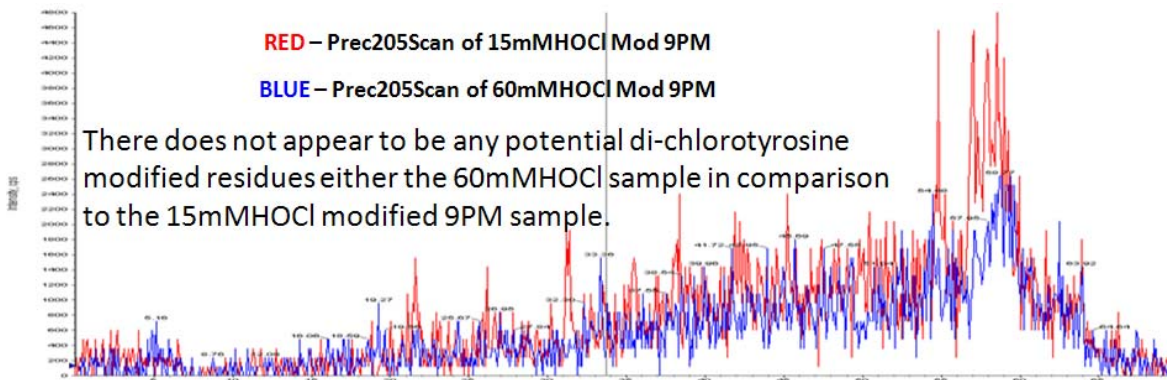


Figure 25: The 205m/z precursor scan for the detection of di-chlorotyrosine in a 15mM and 60mM HOCl modified 9 protein mix sample. The above displays the over-laid TIC (total ion chromatograph) for the analysis of the 15mM (red trace) and 60mM (blue trace) HOCl modified 9 protein mix samples by the precursor scan only. The precursor scan selects for the masses that gives the 205m/z fragment ion which could potentially possess the di-chlorotyrosine modification.

### 2.5.5 Optimising the precursor scan for the detection of chlorotyrosine in complex samples

As discussed in 2.5.2 there are many tyrosines in the proteins present in the 9 protein mix that are potential sites of ClTyr modification. These tyrosines may be modified but are not being detected by the precursor experiment (2.4.1.4). Hence we attempt to improve and optimise the parameters for the precursor scan mass spectrometry method for the sensitive and selective detection of chlorotyrosine modification in a 9 protein mix.

The problems arising with the LC-MSMS method is the low sequence coverage of less abundant proteins and the poor reproducibility of peptide ion selection between replicates. This can be caused by under sampling, a wide concentration dynamic range of the proteins in the mixture and the wide range of electrospray ionization efficiency of the peptides <sup>[168]</sup>. One technique used to solve the problems that are caused by under sampling is dynamic exclusion and the second is gas phase fractionation (GPF). Garza et al used the Finnigan LCQ <sup>[thermo scientific P105 Product Support Bulletin]</sup> (a quadrupole iontrap) to solve under sampling by employing the dynamic exclusion technique. Dynamic exclusion allows the acquisition of MSMS spectra from lower intensity ion species whereas in more complex mixtures different peptides can be eluted close together or overlap and not be seen causing them to be excluded for MSMS in favour of more intense, abundant precursors. When using the dynamic exclusion, masses that have been

previously analyzed will be put on a temporary exclusion list after  $MS^n$  data has been acquired. This then allows the instrument to collect  $MS^n$  data on less intense, less abundant peaks which may have otherwise gone undetected and unanalysed. After a fixed time the excluded ion will be removed from the list so that precursors isobaric to the first intense peak which were analysed can be studied.

### 2.5.6 Improving sensitivity - dynamic exclusion

In the trypsin digested HOCl modified 9 protein mix sample it is possible that precursors of the 170m/z chlorotyrosine immonium ion are being neglected.

The initial precursor scan mass spectrometry method was performed with dynamic exclusion. Dynamic exclusion can either temporarily or permanently enter a mass onto an exclusion list after its MSMS spectrum has been acquired. The experiment was first performed with the dynamic exclusion turned “on” in order to prevent the repetitive collection of data on abundant or very intense precursors giving the 170m/z ClTyr immonium ion. This exclusion of previously seen precursor masses meant that many more low abundant, less intense, precursors may be fragmented by MSMS. However, it is possible that there are some precursors in the sample that are isobaric to each other that are ClTyr modified and will fragment to give the 170m/z ClTyr immonium ion. By setting the dynamic exclusion from “*always* exclude former target ions” to “exclude former target ions for 60seconds *only*” more data will be collected. The two precursor scan mass spectrometry methods where dynamic exclusion is turned “on” always and “on” for 60seconds were used to analyse and detect for the ClTyr modification in the 3mM HOCl sample. The ClTyr modifications identified by Mascot from the analysis of the same sample were compared (Table 6).

Setting the dynamic exclusion time to “exclude former target ions for 60seconds” from “*always* excluding former target ions” led to the detection of a greater number of ClTyr modifications in a 3mM HOCl modified 9 protein mix sample from 2ClTyr to 6ClTyr modifications detected and assigned by Mascot. In simpler samples it is likely the dynamic exclusion parameter would not affect the number of modifications detected as the possibility of there being precursors isobaric to each other is less likely.

**Table 6: Comparison of the analysis of a 3mM HOCl modified 9 protein mix sample by the precursor scan with dynamic exclusion turned “off” and “on”.**

Precursor scan experiment - Dynamic Fill	Protein	Modification	Peptide	No. of Modifications
<b>Always exclude former target ions</b> Dynamic Fill "on"	ALBU_BOVIN	CITyr	K.LGEYGFQNALIVR.Y	2 CITyr Mod
	CAH2_BOVIN	CITyr	K.YGDFGTAAQQPDGLAVVGVFLK.V	
<b>Exclude former target ions for 60seconds</b> Dynamic Fill "off"	ALBU_BOVIN	CITyr	K.LGEYGFQNALIVR.Y	6 CITyr Mod
		CITyr	K.DAFLGSFLYEYSR.R	
	CAH2_BOVIN	CITyr	K.DGPLTGTYSR.L	
	LYSC_CHICK	CITyr	R.NTDGSTDYGIHQINSR.W	
	LACB_BOVIN	CITyr	K.VAGTWYSLAMAASDISLLDAQSAFLR.V	
CASA1_BOVIN	CITyr	R.YLGYLEQLLR.L		

The table displays the comparison of the analysis of a 3mM HOCl modified 9 protein mix sample by the precursor scan when dynamic exclusion is turned “on”. When the dynamic exclusion is set to exclude former target ions for 60seconds more CITyr modifications (6CITyr compared to 2CITyr) are seen in the sample.

### 2.5.7 Improving sensitivity – the gas phase fractionation experiment

We have attempted to employ a gas phase fractionation (GPF) method to combat under sampling and poor sequence coverage within a protein mixture. It is in fact thought possible that a proteome may be characterized effectively using a well developed GPF method by an LC-MSMS without previous protein or peptide fractionation<sup>[169]</sup>. Protein fractionation can increase sequence coverage by making the complex mixture of peptides or proteins less complex by separation. Fractions of the mixture are achieved by separating out proteins by their solubility or isoelectric point. Protein mixtures of great complexity can be first separated out by SDS (sodium dodecyl sulphate) gels, according to their size and charge. Individual protein spots can then be enzymatically digested and then analyzed by MSMS. The steps required in the protocol lead to protein fractionation being very time consuming. Gas phase fractionation therefore represents a significant saving in both cost and time over 2-DE approaches<sup>[170]</sup>.

The precursor scan mass spectrometry method for the detection of CITyr in a HOCl modified 9 protein mix is a selective but not a very sensitive scan. The mass range is wide; between 400 and 1000amu and this takes a long time (5seconds) to scan. The large mass range and long scan time means that when one mass is being scanned for precursors of 170m/z there are others at different masses that are being missed leading to poor sampling.

The dwell time is the time spent at each mass collecting data in the mass range and can affect the sensitivity of the precursor scan. Increasing the scan time will lead to an increase in the signal to noise ratio however a longer dwell time will decrease the number of scans possible. A small step size will improve resolution if dwell time is kept constant and data will be collected for longer again affecting the signal to noise. The scan speed is directly proportional to the dwell time and the mass range scanned but inversely proportional to the step size.

The dwell time can be calculated from the scan time and scan mass range;

$$\text{Dwell Time} = \text{Scan time} / \text{Scan mass range}$$

$$= 5\text{seconds} / 600 \text{ (from 400 to 1000amu)}$$

$$= \underline{8.3}\text{milliseconds}$$

Decreasing the scan range will increase than dwell time (if the total scan time remains the same) meaning that more time is spent at each data point collecting more data and therefore increasing sensitivity.

$$\text{Dwell time} = 5\text{seconds} / 200 \text{ (from 400 to 600amu)}$$

$$= \underline{25}\text{milliseconds}$$

Instead of a wide mass range between 400 and 1000amu being scanned the method was re-written to scan three smaller mass ranges; 400\_600amu, 600\_800amu and 800\_1000amu. Although more sensitive the gas phase fractionation experiment consumes more sample and is more time consuming as the sample must be injected three times to be analysed at each different mass range.

The precursor scan was compared with the GPF experiment by analysis of a 3mM HOCl modified 9 protein mix sample. A 3mM HOCl modified sample is used instead of the 15mM HOCl modified 9 protein mix sample as fewer ClTyr modifications were identified in the initial precursor scan experiment (Table 7). The GPF precursor experiment was found to detect more ClTyr modifications (4ClTyr modifications) in comparison to the precursor scan method (scanning

from 400\_100amu detected 1ClTyr modification) alone. It is noted that the majority of ClTyr modifications were detected within the 400\_600amu mass range.

Table 7: A comparison between the precursor scan method and GPF experiment for the analysis of a 3mM HOCl modified 9 protein mix sample.

Precursor Scan	GPF Experiment
Prec170Scan 400_1000amu	Prec170Scan 400_600amu
ALBU_BOVIN	ALBU_BOVIN
K.YLYEIAR.R + ChloroTyr (Y)	K.YLYEIAR.R + ChloroTyr (Y)
	MYG_EQUBU
	K.YKELGFGG.- + ChloroTyr (Y)
	CYTC_BOVIN
	R.EDLIAYLK.K + ChloroTyr (Y)
	Prec170Scan 600_800amu
	<i>no ClTyr seen</i>
	Prec170Scan 800_1000amu
	MYG_EQUBU
	K.YKELGFGG.- + ChloroTyr (Y)
<b>total modifications = 1</b>	<b>total modifications = 4</b>

The table displays the comparison of the precursor scan and the GPF experiment when both are used to analyse a 3mM HOCl modified 9 protein mix sample. The (left column) precursor scan detected and assigned only 1ClTyr modification whereas in the (right column) GPF experiment 4ClTyr modifications are detected and identified by Mascot.

### 2.5.8 Optimising the Gas Phase Fractionation Experiment

Gas phase fractionation is usually performed by scanning narrow m/z ranges (~100m/z) instead of wider ranges<sup>[171]</sup>. For example, Yi et al approached complete peroxisome characterization by GPF methods, by first scanning a single broad m/z range from 400-1800 followed by three narrower m/z ranges; 400-800, 800-1200 and 1200-1800 followed by scanning sixteen even narrower m/z ranges; 400-510, 490-610, 590-710...1690-1800. More of the proteins in the complex mixture were observed when more scans of narrower m/z ranges were scanned in comparison to fewer scans with a wider m/z range. Although this method was successful and more of the proteome was seen, Yi concluded that ions will be more abundant at some m/z ranges than others and these ranges require deeper “mining” or interrogation than others.

Scherl et al<sup>[169]</sup> demonstrated how optimal mass ranges for GPF could be chosen and calculated based on genomic complexity and experimental data on various organism’s genomes. Calculations to find the most efficient and optimum m/z ranges were executed by performing an in silico digest of the proteins in these

complex mixture and ion density mapping. Ion density mapping or imaging is the presentation of the intensities of mass-to-charge values in a 2-dimensional space. According to both calculations Scherl determined that the  $m/z$  range for the most efficient GPF coverage was that the lower  $m/z$  range needed to be very narrow and increase as the  $m/z$  values increased.

Scherl's GPF experiment was performed again first by scanning one long  $m/z$  range; 400-2000, two narrower scans with the lower  $m/z$  range being narrower than the second; 400-695 and 685-2000 followed by four, six and eight different scan ranges again with the lower  $m/z$  ranges being narrower than the larger  $m/z$  ranges; 400-458, 453-521, 516-596, 591-690, 685-810, 805-968, 963-1243 and 1238-2000. Scherl states in the results and discussion that even though the width of the GPF ranges were based solely on the precursor ion density these might be biased as this was set without taking into account the MS instrument's sensitivity over the entire mass range. The ion density is evidently higher between the  $m/z$  range 400-600amu but this may have been possible as the instrument used, the LTQ-Orbitrap, is tuned for highest sensitivity at these values. Even though a greater number of the proteins or components in a complex sample can be detected using the GPF technique the major drawback is sample consumption due to the repetition of injections into the mass spectrometer.

#### **2.5.8.1 Comparison of sample analysis with conventional MSMS, the precursor scan method and two differing mass ranges for the GPF Experiment**

The mass ranges chosen for a GPF experiment (2) were, 400\_510amu, 490\_610amu, 590\_710amu, 690\_810amu, 790\_910amu, 890\_1010amu and 990\_1110amu. The mass ranges are narrower and overlap by 20amu in order not to "miss" any precursors which may be borderline and missed when the broader mass ranges; 400\_600amu, 600\_800amu and 800\_1000amu were scanned for GPF (1).

To test the precursor scan and these new scan ranges a 15mM HOCl modified 9 protein mix sample was analysed with a conventional MSMS method, the precursor scan method scanning between 400\_1000amu, the GPF experiment (1) scanning 200amu ranges and the GPF experiment (2) scanning 100amu ranges with a 20amu overlap (Figure 26). The conventional MSMS and precursor scan

method (400\_1000amu) both detected and identified 3ClTyr modifications. The GPF experiment scanning 200amu mass ranges detected and identified 2ClTyr modifications and the GPF experiment scanning 100amu mass ranges with a 20amu overlap detected and identified 7ClTyr modifications.

There are ClTyr modified peptides identified in some of the mass spectrometry experiments but not identified in others during the analysis of the 15mM HOCl modified 9 protein mix sample. For example, the LGEYGFQNALIVR + ClTyr peptide from bovine serum albumin is seen in the conventional MSMS experiment, in the mass range 600-800amu in GPF(1) and in the mass range 590\_710amu in GPF(2) but not in the precursor scan experiment scanning between 400\_1000amu. This is unexpected; if a peptide is seen in the conventional MSMS experiment it should be seen in the precursor scan (400\_1000amu) and GPF experiments (1) and (2) as the experiments become more sensitive. It is possible that by repeating the experiment there would be a better correlation or list of ClTyr modified peptides identified by each MS method.

The GPF experiment (2) when scanning the mass range between 400\_510amu detected a 2<sup>+</sup> ion with a 507.0m/z and identified it as the ClTyr modified DGPLTGTYR peptide matched to the carbonic anhydrase protein in the 9 protein mix. Mascot identified the peptide as not being statistically significant as it had an ion score of 28 which was below the statistically significant threshold which was calculated to be 48. The DGPLTGTYR + ClTyr peptide is the second top peptide match identified to possibly be the 507.0m/z ion. The top peptide mass possibly identified as the 507.0m/z ion has a score of 29.4 and is not matched to a protein hit (Figure 27). The DGPLTGTYR + ClTyr peptide's presence in the sample was confirmed manually by its mass spectrum. The mass spectrum data collected for the 507.0m/z ion showed that some of the DGPLTGTYR + ClTyr peptides *y-ions* had been observed (Figure 28). The DGPLTGTYR + ClTyr peptide is not seen in the mass spectrum EPI scan but it is possible that it exists because the peptide is a precursor of the 170m/z ion fragment.

<b>15mM HOCl Mod 9PM - MSMS</b>	
<a href="#">ALBU BOVIN</a>	<b>K.LGEYGFQNALIVR.Y + ChloroTyr (Y)</b>
	<b>K.DAFLGSFLYEYSR.R + ChloroTyr (Y)</b>
<a href="#">OVAL CHICK</a>	<b>R.LYAEER.Y + ChloroTyr (Y)</b>
<b>TOTAL #no. ClTyr Modifications = 3</b>	
<b>15mM HOCl Mod 9PM - Prec170Scan 400_1000amu</b>	
<a href="#">ALBU BOVIN</a>	<b>R.RHPEYAVSVLLR.L + ChloroTyr (Y)</b>
<a href="#">CAH2 BOVIN</a>	<b>K.AVVQDPALKPLALVYGEATSR.R + ChloroTyr (Y)</b>
<a href="#">CASA1 BOVIN</a>	<b>R.YLGYLEQLLR.L + ChloroTyr (Y)</b>
<b>TOTAL #no. ClTyr Modifications = 3</b>	
<b>Gas Phase Fractionation Expt - 1</b>	
15mM HOCl Mod 9PM - Prec170Scan 400_600amu	
<i>no MSMS data</i>	
15mM HOCl Mod 9PM - Prec170Scan 600_800amu	
<a href="#">ALBU BOVIN</a>	<b>K.LGEYGFQNALIVR.Y + ChloroTyr (Y)</b>
<a href="#">CAH2 BOVIN</a>	<b>K.YGDFGTAAQQPDGLAVVGVFLK.V + ChloroTyr (Y)</b>
15mM HOCl Mod 9PM - Prec170Scan 800_1000amu	
<i>no significant hits to report</i>	
<b>TOTAL #no. ClTyr Modifications = 2</b>	
<b>Gas Phase Fractionation Expt - 2</b>	
15mM HOCl Mod 9PM - Prec170Scan 400_510amu	
<a href="#">ALBU BOVIN</a>	<b>R.RHPEYAVSVLLR.L + ChloroTyr (Y)</b>
<a href="#">CAH2 BOVIN</a>	<b>K.DGPLTGTyr.L + ChloroTyr (Y)</b>
15mM HOCl Mod 9PM - Prec170Scan 490_610amu	
<i>no ClTyr modifications</i>	
15mM HOCl Mod 9PM - Prec170Scan 590_710amu	
<a href="#">CASA1 BOVIN</a>	<b>R.YLGYLEQLLR.L + ChloroTyr (Y)</b>
15mM HOCl Mod 9PM - Prec170Scan 690_810amu	
<a href="#">ALBU BOVIN</a>	<b>K.LGEYGFQNALIVR.Y + ChloroTyr (Y)</b>
	<b>K.DAFLGSFLYEYSR.R + ChloroTyr (Y)</b>
<a href="#">CAH2 BOVIN</a>	<b>K.AVVQDPALKPLALVYGEATSR.R + ChloroTyr (Y)</b>
	<b>K.YGDFGTAAQQPDGLAVVGVFLK.V + ChloroTyr (Y)</b>
15mM HOCl Mod 9PM - Prec170Scan 790_910amu	
<i>no ClTyr modifications</i>	
15mM HOCl Mod 9PM - Prec170Scan 890_1010amu	
<i>no MSMS data</i>	
15mM HOCl Mod 9PM - Prec170Scan 990_1110amu	
<i>no MSMS data</i>	
<b>TOTAL #no. ClTyr Modifications = 7</b>	

Figure 26: Analysis of a 15mM HOCl modified 9 protein mix sample with the precursor scan method and the GPF Experiment. The above displays the conventional MSMS, precursor scan method (400\_1000amu), GPF experiment (200amu mass ranges) and the GPF experiment (100amu mass ranges with a 20amu overlap) for the analysis of a 15mM HOCl modified 9 protein mix. The ClTyr modified peptide is statistically insignificant and is displayed in bold black text.

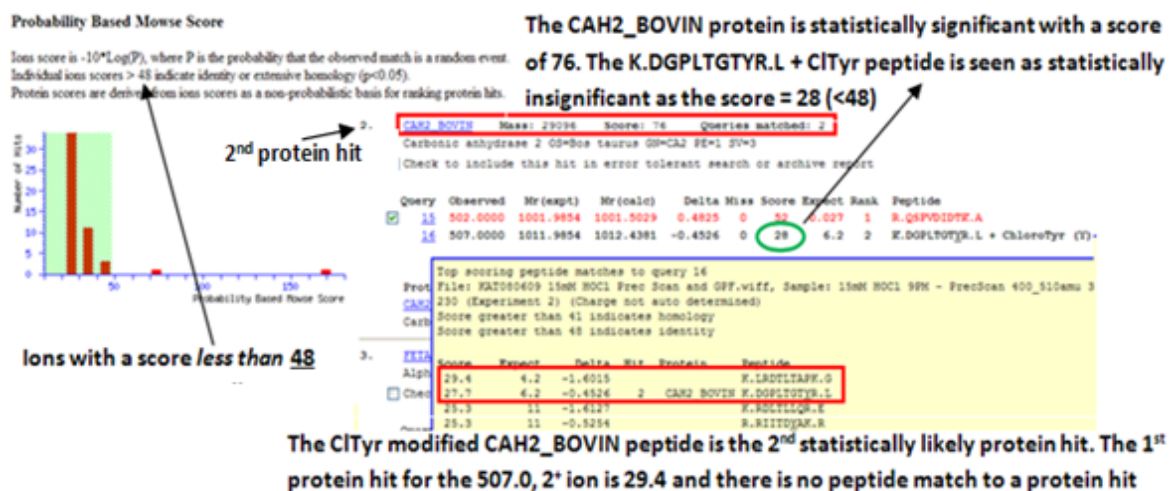


Figure 27: The DGPLTGTYSR + ClTyr peptide detected in the 15mM HOCI modified 9 protein mix sample - Mascot identified insignificant hit - Manual Validation. The above figure displays the probability based Mowse score requirements. Any ions that fall into the green shaded area of the bar chart (an ion score under 48) are not seen to be statistically significant. The DGPLTGTYSR + ClTyr peptide match is assigned to the Carbonic Anhydrase protein hit and is reported in bold black text.

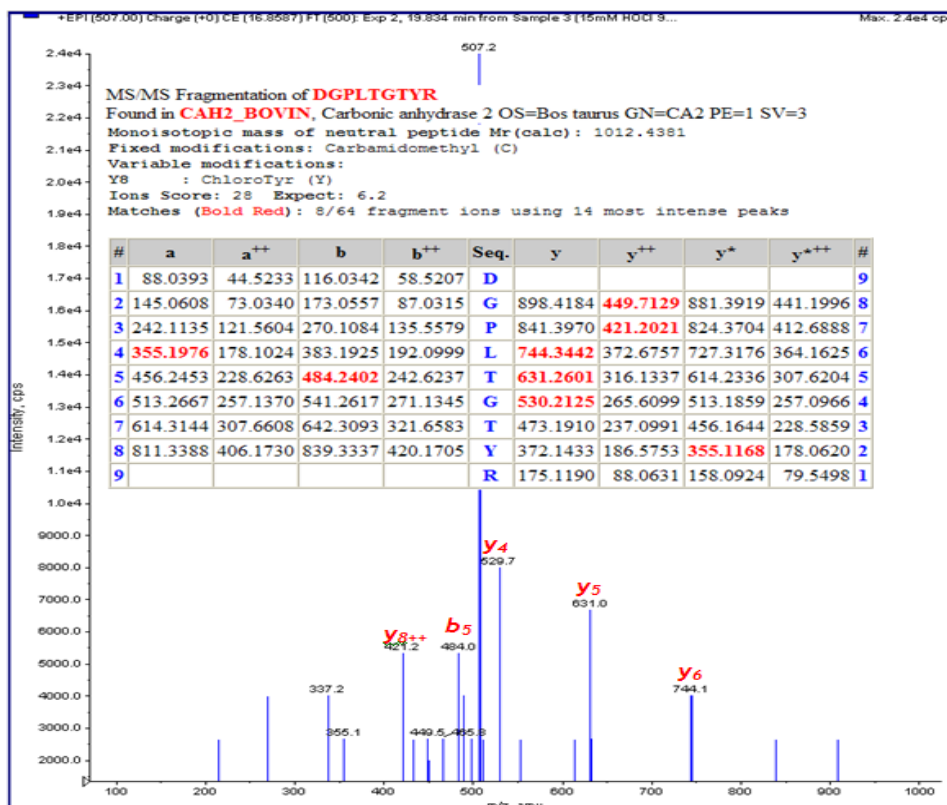


Figure 28: The Mass Spectrum for the manually confirmed DGPLTGTYSR + ClTyr peptide. The Mass Spectrum data for the 507.0m/z ion displays detection of the DGPLTGTYSR + ClTyr peptides y-ion series. The ClTyr modification is not seen but the precursor scan peptide will produce the 170m/z ion which is potentially the ClTyr immonium ion.

The table displaying the comparison between analysis by conventional MSMS, the precursor scan (400\_1000amu) and GPF experiments (1 and 2) (Figure 26) found that when narrower ranges are scanned (100amu mass ranges with a 20amu overlap) more ClTyr modified peptides are identified. Although the consumption of the sample is increased, scanning narrower and overlapping mass ranges is a more sensitive method for the detection of modifications. The conventional MSMS and precursor scan scanning between 400\_1000amu detected and identified the same number of ClTyr modifications. This is unexpected as the precursor scan is a more sensitive and selective method compared to the conventional MSMS method of analysis. The conventional MSMS and precursor scan scanning between 400\_1000amu detected and identified one more ClTyr modification that the GPF experiment (1) scanning 200amu mass ranges. The different mass spectrometry analysis methods were run consecutively so it is unlikely that machine sensitivity has been altered. The GPF experiment (1) should detect and assign a greater number of ClTyr modifications and its success has been observed previously (see 2.5.7).

## **2.6 Discussion - the advantages and disadvantages of the precursor scan method and GPF method**

The precursor scan method and the gas phase fractionation experiments were employed and optimised here to detect ClTyr modifications in HOCl modified 9 protein mix samples. Both methods for the detection of post translational modifications have been shown here and discussed in the reference to sensitively and selectively detect modifications of proteins in complex samples.

The GPF experiment (2.5.7) is more sensitive than the precursor scan alone scanning a broad mass range but involves multiple injections leading to higher sample consumption which may not always be possible if the sample to be analysed is precious and not easily available. Here as discussed in this chapter the GPF experiment should solve the problems with under sampling but for completeness the experiment comparing the different methods for the detection of ClTyr modifications in a HOCl modified 9 protein mix should be repeated and tested again with varying concentration of HOCl modifications.

Multiple reaction monitoring is another example of a sensitive method for the detection of low abundance modifications in a complex sample (to be discussed

in more detail in Chapter 3). Peptides at low-signal-to-noise can be detected and analysed by CID (collision induced dissociation) by multiple reaction monitoring (MRM), such methods are not practical for global analysis. For MRM prior knowledge must be known about the sample to target low abundance ions and their  $m/z$  values. Unlike the MRM method the precursor scan and GPF experiment do not require any prior knowledge of the sample before analysis.

# Chapter 3

---

Detecting nitrotyrosine and chlorotyrosine modifications in human serum albumin and plasma using targeted multiple reaction monitoring

### **3 Chapter – Detecting nitrotyrosine and chlorotyrosine modifications in human serum albumin and plasma using targeted multiple reaction monitoring**

Human serum albumin (HSA) is the most abundant protein found in plasma with a concentration of 5g/100ml in a typical blood sample <sup>[172]</sup>. The blood plasma proteome is highly complex as it contains not only plasma proteins but also tissue proteomes as sub sets; circulating the whole body. The plasma will contain “tissue leakage products” or proteins that have been released into the plasma as a result of cell death or damage, some of which are important biomarkers for disease<sup>[66]</sup>.

#### **3.1 Sensitive techniques for the validation and verification of biomarkers**

In order to search for candidate biomarkers for disease treatment in the plasma proteome one of the biggest problems that must be overcome is the extreme complexity and dynamic range of the plasma proteins <sup>[173]</sup>. In plasma there are many proteins in varying abundances. High abundance proteins will often mask equally important but lower abundance proteins in the sample. To reduce complexity the plasma proteins can be sub-divided into many simpler fractions allowing for hundreds and in many cases thousands of proteins to be characterised but this requires a large number of analyses by complex instruments. Plasma proteins can be fractionated by chromatography and electrophoresis methods <sup>[174-176]</sup>. Pieper et al <sup>[175]</sup> fractionated plasma first by immunoaffinity chromatography to remove the most abundant proteins followed by sequential anion-exchange chromatography and size-exclusion chromatography before displaying the proteins separated out on 2D electrophoresis gels. Fractionation allowed 3,700 distinct proteins to be visualised on a 2D gel (many were post translational modification variants of the plasma proteins) and mass spectrometry enabled 325 distinct proteins to be identified. Aside from the cost implications, labour and the time taken these methods for the fractionation of plasma proteins will also introduce variability

into the results. This is not useful for clinical samples which require fast diagnosis and confirmation of disease specific biomarkers. Scores of samples must be analysed before statistical criteria are satisfied for the diagnostic specificity and sensitivity of disease treatment. The complexity of the plasma as well as the overlap of proteins in each plasma fraction limits biomarker discovery and therefore creates the necessity for more specific and precise assays. Proteins or potential biomarkers that are specific to a plasma fraction due to their molecular weight or electrophoretic mobility will make their extraction more complex and less reproducible. The accumulation of plasma fractions on the other hand, will over complicate assaying and the problems with abundance will occur.

Anderson et al <sup>[173]</sup> reports that the process for developing new diagnostic's (Dx) for the development of new drugs for the treatment of a disease is a three staged process (Figure 29). The first stage will identify statistically valid biomarker candidates by some features, such as their sequence or post-translational modifications and the second stage will attempt to identify these potential candidates in larger sample sets taking into account bio-variability, and specificity in relation to target diseases and their statistical contribution in the context of various biomarker panels. Anderson states that the biomarker panel will consist of five different proteins as larger panels become progressively less economical and more difficult to work with. The third stage of the Dx pipeline is the commercial implementation and clinical test stage of the process relying on the results in the second stage which were evaluated in relation to secondary factors including disease prevalence, availability of treatments, cost reimbursement policies and their compatibility with present clinical laboratory instruments. The pipeline for developing new diagnostics (Dx) is well funded in the first and final, third stage but in many cases the secondary stage for validation of these biomarkers is not <sup>[173]</sup>. Rifai et al <sup>[141]</sup> also calls for better biomarkers for the improvement of diagnosis and molecular guided therapy for the monitoring of disease and has recognised that for novel biomarker candidates antibodies required for their validation by western blotting will not be yet available.

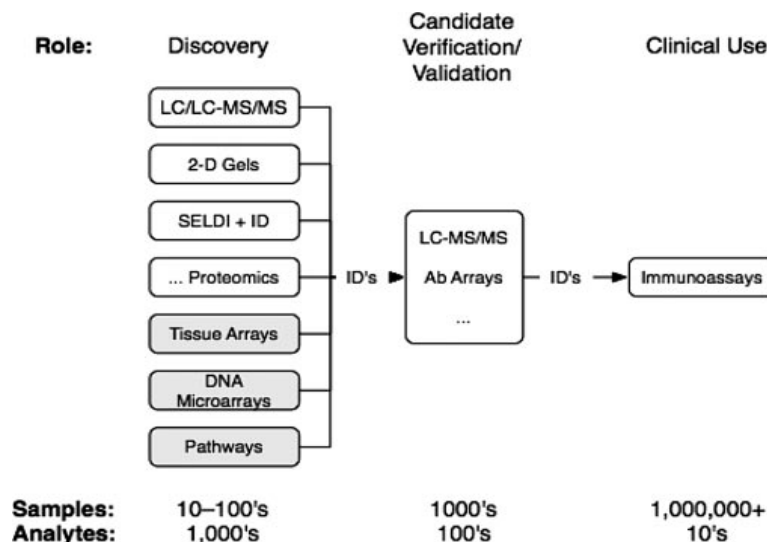


Figure 29: Schematic diagram for a 3-stage diagnostic pipeline exploiting different technologies in each stage and connected by molecular identifications <sup>[173]</sup>. The above figure displays the schematic diagram for a 3-stage diagnostic platform exploiting different technologies in each stage and connected by molecular identifications. (SELDI = Surface-enhanced Laser Desorption Ionisation)

### 3.1.1 Multiple reaction monitoring (MRM) for validation of biomarkers

An alternative method for the validation of potential bio-markers by western blotting is multiple reaction monitoring (MRM) or selected reaction monitoring (SRM). MRM detection using a triple quadrupole mass spectrometer is a sensitive method of detection better throughput than the discovery methods outlined in the above Figure 29. For an MRM program to be written there must first be prior knowledge about the potential biomarker; its primary sequence, charge state and how it fragments, as both the first and second quadrupoles in the instrument are fixed to scan for a targeted precursor ion and fragment ion mass. With MRMs a substantial number of candidates (up to 300 transitions in the case of the *Applied Biosystems*, Qtrap 3200 <sup>[177]</sup>) can be simultaneously targeted and measured in the statistically relevant number of patient samples for verification.

The MRM mass spectrometry technique is focused and targets a precursor and then specifically targets its fragment ion. The first (Q1) and last (Q3) mass analysers of a triple quadrupole mass spectrometer are employed as mass filters therefore isolating a targeted peptide ion and its corresponding fragment ion. The signal of the fragment ion detected in Q3 is then monitored over a chromatographic elution period (Figure 30). The Q1 and Q3 masses targeted for are known as the MRM transitions and by using two mass-filtering stages during

the experiment this allows this mass spectrometry technique to be not only highly selective but with the combination of a high duty cycle results in a quantitative technique with unmatched sensitivity and specificity<sup>[178]</sup>.

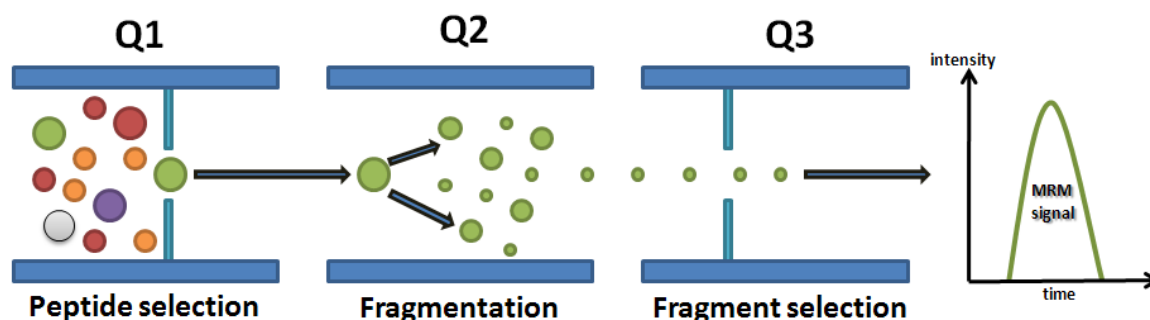


Figure 30: MRM transitions in the triple quadrupole mass spectrometer. The parent ion or precursor mass is detected in Q1 and fragmented in the collision cell (Q2). Fragments of the precursor mass are detected in Q3 and the specific fragment targeted for is allowed through to the detector

### 3.1.1.1 MRMs for the detection of and quantification of oxidative biomarkers

In this study I will focus on potential biomarkers for atherosclerosis. The oxidation of protein side chains is often a sign of stress or inflammation within the body. Methionine is susceptible to oxidation<sup>[179]</sup> to its sulfoxide form and is of particular interest as it has been observed on a wide variety of proteins during periods of oxidative stress in the body. The oxidation of methionine is known to undergo a conformational change eliminating or reducing biological activity and causing protein aggregation and encourages proteolysis. In his study Houde et al<sup>[179]</sup>, monitors and quantifies the methionine oxidation to the sulfoxide form. Extracted ion chromatograms (XICs) were used to quantify the methionine oxidation in a sample. Software added and summed together the peptides of interest and their total peak areas were calculated. The equation below (Equation 6) was used to calculate the relative percentage modification.

#### Equation 6

$$\text{Relative percent oxidation} = \frac{\sum \text{Areas of Met-ox peptide ions}}{(\sum \text{Areas of Met-ox peptide ions}) + (\sum \text{Areas of Met-non-ox peptide ions})} \times 100$$

The laboratory which carried out the quantification of the methionine oxidation traditionally used single ion monitoring (SIM). They suggest that the improved

selectivity of the quantification of methionine oxidation, MRM (plural of SIM) is applied.

## 3.2 Materials and Methods

### 3.2.1 Chlorination of HSA and plasma

Purified HSA (from Sigma Aldrich) was modified in eppendorf tubes at varying concentrations of HOCl (from Sigma Aldrich) as shown in Table 8, in tris buffer ( $C_4H_{11}NO_3$ , pH7, 50mM concentration) at 37°C for 4hours. The modified protein was then dried down using a centrifugal evaporator (eppendorf concentrator 5301) before being trypsin digested.

HSA stock solution = 2mg/ml in tris buffer (pH7, 50mM).

The  $1.5ML^{-1}$  HOCl stock solution was diluted in tris buffer (pH7, 50mM) to give HOCl solutions; 150mML, 15mML and 1.5mML.

#### Samples

Each protein sample for analysis consisted of 10 $\mu$ l (20 $\mu$ g) of the HSA stock solution and HOCl concentrations were adjusted by dilution of the HOCl solution with Tris buffer (Table 8).

Table 8: The HSA samples were oxidized at varying concentrations of HOCl

Sample	Protein	HOCl	Tris Buffer
Unmodified HSA	10 $\mu$ l HSA (20 $\mu$ g)	X	190 $\mu$ l
30mM HOCl Modified HSA	10 $\mu$ l HSA (20 $\mu$ g)	40 $\mu$ l HOCl, 150ML	150 $\mu$ l
15mM HOCl Modified HSA	10 $\mu$ l HSA (20 $\mu$ g)	20 $\mu$ l HOCl, 150ML	170 $\mu$ l
3mM HOCl Modified HSA	10 $\mu$ l HSA (20 $\mu$ g)	40 $\mu$ l HOCl, 15ML	150 $\mu$ l
1.5mM HOCl Modified HSA	10 $\mu$ l HSA (20 $\mu$ g)	20 $\mu$ l HOCl, 15ML	170 $\mu$ l
0.3mM HOCl Modified HSA	10 $\mu$ l HSA (20 $\mu$ g)	40 $\mu$ l HOCl, 15ML	150 $\mu$ l

From left to right; the first column is the HOCl concentration of which the HSA was modified. The second column is how much protein was modified and the third column is the HOCl added to the sample. The fourth column is how much tris buffer was added to the eppendorf to adjust the HOCl concentration.

**Plasma** was taken from a plasma pool of healthy volunteers (by Dr Corinne Spickett and the Oxidative Stress group from Strathclyde University) and a Bradford assay was performed to determine the plasma protein concentrations. The plasma protein concentration was found to be approximately 58mg/ml. A 50µl aliquot (~3mg protein) of the plasma was taken and diluted in an eppendorf tube by 1:20 in 50mM Tris pH7 buffer. The end concentration of the plasma was ~3µg/µl with a 15µl (~44µg protein) aliquot of the diluted plasma to be modified with varying concentrations of HOCl as reported in Table 9, in tris buffer (pH7, 50mM concentration) at 37° C for 4hours. The modified protein was then dried down using the centrifugal evaporator (eppendorf concentrator 5301) before being trypsin digested.

It is to be noted that only approximately 50-75% of blood proteins is albumin so the final concentration of albumin in the plasma will be 22-38.8µg/µl.

## Samples

**Table 9: The Plasma samples were oxidized at varying concentrations of HOCl**

Sample	Protein	HOCl	Tris Buffer
Unmodified Plasma	15µl plasma (44µg)	X	190µl
30mM HOCl Modified Plasma	15µl plasma (44µg)	40µl HOCl, 150ML	150µl
15mM HOCl Modified Plasma	15µl plasma (44µg)	20µl HOCl, 150ML	170µl
3mM HOCl Modified Plasma	15µl plasma (44µg)	40µl HOCl, 15ML	150µl
1.5mM HOCl Modified Plasma	15µl plasma (44µg)	20µl HOCl, 15ML	170µl
0.3mM HOCl Modified Plasma	15µl plasma (44µg)	40µl HOCl, 1.5ML	150µl
0.15mM HOCl Modified Plasma	15µl plasma (44µg)	20µl HOCl, 1.5ML	170µl

From left to right; the first column is the HOCl concentration of which the plasma was modified. The second column is how much protein was modified and the third column is the HOCl added to the sample. The fourth column is how much tris buffer was added to the eppendorf to adjust the HOCl concentration.

### 3.2.2 Nitration of HSA and plasma

Purified human serum albumin (from Sigma Aldrich) was modified in eppendorf tubes using varying concentrations of SIN-1 (3-morpholinosydnonimine from Sigma Aldrich) as shown in Table 10: The HSA samples were oxidised at varying concentrations of SIN-1, in tris buffer (pH7, 50mM concentration) at 37° C for

4hours. The modified protein was then dried down using a centrifugal evaporator (Eppendorf concentrator 5301) before being trypsin digested.

## Samples

Table 10: The HSA samples were oxidised at varying concentrations of SIN-1

Sample	Protein	HOCl	Tris Buffer
Unmodified HSA	10µl HSA (20µg)	X	190µl
25mM SIN-1 modified HSA	10µl HSA (20µg)	50µl SIN-1, 100ML	140µl
10mM SIN-1 modified HSA	10µl HSA (20µg)	20µl SIN-1, 100ML	170µl
2.5mM SIN-1 modified HSA	10µl HSA (20µg)	50µl SIN-1, 10ML	140µl
1mM SIN-1 modified HSA	10µl HSA (20µg)	20µl SIN-1, 10ML	170µl
0.25mM SIN-1 modified HSA	10µl HSA (20µg)	50µl SIN-1, 1ML	140µl

From left to right; the first column is the SIN-1 concentration of which the HSA was modified. The second column is how much protein was modified and the third column is the SIN-1 added to the sample. The fourth column is how much tris buffer was added to the Eppendorf to adjust the SIN-1 concentration.

Plasma was taken from a plasma pool as before (3.2.1) and modified *in vitro* with different concentrations of SIN-1 (3-morpholinopyridone from Sigma Aldrich) in tris buffer, pH7 50mM (as shown in Table 11). The SIN-1 modified protein was then dried down using the centrifugal evaporator (Eppendorf concentrator 5301) before being trypsin digested like before with the HOCl modified plasma samples.

Table 11: The plasma samples were oxidized at varying concentrations of SIN-1

Sample	Protein	HOCl	Tris Buffer
Unmodified Plasma	15µl plasma (44µg)	X	185µl
25mM SIN-1 Modified Plasma	15µl plasma (44µg)	40µl HOCl, 150ML	135µl
10mM SIN-1 Modified Plasma	15µl plasma (44µg)	20µl HOCl, 150ML	165µl
2.5mM SIN-1 Modified Plasma	15µl plasma (44µg)	40µl HOCl, 15ML	135µl
1mM SIN-1 Modified Plasma	15µl plasma (44µg)	20µl HOCl, 15ML	165µl
0.25mM SIN-1 Modified Plasma	15µl plasma (44µg)	40µl HOCl, 1.5ML	135µl

From left to right; the first column is the SIN-1 concentration of which the plasma was modified. The second column is how much protein was modified and the third column is the SIN-1 added to the sample. The fourth column is how much tris buffer was added to the Eppendorf to adjust the SIN-1 concentration.

### 3.2.3 Enzymatic Digestion

#### Trypsin Digestion

The dried down protein samples were trypsin digested as the 9 protein mix (see 2.4.1.2)

#### Glu-C (*Staphylococcus aureus* Protease V8) Digestion

- Tris Buffer 50mM pH 8.4 - 0.6g Tris base was dissolved in 100ml water and the pH was adjusted using 10M HCl to pH 8.4
- 6M Urea - 2g of Urea in 1.25ml Tris Buffer and 3.75ml water.
- 184mM Iodoacetamide (alkylating agent) - 34mg Iodoacetamide in 250µl Tris and 750µl water.
- 194mM Dithiothreitol (DTT) (reducing agent) - 30mg DTT in 250µl Tris buffer and 750µl water.
- Glu-C solution 0.2µg/ul - 100ul of 25mM Ammonium Bicarbonate solution is added to 20µg Glu-C.

100µl 6M Urea and 5µl DTT were added to the dry protein sample in the eppendorf tube. The protein was resuspended by vortexing and incubated at room temperature for one hour. 20µl iodoacetamide was added and vortexed. The solution was again incubated at room temperature for an hour. 20µl DTT was added to react with any unreacted iodoacetamide and to prevent further alkylation of nucleophilic residues such as lysine. The solution was mixed by vortex and left at room temperature. 775µl water is finally added to the protein solution to reduce the urea concentration from 6M to 0.6M. An aliquot of 184µl of this solution was taken and 3µl (0.6µg) Glu-C solution is added. The final digestion solution was mixed and left at 37°C overnight.

### 3.2.4 MIDAS workflow designer

To automatically write a multiple reaction monitoring method the MIDAS workflow designer was used. The protein sequence for human serum albumin was obtained from UniProtKB/Swissprot (P02768) and pasted into the workflow

designer. The user specified enzyme was trypsin and the number of missed-cleaves was set to 1. Fixed modifications were carbamidomethylation and the variable modifications were chloro (Y) and oxidation (M). The charge states were set 2 to 3.

### 3.3 Results and Discussion – detecting chlorotyrosine in HSA

The HOCl modified human serum albumin samples were analysed by conventional MSMS (2.4.1.4) on the Qtrap 2000 (*Applied Biosystems*, Warrington, UK) after being separated by liquid chromatography (2.4.1.3). The mass spectrometry data was searched with Mascot (2.4.1.5). Mascot reported the top protein hit to be human serum albumin and the HSA peptides that were identified as ClTyr modified in a 30mM HOCl modified HSA sample are listed;

Identified ClTyr Modifications

RHPDYSVVLLLR + ChloroTyr (Y)

DVFLGMFLYEYAR + ChloroTyr (Y); Oxidation (M)

RHPYFYAPELLFFAK + ChloroTyr (Y)

ALVLIAFAQYLQQCPFEDHVK + ChloroTyr (Y)

The ALVLIAFAQYLQQCPFEDHVK + ChloroTyr (Y) peptide has a low ion score of 22 which is below the significance threshold calculated to be 48. This peptide has not been identified as ClTyr modified in any of the other HOCl modified HSA samples (15mM, 3mM HOCl modified). The identification of this peptide in this sample is not a Mascot-assigned statistically confident hit and it is unlikely to possess a reduced cysteine residue in the presence of 30mM HOCl. In the ion-match table Mascot has identified very few *y*-ions for this peptide, (*y*7, *y*5 and *y*4), (Figure 31) and when the mass spectrum for the ALVLIAFAQYLQQCPFEDHVK + ChloroTyr (Y) peptide is manually verified (Figure 32) the *y*-ions (*y*4 and *y*5) which are identified are present only in the noise. This suggests that the ALVLIAFAQYLQQCPFEDHVK + ChloroTyr (Y) peptide in the 30mM HOCl modified HSA sample is not a true positive.

Monoisotopic mass of neutral peptide Mr(calc): 2523.2387  
 Fixed modifications: Carbamidomethyl (C)  
 Variable modifications:  
 Y10 : ChloroTyr (Y)  
 Ions Score: 22 Expect: 1.8  
 Matches (bold red): 9/186 fragment ions using 18 most intense peaks

#	b	b <sup>++</sup>	b <sup>*</sup>	b <sup>++</sup>	b <sup>0</sup>	b <sup>0++</sup>	Seq.	y	y <sup>++</sup>	y <sup>*</sup>	y <sup>++</sup>	y <sup>0</sup>	y <sup>0++</sup>	#
1	72.0444	36.5258					A							21
2	<b>185.1285</b>	93.0679					L	2453.2089	1227.1081	2436.1823	1218.5948	2435.1983	1218.1028	20
3	<b>284.1969</b>	142.6021					V	2340.1248	1170.5661	2323.0983	1162.0528	2322.1143	1161.5608	19
4	<b>397.2809</b>	199.1441					L	2241.0564	1121.0318	2224.0299	1112.5186	2223.0459	1112.0266	18
5	510.3650	255.6861					I	2127.9724	<b>1064.4898</b>	2110.9458	1055.9765	2109.9618	1055.4845	17
6	581.4021	291.2047					A	2014.8883	<b>1007.9478</b>	1997.8617	999.4345	1996.8777	998.9425	16
7	728.4705	364.7389					F	1943.8512	972.4292	1926.8246	963.9160	1925.8406	963.4239	15
8	799.5076	400.2575					A	1796.7828	898.8950	1779.7562	890.3817	1778.7722	889.8897	14
9	927.5662	464.2867	910.5397	455.7735			Y	1725.7456	863.3765	1708.7191	854.8632	1707.7351	854.3712	13
10	1124.5906	562.7989	1107.5640	554.2857			Q	1597.6871	799.3472	1580.6605	790.8339	1579.6765	790.3419	12
11	1237.6746	619.3410	1220.6481	610.8277			L	1400.6627	700.8350	1383.6362	692.3217	1382.6521	691.8297	11
12	1365.7332	683.3702	1348.7067	674.8570			Q	1287.5786	644.2930	1270.5521	635.7797	1269.5681	635.2877	10
13	1493.7918	747.3995	1476.7652	738.8863			Q	1159.5201	580.2637	1142.4935	571.7504	1141.5095	571.2584	9
14	1653.8224	827.4149	1636.7959	818.9016			C	1031.4615	516.2344	1014.4349	507.7211	1013.4509	507.2291	8
15	1750.8752	875.9412	1733.8487	867.4280			P	<b>871.4308</b>	436.2191	854.4043	427.7058	853.4203	427.2138	7
16	1897.9436	949.4754	1880.9171	940.9622			F	774.3781	387.6927	757.3515	379.1794	756.3675	378.6874	6
17	2026.9862	1013.9967	2009.9597	1005.4835	2008.9756	1004.9915	E	<b>627.3097</b>	314.1585	610.2831	305.6452	609.2991	305.1532	5
18	2142.0132	1071.5102	2124.9866	<b>1062.9969</b>	2124.0026	1062.5049	D	<b>498.2671</b>	249.6372	481.2405	241.1239	480.2565	240.6319	4
19	2279.0721	1140.0397	2262.0455	1131.5264	2261.0615	1131.0344	H	383.2401	192.1237	366.2136	183.6104			3
20	2378.1405	1189.5739	2361.1139	1181.0606	2360.1299	1180.5686	V	246.1812	123.5942	229.1547	115.0810			2
21							K	147.1128	74.0600	130.0863	65.5468			1

Figure 31: ALVLIAFAQYLQQCPFEDHVK + ChloroTyr (Y) ion-match table. The ALVLIAFAQYLQQCPFEDHVK + ChloroTyr (Y) peptide's ion-match table shows that only a few *y*-ions, *y*7, *y*5 and *y*4, have been detected. The ion's score is 22 which is low for a peptide of this size (especially when the significance threshold is 48) combined with a poor *y*-ion series. There is not much confidence that this is a true identification of a ClTyr modified peptide in this 30mM HOCl sample.

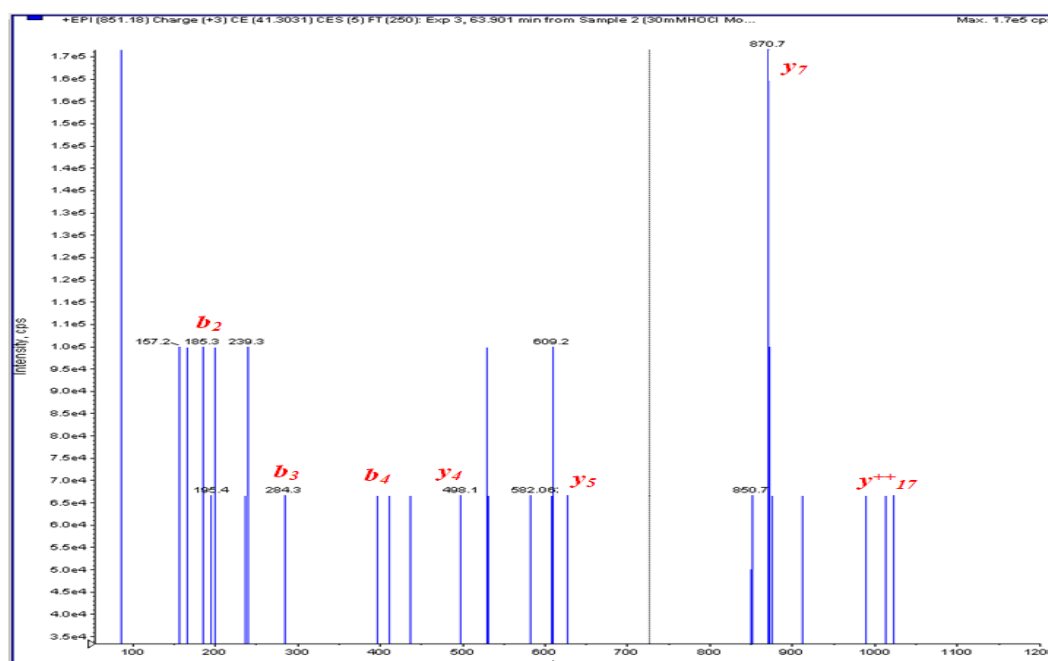


Figure 32: Mass Spectrum for the ALVLIAFAQYLQQCPFEDHVK + ChloroTyr (Y) peptide in the 30mM HOCl modified Human Serum Albumin sample. The above figure displays the Mass Spectrum of the ALVLIAFAQYLQQCPFEDHVK + ChloroTyr (Y) peptide in the 30mM HOCl modified HSA sample.

### 3.3.1 Orthogonal digestion for the detection of ClTyr modified peptides in HSA

To detect any more possible modification sites of chlorotyrosine an orthogonal or “parallel” digest was performed using trypsin and Glu-C. Where trypsin will cleave at lysine (K) and arginine (R) sites, Glu-C will cleave at glutamic (E) and aspartic Acid (D). The specificity of where Glu-C cleaves is dependent on the buffer and pH used as well as the structure around the potential cleavage site. In an ammonium acetate (pH 4.0) buffer or ammonium bicarbonate (pH 7.8) buffer the enzyme will preferentially cleave at the glutamic acid. In phosphate buffer (pH 7.8) Glu-C will cleave at either site although no cleavage at all will occur if a proline residue is on the carboxyl side. The protease is active in the pH range pH 3.5-9.5.

An orthogonal digest will give two different sets of peptide fragments that can be searched and will allow more of the protein’s sequence to be seen. If more of the HSA protein can be seen, more chlorotyrosine modification sites should also be detected (Figure 33). When the Glu-C enzyme was employed a new ClTyr modified peptide was identified (highlighted in purple in the bottom right-hand panel). The ClTyr modification seen in the Glu-C digest for the peptide TYVPKEFNAE was confirmed by conventional MSMS analysis on the Qtrap and Mascot was used to search the MS data generated (Figure 34). A Mascot search of the MS data identified the majority of *y-ions* and *b-ions* for the TYVPKEFNAE peptide and these were confirmed by the peptide’s mass spectrum.



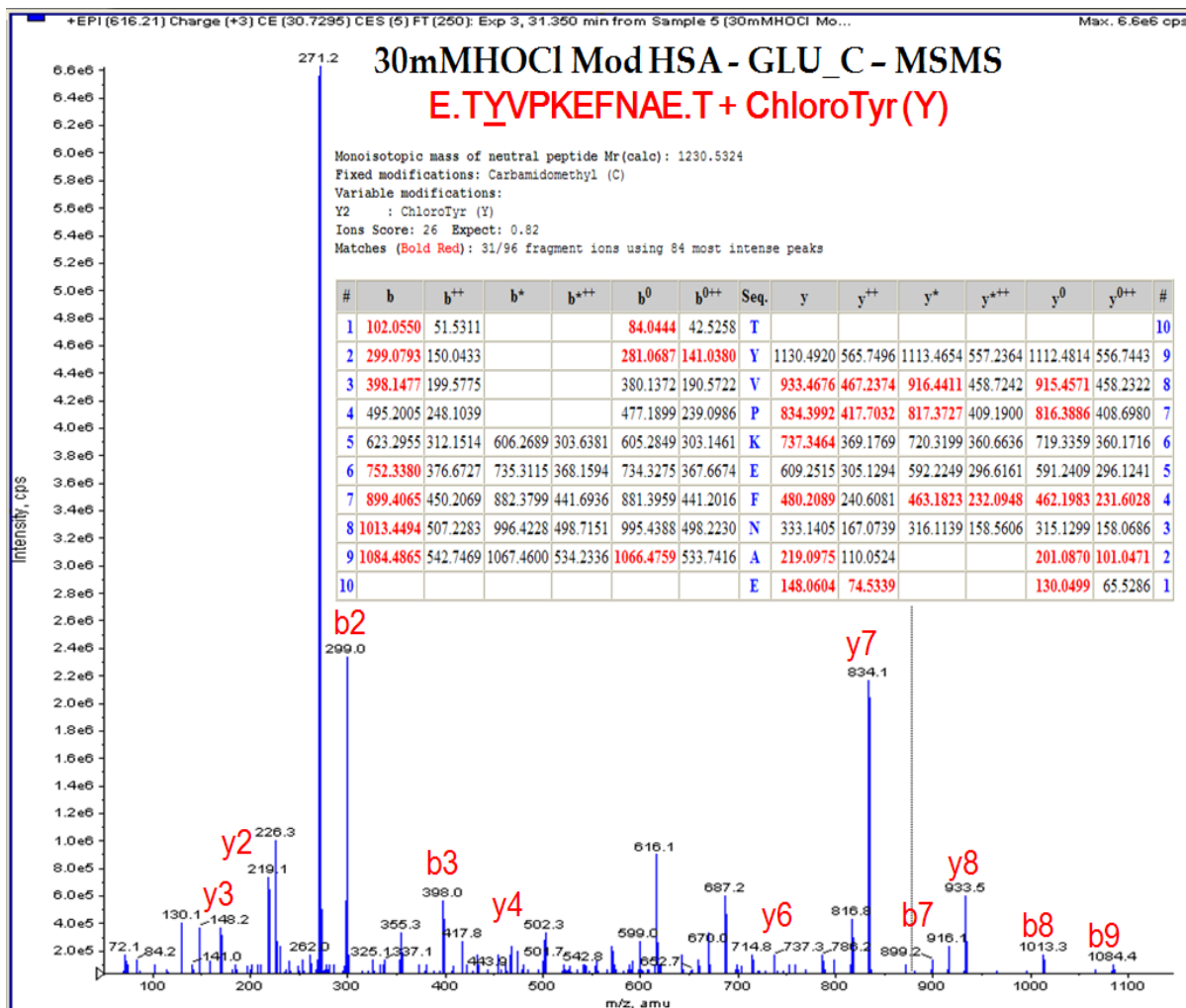


Figure 34: ClTyr modification seen in Glu-C digest. The above figure displays the ion match table and mass spectrum for the ClTyr modified peptide detected from the 30mM HOCl modified HSA, Glu-C digested sample. Mascot identified a number of the *y* and *b-ion* fragment ions in the peptide. The ion-match table is shown and the mass spectrum has been labelled with the assigned ions.

### 3.4 Development of an MRM method to target ClTyr modifications in the HSA protein

The MRM (multiple reaction monitoring) method was developed by using the mass spectrum data generated by the analysis of the various HOCl modified HSA samples. The most commonly identified ClTyr modified peptide observed in the HOCl modified HSA samples was the RHPDYSVLLLR + ClTyr peptide. The transitions used in the MRM method for this peptide were chosen depending on the observations in the mass spectrometry analysis rather than those calculated as these will be optimum for the Qtrap instrument. The collisional energy for the fragmentation of the precursor mass was observed in the mass spectrum data to be 27eV and the most intense and frequent fragment masses observed

(Q3=514.37, 401.28 and 613.44 m/z) were used for the MRM method (Table 12). Three Q3 masses were used in the MRM method as a greater number will lead to lots of information being collected for one individual peptide potentially missing information on others. If less than three Q3 masses are used to identify a peptide this potentially raises the number of false positives possible.

Table 12: Transitions for the modified and unmodified RHPDYSVLLLLR peptide.

Peptide	Q1 m/z	Q3 m/z	Time (msec)	CE (eV)
Modified RHPDYSVLLLLR + ClTyr	501.1	514.37 401.29 613.44	20	27
Unmodified RHPDYSVLLLLR	490.03	514.37 401.29 613.44	20	27

The Q1 masses and Q3 masses for the MRM method were chosen for their frequency and their intensity in the mass spectrometry data. The collisional energy (CE) value was taken from the optimal energy calculated by the mass spectrometer to fragment the peptide.

#### 3.4.1 MRM analysis of a 30mM HOCl HSA sample targeting the unmodified and ClTyr modified RHPDYSVLLLLR peptide

The analysis of a 30mM HOCl HSA sample analysed by the MRM method indicated the detection of both the ClTyr modified and unmodified RHPDYSVLLLLR peptide (Figure 35). The unmodified peptide is seen strongly ( $<3.2 \times 10^4$  cps) at 37 minutes and the ClTyr modified peptide is seen most strongly ( $<4 \times 10^3$  cps) at 40 minutes. The retention time for the ClTyr modified peptide is later than that for the unmodified peptide. The peptides from the sample were separated by reverse-phase liquid chromatography meaning that more polar peptides will be eluted first and less polar peptides eluted later. The chlorine atom on the tyrosine will lead to the peptide becoming less polar meaning it will be eluted later in the chromatography gradient because of the stronger interaction with the stationary phase of the reverse-phase chromatography column.

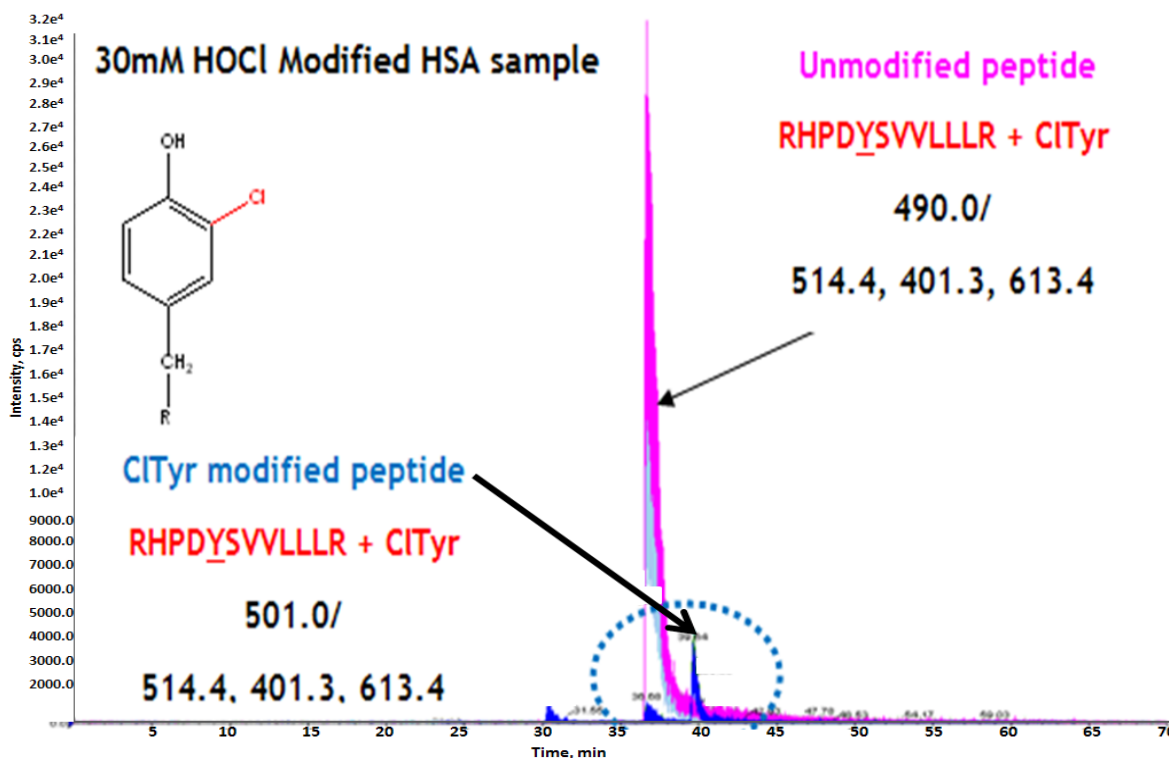


Figure 35: MRM for the CITyr modified and unmodified RHPDYSVLLLLR peptide. The figure displays the signal from the CITyr modified and the unmodified RHPDYSVLLLLR peptide from the analysis of the 30mM HOCl modified HSA sample using the MRM method. The arrows are used to label which peak is the unmodified and CITyr modified peptide.

#### 3.4.1.1 Determining the percentage modification of the RHPDYSVLLLLR peptide in a 30mM HOCl HSA sample

In this study height or intensity is used to calculate the percentage modification of the peptide rather than the area under the peak due to software limitations. This is a reasonable comparison to calculate percentage modification if the peaks to be compared are similar in shape. In a 30mM HOCl sample the percentage modification of the RHPDYSVLLLLR peptide was calculated by the Equation 7;

##### Equation 7

$$\text{Relative percent oxidation} = \frac{\text{Intensity of CITyr peptide}}{\text{Intensity of CITyr peptide} + \text{Intensity of unmodified peptide}} \times 100$$

The intensities of the 501.00m/z (modified)/613.4 and 490.03m/z (unmodified)/613.4 transition signals were compared (Figure 36). The relative percentage modification of the RHPDYSVLLLLR peptide in a 30mM HOCl HSA sample was calculated using the intensities of the signal and under the

assumption that the ionisation energies of the ClTyr modified and unmodified peptide states are similar. Under these assumptions we have calculated that the peptides relative percentage modification in a 30mM HOCl modified sample is approximately 9.1% with the remaining HOCl likely to have reacted with other amino acid side chains.

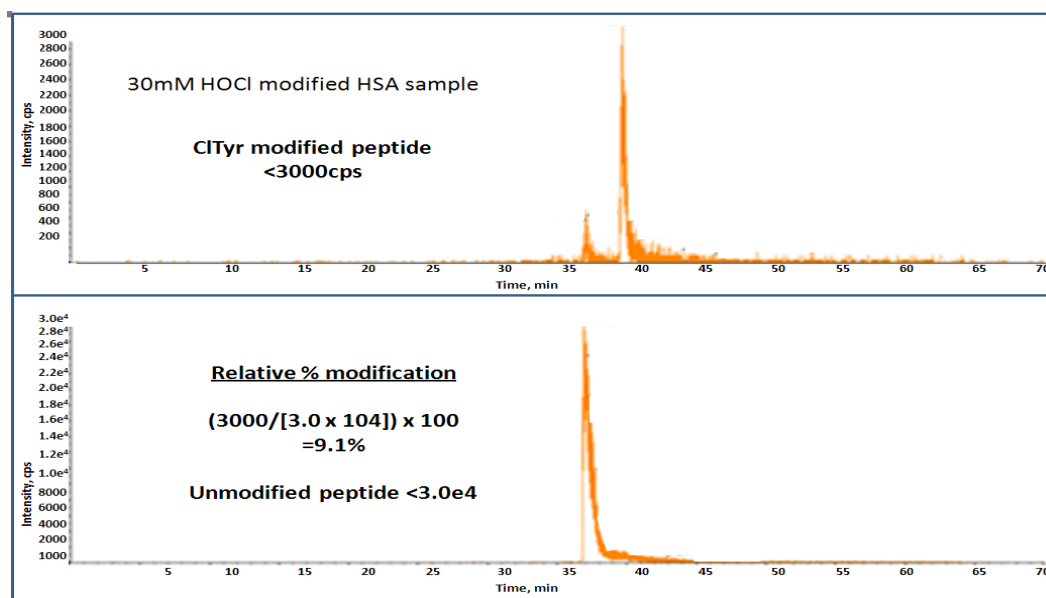


Figure 36: Percentage modification in a 30mM HOCl Modified HSA sample. The calculation of relative percentage modification of the RHPDYSVLLLR peptide in a 30mM HOCl modified HSA sample is displayed above. Signal intensity from the modified peptide, 3000cps (top panel) and the unmodified peptide,  $3.0 \times 10^4$ cps (bottom panel) are used for the calculation.

### 3.4.2 MRM detection of ClTyr modified peptides in HOCl modified HSA samples

The presence of the ClTyr modified and unmodified RHPDYSVLLLR peptide in a 30mM HOCl HSA sample was indicated using an MRM method. A second MRM program to include the other ClTyr modified peptides observed in the conventional MSMS analysis of the HOCl modified HSA samples was written using these observations (Table 13). The CE value for each transition was chosen using the values from the mass spectrometry data collected during MSMS analysis. The Q3 values were also chosen depending on the most frequently seen and intense fragment ions observed previously during conventional MSMS analysis.

To test the sensitivity of the MRM program a lower concentration of HOCl modified HSA (3mM) was analysed instead of the previous 30mM HOCl modified HSA sample (Figure 37). Three MRM transitions for one peptide are used to avoid

false positives. For a true positive and identification of a modified or unmodified peptide in the sample, all three transitions should be eluted at a common point in the chromatography gradient. In Figure 37 elution of single transitions have been labelled in smaller, orange font. The peaks labelled with arrows are the peaks where all three Q3 transitions for the targeted are commonly eluted. The MRM program identifies a peak with two transitions for the RHPDYSVLLLLR + ClTyr peptide (seen at 32 minutes during the chromatography gradient) but this is not an identification of this modified peptide in the unmodified HSA sample as all three transitions for the peptide are not seen. What is believed to be the true RHPDYSVLLLLR + ClTyr modified peptide (ringed in red) is observed to be eluted at 40 minutes during the chromatography gradient. All three transitions for the modified peptide (Q1=501.0/Q3=514.4, 401.3 and 613.3) are all seen to have a common retention time. As a control for the MRM acquisition method is was also used to analyse an unmodified HSA sample targeting for the modified peptides as well as the unmodified peptides (Figure 38).

Table 13: MRM acquisition method for the identification of ClTyr in HOCl modified HSA.

Peptide	Q1 m/z	Q3 m/z	Time (msec)	CE (eV)
Modified RHPDYSVLLLLR + ClTyr	501.1	514.37 401.29 613.44	20	27
Unmodified RHPDYSVLLLLR	490.03	514.37 401.29 613.44	20	27
Modified RHPYFYAPPELLFFAK + ClTyr	593	964.5 867.5 625.3	20	21
Unmodified RHPYFYAPPELLFFAK	582	964.5 867.5 625.3	20	21
Modified DVFLGMFLYEYAR + ClTyr;Ox(M)	837.75	175.1 362.2 475.3	20	31
Unmodified DVFLGMFLYEYAR + Ox(M)	821	175.1 362.2 475.3	20	31

The above table is the program written for the identification of more ClTyr modified peptides observed during conventional MSMS analysis of the HOCl modified HSA samples. From left to right the first column is the peptide to be identified, the second column is the Q1 or precursor mass of that peptide, the third column is the fragment masses or Q3 values used to identify the peptide, the fourth column is the dwell time and the third column is the collisional energy used for fragmentation.

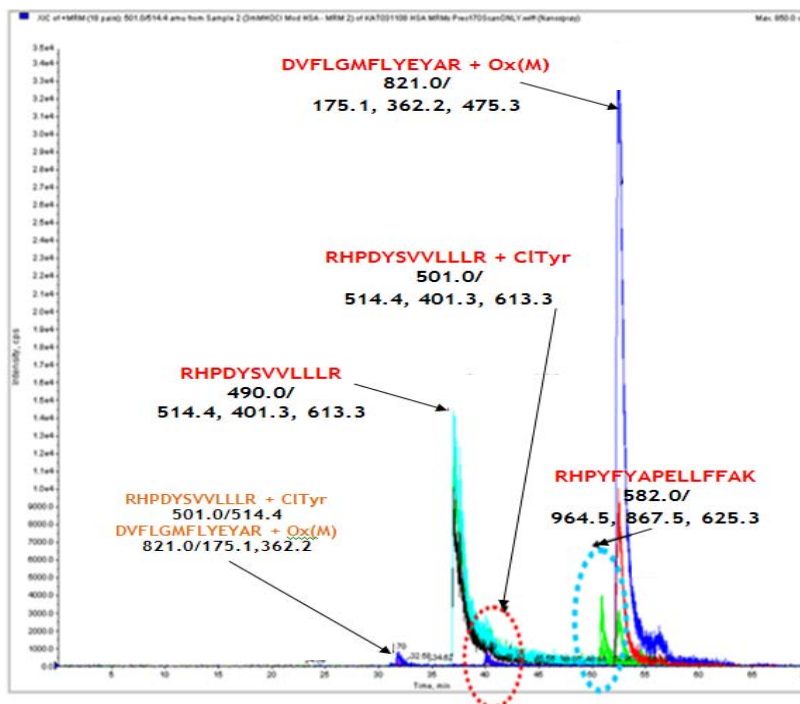


Figure 37: 3mM HOCl modified HSA- MRM. The figure illustrates that the MRM program has identified the targeted peptides in a 3mM HOCl modified sample. The peak signals labelled in red are those where all three Q3 transitions are seen to be commonly eluted. Those that are in the smaller font in orange are peaks where only the signal from a single transition is seen.

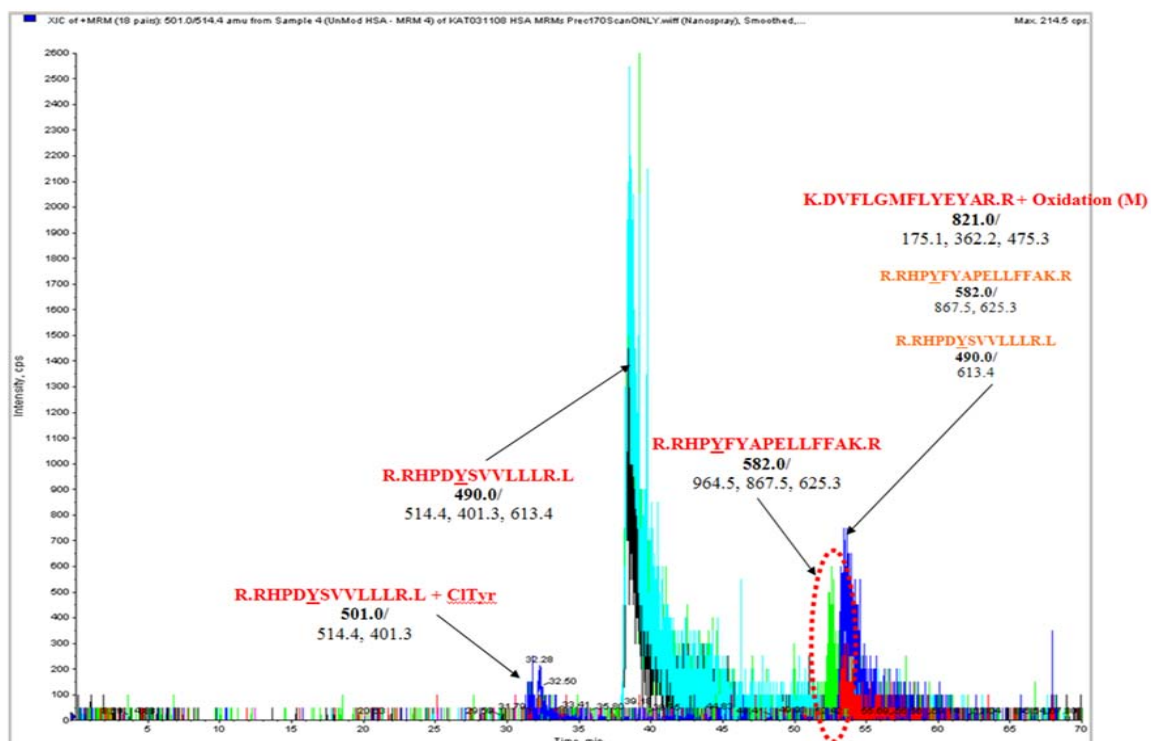


Figure 38: Unmodified HSA- MRM. An analysis of an unmodified HSA sample using the same MRM program targeting for unmodified and CITyr modified peptides. The peptide ringed in the red is the unmodified RHPYFYAPELFFAK peptide.

The degree of modification for each peptide is not known when using this MRM program as the DVFLGMFLYEYAR + Oxidation(M) peptide has been counted as unmodified because it does not contain a ClTyr modification. The oxidation of the methionine residue is not specific to disease and can happen either during sample preparation or be influenced by the increasing HOCl concentration of the sample. The MRM method was re-written to include and target for the unmodified DVFLGMFLYEYAR peptide in the HSA samples.

#### **3.4.2.1 Optimising the ClTyr MRM acquisition method to target all possible modification states for each peptide**

The MRM method was re-written to include the three different DVFLGMFLYEYAR peptide modification states. The MRM will now include the DVFLGMFLYEYAR peptide without any modification, the peptide with the Oxidation(M) modification and the peptide with the Oxidation(M) and ClTyr modification (Table 14). There are some other possible modified peptide states for the targeted peptides such as DVFLGMFLYEYAR + diTyr, DVFLGMFLYEYAR + 2ClTyr and DVFLGMFLYEYAR + 2ClTyr; Ox(M). These oxidation states however were never observed during the conventional MSMS analysis of the various HOCl modified HSA samples so they are not included in the MRM method.

Table 14: The optimised MRM acquisition method.

Peptide	Q1 m/z	Q3 m/z	Time (msec)	CE (eV)
RHPDYSVLLLR + C <sub>1</sub> Tyr	501.1	514.37 401.29 613.44	20	27
RHPDYSVLLLR	490.03	514.37 401.29 613.44	20	27
RHPYFYAPPELLFFAK + C <sub>1</sub> Tyr	593	964.5 867.5 625.3	20	21
RHPYFYAPPELLFFAK	582	964.5 867.5 625.3	20	21
DVFLGMFLYEYAR + 2C <sub>1</sub> Tyr;Ox(M)			Never been seen in MSMS data	
DVFLGMFLYEYAR + 2C <sub>1</sub> Tyr			Never been seen in MSMS data	
DVFLGMFLYEYAR + C <sub>1</sub> Tyr;Ox(M)	837.75	175.1 362.2 475.3	20	31
DVFLGMFLYEYAR + Ox(M)	821	175.1 362.2 475.3	20	31
DVFLGMFLYEYAR	813.45	175.1 362.2 475.3	20	31

From left to right the first column is the peptide targeted for the second column is the Q1 mass, the third column is their Q3 transitions and the fourth column is the dwell time. The fifth column is the CE values which were written and chosen from MSMS data collected as before. The Q3 masses are common to both the modified and unmodified states of a peptide

The newly optimised MRM method was used to analyse additional HOCl modified HSA samples. As a control an unmodified HSA sample was analysed first (Figure 39). All three transitions for each unmodified peptide targeted by the MRM method were identified with common elution times. The unmodified sample is seen to have both the unmodified DVFLGMFLYEYAR peptide and the DVFLGMFLYEYAR + Ox(M) modified peptide.

The RHPDYSVLLLR peptide is the strongest, most intense seen peptide ( $<1.35 \times 10^4$  cps), eluting at 39 minutes, RHPYFYAPPELLFFAK is observed at 54 minutes with an intensity of  $<600,000$  cps and DVFLGMFLYEYAR is seen at 58 minutes with an intensity of 50,000 cps. The DVFLGMFLYEYAR + Ox(M) modified peptide is seen at 56 minutes and is the lowest intensity at approximately

<250cps. There is a single transition (Q1=501.0/Q3=514.5) from the RHPDYSVLLLLR + ClTyr modified peptide which is observed again at 32 minutes (ringed in orange) during the chromatography gradient. This is a false positive; there is only one transition for the RHPDYSVLLLLR + ClTyr peptide with no others confirming its presence in the unmodified sample. Directly below the peak for the unmodified RHPDYSVLLLLR peptide (boxed in red) a peak for all three Q3 transitions for the modified RHPDYSVLLLLR + ClTyr peptide. Elution of this ClTyr modified peptide is unlikely here with respect to elution time for the modified peak. Due to changes in polarity it is unlikely that both the modified and unmodified peptide shall be eluted at the same time. The signals for all three Q3 transitions are seen here so it is likely that this is not the ClTyr modified but in fact breakthrough of signal from the unmodified peptide (for a clearer view of the breakthrough signal see Figure 41). Breakthrough is caused from another signal due to poor selection in Q1. To identify which peak of the three commonly eluted transitions is the elution of the peptide targeted for the retention time of that peak must also be considered.

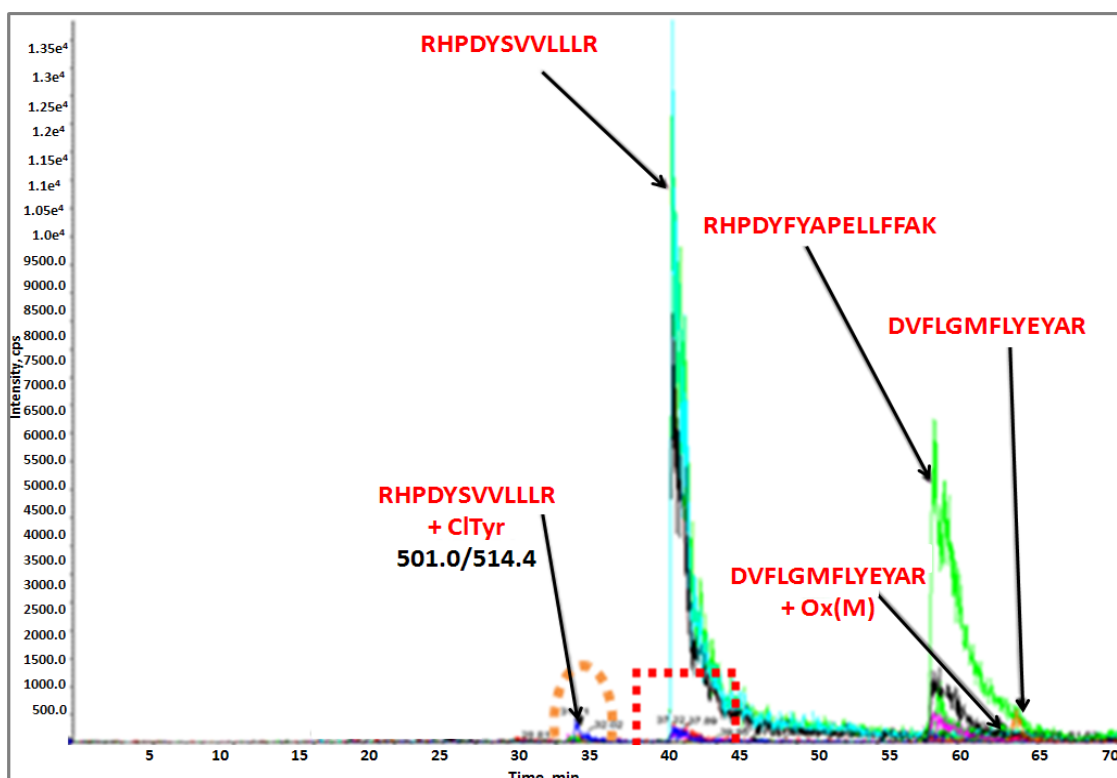


**Figure 39: Unmodified HSA - control - ClTyr MRM method. Illustrates the MRM method has detected the targeted peptides**

In the 10mM HOCl modified HSA sample analysed with the optimised MRM acquisition method to include all modification states of each peptide the

RHPDYSVLLLLR + ClTyr peptide is identified, with all three transitions observed to elute at the same time in the chromatography gradient (Figure 40). The RHPDYSVLLLLR peptide is again seen to be the strongest peak ( $2.4 \times 10^4$  cps) eluted at 28 minutes. The ClTyr modified state of this peptide, RHPDYSVLLLLR + ClTyr, is seen at 32 minutes with an intensity of 200,000 cps. The elution time of the RHPDYSVLLLLR + ClTyr is later as to be expected with respect to the unmodified state. The unmodified RHPYFYAPPELLFFAK peptide has been detected at 44 minutes with an intensity of 400 cps the ClTyr modified state of this peptide may be present but it may be in too low abundance to be seen. In the 10mM HOCl HSA sample there appears to be no DVFLGMFLYEYAR peptide in its unmodified state nor in its Oxidation(M) only state and it is possible that the peptides are present but in low abundance below the limit of detection. This peptide seems to only exist in the Ox(M); ClTyr and Ox(M); 2ClTyr states.

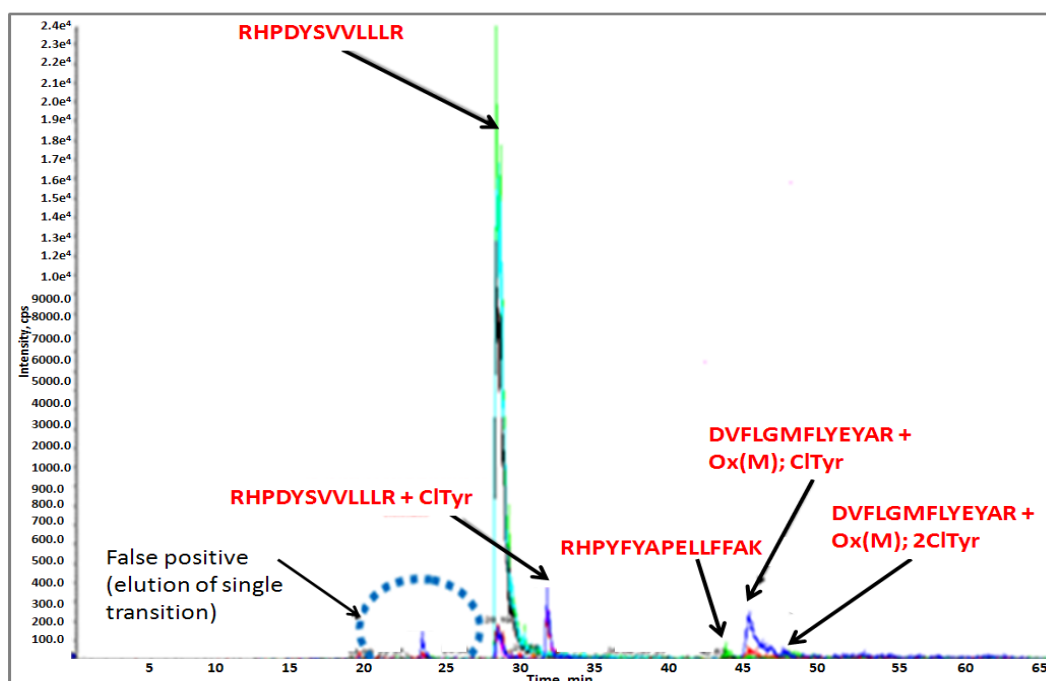


Figure 40: 10mM HOCl Modified HSA - Optimised MRM. The MRM experiment shows that there has been ClTyr modification in the 10mM HOCl HSA sample.

The XICs (Extracted Ion Chromatographs) from the TIC (Total Ion Chromatograph) can be separated out so that low abundance peaks can be analysed and the three transitions for a peptide can be compared when its XICs are isolated and Gaussian smoothed (Figure 41). The peaks were smoothed using a Gaussian filter width (percent of minimal distance between points) = 300 and

the limit of the Gaussian filter (number of minimal distance between points) = 50.

The unmodified RHPDYSVLLLR peptide ( $Q_1=490.0$ ) is seen to elute at 28 minutes (Figure 41). The transitions for the unmodified peptide ( $Q_1=490.0$ ) are in blue and for the C1Tyr modified peptide the transitions are in red ( $Q_1=501.0$ ). The top, middle and bottom panel show the comparison between the modified and unmodified peptide by their common  $Q_3$  masses ( $Q_3=514.4$ ,  $401.3$  and  $613.4$  respectively). In the top panel is the peak ringed in purple which is the false positive peak for the single transition ( $Q_1=501.0/Q_3=514.4$ ) for the C1Tyr modified peptide. All three transitions of the modified peptide have a peak (ringed in green) eluting at the same time as the unmodified peptide ( $Q_1=490.0$ , blue). This is where breakthrough of the signal (as previously discussed) can be clearly seen.

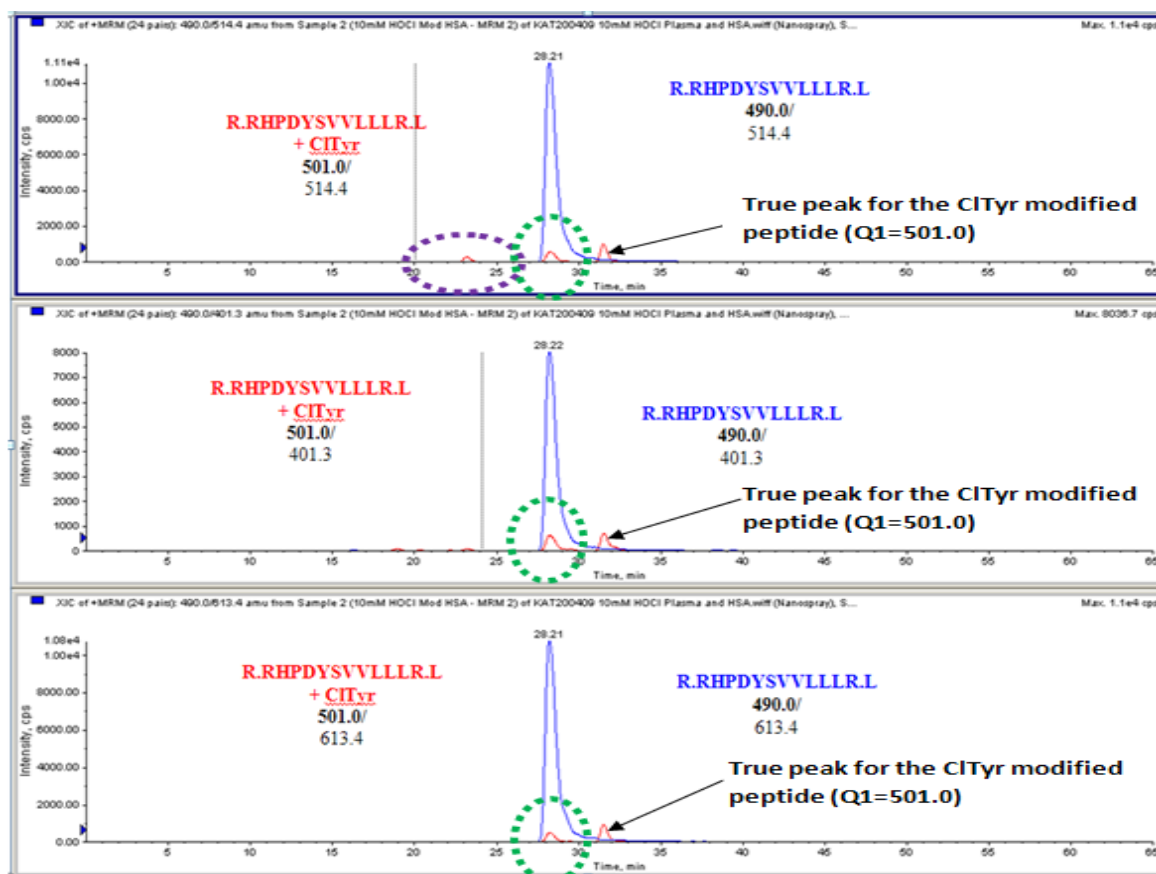


Figure 41: 10mM HOCl HSA Modified sample - RHPDYSVLLLR - modified versus unmodified peptide. The XIC's for the unmodified (blue) and modified peptide (red) are compared. The first peak in the C1Tyr modified 501.0/514.4 transition (circled in purple) is not common to the other two transitions ( $Q_3=401.3$  and  $613.4$ ) and is a false positive. The second peak for the C1Tyr modified peptide (circled in green) under the larger, more intense transition peak

for the unmodified peptide (blue) is common in all three transitions. This is caused by signal breakthrough from the unmodified peptide. The third peak of the modified RHPDYSVLLLR + ClTyr peptide is the most likely to be the true elution time as it is after the unmodified peptide (Q1=490.0, blue) which is to be expected.

### 3.4.3 The investigation of the RHPYFYAPELLFFAK peptide - determination of ClTyr Modification

The RHPYFYAPELLFFAK peptide does not appear to be ClTyr modified in this 10mM HOCl HSA sample (Figure 40). To determine the presence or absence of the peptide's chlorotyrosine modification the XICs (extracted ion chromatograph) were generated and the common transitions (Q3=964.5, 867.5 and 625.3) for the unmodified (Q1=582.0) and the ClTyr modified peptide (Q1=593.0) over-laid (Figure 42). The top panel in this figure displays an overlay of the three transitions of the RHPYFYAPELLFFAK peptide (Q1=582.0). The three transitions for the unmodified peptide (582.0/964.5, 582.0/867.5 and 582.0/625.3) have a common elution at 44 minutes therefore identifying the unmodified peptide in the 10mM HOCl modified HSA sample. The bottom panel displays an overlay of the three transitions of the ClTyr modified RHPYFYAPELLFFAK peptide (593.0/964.5, 593.0/867.5 and 593.0/625.3). The three transitions for the ClTyr modified peptide are not observed at a common retention time leading to the conclusion that there is no RHPYFYAPELLFFAK + ClTyr modified peptide in this 10mM HOCl modified sample.

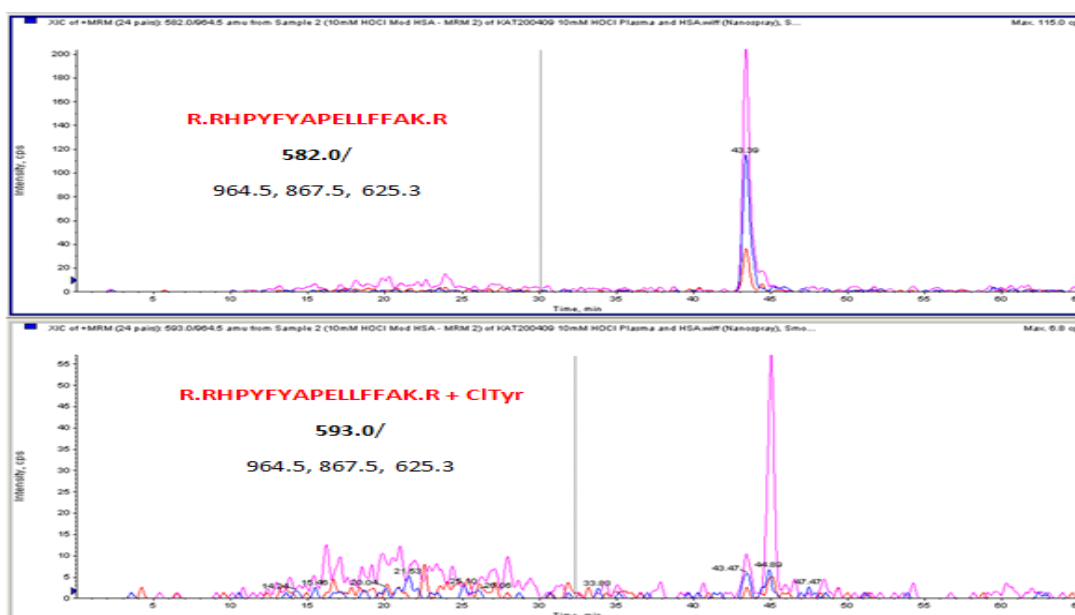


Figure 42: 10mM HOCl modified HSA sample - RHPYFYAPELLFFAK - comparison of the modified and unmodified peptide

In the 0.25mM HOCl modified HSA sample the RHPYFYAPPELLFFAK peptide is observed (Figure 43). The modified RHPYFYAPPELLFFAK + ClTyr peptide (Q1=593.0) however is seen to be eluted at the same time as the unmodified peptide (55 minutes) in very low abundance with a signal of 45cps in comparison with the unmodified peptides signal intensity of 1,300cps. Elution of the “unmodified peptide” at the same time as the modified peptide is unlikely due to the change in the peptide’s polarity. This is another example of the breakthrough of signal from the unmodified peptide. The modified RHPYFYAPPELLFFAK + ClTyr peptide in the 0.25mm HOCl modified HSA sample is therefore unlikely to be present.

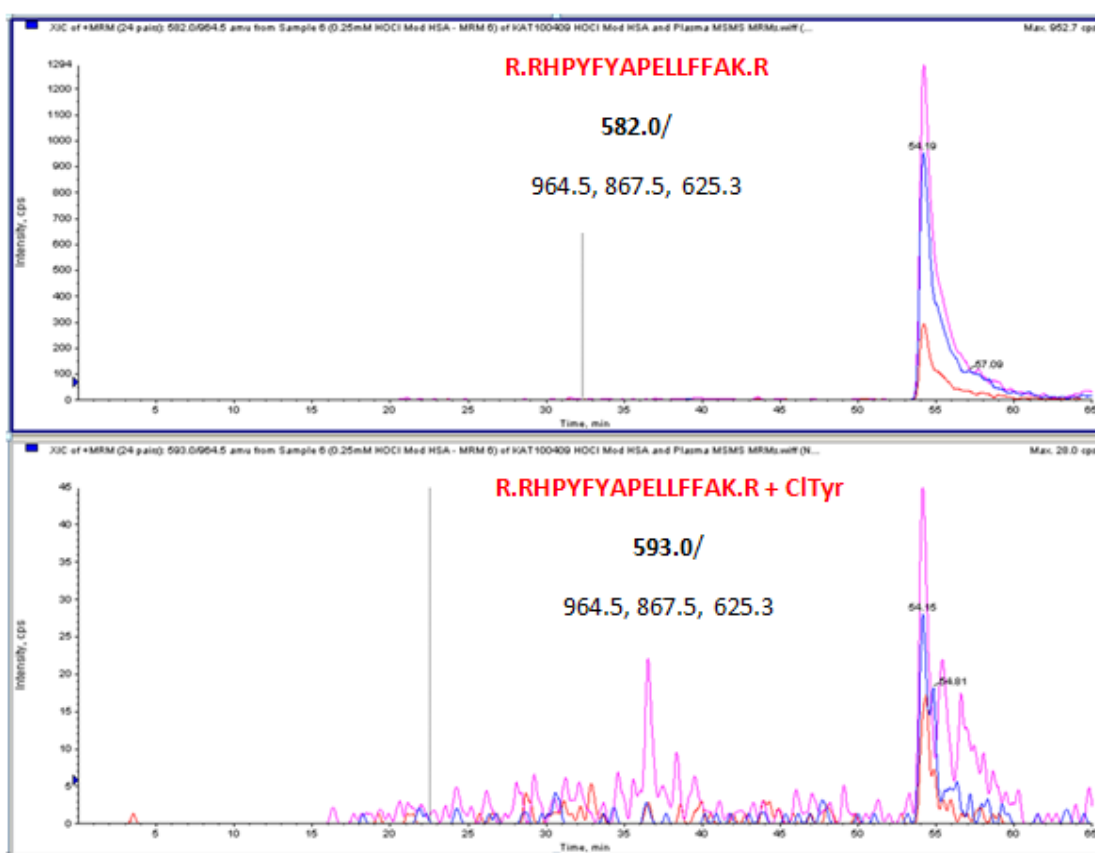


Figure 43: A 0.25mM HOCl modified HSA sample - RHPYFYAPPELLFFAK - comparison of the modified and unmodified peptide. This figure displays the three transitions (Q3=964.5, 867.5 and 625.3) over-laid for the unmodified (Q1=582.0, top panel) RHPYFYAPPELLFFAK peptide eluted at 55minutes and the ClTyr modified RHPYFYAPPELLFFAK peptide (Q1=593.0, bottom panel) eluted at 55minutes in the 0.25mM HOCl modified HSA sample. Both the modified and unmodified states of the peptide are unlikely to be eluted at the same time. This is another example of signal breakthrough from the unmodified peptide.

### 3.4.4 The investigation of the DVFLGMFLYEYAR peptide's modification states in various HOCl in vitro modified HSA samples

The XIC's for the DVFLGMFLYEYAR peptide and its modified states are generated and compared and the most abundant modified state of the peptide in the 10mM HOCl modified HSA sample is identified (Figure 44). Panel A displays the three transitions (Q3=175.1, 362.2 and 475.3) over-laid for the unmodified DVFLGMFLYEYAR peptide (Q1=813.45). There is no common elution time for the three transitions so it is likely that this peptide either does not exist in the unmodified form in a 10mM HOCl HSA sample or is in such low abundance that it is below the limit of detection. Panel B displays the three transitions (Q3=175.1, 362.2 and 475.3) over-laid for the Oxidation(M) modified peptide (Q1=821.0, panel B). There is a common elution time at 44 minutes and it is common to all three transitions indicating that the DVFLGMFLYEYAR + Ox(M) peptide is present in the 10mM HOCl HSA sample. Panel C displays the three transitions (Q3=175.1, 362.2 and 475.3) over-laid for the Oxidation(M) and ClTyr modified peptide (Q1=837.75, panel C). The three transitions are commonly eluted for the Ox(M) + ClTyr modified peptide and are seen at 46 minutes also indicating the presence of the Ox(M);ClTyr modified state of the peptide in the 10mM HOCl sample. Panel D displays the three transitions (Q3=175.1, 362.2 and 475.3) over-laid for the Oxidation(M) and 2ClTyr (Q1=855.0, panel D) modified state of the peptide. Although low in intensity (150cps) and therefore abundance the common elution times for the Ox(M);2ClTyr modified state is seen at 47 minutes indicating the modified state of this peptide is present in the 10mM HOCl sample.

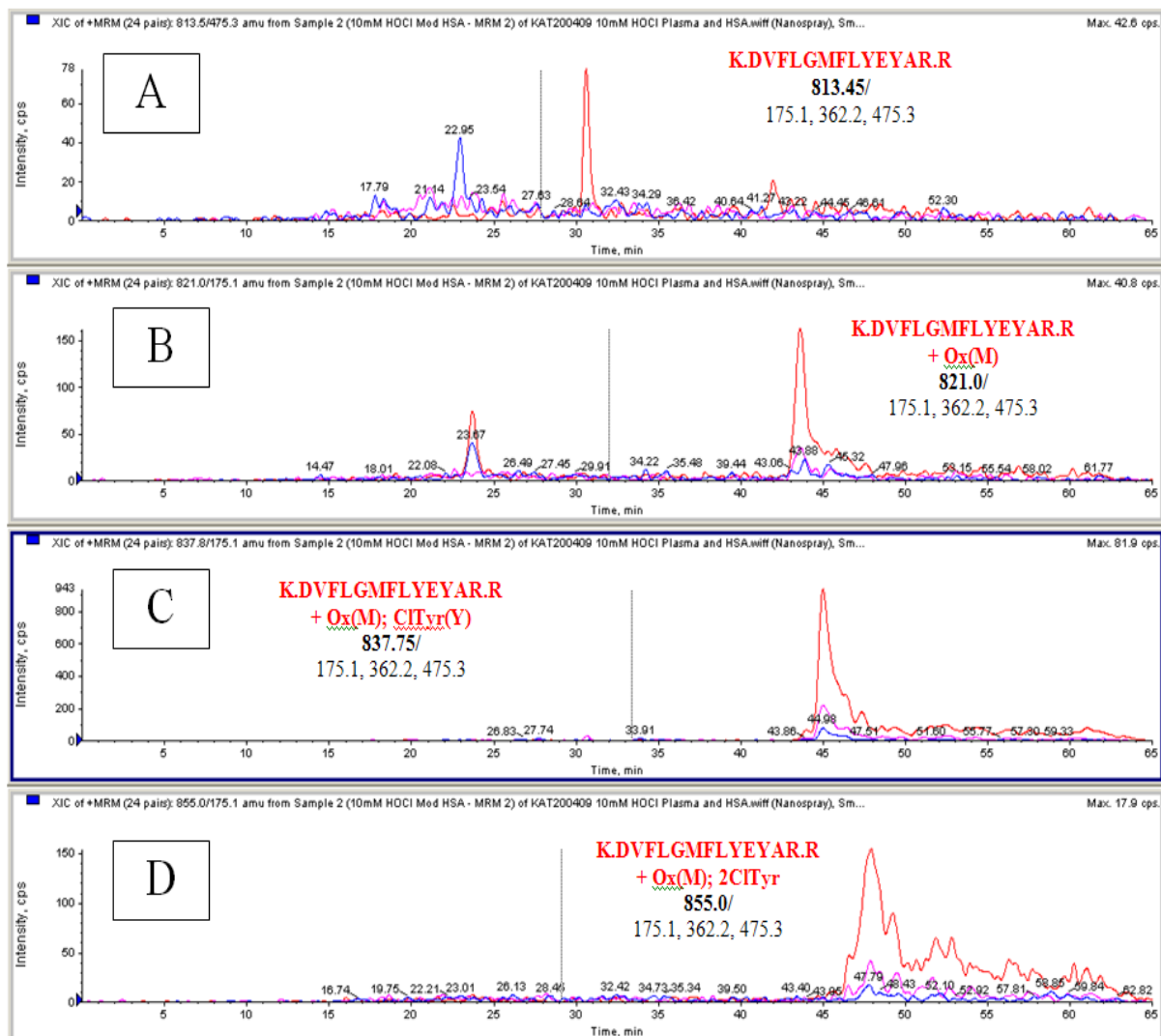


Figure 44: 10mM HOCl Modified HSA sample - DVFLGMFLYEYAR - comparison of the modified and unmodified peptide.

There does not seem to be any of the unmodified DVFLGMFLYEYAR peptide (Q1=813.0) in the 10mM HOCl modified HSA sample meaning that the peptide at this concentration is in one modified state or another. The elution times for the DVFLGMFLYEYAR + Ox(M) (Q1=821.0), DVFLGMFLYEYAR + Ox(M);ClTyr (Q1=837.75) and DVFLGMFLYEYAR + Ox(M);2ClTyr (Q1=855.0) modified peptides are to be expected. The oxidation of the DVFLGMFLYEYAR peptide will make the peptide more polar so the signal of the Ox(M) (Q1=821.0) modified peptide will be earlier than the unmodified peptide (not observed) if it were detected and indeed the Ox(M);ClTyr and Ox(M);2ClTyr modified peptides. The chlorination of the first and second tyrosine residues will make the DVFLGMFLYEYAR peptide less polar leading to the modified peptides Ox(M);ClTyr (Q1=837.75) and Ox(M);2ClTyr (Q1=855.0) having later retention times respectively.

To investigate which modified state is the most predominant in the 10mM HOCl modified HSA sample the common transition (Q3=175.1, 362.2 and 475.3) from each modified state of the DVFLGMFLYEYAR peptide were compared (Figure 45). The three transitions (Q3=475.3 - top panel, 362.2 - middle panel and 175.1 - bottom panel) of each modified state; unmodified (Q1=813.45, blue), Ox(M) modified (Q1=821.0, red), Ox(M);ClTyr modified (Q1=837.75, pink) and Ox(M);2ClTyr modified (Q1=855.0, green) of the DVFLGMFLYEYAR peptide.

In all three panels the most intense signal is from the Ox(M);ClTyr (Q1=837.75) modified state. In the 10mM HOCl HSA modified sample the DVFLGMFLYEYAR peptide is most abundant in the Ox(M);ClTyr modified state. From this observation it can be assumed that the peptide will be modified at certain side chains which are more susceptible to oxidation than others.

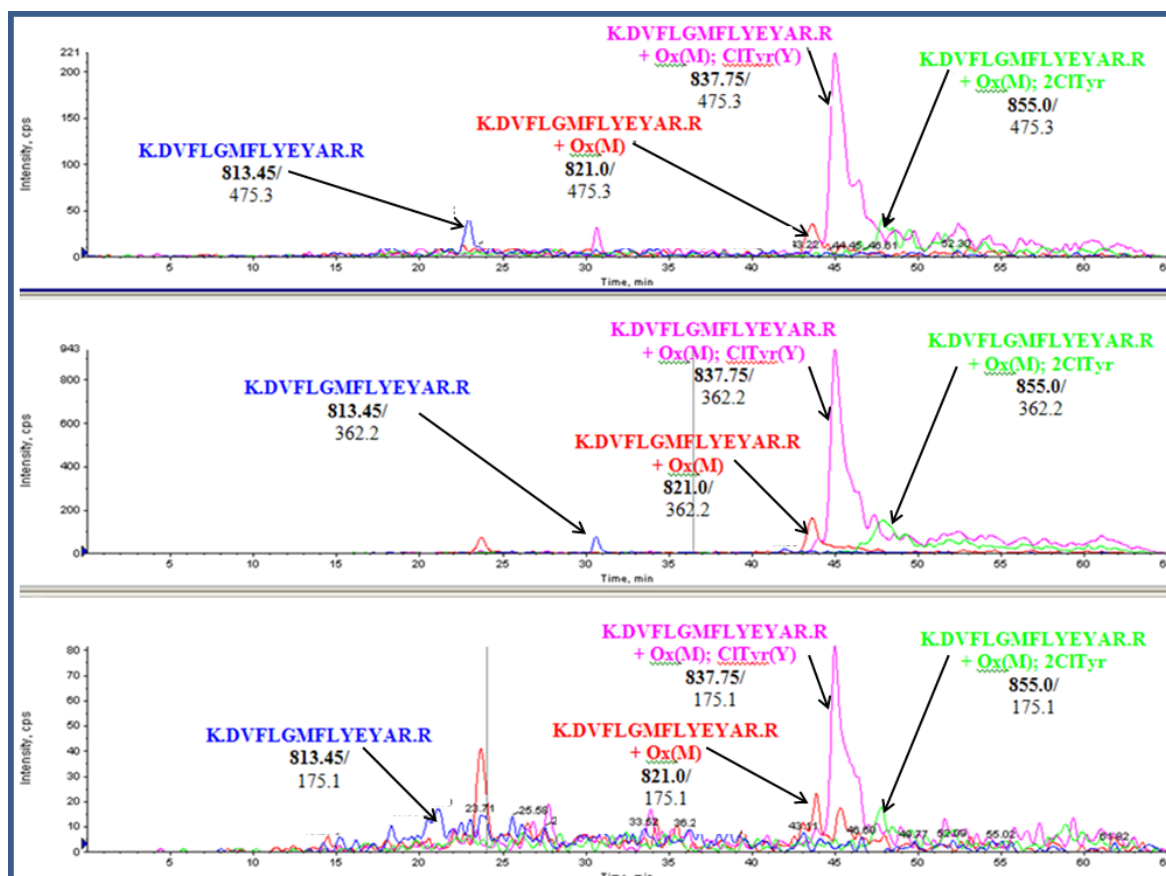


Figure 45: 10mM HOCl modified HSA sample - DVFLGMFLYEYAR - comparison of the modified states peptide. By comparing the three MRM transitions (Q3=175.1, 362.2 and 475.3) of each modified state we can clearly see that in the 10mM HOCl modified HSA sample the Oxidation(M); ClTyr (Q1=837.75) modified state is the most predominant.

### 3.5 The application of the ClTyr MRM acquisition method for the analysis of plasma

The MRM method has detected and identified the targeted chlorotyrosine modifications on a purified HSA protein modified by HOCl *in vitro*. The method was first optimised on purified HSA so that it could then be employed for the detection of ClTyr modifications in a real life biological sample. Albumin is the most abundant protein in plasma (50-75%) so a method developed to target for ClTyr modifications on purified HSA can be successfully applied to target ClTyr modifications on albumin in plasma. Plasma from a plasma pool of healthy volunteers was modified *in vitro* using the same protocol as the purified HSA (see 3.2.1) and was analysed by the ClTyr MRM method. An unmodified plasma sample was analysed using the ClTyr MRM method as a control (Figure 46). The false positive peak from the (501.0/514.4m/z) transition for the RHPDYSVLLLLR.L + ClTyr modified peptide is observed in the unmodified plasma sample (as seen before in the unmodified HSA sample) eluting at 30 minutes. The unmodified RHPDYSVLLLLR peptide (Q1=490.0) is seen at 36 minutes, the unmodified RHPYFYAPELLFFAK peptide (Q1=582.0) at 54 minutes, the unmodified DVFLGMFLYEYAR peptide (Q1=813.45) at 59 minutes and the DVFLGMFLYEYAR + Ox(M) modified peptide (Q1=821.0) at 56 minutes. The DVFLGMFLYEYAR + Ox(M) peptide can become methionine oxidised non specifically during sample preparation or biologically in the volunteer or patient and is eluted before the unmodified DVFLGMFLYEYAR peptide as expected due to the change in the peptide's polarity after modification.

The ClTyr MRM method was then employed to detect the targeted ClTyr modifications in the 10mM HOCl modified plasma sample (Figure 47). The RHPDYSVLLLLR unmodified peptide (Q1=490.0) was seen at 31 minutes with its ClTyr modified state RHPDYSVLLLLR + ClTyr (Q1=501.0) at 34 minutes. The unmodified RHPYFYAPELLFFAK peptide (Q1=582.0) was seen at 44 minutes but its ClTyr modified state was not initially obvious and it was possible that it was present at low intensity. The modified DVFLGMFLYEYAR + Ox(M);ClTyr peptide (Q1=837.75) was seen at 47 minutes and its methionine oxidation only state, DVFLGMFLYEYAR + Ox(M) (Q1=821.0) was seen as expected before in the gradient at 46 minutes. The modified DVFLGMFLYEYAR + Ox(M);2ClTyr state (Q1=855.0) was eluted last as expected at 49 minutes.

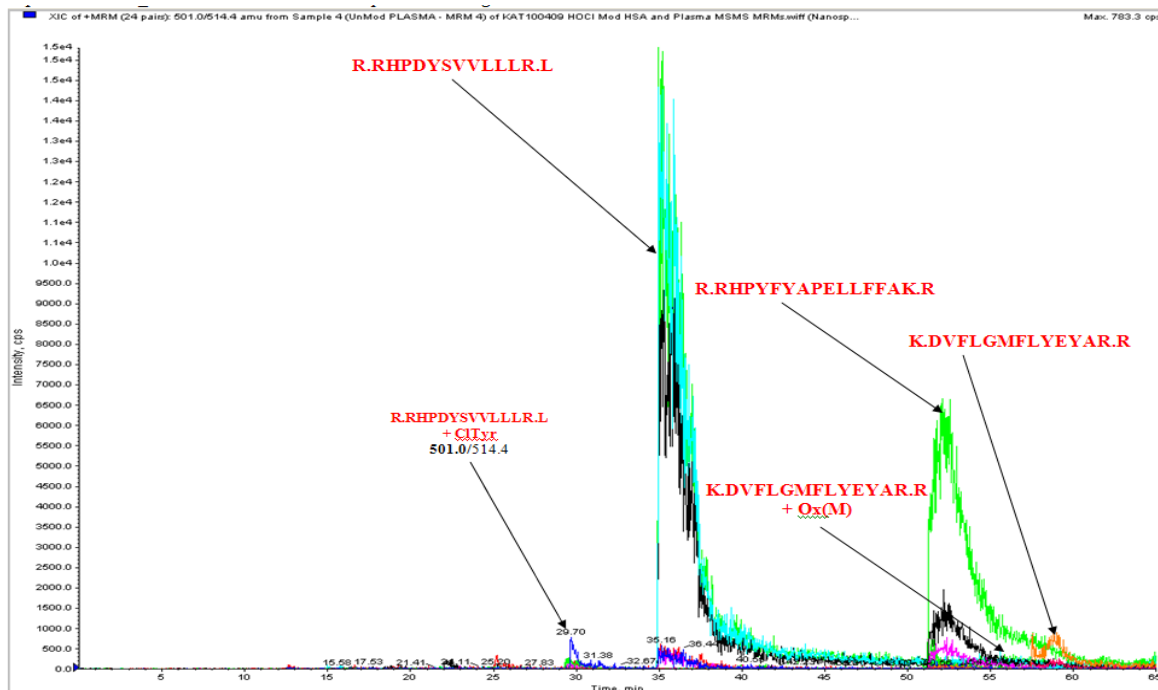


Figure 46: Unmodified plasma sample - control - CITyr MRM. The unmodified peptides targeted by the MRM are identified in the unmodified plasma sample.

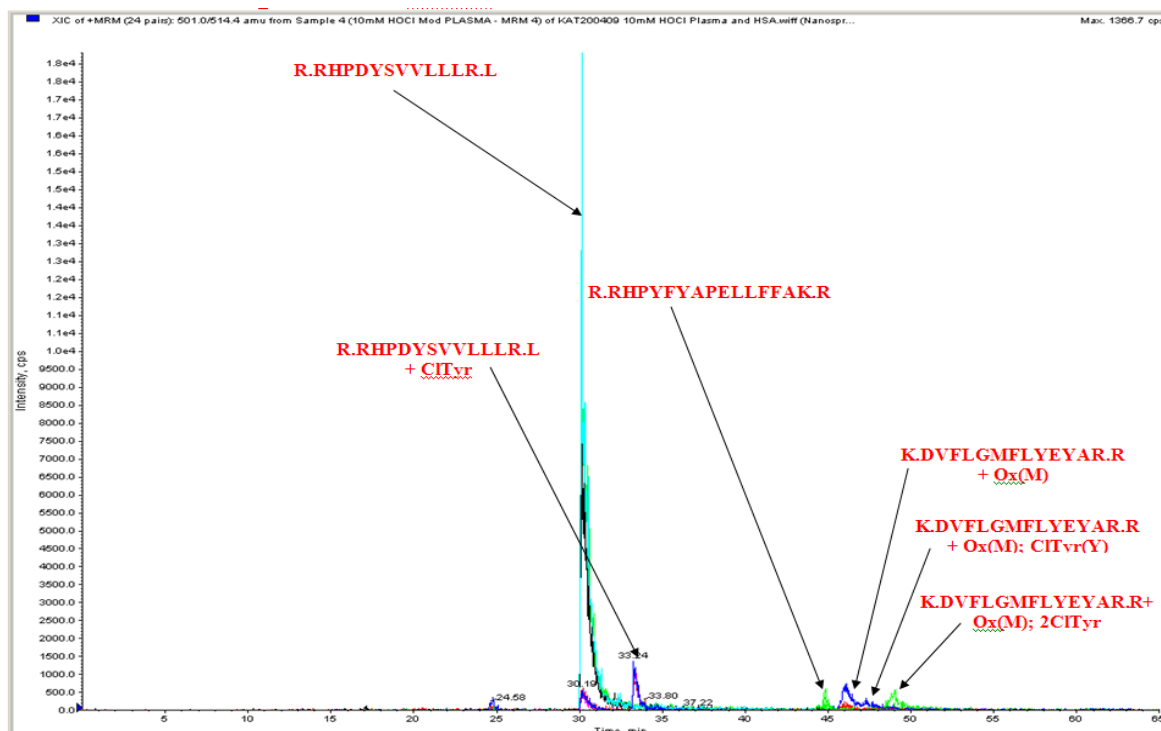


Figure 47: 10mM HOCl modified plasma - CITyr MRM. The figure illustrates that the MRM method has detected the targeted unmodified peptides and CITyr modified peptides in the 10mM HOCl modified plasma sample.

### 3.5.1 Comparing the XICs of the unmodified and ClTyr modified RHPYFYAPPELLFFAK peptide in the 10mM HOCl plasma sample

The RHPYFYAPPELLFFAK + ClTyr modified peptide may be in low abundance in the 10mM HOCl modified plasma sample. To assess for the peptide the individual XICs of the three transitions for the peptide were isolated.

The XICs for the transitions of the RHPYFYAPPELLFFAK + ClTyr modified peptide were Gaussian smoothed for comparison and to look at in more detail (Figure 48). The top panel shows the unmodified RHPYFYAPPELLFFAK peptide (Q1=582.0) is in low abundance but present as all three transitions have a common elution time. The ClTyr modified RHPYFYAPPELLFFAK + ClTyr peptide (Q1=593.0) is in low abundance with a signal intensity of <80cps in comparison with the unmodified peptide (intensity <347cps). There is a common elution time for all three transitions for the ClTyr modified peptide (41 minutes) indicating the modified peptides probable presence in the sample but the signal is low so it is not easily observed in the TIC (Figure 47). Before a conclusion can be made about the presence of a peptide in a sample when analysed by an MRM method for lower, less abundant peptides it is necessary to extract individual XIC's for analysis.

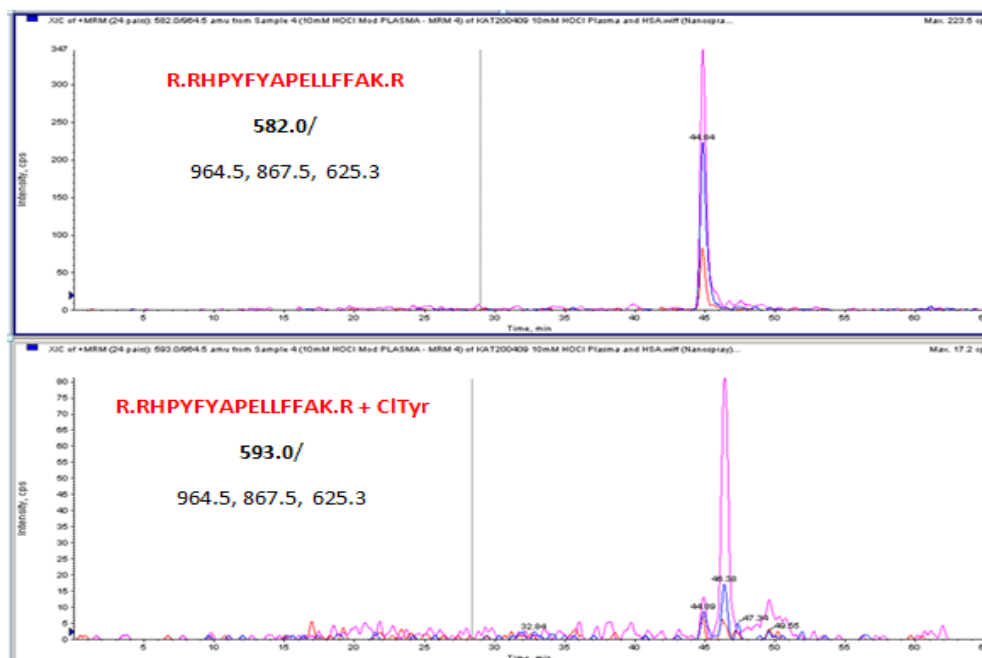


Figure 48: 10mM HOCl HSA Modified sample - RHPYFYAPPELLFFAK - comparison of the modified and unmodified peptide. The figure illustrates the over-laying of the three transitions (Q3=964.5, 867.5 and 625.3) for the unmodified RHPYFYAPPELLFFAK peptide (Q1=582.0 - top panel) and the modified RHPYFYAPPELLFFAK + ClTyr peptide (Q1=593.0 - bottom panel).

### 3.5.2 The relative percentage modification in the 10mM HOCl modified plasma sample for the RHPDYSVLLLLR peptide

The relative percentage oxidation was calculated for the RHPDYSVLLLLR peptide in the 10mM HOCl modified plasma sample. Relative percentage modification was found by comparing the Gaussian smoothed XICs of the unmodified RHPDYSVLLLLR and modified RHPDYSVLLLLR +ClTyr peptide (Figure 49). This assumes that the ionisation energies for the modified and unmodified peptide are equal. Equation 7 (as first described in 3.4.1.1) was used to calculate approximate relative percentage modification.

Equation 7

$$\text{Relative percent oxidation} = \frac{\text{Intensity of ClTyr peptide}}{\text{Intensity of ClTyr peptide} + \text{Intensity of unmodified peptide}} \times 100$$

The three transitions for the RHPDYSVLLLLR unmodified peptide ( $Q_1=490.0$ ) and the ClTyr modified peptide ( $Q_1=501.0$ ) were compared. For the transitions;  $Q_3 = 514.4$ ,  $401.3$  and  $613.4$  the relative percentage oxidation were approximately 12.4%, 16.5% and 12.4% respectively. The average approximate relative percentage oxidation for this peptide in a 10mM HOCl modified plasma sample was 13.77%.

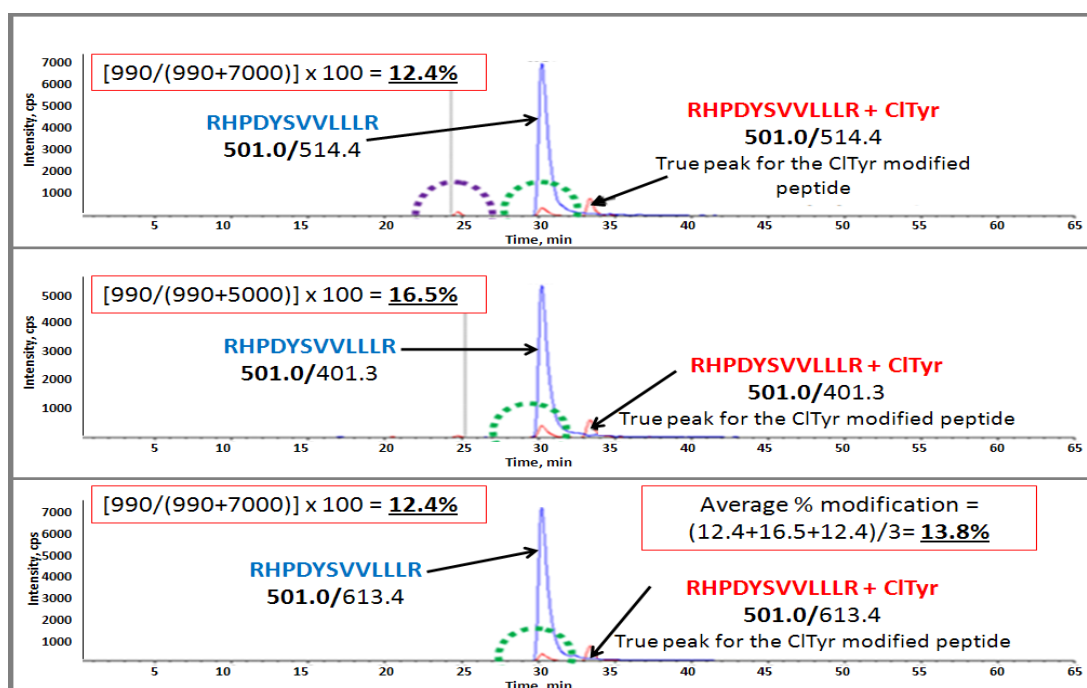


Figure 49: 10mM HOCl HSA Modified sample - RHPDYSVLLLLR - modified versus unmodified peptide. The above figure illustrates the comparison of the three common transitions ( $Q_3=514.4$  - top panel,  $401.3$  - middle panel and  $613.4$  - bottom panel) for the unmodified

RHPDYSVLLLLR peptide (Q1=490.0, blue) and the modified RHPDYSVLLLLR + CITyr peptide (Q1=501.0, red). As seen previously in HOCl modified HSA samples the false positive peak (circled in purple) is seen in the modified RHPDYSVLLLLR + CITyr peptide (501.0/514.4, red - top panel). Circled in green is breakthrough from the signal from the unmodified peptide.

The unmodified and CITyr modified DVFLGMFLYEYAR peptide is detected in the 10mM HOCl modified plasma sample (Figure 50). Panel A indicates that the unmodified DVFLGMFLYEYAR peptide (Q1=813.45) exists in very low abundance (<30cps) in the 10mM HOCl plasma sample. Panel B displays the DVFLGMFLYEYAR + Ox(M) modified peptide (Q1=821.0) state seen at 45 minutes. Panel C displays the DVFLGMFLYEYAR + Ox(M);CITyr (Q1=837.75) peptide. The three transitions have a common elution time seen at 47 minutes in the chromatography gradient. Panel D shows the transitions of the DVFLGMFLYEYAR + Ox(M);2CITyr (Q1=855.0) peptide eluting at a common time at 49 minutes into the chromatography gradient.

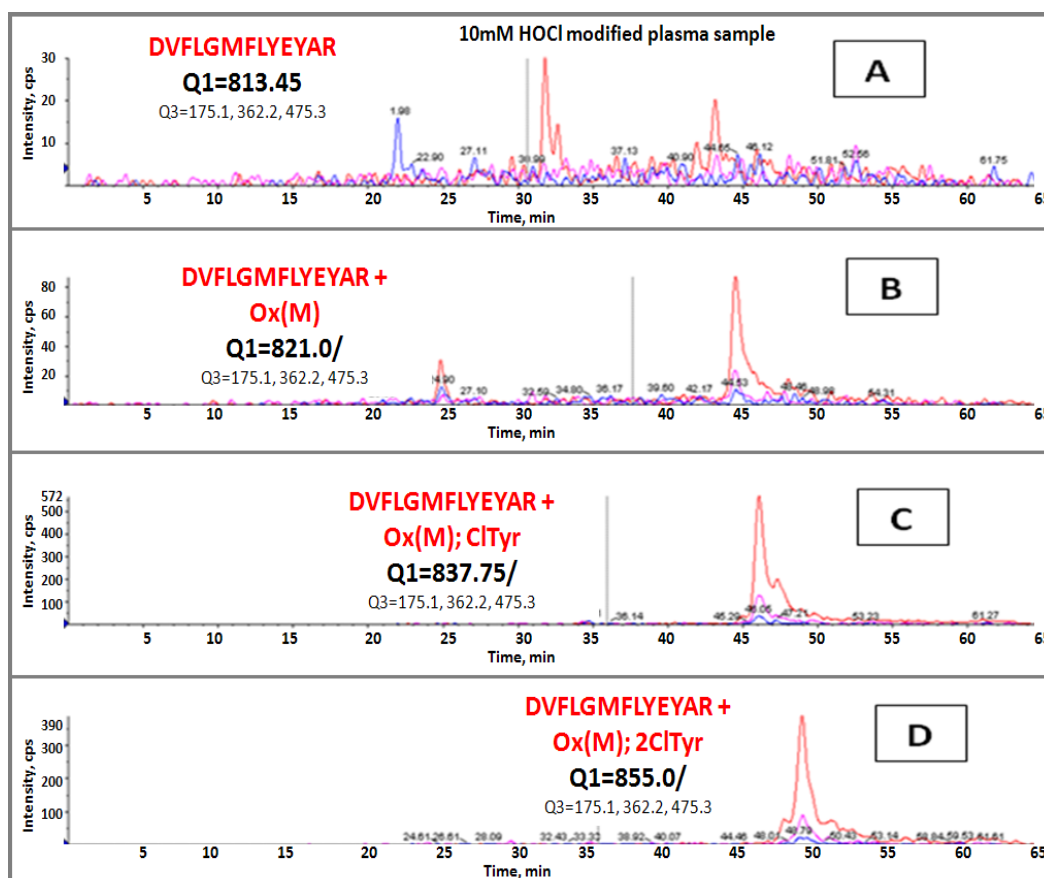


Figure 50: 10mM HOCl Modified plasma sample - DVFLGMFLYEYAR - comparison of the modified states. The figure illustrates the over-laid three transitions (Q3=175.1, 362.2 and 475.3) for each modified state of the DVFLGMFLYEYAR peptide in the 10mM HOCl modified plasma sample.

From the XICs we can calculate an approximation of the relative percentage oxidation of the DVFLGMFLYEYAR peptide in a 10mM HOCl modified plasma sample using the previous equation used (3.4.1.1 and 3.5.2). The calculation was performed using the values of the most intense (Q3=475.3 - red) transition in each modified state (unmodified=30cps, Ox(M)=80cps, Ox(M);ClTyr=572cps and Ox(M);2ClTyr=390cps).

$$\text{Relative percentage oxidation} = [(80 + 572 + 390) / (30 + 80 + 572 + 390)] \times 100$$

$$= 97.22\% \text{ (approximate)}$$

The relative percentage oxidation for the DVFLGMFLYEYAR peptide was found to be 97.22%. This appears high in comparison to the RHPDYSVLLLLR peptide (13.8%) in a 10mM HOCl modified plasma sample. This may be because there are a greater number of residues susceptible to oxidation on the DVFLGMFLYEYAR peptide than the RHPDYSVLLLLR peptide. The DVFLGMFLYEYAR peptide has a greater number of potential oxidation sites possessing the methionine residue, which is susceptible to oxidation and two tyrosines both susceptible to chlorination.

### 3.5.3 The relative percentage modification in the 0.25mM HOCl modified plasma sample for the RHPDYSVLLLLR

In a 0.25mM HOCl *in vitro* modified plasma sample the Oxidation(M) modified DVFLGMFLYEYAR peptide and the unmodified DVFLGMFLYEYAR peptide are the most predominant peptides (Figure 51). In panel A the unmodified DVFLGMFLYEYAR peptide (Q1=813.45) has a common elution time seen at about 47 minutes in the chromatography gradient. In panel B the three transitions for the DVFLGMFLYEYAR + Ox(M) peptide (Q1=821.0) also have a common elution time seen at 46 minutes. This will be the most abundant modified state of the DVFLGMFLYEYAR +Ox(M) peptide in the 0.25mM HOCl plasma sample as the signal intensity for this modification is  $\leq 1.4 \times 10^4$  cps in comparison to the signal for the unmodified peptide (panel A) which is  $\leq 100$  cps. In panel C for the DVFLGMFLYEYAR + Ox(M);ClTyr peptide (Q1=837.75) the three transitions commonly elute at 46 minutes. Due to the unexpected retention time this is possibly a false positive and breakthrough signal from the Ox(M) modified peptide. In panel D for the DVFLGMFLYEYAR + Ox(M);2ClTyr peptide (Q1=855.0)

there is no common elution time for all the transitions indicating that this modified state of the DVFLGMFLYEYAR + Ox(M);2ClTyr peptide does not exist in the 0.25mM HOCl plasma sample or is in abundance below the limit of detection. The unmodified and Oxidation(M) states of the DVFLGMFLYEYAR peptide therefore appear the most predominant.

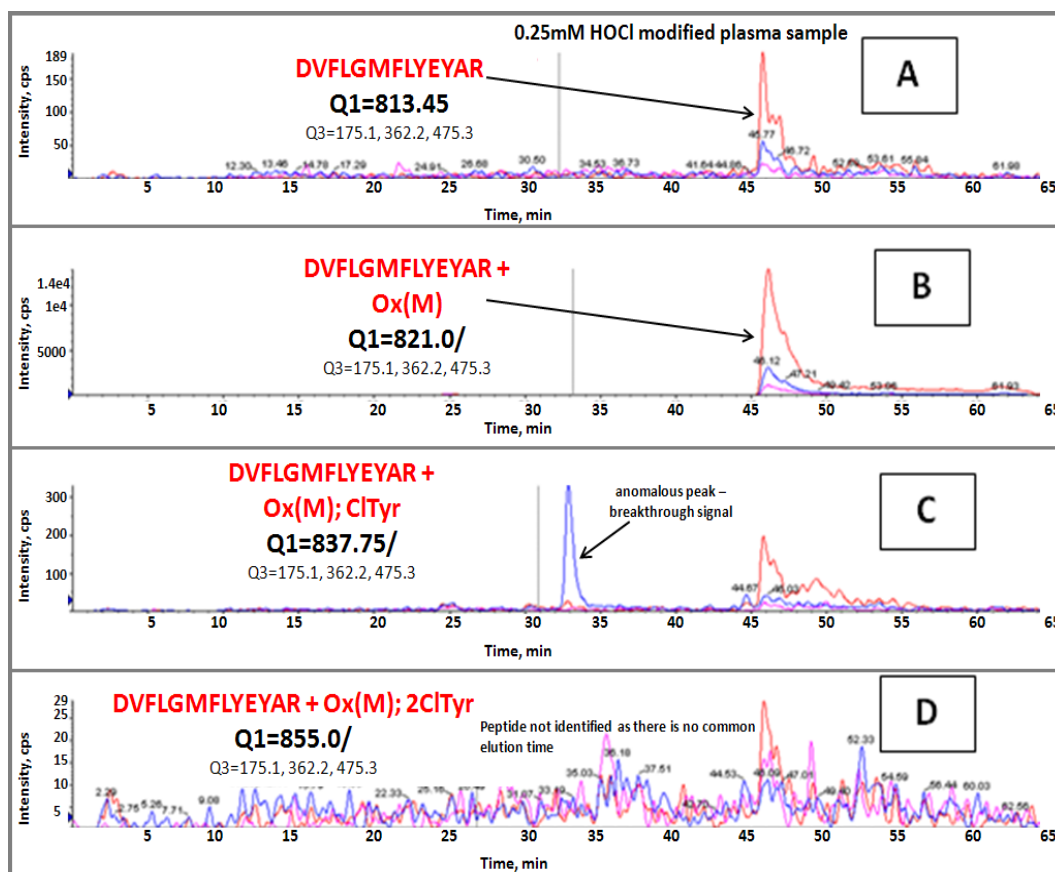


Figure 51: A 0.25mM HOCl Modified plasma sample - DVFLGMFLYEYAR - comparison of the modified states. The figure illustrates the DVFLGMFLYEYAR peptide's modified states with their three common transitions (Q3=175.1, 362.2 and 475.3) over-laid.

The approximate relative percentage oxidation of this peptide was calculated as before (3.4.1.1 and 3.5.2) using the most intense Q3 transition (Q3=475.3 - red) in each modified state. The intensities for each modified state of the peptide were 189cps,  $1.4 \times 10^4$  cps and 300cps for the unmodified state, Ox(M) modified state and the Ox(M);ClTyr modified state respectively.

$$\text{Relative percentage oxidation} = \left[ \frac{(1.4 \times 10^4 + 300)}{(189 + 1.4 \times 10^4 + 300)} \right] \times 100$$

$$= 98.7\% \text{ (approximately).}$$

The percentage modification for the DVFLGMFLYEYAR peptide is similar in the 0.25mM and 10mM HOCl modified plasma samples (approximately 98.7% and 97.2% respectively). In the 0.25mM HOCl modified plasma samples the DVFLGMFLYEYAR peptide is predominantly methionine oxidized (in the Ox(M) state). In the higher 10mM HOCl modified plasma sample the peptide is predominantly in the Ox(M);ClTyr and Ox(M);2ClTyr modified states. Although relative percentage oxidation of the peptide is close in the 0.25mM and 10mM HOCl modified plasma samples at the higher HOCl concentration the peptide is in higher-level modified states.

#### 3.5.4 Conclusion of the development of the ClTyr MRM acquisition method

The ClTyr MRM has been able to identify the targeted ClTyr modified peptides in both the model purified protein HSA and in a biological sample, plasma. We have demonstrated by the ClTyr MRM analysis of various concentrations of HOCl *in vitro* modified plasma samples the degree of oxidation in individual peptides. The ClTyr modification as discussed could be an important biomarker for inflammatory diseases. The ClTyr MRM for the albumin may therefore be of use for the diagnosis of oxidative stress and its diseases in clinical plasma samples.

### 3.6 Nitration of HSA

Myeloperoxidase (MPO) is both present and active in inflammatory conditions and will lead to the formation of nitrotyrosine and chlorotyrosine. These molecules have been found to be elevated in atherosclerosis <sup>[57]</sup>. It is likely that a combination of biomarkers is required for the diagnosis of disease and if an MRM acquisition method can be written for ClTyr modifications in human serum albumin one for NiTyr should also be possible.

The compound, 3-morpholinosydnonimine (SIN-1) (Figure 52) is unstable and will release nitric oxide ( $\cdot\text{NO}$ ) and superoxide ( $\text{O}_2^{\cdot-}$ ) to form peroxynitrite ( $-\text{ONOO}$ ) which will then decompose to modify tyrosine side chains. To mimic the formation of nitrotyrosine, SIN-1 is commonly used to modify proteins *in vitro* [180-184].

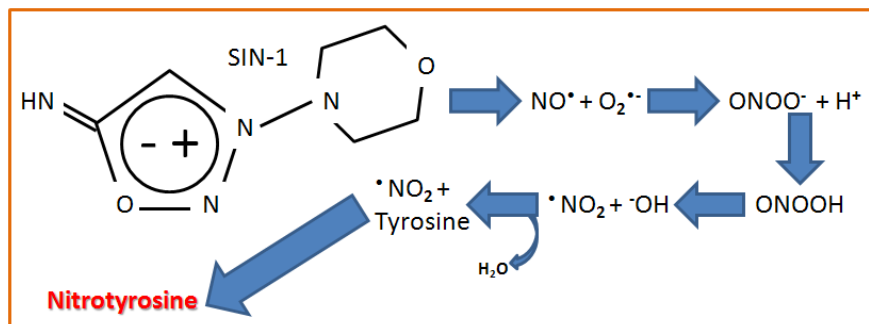


Figure 52: The above is the structure for SIN-1. It is an unstable compound and will release nitric oxide ( $\text{NO}^\bullet$ ) and superoxide ( $\text{O}_2^{\bullet-}$ ) to form peroxynitrite ( $\text{-OONO}$ ) leading to the formation of nitrotyrosine.

### 3.6.1 Results and Discussion – Detecting Nitrotyrosine in HSA

The various concentrations of the SIN-1 modified HSA samples were trypsin digested and analysed by separation of the peptides on the LC then detected by MSMS on the *Analyst Biosystems QTrap 2000*.

The SIN-1 modified human serum albumin samples were analyzed by conventional MSMS (2.4.1.4) on the Qtrap 2000 (*Applied Biosystems*, Warrington, UK) after being separated by liquid chromatography (2.4.1.3). The mass spectrometry data was searched with Mascot (2.4.1.5). Mascot reported the top protein hit to be human serum albumin and the HSA peptides that were identified as Nitrotyrosine (NiTyr) modified in the various SIN-1 modified HSA samples were;

YLYEIAR + NitroTyr (Y)

RHPDYSVLLLLR + NitroTyr (Y)

DVFLGMFLYEYAR + NitroTyr (Y); Oxidation (M)

RHPYFYAPELLFFAK + NitroTyr (Y)

The NiTyr modified peptides assigned by Mascot were then cross-referenced with their mass spectrometry data and the Mascot ion-match table. For a true match a good coverage of the y-ion series for a peptide should be identified and the y-ions should be identifiable in the signal. For an example of a NiTyr modified peptides with good confidence see the MSMS analysis of the YLYEIAR + NiTyr and

its ion-match table (Figure 53). In the ion-match table we can clearly see the full y-ion series has been identified from the mass spectrum data. The mass spectrum for the YLYEIAR + NiTyr modified peptide is labelled to show which y and b-ions have been identified. Those present in the ion-match table that are not labelled in the spectrum are of low intensity and can be seen when zoomed in. The peptides ion-score was 86 which is above the significance threshold calculated to be 48.

Observations from the mass spectrometry data collected during the conventional MSMS analysis of the various concentrations of SIN-1 modified HSA samples were used to write a MRM method. The MRM method was to be applied to detect targeted NiTyr modifications in the model purified protein, HSA, and a real biological sample, SIN-1 modified plasma (Table 15). The Q3 masses of the targeted peptides for the NiTyr MRM acquisition method were chosen due to their intensity and frequency seen in the MSMS analysis.

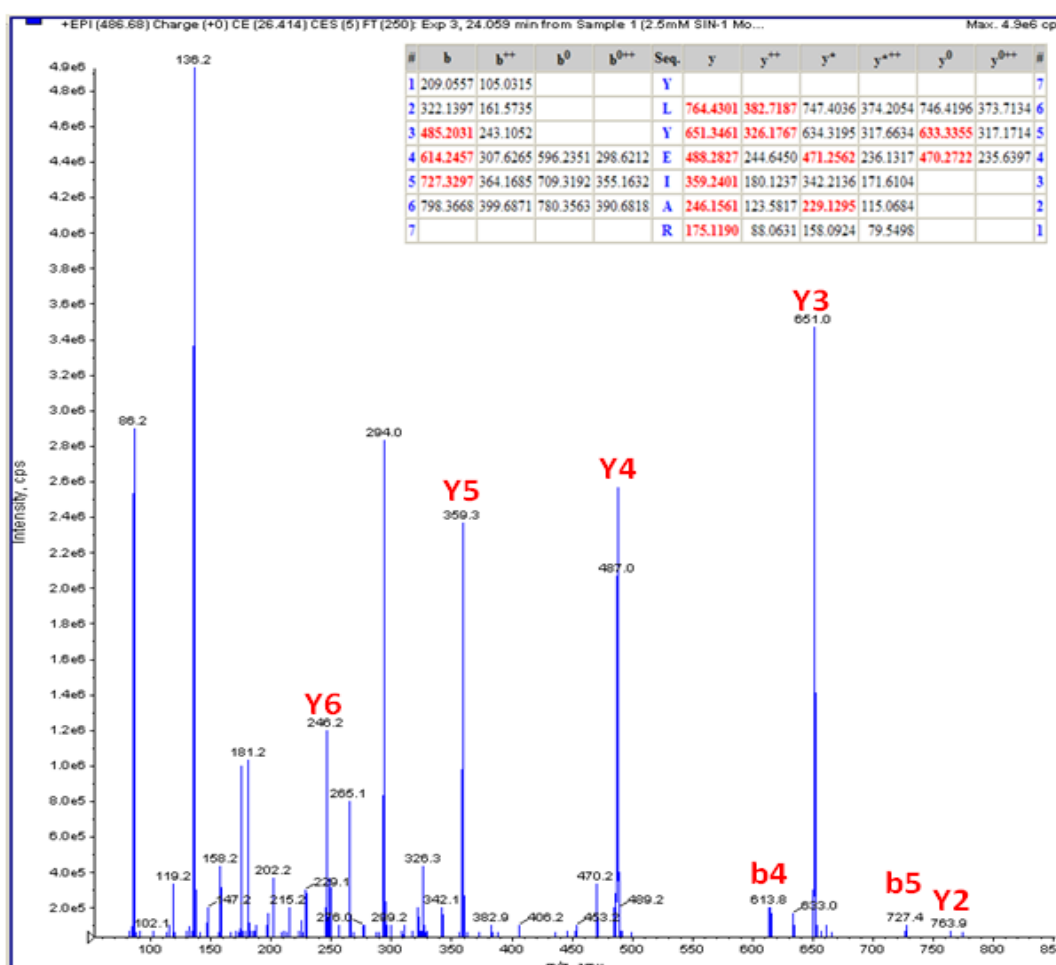


Figure 53: MSMS analysis of the YLYEIAR NiTyr modified peptide - Mass Spectrum and MASCOT ion-match table.

Table 15: MRM acquisition method for NiTyr modifications in HSA and plasma.

Peptide	Q1 m/z	Q3 m/z	CE (eV)
DVFLGMFLYEYAR + NiTyr;Ox(M)	842.72	746.31 859.39 1006.5	45
DVFLGMFLYEYAR + Ox(M)	820.57	1214.6 1101.5 961.48	45
YLVEIAR + NiTyr	487	651.35 359.24 246.16	28
YLVEIAR	464.2	764.43 651.35 246.16	28
RHPYFYAPELFFAK + NiTyr	648.6	625.37 964.55 365.22	35
RHPYFYAPELFFAK	634.05	1035.6 964.55 701.35	35
TYETTLEK + NiTyr	515.1	928.43 276.16 389.24	25
TYETTLEK	492.68	720.38 591.33 490.29	25

The NiTyr MRM acquisition method was written from the MSMS observations from MSMS analysis of HSA samples modified *in vitro* with varying concentrations of [SIN-1]. From left to right the first column is the peptide targeted for, the second column is the precursor mass and the third column is the Q3 m/z which were chosen due to their intensity and their frequency seen in the MSMS spectra. The fourth column is the collisional energy used.

### 3.6.2 The analysis of an unmodified HSA sample in comparison to a 2.5mM SIN-1 in vitro modified HSA and plasma sample by the NiTyr MRM acquisition method

To test the NiTyr MRM program a control unmodified HSA sample was analysed previous to the SIN-1 modified samples to ensure no cross-contamination (Figure 54). In the unmodified HSA sample we do not see the DVFLGMFLYEYAR + Ox(M) peptide when analysed with the NiTyr MRM program. The DVFLGMFLYEYAR + Oxidation(M) is seen in the 2.5mM SIN-1 modified sample (Figure 55) but not the unmodified sample (Figure 54). Although not detected by the MRM program, it is unlikely that there is no oxidation of the methionine present in this peptide in the unmodified sample as methionine oxidation is a process which happens naturally in the air and cannot be prevented or controlled.

The analysis of 2.5mM SIN-1 modified HSA and plasma samples by the NiTyr MRM, detected the targeted NiTyr modified peptides (Figure 55). The top panel in the figure is the TIC (total ion chromatography) of the 2.5mM SIN-1 modified HSA sample. The unmodified TYETTLEK peptide (Q1=492.7) is seen at 10 minutes, the unmodified YLYEIAR peptide (Q1=464.2) is seen at 20 minutes and its NiTyr modified state is seen at 23 minutes. The unmodified RHPYFYAPELLFFAK peptide (Q1=634.0) is seen at 33 minutes and the DVFLGMFLYEYAR + Ox(M) is seen at 41 minutes and the DVFLGMFLYEYAR + Ox(M);NiTyr is seen at 46 minutes in the 2.5mM SIN-1 HSA sample. The bottom panel in the figure displays the TIC of the SIN-1 modified plasma sample and the targeted peptides are again detected.

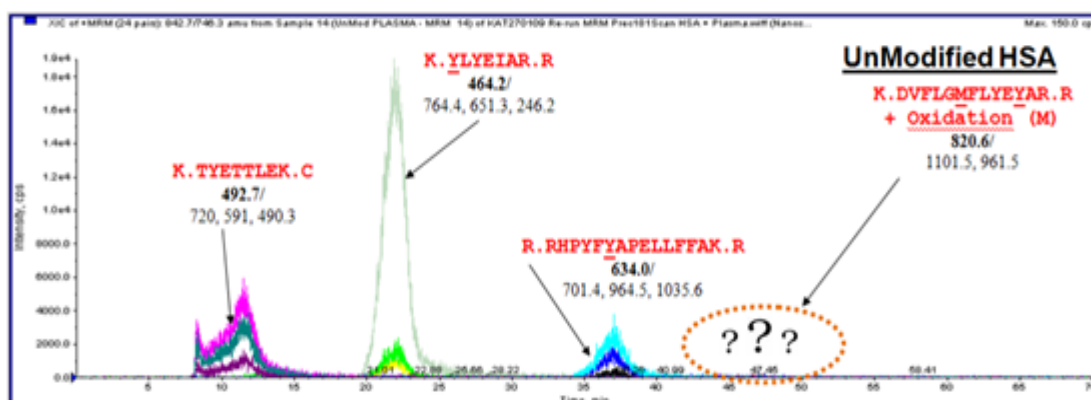


Figure 54: Unmodified HSA. The above figure shows that the NiTyr MRM for the detection of NiTyr modification in HSA has detected the targeted unmodified peptides.

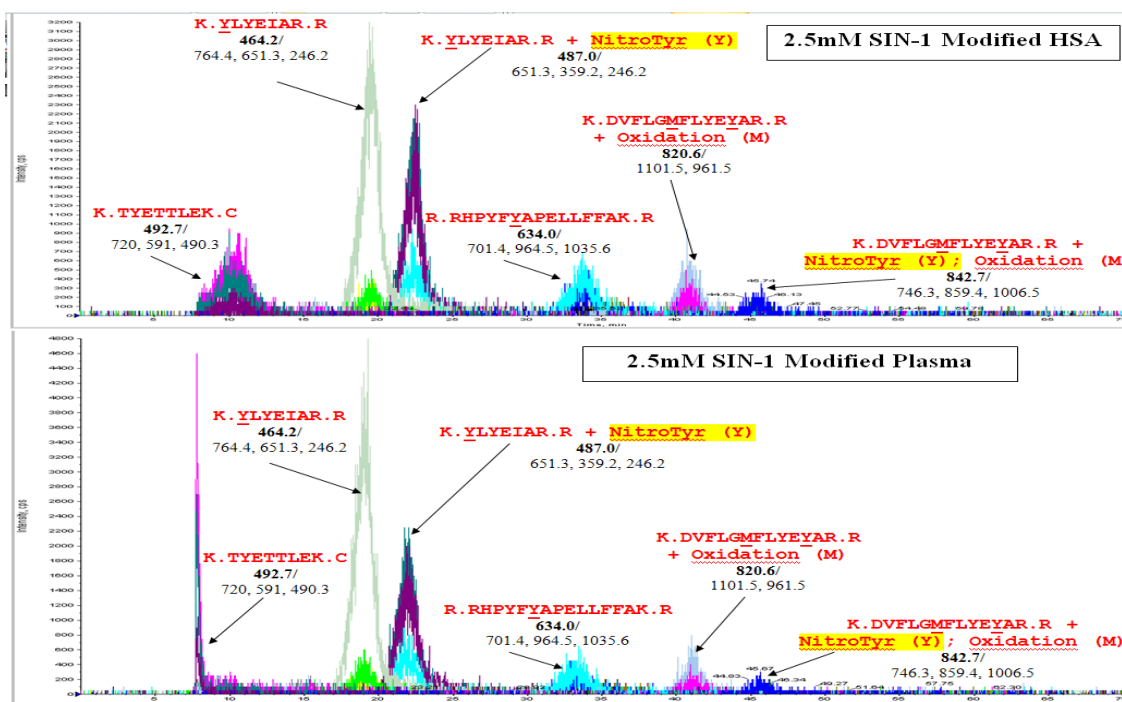


Figure 55: 2.5mM SIN-1 modified HSA and Plasma - NiTyR MRM. The above figure illustrates that the NiTyR MRM has detected the targeted NiTyR modifications in both the SIN-1 modified purified HSA protein and the real life biological sample plasma.

### 3.6.3 Optimising the NiTyR MRM method by increasing the scan time

To optimise the NiTyR MRM acquisition method and to ensure all peptides which are present in the sample are being detected the method's sensitivity was increased by increasing the dwell time from 20ms to 60ms. The total scan time for the method was therefore increased from 0.4sec to 1.952sec. Increasing the scan time means that more time will be spent "looking" for the chosen masses in Q1. Increasing the sensitivity of the method will decrease the resolution of the acquisition method which can lead to problems with quantification.

To test the new optimised NiTyR MRM method an unmodified HSA sample was analysed (Figure 56). Two false positive peaks for two NiTyR modified peptides were detected in the unmodified HSA sample. The single transitions for the modified RHPYFYAPELLFFAK + NiTyR ( $Q1=648.6/Q3=136.3$ ) peptide were seen at 32 minutes and a single transition for the RHPDYSVLLLLR + NiTyR ( $Q1=505.1/Q3=401.2$ ) peptide was seen at 37 minutes during the chromatography gradient. For a targeted peptide to be identified all three transitions must be seen commonly eluted so these signals are likely false positives caused by breakthrough from another signal. The false positive single transition for the RHPYFYAPELLFFAK + NiTyR peptide ( $Q1=648.6$ ) is also seen *before* the

unmodified state (Q1=634.0 seen at 45 minutes). When a peptide's tyrosine becomes nitrated the peptide becomes less polar and therefore has a longer retention time.

The newly optimised NiTyr MRM method was then used to analyse a 1mM SIN-1 modified plasma sample (Figure 57). The NiTyr MRM acquisition method detected all the targeted peptides in the 1mM SIN-1 modified plasma sample. What is interesting in the repetitive targeted MRM analysis of both the SIN-1 modified HSA and the SIN-1 modified plasma sample is that the YLYEIAR + NiTyr peptide's transitions form a split peak whereas all other transitions from the targeted peptides form a single peak.

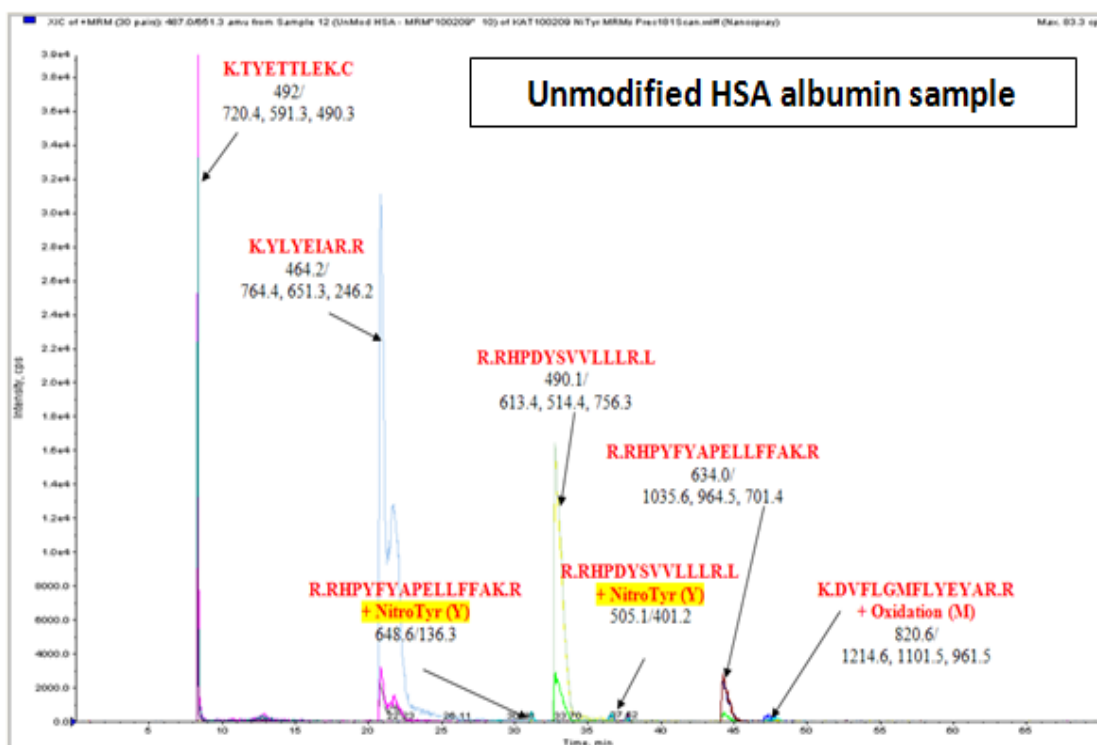


Figure 56: New optimised NiTyr MRM method - Test - Unmodified HSA sample. The figure illustrates that the newly optimised NiTyr MRM method has now detected all the targeted unmodified peptides.

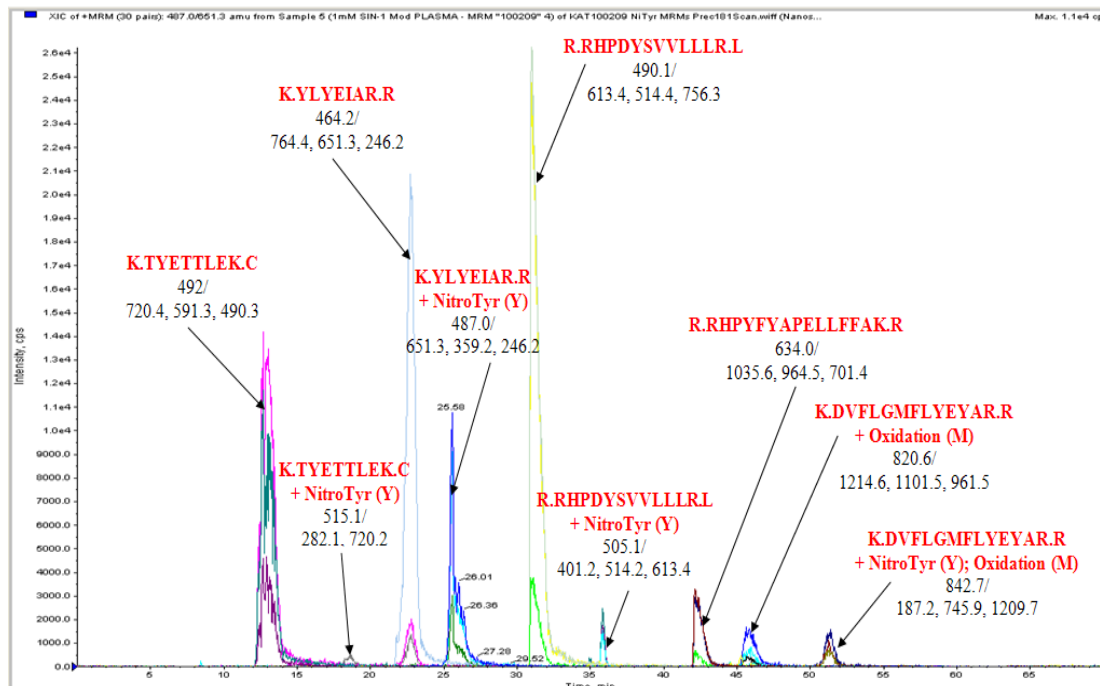


Figure 57: Newly optimised NiTyr MRM Method - 1mM SIN-1 modified plasma. The figure illustrates the analysis of a 1mM SIN-1 modified biological sample, plasma, with the optimised NiTyr MRM method. The newly optimised MRM method has detected the targeted unmodified and NiTyr modified peptides in the SIN-1 modified plasma sample.

### 3.6.4 Searching for the YLY<sup>2</sup>EIAR + NiTyr modified peptide by MSMS and the omission of the dynamic exclusion parameter

The “split-peak” elution of the Y<sup>1</sup>L<sup>2</sup>EIAR + NiTyr modified peptide could mean that there are two close possible elution times of the modified peptide in comparison to the unmodified state whose transitions form a single peak meaning one single elution time (Figure 58). The split-peak appears not to be an artefact as all three transitions for the modified YLYE<sup>1</sup>IAR + NiTyr peptide (Q1=487.0, Q3=651.3, 359.2 and 246.2) have a common elution time and all form the same split-peak pattern and the “split-peak” anomaly of the YLYE<sup>1</sup>IAR + NiTyr peptide was seen in various SIN-1 modified HSA and SIN-1 modified plasma samples.

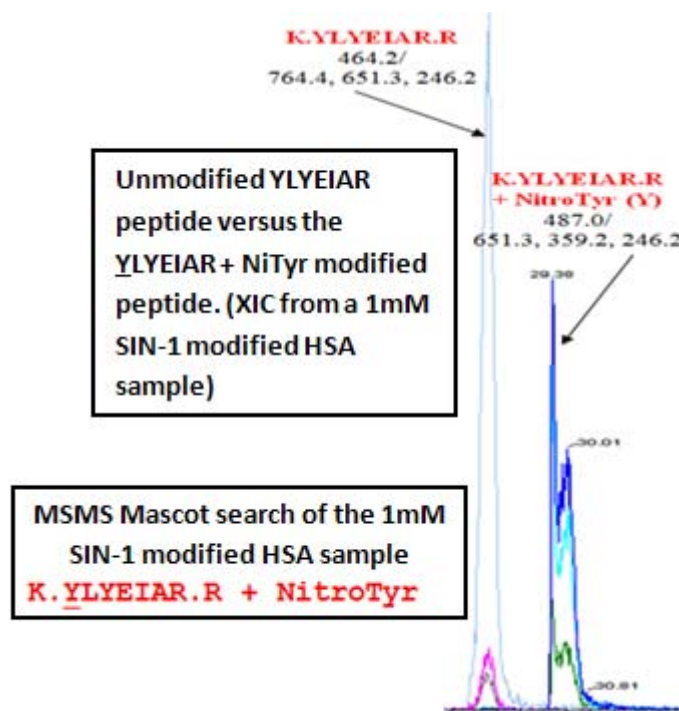


Figure 58: The YLYEIAK unmodified peptide compared with YLYEIAK + NiTyr peptide. The above figure illustrates the “split-peak” anomaly in a purified protein HSA sample.

When the MSMS data of these SIN-1 modified HSA and plasma samples is searched with Mascot the NiTyr modification is assigned to Y<sup>1</sup> in the peptide Y<sup>1</sup>LY<sup>2</sup>EIAK + NiTyr. The MSMS spectra and ion-match table confirms the modification on the Y<sup>1</sup> tyrosine in the peptide. When the SIN-1 modified samples were analysed with a conventional MSMS acquisition method the dynamic exclusion parameter was turned on to always exclude former target ions (2.4.1.4). When a mass is detected it will then be added to an exclusion list and no more data will be collected on this mass to ensure that other masses in the sample are seen and data is not collected repeatedly on the same mass. The YLY<sup>2</sup>EIAK + NiTyr (Y) and the Y<sup>1</sup>LYEIAK + NiTyr (Y) peptides will have the same masses. It is therefore possible that the modified YLY<sup>2</sup>EIAK + NiTyr (Y) peptide is present but the second peak is then ignored or rejected for MSMS analysis by the dynamic exclusion parameter in the information dependant acquisition experiment in the MSMS method. The MSMS acquisition method with the dynamic exclusion turned ‘on’ was compared with the MSMS acquisition method with the dynamic exclusion turned ‘off’ (Table 16). The table displays the Mascot identifications of the NiTyr modified peptides detected in a 2.5mM SIN-1 modified protein sample when the dynamic exclusion parameter in the MSMS

acquisition method is turned off. The YLY<sup>2</sup>EIAR + NiTyr peptide is not observed only the Y<sup>1</sup>LYEIAR + NiTyr peptide is.

Table 16: MSMS analysis of 2.5mM SIN-1 modified HSA and plasma with dynamic exclusion turned off

NiTyr modifications found with....		
	Dynamic Exclusion turned ON	Dynamic Exclusion turned OFF
HSA	K.YLYEIAR.R + NitroTyr (Y)	K.YLYEIAR.R + NitroTyr (Y)
	R.RHPDYSVLLLR.L + NitroTyr (Y)	K.TYETTLEK.C + NitroTyr (Y)
	K.DVFLGMFLYEYAR.R + NitroTyr (Y); Oxidation (M)	R.RHPDYSVLLLR.L + NitroTyr (Y)
		K.DVFLGMFLYEYAR.R + NitroTyr (Y); Oxidation (M)
Plasma	K.KYLYEIAR.R + NitroTyr (Y)	R.RHPDYSVLLLR.L + NitroTyr (Y)
	R.RHPDYSVLLLR.L + NitroTyr (Y)	K.DVFLGMFLYEYAR.R + NitroTyr (Y); Oxidation (M)
	K.DVFLGMFLYEYAR.R + NitroTyr (Y); Oxidation (M)	

The above displays from left to right in the first column the 2.5mM SIN-1 modified sample which was analysed (either HSA or plasma) and the second and third columns display the NiTyr modifications identified by Mascot with the dynamic exclusion turned “on” and “off”.

The Y<sup>1</sup>LYEIAR + NiTyr peptide is seen when the dynamic exclusion is ‘on’ and ‘off’ in the MSMS acquisition method but the modified YLY<sup>2</sup>EIAR + NiTyr, peptide is not. In reference to Bergt et al <sup>[185]</sup>, the modification patterns are consistent. The Y1 tyrosine is close to the lysine (K) residue making it more susceptible to nitration as the lysine directs the modification of tyrosine. The lysine is the initial site of attack by oxidation forming, in this case, nitroamine making the product Y<sup>1</sup>LYEIAR + NiTyr and not YLY<sup>2</sup>EIAR + NiTyr. The YLY<sup>2</sup>EIAR + NiTyr modified peptide is less favourable so its formation is unlikely or will occur at low abundance and in this case is below the limit of detection.

#### 3.6.4.1 An MRM targeted analysis for the Y<sup>1</sup>LY<sup>2</sup>EIAR + 2NiTyr peptide

To target for the di-nitro modified peptide, Y<sup>1</sup>LY<sup>2</sup>EIAR + 2NiTyr, an MRM method looking specifically for this double modified peptide was written from MSMS data observations (Table 17). The Y<sup>1</sup>LY<sup>2</sup>EIAR + 2NiTyr peptide was observed only once in the MSMS data after the conventional MSMS analysis of a 10mM SIN-1 modified HSA sample. The Q3 masses were chosen due to their intensity and frequency seen in the MSMS data. The di-NiTyr peptide, YLYEIAR + 2NiTyr (Q1=510.0, Q3=696.3, 488.3 and 359.2), has a 2NiTyr-confirmatory Q3 mass, 696.3m/z, and is its y5-ion. The y5-ion is also targeted for in the detection for the mono-NiTyr peptide and its mass is Q3=651.3.

Table 17: MRM for Y<sup>1</sup>LY<sup>2</sup>EIAR + 2NiTyr peptide

Peptide	Q1	Transitions seen	Transitions used
K. <u>Y</u> LYE <sup>1</sup> IAR.R + 2 NitroTyr (Y)	510.000 (2+)	696.3311 488.2827 359.2401	696.3311 488.2827 359.2401
K. <u>Y</u> LYE <sup>1</sup> IAR.R + NitroTyr (Y)	486.010 (2+)	764.4301 651.3461 488.2827 359.2401 246.1561 175.119	651.3461 488.2827 359.2401
K. <u>Y</u> LYE <sup>1</sup> IAR.R	464.190 (2+)	764.4301 651.3461 488.2827 359.2401 175.119	651.3461 488.2827 359.2401

The above displays from left to right the peptide targeted for, in the second column is the Q1 mass, the third column is the Q3 masses observed from MSMS data and the fourth column displays which transitions were used in the acquisition method.

The MRM method was applied to analyse a 1mM SIN-1 modified HSA sample (Figure 59). The unmodified YLYE<sup>1</sup>IAR peptide was seen at 25 minutes and the Y<sup>1</sup>LYE<sup>1</sup>IAR + NiTyr peptide at 28 minutes. The Y<sup>1</sup>LY<sup>2</sup>EIAR + 2NiTyr peptide is not detected in the 1mM SIN-1 modified HSA sample. The MRM method of detection is sensitive so it is likely the peptide has not been significantly di-nitrotyrosine modified when exposed to a 1mM SIN-1 concentration. Ringed in purple are single signal transitions for the unmodified YLYE<sup>1</sup>IAR peptide and the modified Y<sup>1</sup>LYE<sup>1</sup>IAR + NiTyr peptide. The Y<sup>1</sup>LYE<sup>1</sup>IAR + NiTyr peptide is in very low abundance so the Y<sup>1</sup>LY<sup>2</sup>EIAR + 2NiTyr peptide is unlikely to be formed or at abundance where it can be detected.

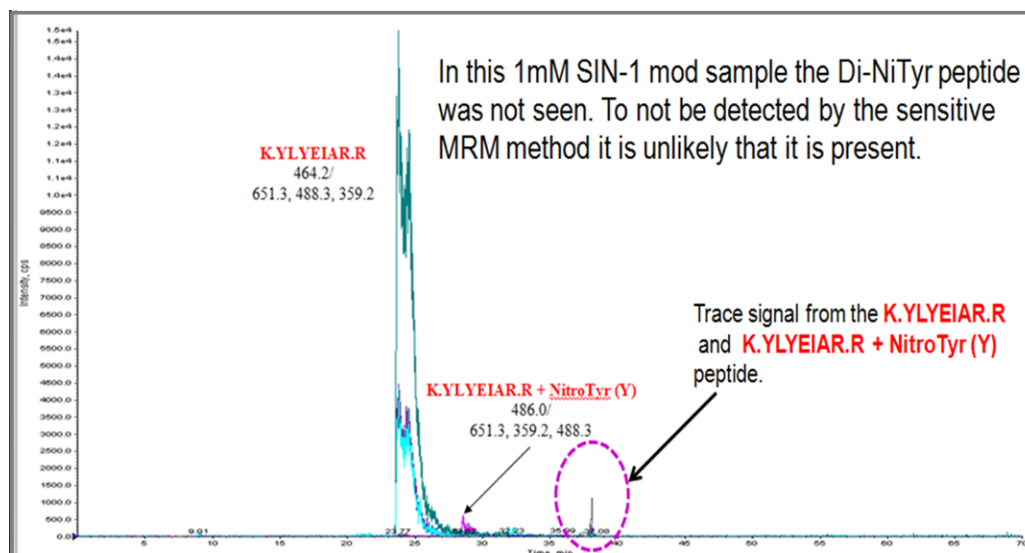


Figure 59: Di-nitrotyrosine MRM of 1mM SIN-1 modified HSA sample. The figure displays the analysis of a 1mM SIN-1 modified HSA sample with the “Di-nitrotyrosine MRM”.

### 3.7 Optimisation of the NiTyr MRM method to target all possible modified states of the peptides

Using the improved NiTyr MRM a new MRM was written to include all possible oxidation states (Table18). The newly optimised NiTyr MRM method although more sensitive does not take into account possible oxidised states that have not been seen by MSMS analysis in previous MSMS analysis of the SIN-1 modified HSA or plasma samples. The DVFLGMFLYEYAR + 2NiTyr peptide (Q1 = 858.45) is unlikely to form, as was discussed previously, methionine is the initial target for tyrosine modification. The DVFLGMFLYEYAR + Ox(M);2NiTyr peptide (Q1 = 866.45) is possible but a high SIN-1 concentration would be required and it is likely that the protein would aggregate at those required concentrations before the methionine plus both tyrosines of this peptide were modified.

The optimised NiTyr MRM program with all possible oxidation states was used to analyse the unmodified HSA and plasma samples as a control (Figure 60). Modified peptides RHPDYSVLLLR + Nityr (Q1=505.11, seen at 42 minutes in the unmodified HSA sample and 41 minutes in the plasma sample) are seen but the intensity of the transitions of these modifications is low. Zero modification of each peptide cannot be guaranteed as the sources of the plasma and purified HSA are variable due to the number of “healthy” individuals.

Table 18: Optimised NiTyr MRM method with all possible oxidation states

Peptide	Q1	ransition	CE
K.YLYEIAR.R + 2 NitroTyr (Y)	510.000 (2+)	696.33	28
		488.28	
		359.24	
K.YLYEIAR.R + NitroTyr (Y)	486.010 (2+)	651.35	28
		488.28	
		359.24	
K.YLYEIAR.R	464.190 (2+)	651.35	28
		488.28	
		359.24	
R.RHPDYSVLLLR.L + NitroTyr (Y)	505.11 (3+)	613.44	28
		514.37	
		401.29	
R.RHPDYSVLLLR.L	490.06 (3+)	613.44	28
		514.37	
		401.29	
K.DVFLGMFLY <del>Y</del> AR.R + 2NitroTyr (Y) ; Oxidation (M)	866.45 (2+)		
		Transitions never been seen	
K.DVFLGMFLY <del>Y</del> AR.R + 2NitroTyr (Y)	858.45 (2+)		
		Transitions never been seen	
K.DVFLGMFLY <del>Y</del> AR.R + NitroTyr (Y) ; Oxidation (M)	842.89 (2+)	1146.5	40
		859.39	
		746.31	
K.DVFLGMFLY <del>Y</del> AR.R + Oxidation (M)	820.57 (2+)	1101.5	40
		961.48	
		538.26	
K.DVFLGMFLY <del>Y</del> AR.R	813.45 (2+)	814.41	40
		961.48	
		538.26	
K.TYET <del>T</del> LEK.C + NitroTyr (Y)	515.10 (2+)	720.38	25
		591.33	
		490.29	
K.TYET <del>T</del> LEK.C	492.68 (2+)	720.38	25
		591.33	
		490.29	
R.RHPYFYAPE <del>L</del> LFFAK.R + NitroTyr (Y)	649.15 (3+)	738.45	35
		554.28	
		294.17	
R.RHPYFYAPE <del>L</del> LFFAK.R	633.70 (3+)	738.45	35
		554.28	
		294.17	

The table displaying the acquisition method from left to right in the first column shows the peptide targeted for, the second column is the Q1 mass, the third column is the Q3 masses used to identify the peptide and the fourth column is the collision energy used.

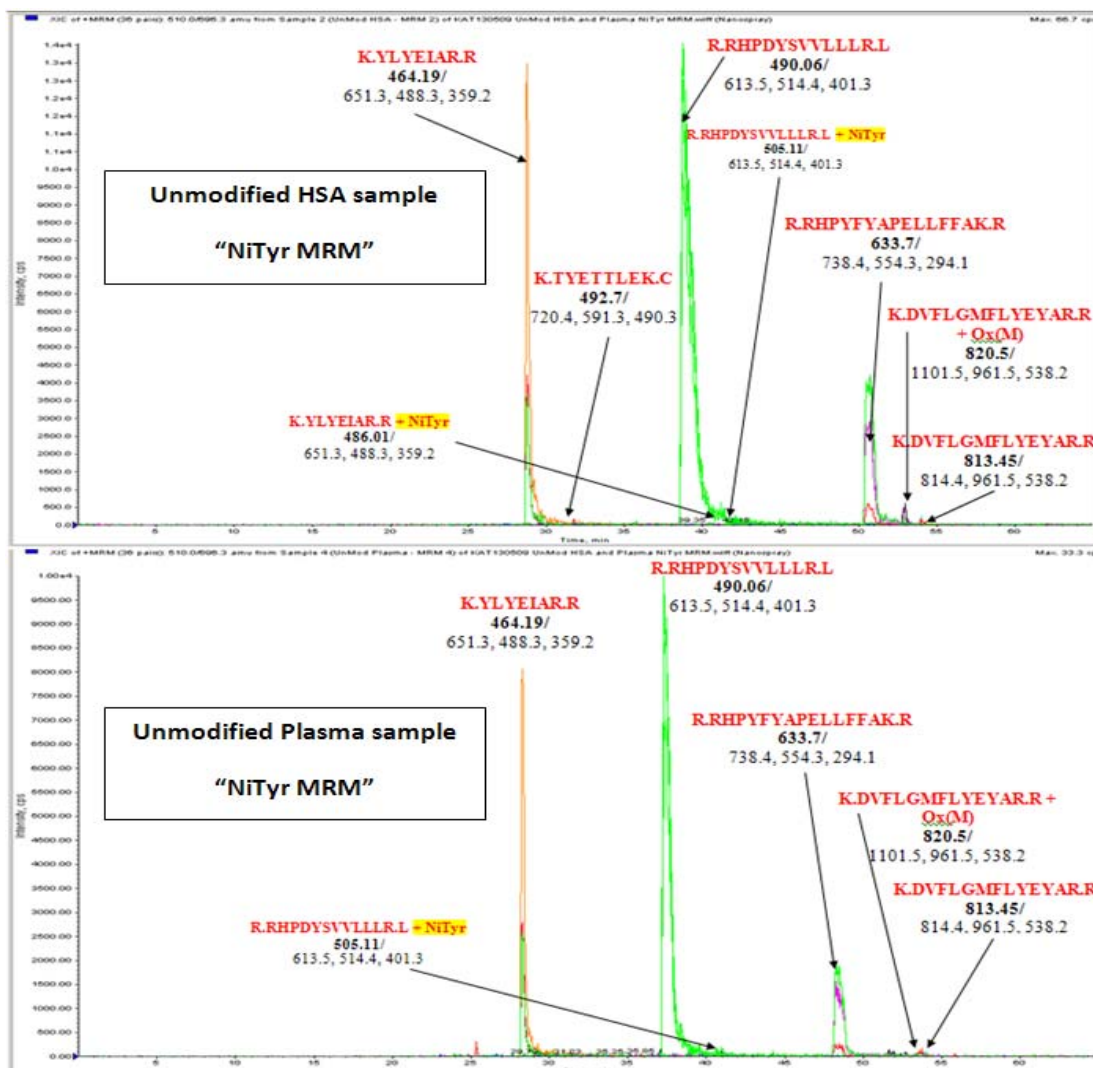
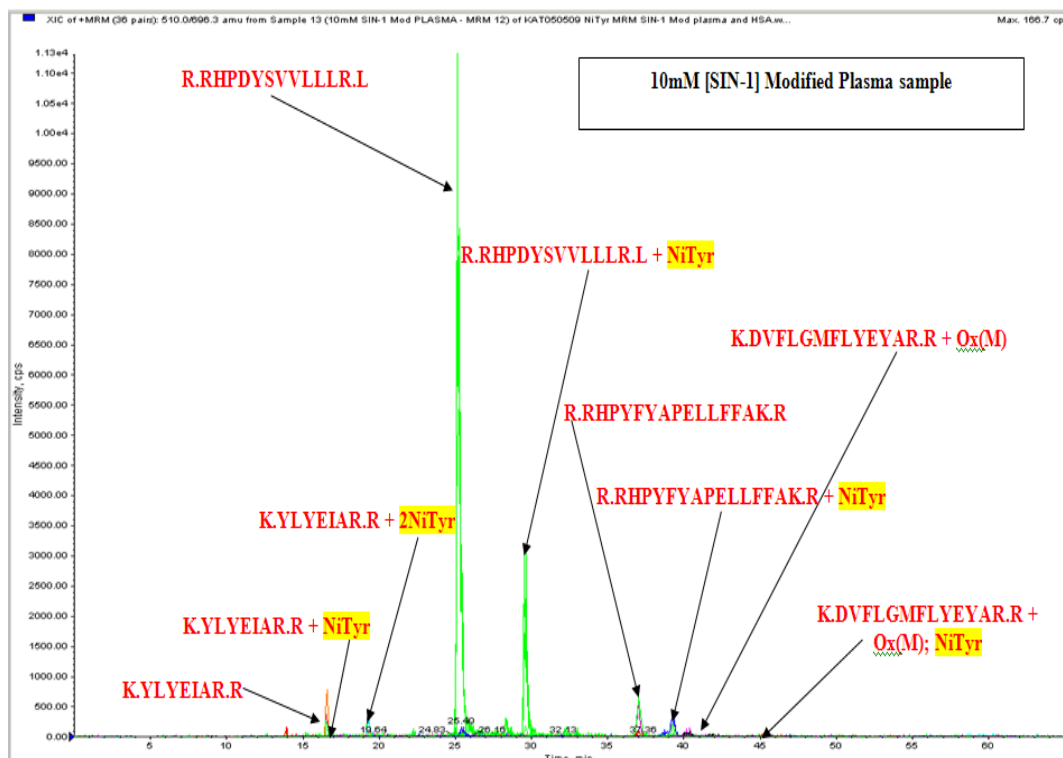


Figure 60: Unmodified HSA and plasma - Optimised NiTyr MRM method - Control. The figure illustrates the analysis of an unmodified HSA (top panel) and an unmodified plasma (bottom panel) sample with the optimised NiTyr MRM acquisition method.

In a 10mM SIN-1 modified plasma sample, for example, all targeted peptides were identified by the MRM method apart from the unmodified DVFLGMFLYEYAR peptide (Figure 61). The DVFLGMFLYEYAR + Ox(M) peptide's modified state is observed at 41 minutes and the Ox(M),NiTyr modified state is observed at 45 minutes. When modified at a 10mM SIN-1 concentration it is unlikely that there is significant unmodified DVFLGMFLYEYAR peptide present in the sample. The NiTyr MRM has effectively detected the NiTyr peptides. By comparing individual XICs from each modification state for a peptide the relative abundance of each modification can be compared.



**Figure 61:** 10mM SIN-1 plasma sample analysed by the optimised NiTyr MRM acquisition method. The above figure illustrates the detection of the peptide and their modified states in a 10mM SIN-1 modified plasma sample using the Optimised NiTyr MRM method.

The NiTyr MRM acquisition method does not search for the DVFLGMFLYEYAR + Ox(M); 2NiTyr or DVFLGMFLYEYAR + 2NiTyr oxidation states because there has been no MSMS data collected on these modifications so these transitions have never been seen. The Ox(M); 2NiTyr modification state would indicate a very oxidized peptide but when modified at high SIN-1 concentrations the purified protein, HSA and the real life biological sample, plasma may aggregate. The 2NiTyr modification state of the DVFLGMFLYEYAR peptide is unlikely as, with reference to the Bergt<sup>[185]</sup> and Zhang<sup>[185;186]</sup>, the methionine residue on the peptide is the primary target for nitration. It is logical to say that the first stage of modification in the DVFLGMFLYEYAR peptide is the oxidation of the methionine followed by the nitration of a tyrosine residue and finally when the peptide is exposed to high concentrations of oxidant (>10mM SIN-1 modified samples) the nitration of both tyrosines.

### 3.7.1 The extraction of XIC's to investigate the most abundant modified state of targeted peptides

The XIC's for the unmodified YLYEIAR peptide and its NiTyr and 2NiTYr modified states were compared to investigate which state was most abundant in the

10mM SIN-1 modified plasma sample (Figure 62). In the figure the top panel displays the unmodified peptides (Q1=464.19, blue), NiTyr modified (Q1=486.01, red) and the 2NiTyr modified (Q1=510.0, pink) *y5-ion* Q3 masses. The unmodified state appears more abundant with a signal intensity of 400cps in comparison with the NiTyr modified and di-NiTyr modified peptides 200 and 100cps respectively. The middle panel shows the comparison between the peptides modified states by comparing the common Q3=488.3 mass. The peak ringed in green from the 2NiTyr peptide is a false positive peak as this peak is from a single transition uncommon to the other Q3 masses for this peptide and is likely to be a signal from breakthrough. In this comparison of the transitions the NiTyr modified state appears more abundant. The 2NiTyr modification is in low abundance and was not detected by the conventional MSMS analysis of the 10mM SIN-1 modified sample only by the MRM method.

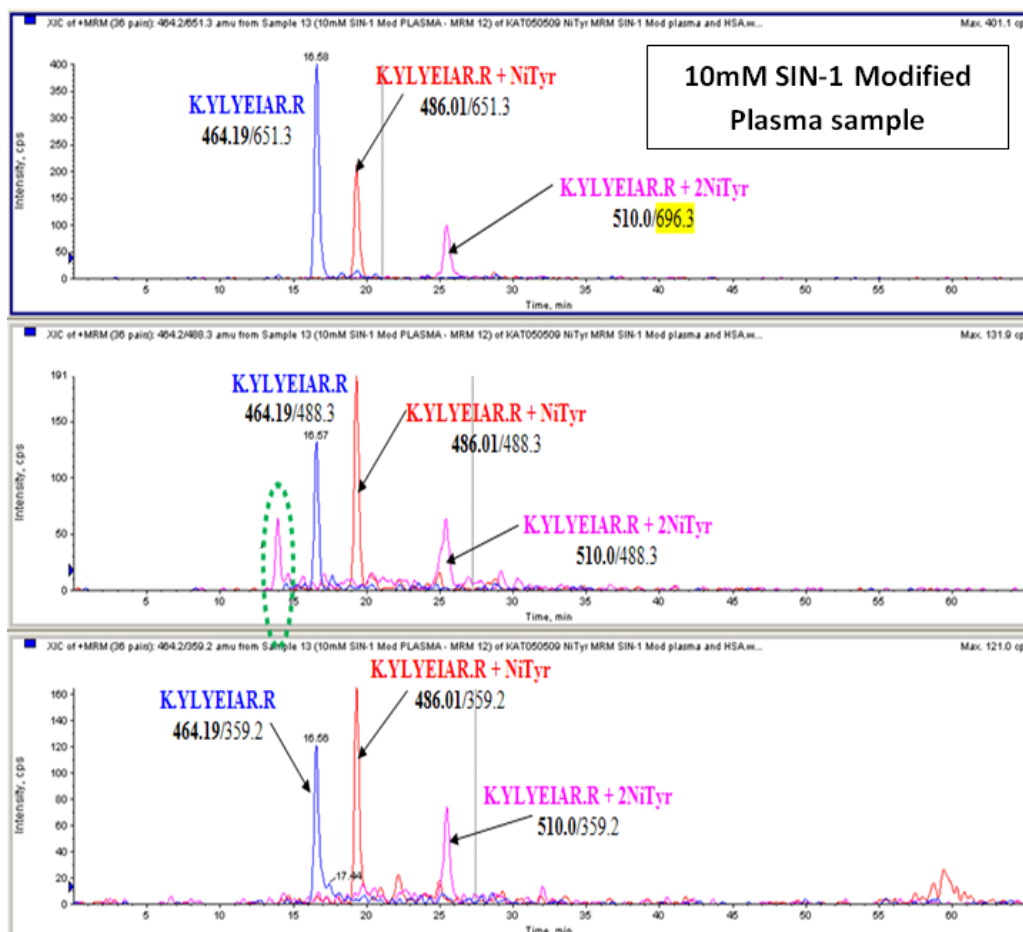


Figure 62: YLYEIKR modification in the 10mM SIN-1 plasma sample. The above figure illustrates the comparison of the YLYEIKR peptides common transitions (apart from the di-nitro tyrosine peptide's *y5-ion*, Q3=696.3 - top panel) for the three modified states.

### 3.8 The comparison of the automated generation of an MRM acquisition method to the manual generation by MSMS observations

The Analyst software includes the MIDAS program (1.7.3.1, 3.2.4) (Figure 63) which is an *in silico* digest and is performed with the user-specified protease, automatically generating and calculating theoretical MRM precursor masses; their transitions and optimal collisional energy. Only one transition per Q1 mass or peptide is chosen and an acquisition method is automatically written. The peptides searched for are then confirmed by their mass (Q1) and fragment (Q3).

It seems inefficient to write our own MRM program when MIDAS can calculate the acquisition method for us. One of the benefits with writing our own MRM method is that we choose three transitions whereas MIDAS only chooses one. One transition for a peptide mass should be adequate but we have found with previous MRM analysis on the SIN-1 and HOCl modified HSA and plasma samples that, especially when a transition is in low abundance, it is helpful to have two other confirmatory transitions. Identification of breakthrough signal is also possible when there is more than one confirmatory transition for a targeted peptide. It is possible that there will be one isobaric transition in a sample especially in complex samples but for there to be three isobaric and transitions is fairly unlikely. Using only one transition for peptides will increase the chance of false positives in the resulting data. To compare the MIDAS calculated transitions and the transitions written from our MSMS data analysis a MIDAS program was written for the NiTyr modifications in HSA (Table 19). Displayed are the differences between the NiTyr MRM written from MSMS observations and the NiTyr MRM written by MIDAS. The MIDAS transitions that were different to the ones we chose from MSMS observation are circled in red. Most of the transitions for the peptides calculated by MIDAS are the same as those chosen by the MSMS observations. Where a mass is within the appropriate mass ranges (400\_1500amu), the MIDAS program will search for both the (2+) and (3+) charges for a peptide.

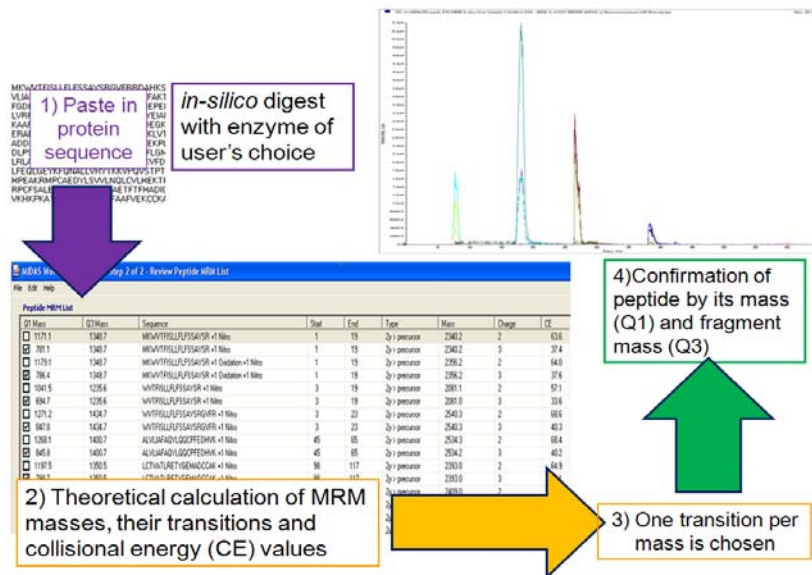


Figure 63: The MIDAS Workflow.

Table 19: NiTyr MRM written from MSMS observations versus NiTyr MRM written by MIDAS

250209 MRM for NiTyr Modifications - written from previous MS observations				250209 NiTyr MIDAS - compare.dam					
Peptide	Q1	Transitions	CE	Q1 assigned by MIDAS	Transition	CE			
K.YLYEIAR.R + 2 NitroTyr (Y)	510.000 (2+)	696.3311	28	509.2 (2+)	696.3	30.5			
		488.2827							
		359.2401							
K.YLYEIAR.R + NitroTyr (Y)	486.010 (2+)	651.3461	28	486.7 (2+)	651.3	29.3			
		488.2827							
		359.2401							
K.YLYEIAR.R	464.190 (2+)	651.3461	28	464.2 (2+)	488.3	28.2			
		488.2827							
		359.2401							
R.RHPDYVSVLLLR.L + NitroTyr (Y)	505.11 (3+)	613.4396	28	504.9 (3+)	1219.7	25.2			
		514.3711			756.9 (2+)	1219.7	42.8		
		401.2871							
R.RHPDYVSVLLLR.L	490.06 (3+)	613.4396	28	489.9 (3+)	1174.7	24.6			
		514.3711			734.4 (2+)	1174.7	41.7		
		401.2871							
K.DVFLGMFLYEYAR.R + NitroTyr (Y); Oxidation (M)	842.89 (2+)	1146.5215	40	842.9 (2+)	859.4	47.1			
		859.3945					562.3 (3+)	859.4	27.7
		746.3104							
K.DVFLGMFLYEYAR.R + Oxidation (M)	820.57 (2+)	1101.5364	40	820.4 (2+)	961.5	46			
		961.4778					547.3 (3+)	961.5	27.1
		538.262							
K.TYETTLEK.C + NitroTyr (Y)	515.10 (2+)	720.3774	25	515.2 (2+)	591.3	30.8			
		591.3348					343.8 (3+)	591.3	18.1
		490.2871							
K.TYETTLEK.C	492.68 (2+)	720.3774	25	492.7 (2+)	591.3	29.6			
		591.3348					328.8 (3+)	591.3	17.5
		490.2871							
R.RHPFYAPELLFFAK.R + NitroTyr (Y)	649.15 (3+)	738.4549	35	648.7 (3+)	964.5	31.5			
		554.2834			972.5 (2+)	964.5	53.6		
		294.1673							
R.RHPFYAPELLFFAK.R	633.70 (3+)	738.4549	35	633.7 (3+)	964.5	30.9			
		554.2834			950.0 (2+)	964.5	52.5		
		294.1673							

The table compares the MRM acquisition method written from MSMS observations and that written automatically by MIDAS. The Q3 transitions used (ringed in red) are those which differ from the ones used in the acquisition method written from MSMS observations.

### 3.8.1.1 The analysis of an unmodified HSA sample by the MIDAS MRM program and the NiTyr MRM program written from MSMS observations

To compare the MIDAS MRM program and the NiTyr MRM program written from MSMS observation an unmodified HSA sample was analysed. The MIDAS MRM acquisition method detected a number of “NiTyr modified” peptides in the unmodified HSA sample (Figure 64). The MIDAS program displaying a lot of false positives in the unmodified sample is therefore not as reliable as the MRM acquisition method generated from MSMS observations. The false positives are also hard to identify. In the MIDAS program only one transition from each mass is chosen so there are no affirmation transitions to verify the existence of the nitrotyrosine modifications in the unmodified sample. Instead of secondary or tertiary transitions to confirm or deny the existence of NiTyr modified peptides in the unmodified human serum albumin sample we can use the theoretical retention times for a NiTyr modified and unmodified peptide. The nitration of a tyrosine will decrease the polarity of a peptide therefore making the peptide more hydrophobic meaning a greater retention time and later elution time of the NiTyr modified peptide than the unmodified peptide. The MIDAS program analysis places the YLYEIAR + NiTyr peptide directly underneath the unmodified YLYEIAR peptide suggesting a common retention time. Due to the change in the peptide’s polarity when it becomes modified we know this is not true and must be a false positive. The MIDAS program also includes the RHPYFYAPELLFFAK + NiTyr (2+) and (3+) modified peptide charge states. If both NiTyr modified peptide charge states are truly present in the unmodified HSA sample they are expected to be eluted at the same time as each other and be eluted after the unmodified RHPYFYAPELLFFAK peptide.

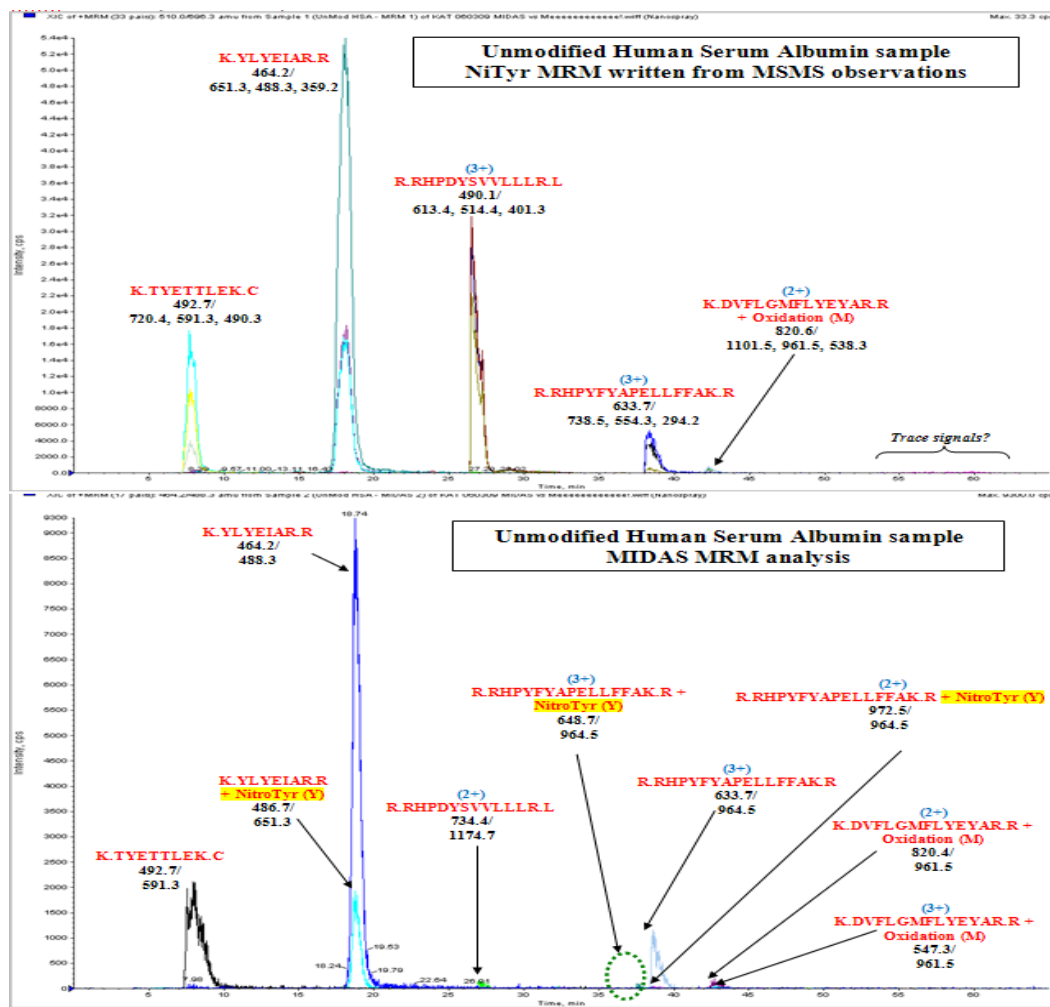


Figure 64: Unmodified HSA with MIDAS and NiTyr MRMs written from MSMS analysis. The above figure compares the analysis of an unmodified human serum albumin sample by the MIDAS MRM method and by the NiTyr MRM written from MSMS observations.

For a fair comparison both the automated MIDAS acquisition program and the manually generated NiTyr acquisition methods were used to analyse and detect NiTyr modifications in a 1mM SIN-1 HSA sample (Figure 65).

The MIDAS analysis of the sample (bottom panel) indicates that the YLYEIAR unmodified peptide (Q1=464.2) and the YLYEIAR + NiTyr (Q1=486.7) modified peptide being eluted at the same time (17 minutes). It is a likely false positive as the NiTyr modified peptide is expected to be seen after the unmodified peptide due to the changes in the peptides polarity when it becomes modified. This peak at 17 minutes is more likely to be the unmodified peptide as the YLYEIAR + NiTyr modified peptide is also seen at 22 minutes and this is concurrent with the retention time expected. The MIDAS program also detects the di-nitro tyrosine YLYEIAR + 2NiTyr peptide (Q1=509.2) whereas the MRM written from MSMS observations (top panel) does not. It is hard to have full

confidence in the detection of the di-nitrotyrosine peptide even though it is seen at the expected time (29 minutes *after* the unmodified - 17 minutes - and the NiTyr modified YLYEIAR peptide - 22 minutes) because the SIN-1 concentration is low. The RHPDYSVLLLR (2+) peptide (Q1=734.4, 28 minutes, MIDAS analysis bottom panel) is very low in intensity in comparison with the same peptide RHPDYSVLLLR (3+) peptide (Q1= 490.1, 30 minutes, MRM MSMS observations top panel). As the 3+ peptide was chosen due to its observation in the MSMS for the MRM method this charge state must be the most abundant charge. The RHPYFYAPPELLFFAK peptide is seen in both the MIDAS analysis and the MRM written from MSMS observations (Q1=633.7, 38 minutes, MIDAS bottom panel) and (Q1=633.7, 40 minutes, MRM MSMS observations top panel) leading to the conclusion that the MIDAS generated Q3=964.5 is just as efficient as those chosen from MSMS observation Q3=738.5, 554.3 and 294.5.

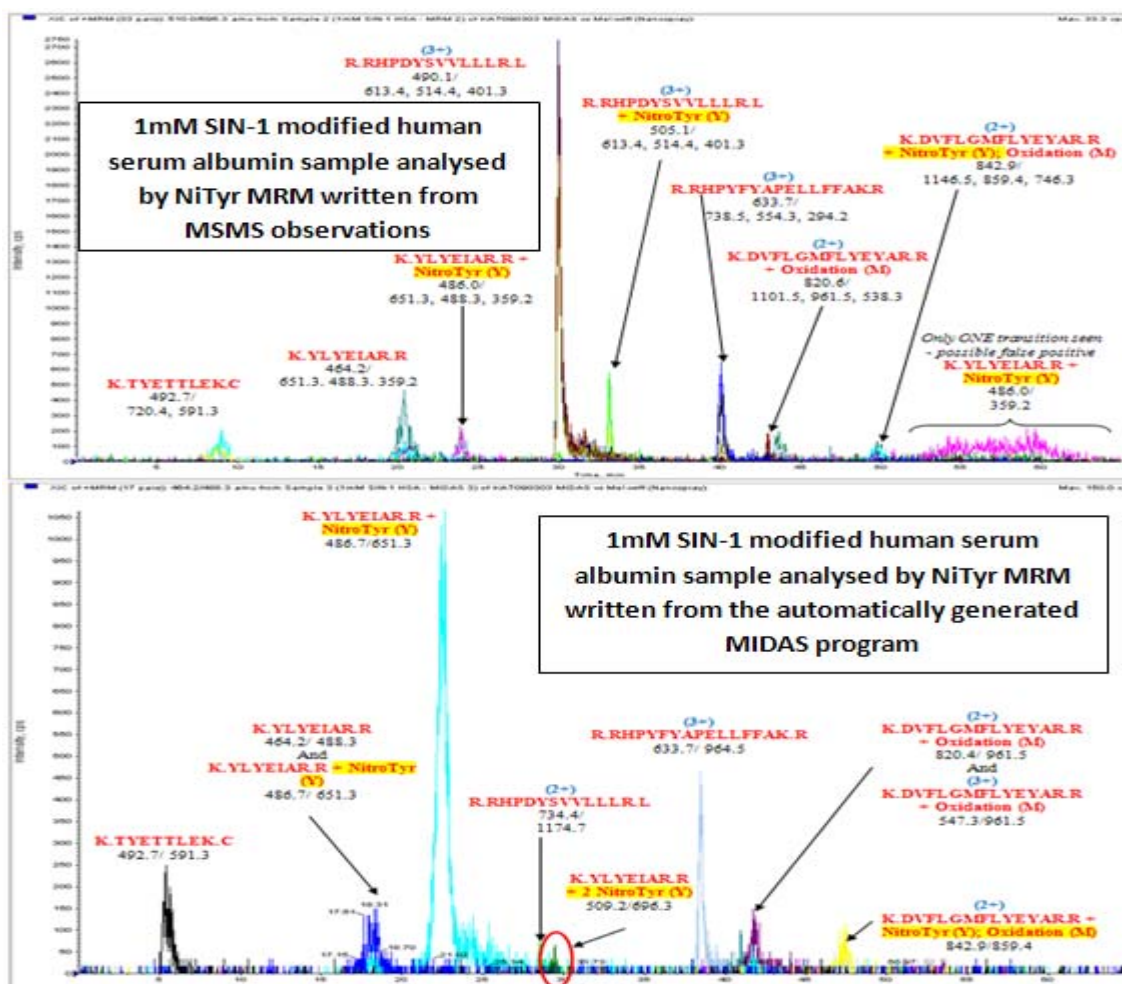


Figure 65: 1mM SIN-1 modified HSA sample analysed with MIDAS MRM and NiTyr MRM Acquisition method written from MSMS observations. The above figure displays the analysis of a 1mM SIN-1 modified HSA sample by the NiTyr MRM written from MSMS observations (top panel) and the MIDAS MRM acquisition method (bottom panel).

The problem with only one transition is that we cannot have full confidence in the presence of the peptide as there are no confirmation transitions. Identification of a peptide using only one transition becomes ambiguous.

The MIDAS acquisition method has its limitations. However, Unwin et al <sup>[144]</sup> reports that the value in MIDAS lies in the sensitivity and selectivity afforded by the MRM. The instrument allows only targeted, chosen precursor ions into the collision cell and the secondary confirmatory fragment ions monitored to the detector. This means that the background level becomes extremely low therefore enhancing signal to noise ratio.

The conclusion of the comparison between the Analyst software program, MIDAS, and writing MRM acquisition methods from MSMS observation in this study is that writing MRM programs manually is optimal to obtain the best transitions and prevent false positives.

### **3.9 Discussion**

The peptides identified as NiTyr modified were the same ones that were ClTyr modified. One potential explanation is that this is due to the folding of the HSA globular structure and that these tyrosines may be more exposed at the protein's surface and therefore more susceptible to oxidation. The crystallographic structure of the HSA shows that some of the tyrosines found to be NiTyr or ClTyr modified are in fact found to be buried or folded inside the protein's structure. Surface exposure of the tyrosine is therefore not important in relation to which tyrosine is ClTyr or NiTyr is modified as the NO<sub>2</sub> and Cl are relatively small in size.

#### **3.9.1 The presence of lysine leading to specific oxidative products**

Bergt et al <sup>[185]</sup> demonstrated that lysine residues will direct the chlorination of tyrosines. To investigate and explore the chlorination mechanism of tyrosine synthetic peptides they exposed to HOCl. The synthetic peptides sequences constituted the amino acids; YKXXY, YXXKY and YXXX Y, where X represents an unreactive amino acid. Analysis of the modified synthetic peptides by MS/ MS confirmed that the chlorination of tyrosines in peptides that contained lysine were regioselective and occurred in high yield when the peptide encompassed KXXY or YXXK sequences. NMR (nuclear magnetic resonance) was employed with

MS to show that the nitrogen on the lysines side chain was initially chlorinated implying that chloroamine formation is the initial step before tyrosine chlorination. In comparison, synthetic peptides without a lysine (K), with the general sequence; YXXXY, were not found to modify regiospecifically. The YXXXY synthetic peptides were found to form equal amounts of 3-chlorotyrosine and 3,5-dichlorotyrosine (*ClYXXXY*, *Cl<sub>2</sub>YXXXY*, *YXXXYCl* and *YXXYCl<sub>2</sub>*) but they were unable to modify both of the tyrosines in the one peptide (*ClYXXXYCl*). The tyrosine residue identified to be commonly NiTyr or ClTyr modified in the HSA protein are likely to be close in space to lysine residues in the secondary structure or close in space to residues in the tertiary structure.

### 3.9.2 The effect of methionine and the modification of a tyrosine residue

How the proximity of a methionine residue affects a neighbouring tyrosine's potential to be NiTyr modified was investigated by Zhang et al<sup>[186]</sup>. Previously, they reported how the tyrosylcysteine (YC- another sulphur containing residue) type peptides inhibited nitration or oxidation of a tyrosyl in comparison to free tyrosine alone<sup>[187]</sup>. Their most recent research, however, was focused on investigating the effects of a methionine residue on tyrosine nitration and oxidation when induced by myeloperoxidase (MPO, a heme enzyme), hydrogen peroxidase, nitrogen dioxide, peroxyxynitrite (ONOO<sup>-</sup>) and bicarbonate in model peptides. The nitration and oxidation products of these model peptides were analysed by HPLC with UV/Vis and fluorescence detection and mass spectrometry. The radical intermediates were detected by electron paramagnetic resonance (EPR)-spin-trapping. Spin-trapping is an assay for the detection and identification of free radicals. The analytical technique involves the formation of a spin adduct, a nitroxide-based persistent radical, that can be detected by EPR. The spin-adduct will then give a characteristic electron paramagnetic resonance spectrum depending on which radical is trapped. The enhancement of the nitration of the tyrosine radical in the close proximity of methionine is explained by a possible intramolecular electron transfer between the methionine sulphide cation radical and the tyrosine residue. The primary attack of the oxidising radical is the methionine but the end resulting product is the nitrated tyrosine residue indicating a fast intramolecular electron transfer from the tyrosine residue to the one-electron oxidised methionine moiety. During analysis of the SIN-1 modified HSA samples I noted that the most frequently observed peptide identified to be NiTyr modified was the

DVFLGMFLY<sub>1</sub>EY<sub>2</sub>AR + NiTyr peptide. The DVFLGMFLY<sub>1</sub>EY<sub>2</sub>AR + NiTyr modified peptide possesses a methionine residue and the most susceptible tyrosine to become modified in this peptide is Y<sup>1</sup> due to its close proximity to methionine.

### 3.10 Conclusion

I have been able to develop and optimize MRM acquisition methods from the observations of MSMS data to target and detect ClTyr and NiTyr in HOCl and SIN-1 modified purified protein, HSA, and in a real life biological sample, plasma. Through the development and testing of these MRM methods NiTyr and ClTyr modifications have been detected and the oxidation process of the residues in a peptide have been greater understood. The next stage of work would be to apply these MRM acquisition methods to clinical samples. This work was performed and discussed in more detail in Chapter 4.

# Chapter 4

---

The application of MRM (Multiple Reaction Monitoring) methods for the detection of nitrotyrosine and chlorotyrosine in clinical samples

## **4 Chapter - The application of MRM (Multiple Reaction Monitoring) methods for the detection of nitrotyrosine and chlorotyrosine in clinical samples.**

Mass spectrometry has been applied to screen, validate and quantify disease and monitor drug therapy in patients [76;188;189]. The use of mass spectrometry techniques has revolutionised and advanced the detection of disease classes such as the fatty acid oxidation defects [190]. A triple quadrupole is capable of performing the different scan functions (precursor ion scan, neutral loss scan, product ion scan) while maintaining high enough scan speeds for analysis. As discussed in sections 2.2 and 3.1.1 data can be acquired in two ways the first being *class specific analysis* for example neutral loss off-set mass scanning for acidic and neutral amino acids and precursor ion scanning for known  $m/z$ 's [130;161;191-195]. The second method for the acquisition of data can be by *targeted compound analysis* either by Selected Ion Monitoring (SIM) or Multiple Reaction Monitoring (MRM) where certain transitions of the precursor  $m/z$  and product ion  $m/z$  are monitored. Throughout the literature it has been found that the use of MRMs provides a more sensitive technique when targeting for low abundance proteins in biological samples [120;136;139;161;178;196-198].

### **4.1.1 MRM methods used to classify disease in biological samples**

Using MRMs is an effective way to classify disease and detect differences between diseased and healthy biological samples. An example of this technique is its use to study metabolites. There is a requirement for rapid and comprehensive screening methods for the detection of abnormal metabolites in urine for the diagnosis of many inborn errors of metabolism (IEM) [198]. MRMs have been used to assay post translational modifications as well as inborn errors of metabolism and the quantitative assay of drug metabolism [136;199]. Analysis of the urine was performed by direct injection into the tandem mass spectrometer with an MRM method for 32 targeted metabolites. This procedure was faster and less laborious than the previous conventional methods for testing for inborn errors of metabolism (IEM) by amino acid or organic acid profiling with similar diagnostic sensitivity. The conventional methods are by chromatographic

separation to first generate the metabolite profiles. Amino acid profiling can be generated by ion-exchange chromatography (IEX), thin-layer chromatography (TLC), paper electrophoresis and gas-phase chromatography. Organic acid testing is normally performed by HPLC (high performance liquid chromatography) and GC-MS (gas-phase mass spectrometry). These original tried and tested methods although successful have limited throughput. Using the MRM method increases throughput and reduces the time taken for the metabolic profiling.

Yang et al, also uses MRM for the discovery of novel biomarkers that are essential in a clinical setting to enable early disease diagnosis <sup>[200]</sup>. Using tandem based MSMS based protein profiling an MRM technique was developed by generating a library of 9,677 peptides representing approximately 1,572 proteins from human breast cancer cells. The library provides information about each cancer-related protein's peptides including their charge state, molecular weight, retention time etc, allowing for an informative MRM based biomarker screening study. Preliminary experiments demonstrated that putative biomarkers for human breast cancer that were not detected by traditional data dependant MS acquisition methods can be reliably identified using an MRM technique created by the information in the library. The MRM targeted methods meant there was no need for the fractionation of cell-lysis samples leading to faster, more reliable analysis with greater throughput.

Due to the high throughput and lower labour requirements, MRM techniques have also been used for the study of normal and atherosclerotic diseased arteries. Bagnato et al <sup>[201]</sup> reports the detection and quantification of SDF-1 $\alpha$  (stromal cell-derived factor 1 $\alpha$ ) and growth factors in atherosclerotic coronary arteries using direct tissue proteomics (DTP) and MRMs coupled to AQUA (absolute quantification). SDF-1 $\alpha$  is a chemokine and its interaction with CXCR4 (a CXC chemokine receptor) has been implicated in various inflammatory conditions <sup>[202]</sup>. The SDF-1 $\alpha$ /CXCR4 interaction regulates multiple cell signal pathways, cell migration, proliferation (important in stages of atherosclerosis), cell survival and angiogenesis (the growth of new blood vessels from pre-existing vessels) <sup>[203]</sup>. Chemokines are produced from multiple vascular cells and atherosclerotic vessels prone to developing thrombi. The SDF-1 $\alpha$  protein is highly expressed in smooth muscle cells, endothelial cells and, macrophages in human

atherosclerotic plaques but not in normal vessels <sup>[204]</sup>. The DTP method can be used to target paraformaldehyde-fixed, paraffin embedded and frozen coronary arteries. SDF-1 $\alpha$  and growth factors in the atherosclerotic artery were detected and quantified using the AQUA method. AQUA is absolute quantification using a selected suitable tryptic peptide as a unique identifier for the protein of interest and the addition of the synthetic heavy isotope-labelled counterpart as the internal standard for quantification by mass spectrometry. Using MRM coupled to AQUA, Bagnato et al, found they could detect and quantify SDF-1 $\alpha$  in the atherosclerotic vessel wall although the SDF-1 $\alpha$  protein was undetectable when using the less sensitive DTP technique. This study suggests that using MRM coupled to AQUA is a better method for the detection and quantification of low abundance proteins in histological tissue.

#### **4.1.2 Using MRMs to detect targeted NiTyr and CiTyr modified peptides in clinical samples**

The MRM methods from Chapter 3 were used to detect nitrotyrosine and chlorotyrosine modifications in purified HSA and plasma samples that had been chemically modified by SIN-1 or HOCl. Our goal here is to apply the MRM methods to detect chlorotyrosine and nitrotyrosine modification in clinical samples. The clinical samples were provided by Dr Christian Delles from the British Heart Foundation Glasgow Cardiovascular Research centre. The individuals from who these samples were obtained from were made aware of the circumstances in which they would be used and had given their consent. The use of these samples in this research project had been ethically approved. The clinical samples consisted of 24 plasma samples taken from 12 healthy volunteers and 12 patients. The patients and volunteers were all male. The diseased samples were from patients who all were currently suffering from severe coronary artery disease and placed on the list for major surgery by the cardiothoracic surgeon. The diseased samples had previously been classified from the healthy by Delles et al by the increased presence of malondialdehyde. All samples had been stored at -80°C for two years. The Cl and NO<sub>2</sub> groups are covalently bound to the tyrosine so are stable post translational modifications. Due to storage time there may be degradation of the proteins in the plasma samples but any chloro- or nitrotyrosine modifications of the albumin protein caused by oxidative stress will still be present and able to be detected.

In order for a fair and unbiased comparison of the clinical samples to be achieved it was decided that the analysis should be performed “blinded”. To carry out the analysis blinded this means that it is unknown which plasma sample is from a diseased patient and which is from a healthy volunteer. Only after analysis and when a conclusion is drawn about which samples are from healthy volunteers and which are from diseased patients will the samples be un-blinded and a comparison made between our diagnosis and the source of the plasma sample.

## 4.2 Aims

In this chapter I aim to analyse blinded clinical samples using the MRM methods previously developed in Chapter 3 in the hope that I am able to classify healthy and diseased samples by the chloro and nitrotyrosine modifications present.

## 4.3 Materials and Methods

I had previously carried out a Bradford assay on raw plasma (see 3.2) and due to the small volume of clinical samples available it was decided to assume protein concentration was similar for the clinical samples to avoid sample loss. The clinical samples were 100 $\mu$ l aliquots and the protein concentration was assumed to be approximately 60mg/ml. A 50 $\mu$ l aliquot (approximately 30mg protein) of the plasma was taken and diluted by 1:20 in 50mM Tris pH7 buffer. The end concentration of the plasma was then approximated to be 3 $\mu$ g/ $\mu$ l with 10 $\mu$ l (~30 $\mu$ g protein) to be trypsin digested as before (2.4.1.2) and analysed on the Qtrap 2000 (*Applied Biosystems*, Warrington, UK) by MSMS and the MRM method.

### 4.3.1 Mass Spectrometry Methods

#### 4.3.1.1 Conventional MSMS

As described in 2.4.1.4

#### 4.3.1.2 Targeted MSMS

The targeted MSMS was set to fragment the precursor m/z only. The enhanced product ion experiment scanned between 50 and 1500amu in positive ion mode. The step size was 0.06amu and the scan rate 1000amu/s. The resolution of Q1 was set to unit and the total scan time including pauses was 5.4 seconds. The collisional energy employed was 30eV and the ion spray voltage was 2500V.

### 4.3.1.3 The ClTyr and NiTyr MRM method

The MRM acquisition method below (Table 20) is a union of the NiTyr and ClTyr MRM methods used in Chapter 3 that were written from the MSMS observations from chemically modified HSA and plasma samples. Out of the four targeted peptides to be detected for chloro- or nitrotyrosine modification, three had been seen to be modified by either the Cl or NO<sub>2</sub> group. The YLYEIAR peptide however has only been seen to be nitrotyrosine modified and not chlorotyrosine modified.

Table 20: The MRM acquisition method for the diagnosis of clinical samples.

Peptide	Q1 m/z	Q3 m/z		
YLYEIAR + 2NiTyr	510	696.3	359.2	246.2
YLYEIAR + NiTyr	487	651.3	359.2	246.2
YLYEIAR	464.2	651.3	359.2	246.2
RHPDYSVLLLR + ClTyr	501.1	514.4	401.3	613.4
RHPDYSVLLLR + NiTyr	505.1	514.4	401.3	613.4
RHPDYSVLLLR	490	514.4	401.3	613.4
DVFLGMFLYEYAR + NiTyr;Ox(M)	842.9	746.3	859.4	1147
DVFLGMFLYEYAR + 2ClTyr;Ox(M)	855	175.1	362.2	475.3
DVFLGMFLYEYAR + ClTyr;Ox(M)	837.75	175.1	362.2	475.3
DVFLGMFLYEYAR + Ox(M)	820.57	1101.5	965.5	538.3
DVFLGMFLYEYAR	813.45	814.4	961.5	538.3
RHPYFYAPPELLFFAK + NiTyr	648.6	738.4	554.3	294.2
RHPYFYAPPELLFFAK + ClTyr	593	964.5	867.5	625.3
RHPYFYAPPELLFFAK	582	738.4	554.3	294.2

From left to right the above displays the targeted peptides in the first column, their parent masses (Q1) in the second column and fragment ions (Q3) that are searched for using the MRM method. The MRM method was written from MSMS observations from the analysis of chemically modified HSA and plasma samples.

## 4.4 Results and Discussion

### 4.4.1 MSMS Analysis of the 24 Clinical Samples

Each clinical sample (10µl, ~3µg total protein) was analysed by conventional MSMS on the Qtrap 2000 (*Applied Biosystems*, Warrington, UK) and the data searched with Mascot, a MS data searching algorithm, version 1.6b9 (2.4.1.5). The mass spectrometry data collected from the MSMS analysis of all 24 clinical samples did not identify any peptide where a nitro- or chlorotyrosine modification was assigned to any of the identified peptides when searched using Mascot (Figure 66) (further discussed in 4.6).

1. **ALBU HUMAN** Mass: 71317 Score: 453 Queries matched: 21 emPAI: 1.49  
 Serum albumin OS=Homo sapiens GN=ALB PE=1 SV=2  
 Check to include this hit in error tolerant search or archive report

Query	Observed	Mr(expt)	Mr(calc)	Delta	Miss	Score	Expect	Rank	Peptide
<input checked="" type="checkbox"/> <a href="#">94</a>	438.2852	874.5559	874.5025	0.0534	1	28	0.4	1	R.LSQRFPK.A
<input checked="" type="checkbox"/> <a href="#">96</a>	440.6829	879.3513	879.4338	-0.0825	0	39	0.027	1	K.AEFAEVS <i>K</i> .I
<input checked="" type="checkbox"/> <a href="#">111</a>	464.2316	926.4487	926.4861	-0.0375	0	32	0.14	1	K.YLYEIA <i>R</i> .R
<input checked="" type="checkbox"/> <a href="#">114</a>	476.2355	950.4565	950.4345	0.0220	0	40	0.024	1	K.DLGEENFK.A
<input checked="" type="checkbox"/> <a href="#">117</a>	480.7563	959.4981	959.5552	-0.0571	0	54	0.00097	1	K.FQNALLVR.Y
<input checked="" type="checkbox"/> <a href="#">124</a>	500.8380	999.6614	999.5964	0.0650	0	49	0.0027	1	K.QTALVELVK.H
<input checked="" type="checkbox"/> <a href="#">126</a>	501.8530	1001.6915	1001.5506	0.1410	1	21	1.9	1	K.TPVSDRVTK.C
<input checked="" type="checkbox"/> <a href="#">130</a>	510.2962	1018.5778	1018.5712	0.0066	1	57	0.00047	1	R.AFKAAVAR.L
<input checked="" type="checkbox"/> <a href="#">151</a>	564.9003	1127.7860	1127.6914	0.0946	1	75	6.3e-06	1	K.KQTALVELVK.H
<input checked="" type="checkbox"/> <a href="#">154</a>	575.3198	1148.6251	1148.6077	0.0173	0	52	0.0012	1	K.LVNEVTEFAK.T
<input checked="" type="checkbox"/> <a href="#">155</a>	575.4082	1148.8019	1148.5686	0.2333	1	39	0.023	1	R.DAHKSEVAMR.F
<input checked="" type="checkbox"/> <a href="#">177</a>	613.8459	1225.6773	1225.5979	0.0794	1	44	0.0084	1	R.FKDLGEENFK.A
<input checked="" type="checkbox"/> <a href="#">178</a>	409.6625	1225.9657	1225.5979	0.3678	1	(32)	0.09	1	R.FKDLGEENFK.A
<input checked="" type="checkbox"/> <a href="#">198</a>	656.4816	1310.9487	1310.7347	0.2140	0	70	1.4e-05	1	R.HPDYSVLLLR.L
<input checked="" type="checkbox"/> <a href="#">221</a>	734.5087	1467.0028	1466.8358	0.1670	1	65	4.9e-05	1	R.HPDYSVLLLR.L
<input checked="" type="checkbox"/> <a href="#">231</a>	756.5394	1511.0643	1510.8355	0.2288	0	76	4.1e-06	1	K.VPQVSTPLVEVSR.H
<input checked="" type="checkbox"/> <a href="#">244</a>	547.5631	1639.6674	1638.9305	0.7370	1	77	3.9e-06	1	K.KVPQVSTPLVEVSR.N
<input checked="" type="checkbox"/> <a href="#">245</a>	820.9429	1639.8713	1638.9305	0.9408	1	(50)	0.0019	1	K.KVPQVSTPLVEVSR.N
<input checked="" type="checkbox"/> <a href="#">247</a>	825.9787	1649.9428	1649.8876	0.0552	1	110	2e-09	1	K.AEFAEVS <i>K</i> LVDTLK.V
<input checked="" type="checkbox"/> <a href="#">282</a>	682.6165	2044.8277	2044.0881	0.7396	0	39	0.02	1	K.VFDEFKPLVEEPQNLK.Q
<input checked="" type="checkbox"/> <a href="#">283</a>	1023.5208	2045.0271	2044.0881	0.9390	0	(10)	17	1	K.VFDEFKPLVEEPQNLK.Q

Figure 66: An example of Mascot Results for the MSMS analysis of the Clinical Samples - Protein Hits and Matched Queries for Clinical Sample 13. The above figure displays the Mascot protein hits and queries assigned from searching the data collected from the MSMS analysis on Clinical Sample 13. There are no NiTyr or ClTyr modifications assigned. The peptides boxed in purple are the unmodified peptides targeted for in the MRM acquisition method.

#### 4.4.2 Random analysis of the 24 Clinical Samples by the MRM Method

Previously an MRM acquisition method was used to detect nitro- and chlorotyrosine modifications of targeted peptides in chemically modified HSA and plasma samples (see Chapter 3). The MRM method was applied to all 24 clinical samples with the aim of classifying which of the 12 samples were from healthy volunteers and of which remaining 12 was from diseased patients. Samples; 1, 3, 5, 7, and 9 were chosen randomly for initial analysis.

##### 4.4.2.1 Comparison of the signal intensity for the modified YLYEIA*R* + NiTyr peptide

The targeted nitro- and chlorotyrosine modified and unmodified peptides were identified in the clinical samples. Nitro- and chlorotyrosine modifications were found to be more abundant in some samples than in other samples (4.4.2.4 Figure 67). The peaks ringed in purple are where the NiTyr modified peptide is eluted. For an identification of the NiTyr modified peptide three transitions must be eluted at the common time in the chromatography gradient. The common elution time (approximately 37 minutes) for the modified YLYEIA*R* +

NiTyr peptide is seen in samples 1, 5, 7 and 9. The intensity of signal for the NiTyr modified peptide in these samples is low ranging from >40cps to >100cps. The false positive peaks are where there is only one transition observed and they are present in all samples analysed here. In sample 3 there is no common elution time for the three transitions so the peptide in sample 3 is not expected to be NiTyr modified.

From Figure 67 we can assume at this point in the analysis of the clinical samples that although low in intensity the modified YLYEIAR + NiTyr peptide is present in samples 1, 5, 7 and 9. The modified YLYEIAR + NiTyr peptide is not present in sample 3 which would indicate that sample 3 is in fact one of the 12 healthy samples and that samples 1, 5, 7 and 9 are from diseased patients.

#### 4.4.2.2 Comparison of the signal intensity for the modified RHPYFYAPPELLFFAK + ClTyr peptide

The MRM method also targets other possible modified peptides and these were also compared between the samples (4.4.2.4 Figure 68). The peak ringed in purple is where the ClTyr modified peptide is eluted (approximately 40 minutes). The modified RHPYFYAPPELLFFAK + ClTyr peptide is seen in sample 3 only although the signal is low in intensity at >53cps. In samples 1, 5, 7 and 9 there are no common elution times for the three transitions so the peptide in these samples is not significantly ClTyr modified. The previous comparison of the modified YLYEIAR + NiTyr peptide (4.4.2.4 Figure 68) between these samples all *but* sample 3 was indicated to have this modified peptide present. This inconsistency suggests that to classify disease there is a need for more than one biomarker and or a threshold intensity for a signal.

#### 4.4.2.3 Comparison of the signal intensity for the modified RHPDYSVLLLLR + NiTyr peptide

In samples 1, 3, 5, 7 and 9 the modified YLYEIAR + NiTyr peptide was *not* present in sample 3 but present in samples 1, 5, 7 and 9. The modified RHPYFYAPPELLFFAK + ClTyr peptide, however, was *only* identified to be present in sample 3. A comparison was made between samples for the presence of the modified RHPDYSVLLLLR + NiTyr peptide (4.4.2.4 Figure 69). The peaks ringed in purple are where the NiTyr modified peptide is eluted (approximately at 30 minutes). The modified RHPDYSVLLLLR + NiTyr peptide is seen in all samples 1,

3, 5, 7 and 9 although the signal is low in intensity ranging from >30cps - >150cps. The modified RHPDYSVLLLLR + NiTyr peptide was seen in *all* samples 1, 3, 5, 7 and 9 at approximately 30 minutes into the gradient and the signal intensity varied from >30cps to >150cps in sample to sample. Because there is modification of some peptides but not of all peptides targeted in some samples it may be signal intensity as well as a combination of more than one biomarker which is more important when classifying if a sample is from a diseased source or not.

#### 4.4.2.4 Figures from the MRM analysis of samples 1, 3, 5, 7 and 9

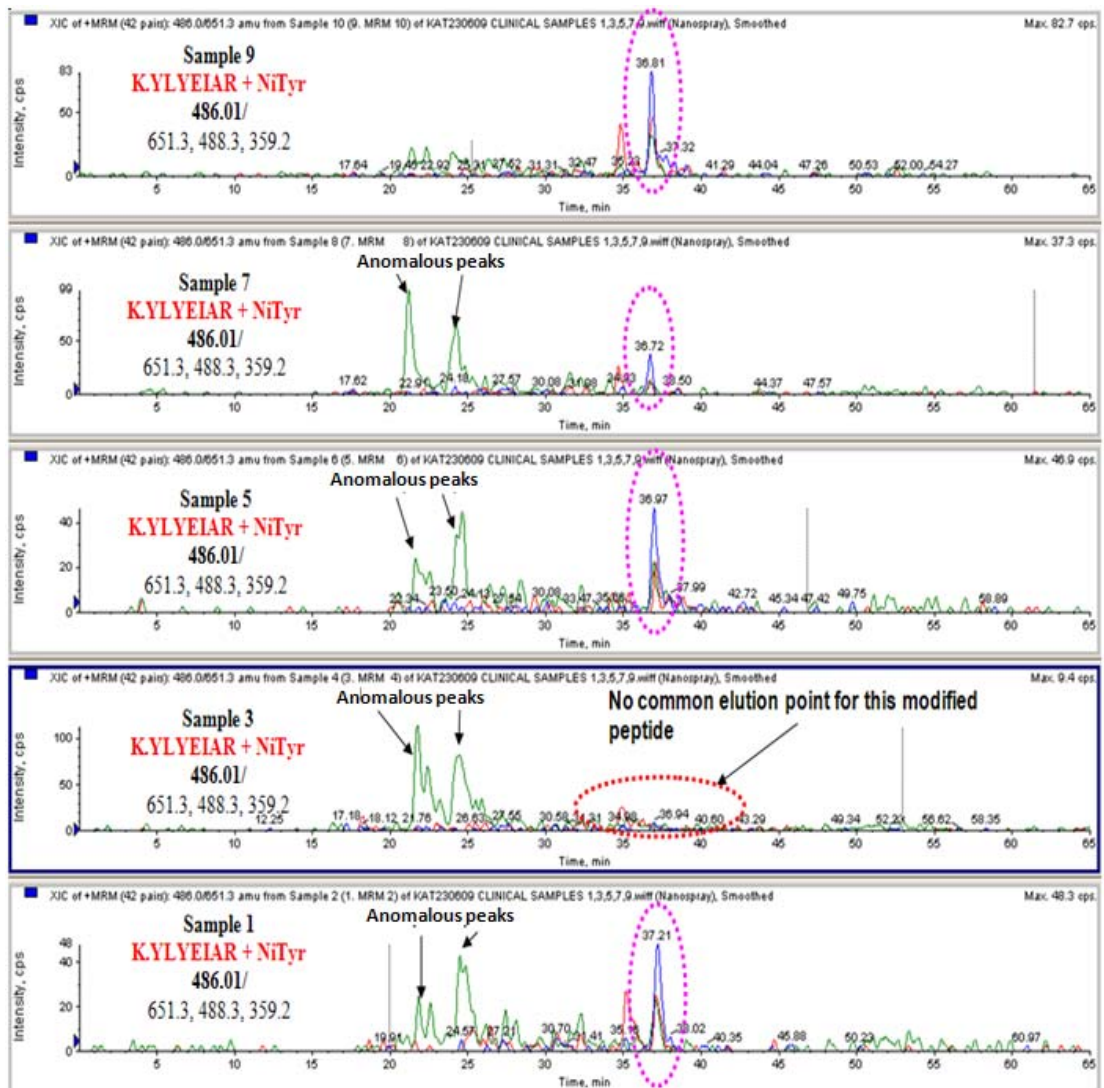


Figure 67: Comparison of the modified YLYEYIAR + NiTyr peptide in samples 1, 3, 5, 7, and 9. The above figure displays the over-laid Q3=651.3, 488.3 and 359.2 m/z traces for the modified YLYEYIAR + NiTyr peptide (Q1=486.01 m/z) for the clinical samples 1, 3, 5, 7, and 9.

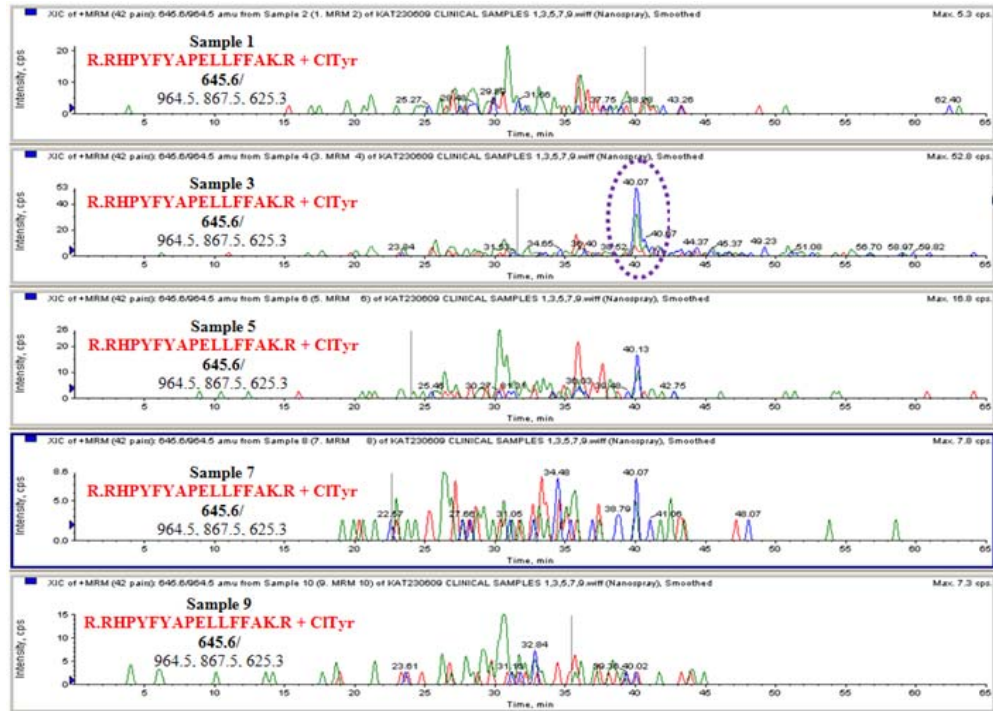


Figure 68: Relative comparison of the modified RHPYFYAPPELLFFAK + CItyr peptide samples 1, 3, 5, 7, and 9. The above figure displays the over-laid Q3=964.5, 867.5 and 625.3m/z traces for the modified RHPYFYAPPELLFFAK + CItyr peptide (Q1=645.6m/z) for clinical samples 1, 3, 5, 7, and 9. Ringed in purple is the identified modified peptide.

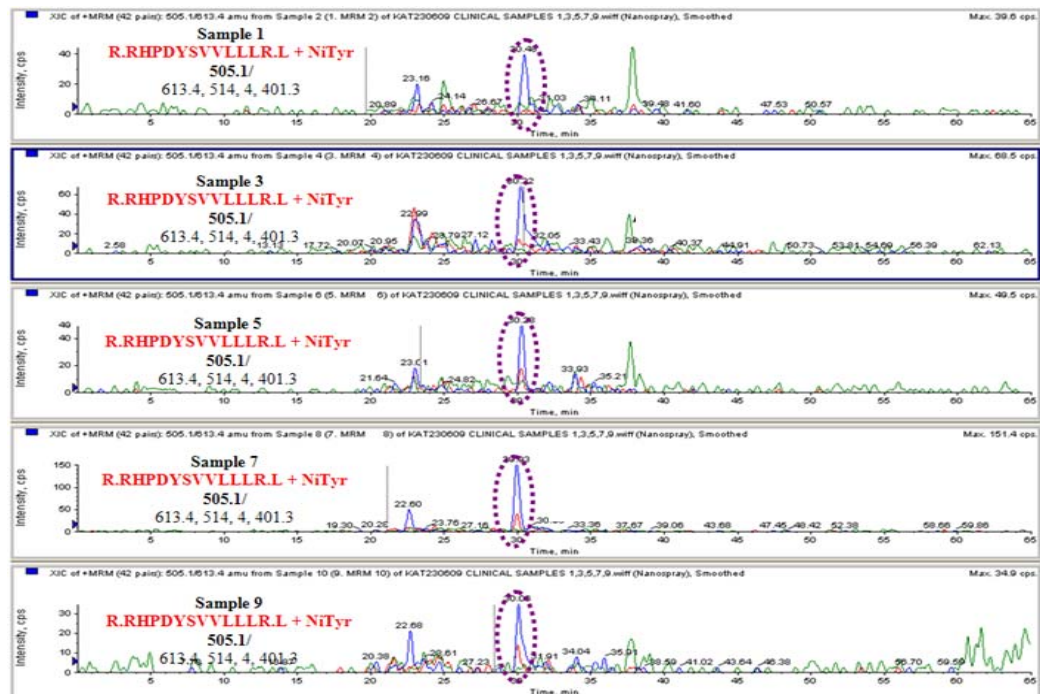
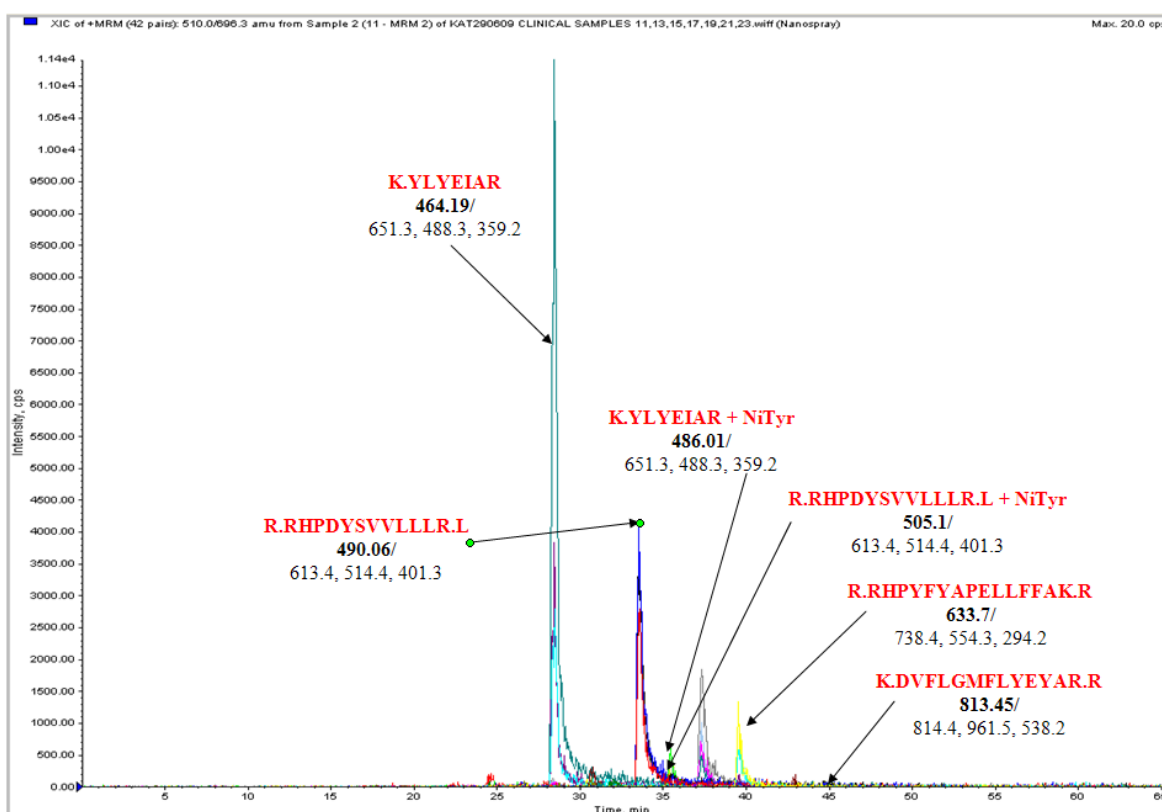


Figure 69: Relative comparison of the modified RHPDYSVLLLLL + NiTyr peptide in samples 1, 3, 5, 7, and 9. The above figure displays the over-laid Q3=613.4, 514.4, 401.3m/z traces for the modified RHPDYSVLLLLL + NiTyr peptide (Q1=505.1m/z) for clinical samples 1, 3, 5, 7, and 9. Ringed in purple is the identified modified peptide.

#### 4.4.3 Confirmation of the modified peptides detected

Before criteria could be defined to classify healthy samples from diseased, all 24 clinical samples were analysed using the MRM method. Modification of the YLYEIAR + NiTyr and the RHPDYSVLLLLR + NiTyr peptide was seen in a number of samples (see 4.5) but when the clinical samples were randomly analysed these modifications were first seen in sample 11. Here we use sample 11 as an example and target these modified peptides by MSMS to confirm the assumed peptide is what we have targeted for. The MRM method indicated the presence of the modified YLYEIAR + NiTyr and the RHPDYSVLLLLR + NiTyr peptide in sample 11 (Figure 70).



**Figure 70:** The detection of the modified and unmodified target peptides in clinical sample 11. The figure displays the XIC (extracted ion chromatograph) of the peptides targeted by the MRM. The YLYEIAR unmodified peptide is seen at 28 minutes, the modified YLYEIAR + NiTyr peptide is seen at 35 minutes, the unmodified RHPDYSVLLLLR peptide is seen at 33 minutes, the modified RHPDYSVLLLLR + NiTyr peptide is seen 34 minutes, the unmodified RHPYFYAPPELLFFAK peptide is seen at 40 minutes and the unmodified DVFLGMFLYEYAR peptide is seen at 45 minutes into the chromatography gradient.

#### 4.4.3.1 Relative Quantitation of Modification of the YLYEIAR peptide

The MRM has detected the targeted peptides and indicates modification in sample 11. Although the nitrotyrosine modified peptides are seen in sample 11 the chlorotyrosine modified peptides were not (Figure 71). The unmodified peptide (red) is seen to be eluted at 28 minutes and the NiTyr modified peptide (blue) is seen to be eluted at 37 minutes into the chromatography gradient. Underneath the peak for the unmodified peptide (red) there is a trace from the NiTyr Modified peptide (blue) ringed in orange. It is impossible for the unmodified and modified peptide to be eluted at the same time due to the peptide's changes in polarity. An explanation for the modified peptide being observed at the same time as the unmodified peptide could be caused by breakthrough (as previously discussed). The Q1 resolution in the MRM method is set to low. The emergence of the modified peptide could be caused by poor selection in Q1. The relative percentage modification of the YLYEIAR peptide in Sample 11 was calculated using the transitions intensities and not area under the peak and the equation 7 (3.4.1.1). The calculated approximate percentage modification is calculated under the assumption that the modified and unmodified states of the peptide have similar ionisation energies.

$$Q3 = 651.3 \quad [2000 / (2000 + 7608)] \times 100 = 20.8\%$$

$$Q3 = 488.3 \quad [900 / (900 + 2331)] \times 100 = 27.8\%$$

$$Q3 = 359.2 \quad [500 / (500 + 2000)] \times 100 = 20.0\%$$

Average relative percentage modification for clinical sample 11 = **22.8%**

To confirm that the MRM method has successfully detected the YLYEIAR peptide and that it is indeed NiTyr modified and not a false positive a targeted MSMS experiment was performed.

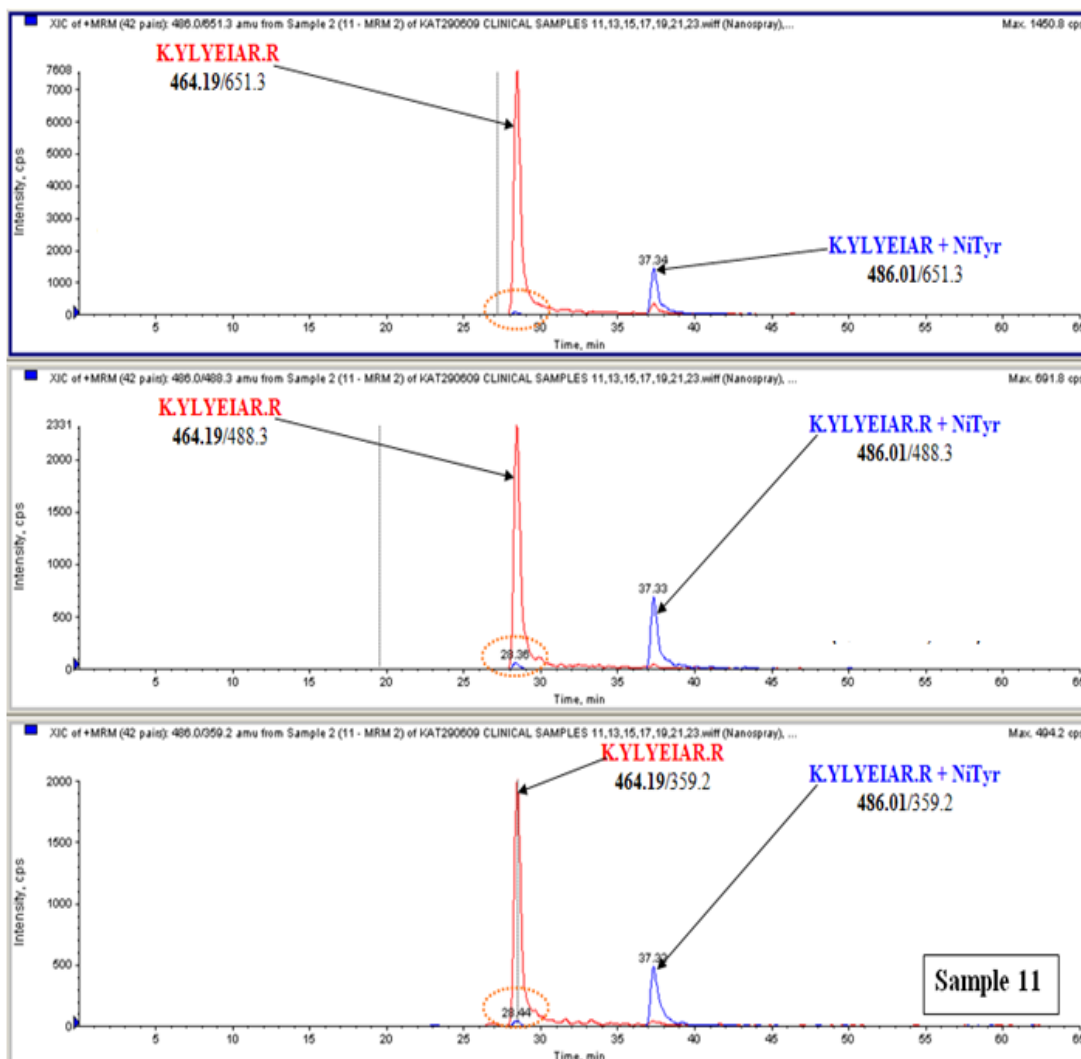


Figure 71: Comparison of the unmodified YLYEIQAR peptide and the YLYEIQAR + NiTyr peptide in sample 11. The figure displays the three Q3 masses (651.3 - top panel, 488.3 - middle panel and 359.2 - bottom panel) for the NiTyr modified (Q1=486.01, blue) and unmodified YLYEIQAR (Q1=464.19 - red) peptide. Ringed in orange is breakthrough signal from the unmodified peptide.

#### 4.4.3.2 A targeted MSMS experiment

The modified YLYEIQAR + NiTyr peptide was also detected in sample 24. To determine and confirm the presence of the detection of the modified YLYEIQAR + NiTyr peptide in clinical sample 24 a targeted MSMS experiment (4.3.1) was performed where MSMS is carried out on a specific precursor mass only (496m/z). The resulting MSMS data was then searched using Mascot and the resulting ion score for the YLYEIQAR + NiTyr peptide was 34. The targeted MSMS experiment on sample 24 was run concurrent to the MRM analysis of the sample then the MSMS data was searched with Mascot. If the targeted MSMS experiment confirms the presence of the modified YLYEIQAR + NiTyr peptide in Sample 24 it also strongly suggests that the MRM acquisition method has successfully targeted

the modified peptide when it is detected by the MRM method in a sample (Figure 72). The figure displays the total ion chromatograph (TIC) in the top panel and the region where the modified YLYEIAR + NiTyr peptide is known to be eluted from (between 36-37 minutes) is highlighted. The middle panel is the enhanced product ion (EPI) scan for the Q1=486.0 precursor between 36 and 37 minutes into the chromatography gradient and the ion-match table from Mascot. The *y*-ions not labelled in the EPI scan but reported in the ion-match table are present but in low intensity so are difficult to see in the mass spectrometry data. The bottom panel is the MRM of the YLYEIAR + NiTyr with the three transitions (Q3=488.3, 651.3 and 359.2) that are targeted in the MRM method overlaid. There is a common peak where all three transitions or Q3 masses are eluted (ringed in red) seen between 36 and 37 minutes. There is a false positive observed at 27 minutes ringed in orange that is breakthrough from the unmodified peptide.

The mass spectrometry data suggests that the modified YLYEIAR + NiTyr peptide is present. The Q3 masses targeted in the MRM Acquisition method are commonly seen at the expected elution times (between 36 and 37 minutes) and a Mascot search of the MSMS data is performed for confidence in confirmation.

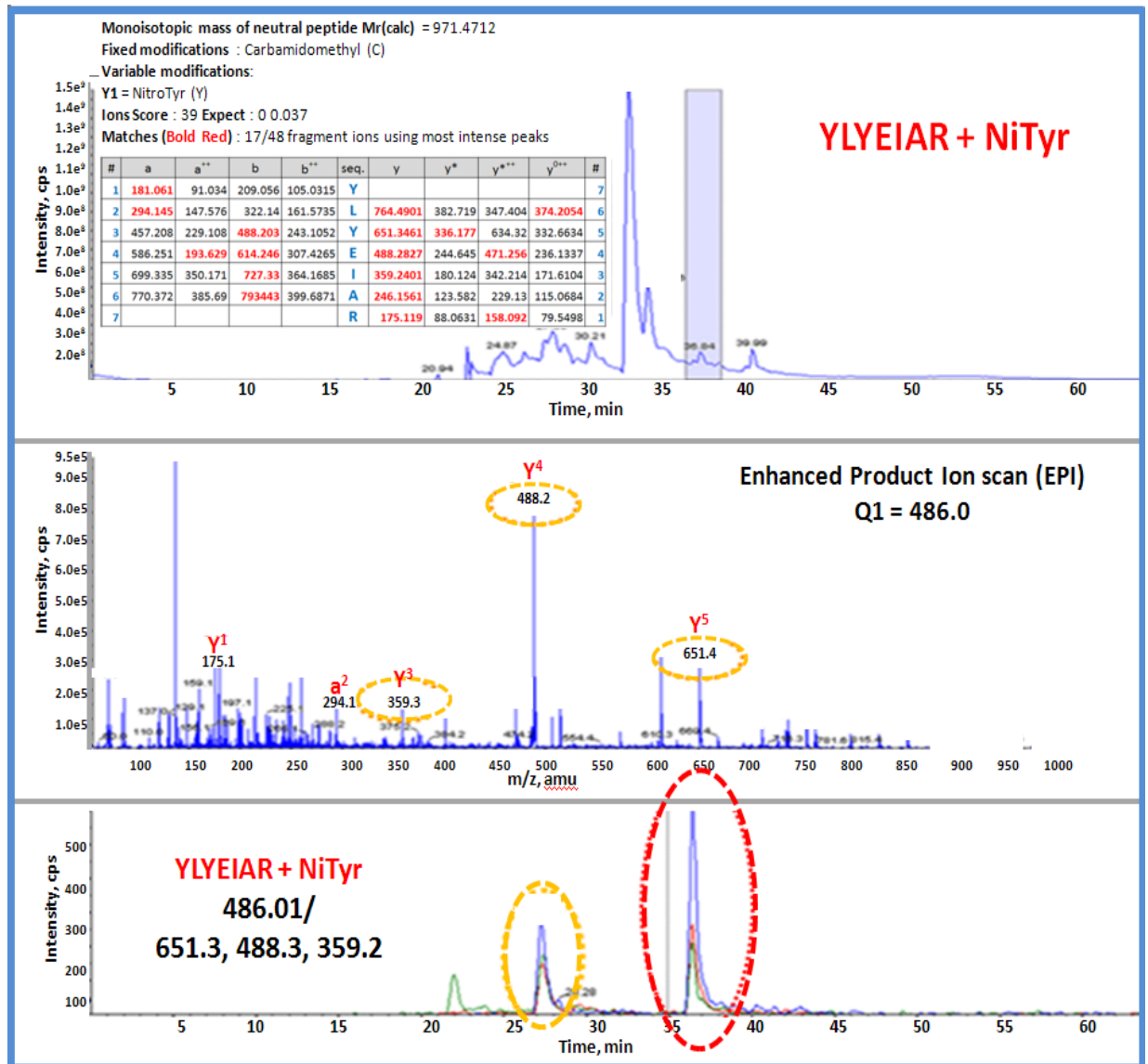


Figure 72: Confirmatory targeted MSMS on YLYEIAR + NiTyr (Q1= 486.01) peptide.

#### 4.4.3.3 Detection of the modified RHPDYSVLLLLR + NiTyr peptide in clinical sample 11

The second NiTyr modified peptide, RHPDYSVLLLLR + NiTyr, whose signal was seen strongly in sample 11 was also confirmed by a targeted MSMS experiment.

The presence of the RHPDYSVLLLLR + NiTyr modified peptide was indicated by the MRM acquisition method analysis of clinical sample 11 (Figure 73). The unmodified RHPDYSVLLLLR peptide (top panel) is seen at 34 minutes into the chromatography gradient with an intensity of <2908cps. The middle panel shows the common elution of transitions Q3=613.4 and 514.4 with an intensity of >200cps but not the third confirmatory transition, Q3=401.3. The retention time (31 minutes) for these two transitions is also observed too early in the chromatography gradient with respect to the unmodified peptide which also

suggests that the RHPDYSVLLLLR + ClTyr modified peptide is not seen in the sample. When the peptide becomes modified by ClTyr or NiTyr the peptide becomes less polar and the retention time of the modified peptide is therefore later than the unmodified state due to the peptide's change in polarity. The bottom panel displays the modified RHPDYSVLLLLR + NiTyr peptide seen at 36minutes with an intensity of >400cps. The modified RHPDYSVLLLLR + NiTyr peptide's Q3 masses have a clear, common elution time and are eluted at an expected time with respect to the unmodified peptide.

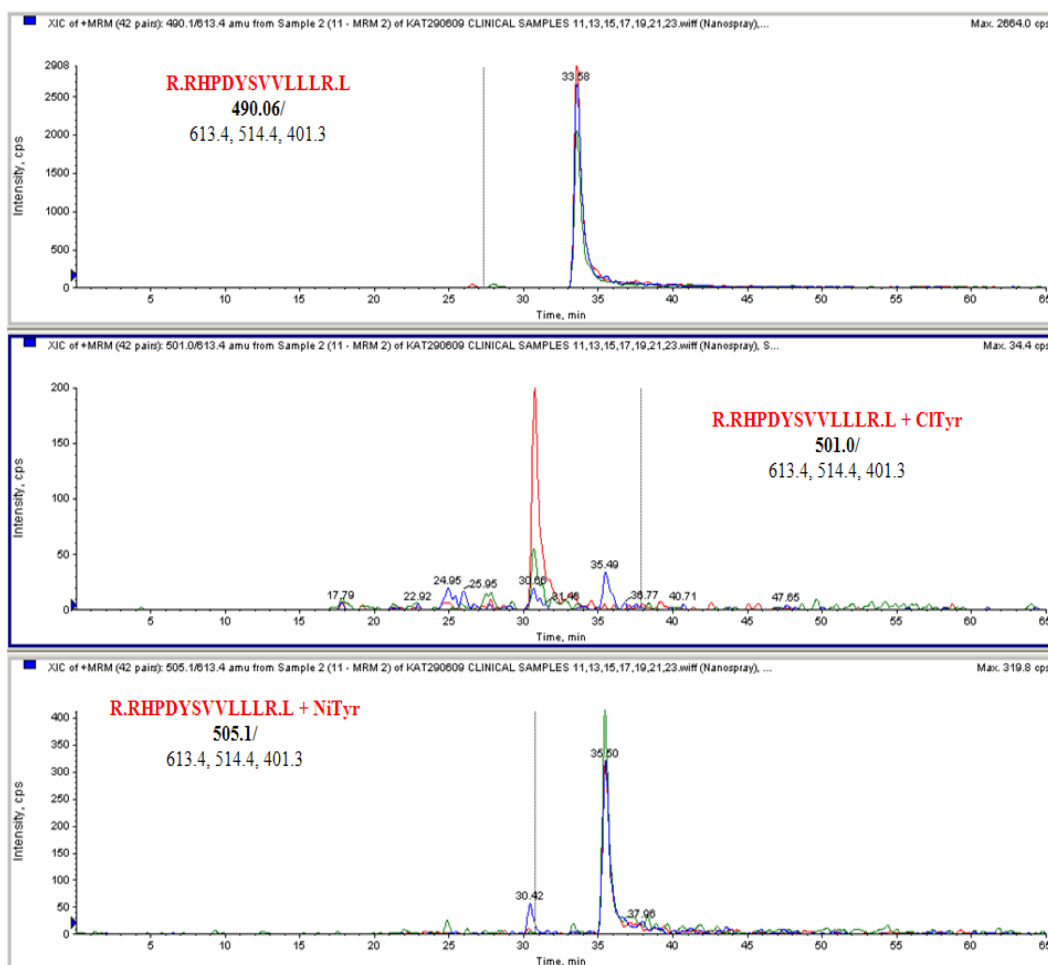


**Figure 73:** The detection of the RHPDYSVLLLLR + NiTyr modified peptide in clinical sample 11. The figure displays the unmodified RHPDYSVLLLLR peptide (top panel) seen at 34minutes into the chromatography gradient with an intensity of <2908cps. The ClTyr modified peptide is not identified but breakthrough signal is observed at 31minutes (middle panel). It is not a true identification of the ClTyr modified peptide when expected retention time is considered with respect to the unmodified peptide. The NiTyr modified peptide is identified at 36minutes (<400cps) into the chromatography gradient with all three transitions seen clearly.

#### 4.4.3.4 Relative quantitation of modification of the RHPDYSVLLLR peptide in clinical sample 11

The modified RHPDYSVLLLR + NiTyr peptide is in high enough abundance (>400cps) to calculate the relative percentage modification (Figure 74). The modified RHPDYSVLLLR + ClTyr peptide is however not seen to be present in sample 11. The relative percentage modification of the RHPDYSVLLLR peptide in Sample 11 was calculated using the transitions intensities and not area under the peak and the equation 7 (3.4.1.1). The calculated percentage modification is approximate and calculated under the assumption that the modified and unmodified states of the peptide have equal ionisation energies.

$$Q3 = 613.4 \quad [300 / (300 + 2500)] \times 100 = 10.7\%$$

$$Q3 = 514.4 \quad [300 / (300 + 2908)] \times 100 = 9.3\%$$

$$Q3 = 401.3 \quad [500 / (500 + 2000)] \times 100 = 20.0\%$$

Average relative percentage modification for clinical sample 11 = **13.3%**

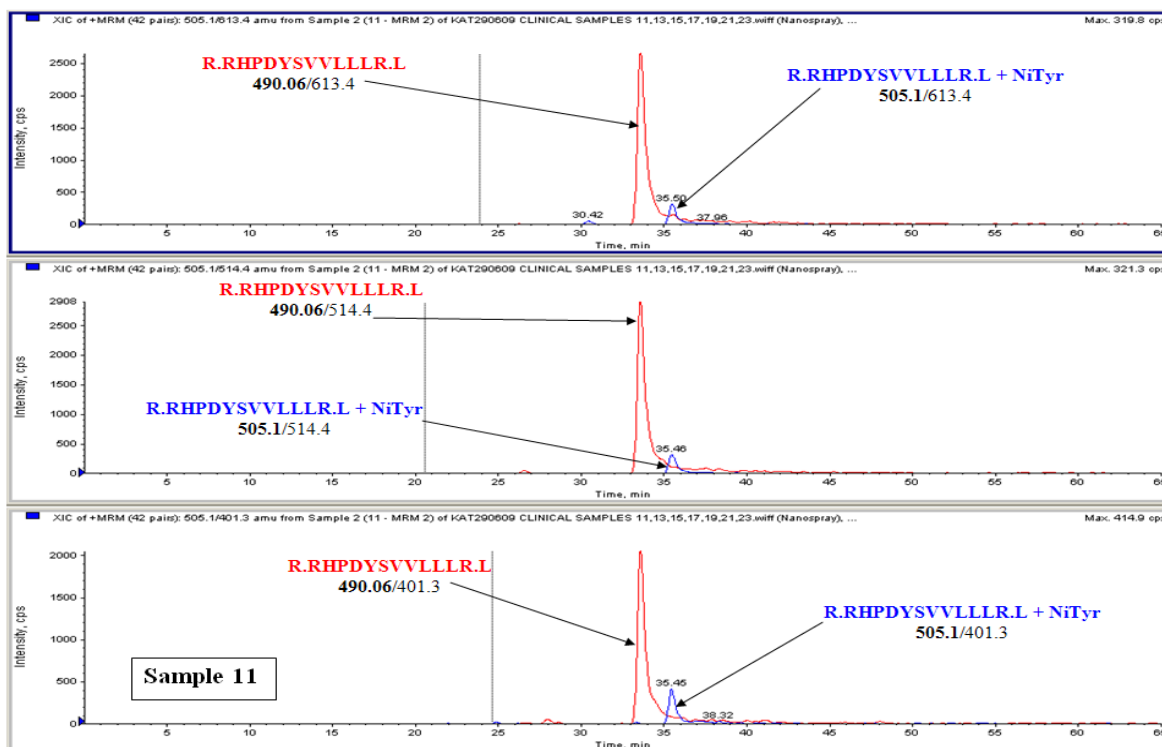
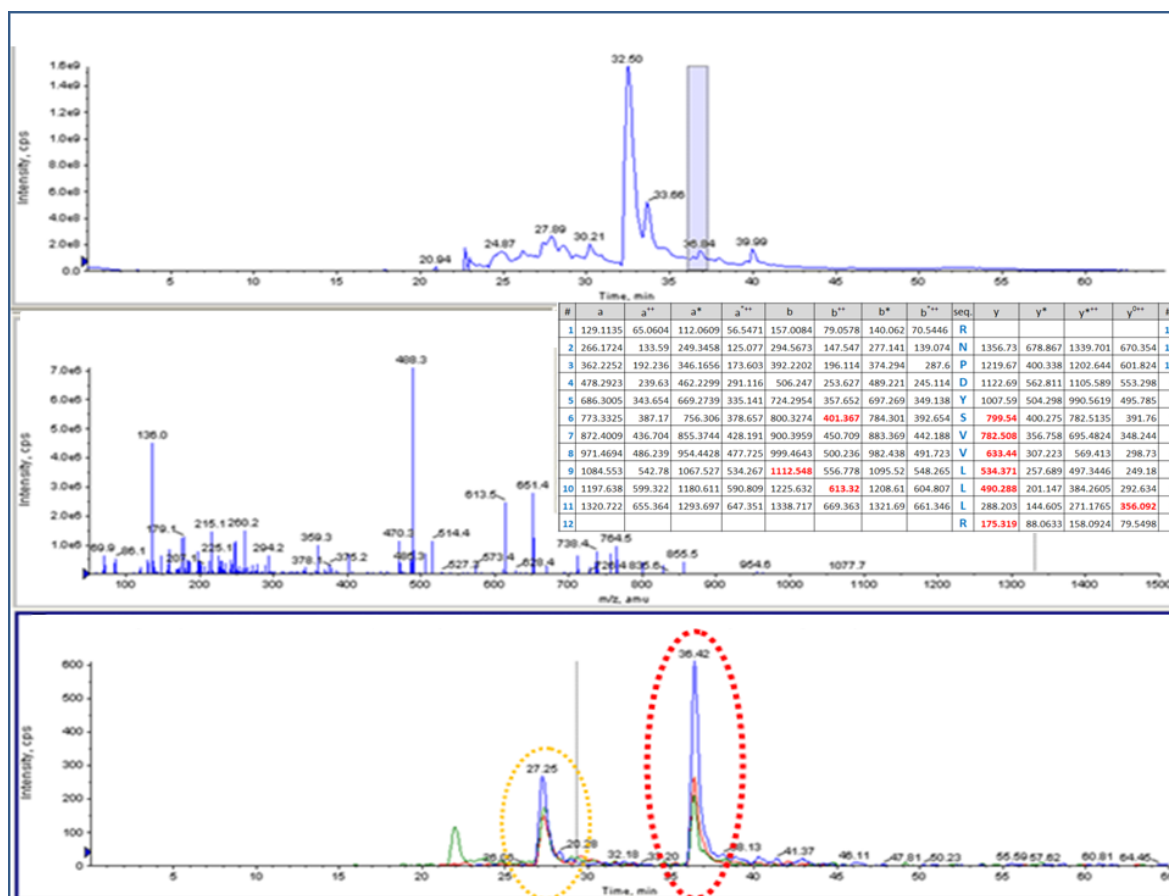


Figure 74: The comparison of the unmodified and modified RHPDYSVLLLR + NiTyr peptide in clinical sample 11. The figure displays the three common Q3 transitions (Q3=613.4 - top panel, 514.4 - middle panel and 401.3 - bottom panel) of the unmodified RHPDYSVLLLR (Q1=490.06, red) and modified RHPDYSVLLLR + NiTyr peptide (Q1=505.1, blue).

#### 4.4.3.5 A targeted MSMS experiment

To confirm the presence of the modified RHPDYSVLLLLR + NiTyr peptide in the clinical sample 11 and the reliability of the MRM methods ability to successfully detect the NiTyr modified peptide in samples a targeted MSMS experiment was performed (Figure 75). The MSMS was targeted to fragment a specific chosen precursor (Q1=505.1) only across the chromatography gradient and the resulting MSMS data was searched using Mascot. Mascot identified the RHPDYSVLLLLR + NiTyr peptide with an ion score of 22. The targeted MSMS experiment was run concurrently with the analysis of sample 11 with the MRM method. The total ion chromatogram (TIC) is displayed in the top panel and where the RHPDYSVLLLLR + NiTyr peptide is known to be eluted is highlighted. The middle panel is the EPI and the Mascot ion match table. The three transitions (Q3= 613.4, 514.4 and 401.3) for the NiTyr modified peptide are commonly eluted (ringed in red) and observed after 35 minutes into the chromatography gradient. There is breakthrough from the unmodified peak seen at 27 minutes (ringed in orange).

Figure 75: Confirmed targeted MSMS of the RHPDYSVLLLLR + NiTyr, (Q1=505.1) peptide in clinical sample 11.



The three transitions (Q3= 613.4, 514.4 and 401.3) for the NiTyr modified peptide are commonly eluted (ringed in red) and observed after 35 minutes into the chromatography

gradient (bottom panel). There is breakthrough from the unmodified peak seen at 27 minutes (ringed in orange). The highlighted window in the top panel is where the targeted peptide has been seen to be eluted and the EPI from this area searched (middle panel). The middle panel also displays the ion-match table from the peptide.

#### 4.5 Summary and comparison of the clinical samples 1- 24

All 24 clinical samples were analysed by MSMS and by the MRM method before being compared (Table 21).

The most common and most intensely seen targeted modified peptide that was detected by the MRM acquisition method was the YLYEIAR + NiTyr peptide. The samples were therefore considered to be from a diseased patient if the following criteria were true;

##### Criteria to be met before a sample can be considered diseased

- The YLYEIAR peptide is nitrotyrosine modified and the signal is seen to be *above* 100cps in intensity.
- If the YLYEIAR peptide is *not* nitrotyrosine modified or *is* but the signal is seen to be *below* 100cps in intensity there must be at least *one or more* other ClTyr/NiTyr modified peptides detected.
- The modified peptide either ClTyr or NiTyr must be eluted and seen in the chromatography gradient *after* the unmodified peptide

Following the above criteria in the Table 21 if the samples were classified healthy they were coloured yellow. If classified by our criteria to be diseased were coloured in blue. MRM signals from a modified peptide with an intensity below 100cps were coloured orange and those above 100cps were coloured in green. Unmodified peptides detected were left white and where no MRM signal for the peptide targeted for was observed a “X” was used.

The data collected from the study of the clinical samples is incomplete (all unmodified peptides targeted for should *always* be detected regardless if sample is diseased or healthy) and the data is fragmented. From the data summarised in Table 22 we see that there are samples; 3, 7 and 9 where the modified peptide

is identified from the MRM analysis but the unmodified peptide is not. From previous discussion it is suggested that the ClTyr and NiTyr post translational modifications resulting from oxidative stress are in low abundance. It then seems unreasonable for the modification to be seen but not the unmodified counterpart. What is also unexpected is that for all 24 samples not all the unmodified peptides targeted for by the MRM method are observed. Due to the abundance of albumin in the plasma all unmodified peptides targeted for should be identified. This leads us to the conclusion that there may have been a problem with sampling during the analysis. There was only one analysis carried out for each clinical sample and more technical replicates are required to know the variables from the analysis of each sample. If more technical replicates are performed we can then decide what is statistically significant and determine the reproducibility of this analysis by comparing XIC's.

Table 21: Summary and comparison of clinical samples.

Peptide	1	2	3	4	5	6	7	8	9	10	11	12	13	14	15	16	17	18	19	20	21	22	23	24
K_YLYEIAR.R	29mins 1.14E-04	29mins 5777	28mins 1600	28mins 3.80E-04	28mins 5799	28mins 2000	28mins 1564	28mins 3.50E-04	28mins 7747	28mins 5777	29mins 7608	28mins 3354	29mins 1400	28mins 3450	30mins 6000	28mins 3.30E-04	30mins 4000	28mins 4.40E-04	29mins 2500	28mins 1945	29mins 2000	28mins 5.90E-04	29mins 1.60E-04	27mins 6.05E-04
K_YLYEIAR.R + NitroTyr (Y)	37mins 48	x	x	37mins 100	37mins 47	37mins 44	37mins 40	37mins 300	37mins 80	37mins 57	37mins 1400	x	x	x	38mins 50	37mins 169	38mins 50	37mins 250	38mins 25	x	38mins 13	37mins 381	37mins 60	37mins 600
K_YLYEIAR.R + 2 NitroTyr (Y)	x	x	x	x	x	x	x	x	x	x	x	x	x	x	x	x	x	x	x	x	x	x	x	x
R.RHPDYSVVLRL.L	x	34mins 1600	x	33mins 1.00E-04	33mins 50	33mins 1150	x	33mins 9112	x	33mins 2500	38mins 2908	33mins 800	35mins 184	33mins 1000	35mins 100	33mins 9993	35mins 442	33mins 1.40E-04	35mins 60	33mins 668	34mins 79	33mins 9734	34mins 4000	33mins 1.30E-04
R.RHPDYSVVLRL.L + ChloroTyr (Y)	x	x	x	x	x	x	x	x	x	x	x	x	x	x	x	x	x	x	x	x	x	x	x	x
R.RHPDYSVVLRL.L + NitroTyr (Y)	x	x	34mins 68	x	x	x	x	34mins 151	35mins 56	35mins 35	x	36mins 400	x	x	x	35mins 60	x	35mins 140	x	x	x	35mins 60	x	35mins 221
K.DVFLGMFLYEYAR.R	28mins 96	45mins 48	x	45mins 91	x	45mins 36	x	45mins 60	x	45mins 60	45mins 59	x	x	x	x	44mins 60	x	45mins 83	x	x	x	44mins 86	45mins 60	44mins 100
K.DVFLGMFLYEYAR.R + Oxidation (M)	x	x	x	x	x	x	41mins 149	x	x	x	43mins 95	x	x	x	x	x	x	x	x	x	x	x	x	x
K.DVFLGMFLYEYAR.R + ChloroTyr(Y); Oxidation (M)	x	x	x	x	x	x	x	x	x	x	x	x	x	x	x	x	x	44mins 60	x	x	x	44mins 53	x	x
K.DVFLGMFLYEYAR.R + 2ChloroTyr(Y); Oxidation (M)	x	x	x	x	x	x	x	x	x	x	x	x	x	x	x	x	x	x	x	x	x	x	x	x
K.DVFLGMFLYEYAR.R + NitroTyr (Y); Oxidation (M)	x	x	x	x	x	x	x	x	x	x	x	x	x	x	x	x	x	x	x	x	x	x	x	x
R.RHP_YFYAPELFFAK.R	x	39mins 400	x	39mins 4000	x	39mins 250	x	38mins 3940	x	38mins 500	40mins 658	39mins 192	41mins 80	39mins 228	x	39mins 3922	41mins 179	38mins 4758	x	38mins 160	x	38mins 6943	40mins 1786	38mins 1.20E-05
R.RHP_YFYAPELFFAK.R + ChloroTyr(Y)	x	x	40mins 50cps	x	x	x	x	39mins 20	x	x	x	x	x	x	x	x	x	x	x	x	x	x	x	x
R.RHP_YFYAPELFFAK.R + NitroTyr (Y)	x	x	34mins 80	x	x	x	x	33mins 177	x	x	41mins 30	x	x	x	x	x	x	x	x	x	x	x	x	x

## KEY

x	Peptide is not seen to be modified. No common elution of the three transitions
Green box	Peptide is seen to be modified. There is a common elution of the three transitions and intensity is above >100cps
Orange box	Peptide is seen to be modified. There is a common elution of the three transitions but intensity is below <100cps
Yellow box	HEALTHY - Sample analysis has not met the criteria to be considered diseased
Blue box	DISEASED - Sample analysis has met the criteria to be considered diseased

The above table displays the time the peptide is seen to be eluted and the intensity (cps) of which the signal is seen. The white box with the “x” denotes that the Ni/CITyr modified targeted peptide was definitely not seen. The dark orange box denotes that the Ni/Tyr modified targeted peptide was seen but in low abundance (<100cps). The green box denotes that either the Ni- or CITyr modified targeted peptide was definitely seen (>100cps)

The clinical samples classified by our criteria said to be from diseased patients are 3, 4, 7, 8, 11, 18, 22 and 24 and the clinical samples said to be from healthy volunteers are 1, 2, 5, 6, 9, 10, 12, 13, 14, 15, 17, 19, 20, 21 and 23. We already know from these results that we cannot be correct as from the 24 samples analysed we know 12 are from healthy and 12 were from diseased sources.

As discussed before, the analysis of the 24 samples was performed blinded to avoid any bias in the comparison of the samples. The MRM acquisition methods were developed on plasma and a model protein, HSA. Building criterium for the classification of healthy and diseased samples was developed by first identifying which human serum albumin peptides were seen to be modified *in vitro* by HOCl and SIN-1. It is hypothesised that sites of modification identified from chemical modification *in vitro* should also be seen *in vivo* as the modification was performed on native protein meaning the same sites of modification will be susceptible.

#### **4.5.1 The clinical samples “un-blinded”**

After analysis of the 24 clinical samples Christian Delles, who provided the samples, informed us which of the samples were from healthy volunteers and which of those were from diseased patients. The known diseased and healthy samples were compared with our classifications (Table 22).

The un-blinding of the samples showed that out of the 24 clinical samples only 13 were classified correctly by our criteria. This result is close to random suggesting that the MRM method and our set criteria cannot be used as a way to classify healthy from diseased samples. It is possible that to classify for disease a more complex approach should be taken. The most intense peptides seen to be modified may be very susceptible to modification and these modified peptides will be observed regardless if a sample is from a healthy or diseased source. The modified peptides specific to disease could be low level and below our limit of detection so were therefore not detected and identified in our MSMS observations from which the MRM acquisition methods were written.

Table 22: Clinical Samples un-blinded.

Source	Clinical sample	Classified	Result
2056-HEA	1	H	right
2044-HEA	2	H	right
313-CAB	3	D	right
2048-HEA	4	D	wrong
320-CAB	5	H	right
2075-HEA	6	H	right
2066-HEA	7	D	wrong
296-CAB	8	D	right
2074-HEA	9	H	right
2057-HEA	10	H	right
318-HEA	11	D	wrong
2042-HEA	12	H	right
295-CAB	13	H	wrong
307-CAB	14	H	wrong
319-CAB	15	H	wrong
157-CAB	16	D	right
2071-HEA	17	H	right
284-CAB	18	D	right
314-CAB	19	H	wrong
300-CAB	20	H	wrong
327-CAB	21	H	wrong
2065-HEA	22	D	wrong
2045-HEA	23	H	right
2059-HEA	24	D	wrong

CAB - Diseased	D - Diseased
HEA - Healthy	H - Healthy
<b>13 out of 24 correct classifications = 41.46% success</b>	

The table (from left to right) illustrates the source from which the clinical sample is from; HEA=healthy volunteer or CAB=coronary artery diseased patient, the Clinical Sample Number (1-24), the results from the MRM results (either H=healthy or D=diseased) and the results from the “un-blinding” of the clinical samples (wrong = no match and right=match).

To improve the results samples which did not show all four unmodified targeted peptides were discarded (Table 23). This improved the classification by our criteria (from 41.46% success to 55.5%) slightly but still not enough to be statistically viable as a method for classification of diseased and healthy samples. It is possible that to classify diseased samples (from patients that have suffered/suffer symptoms of atherosclerosis i.e. strokes, heart attacks, high

blood pressure etc) from healthy samples that more than one and indeed a combination of certain biomarkers are required. The MRM method was written from MSMS observations from the conventional analysis of *in vitro* chemically modified purified HSA samples. There may be other lower abundance NiTyr and ClTyr modifications that were not identified by the initial conventional MSMS analysis and were therefore not targeted for in the MRM method for disease classification. It is possible that these potential biomarkers that were not observed could then be used alone or as a combination for the classification of disease.

Table 23: Discarding of samples where all unmodified peptides targeted for were not detected.

Peptide	2	4	6	8	10	11	16	18	22	23	24
K.YLYEIAR.R	29mins 5777	28mins 3.80E+04	28mins 2000	28mins 3.50E+04	28mins 5777	29mins 7608	28mins 3.30E+04	28mins 4.40E+04	28mins 5.90E+04	29mins 1.60E+04	27mins 6.05E+04
K.YLYEIAR.R + NitroTyr (Y)	x	37mins 100	37mins 44	37mins 300	37mins 57	37mins 1400	37mins 169	37mins 250	37mins 381	37mins 60	37mins 600
K.YLYEIAR.R + 2 NitroTyr (Y)	x	x	x	x	x	x	x	x	x	x	x
R.RHPDYSVYLLLR.L	34mins 1600	33mins 1.00E+04	33mins 1150	33mins 9112	33mins 2500	38mins 2908	33mins 9993	33mins 1.40E+04	33mins 9734	34mins 4000	33mins 1.30E+04
R.RHPDYSVYLLLR.L + ChloroTyr (Y)	x	x	x	x	x	x	x	x	x	x	x
R.RHPDYSVYLLLR.L + NitroTyr (Y)	x	x	x	35mins 56	x	36mins 400	35mins 60	35mins 140	35mins 60	x	35mins 221
K.DVFLGMFLYEYAR.R	45mins 48	45mins 91	45mins 36	45mins 60	45mins 60	45mins 59	44mins 60	45mins 83	44mins 86	45mins 60	44mins 100
K.DVFLGMFLYEYAR.R + Oxidation (M)	x	x	x	x	x	43mins 95	x	x	x	x	x
K.DVFLGMFLYEYAR.R + Chloroty(Y); Oxidation (M)	x	x	x	x	x	x	x	44mins 60	44mins 53	x	x
K.DVFLGMFLYEYAR.R + 2Chloroty(Y); Oxidation (M)	x	x	x	x	x	x	x	x	x	x	x
K.DVFLGMFLYEYAR.R + NitroTyr (Y); Oxidation (M)	x	x	x	x	x	x	x	x	x	x	x
R.RHPYFYAPELFFAK.R	39mins 400	39mins 4000	39mins 250	38mins 3940	38mins 500	40mins 658	39mins 3922	38mins 4758	38mins 6943	40mins 1786	38mins 1.20E+05
R.RHPYFYAPELFFAK.R + Chloroty(Y)	x	x	x	39mins 20	x	x	x	x	x	x	x
R.RHPYFYAPELFFAK.R + NitroTyr (Y)	x	x	x	39mins 177	x	41mins 30	x	x	x	x	x

Source	Clinical sample	Classified	Result
2044-HEA	2	H	right
2048-HEA	4	D	wrong
296-CAB	8	D	right
2057-HEA	10	H	right
318-HEA	11	D	wrong
284-CAB	18	D	right
2065-HEA	22	D	wrong
2045-HEA	23	H	right
2059-HEA	24	D	wrong

CAB - Diseased	D - Diseased
HEA - Healthy	H - Healthy
5 out of 9 correct classifications = 55.55% success	

The above displays the table of clinical samples from which all unmodified peptides targeted for were identified. On the left displays which of the clinical samples were classified correctly.

## 4.6 Comparison of conventional MSMS with the MRM

Analysis of the clinical samples by conventional MSMS did not result in any chloro or nitrotyrosine modifications being detected and assigned using the search engine Mascot. The conventional MSMS method of analysis is a less sensitive method of the detection of low abundance proteins or post translational modifications of proteins in comparison with the MRM technique (Figure 76). The top scan in the figure, the product ion scan, also known as conventional MSMS works by MS1 also known as Q1 being fixed to fragment the top most intense precursor to be fragmented by CID. The MS2 also known as Q3 then scans these fragments out to be detected by the detector. The multiple ion monitoring method is shown below the product ion scan and analyses by fixing both the MS1 and MS2. The technique is carried out by the instrument cycling through a series of transitions (specific precursor-fragment pairs) and records the signal as a function of time. Because both the MS1 and MS2 are fixed to target specific masses the MRM method is more selective and sensitive for the detection of low abundant proteins or modification of proteins in complex samples.

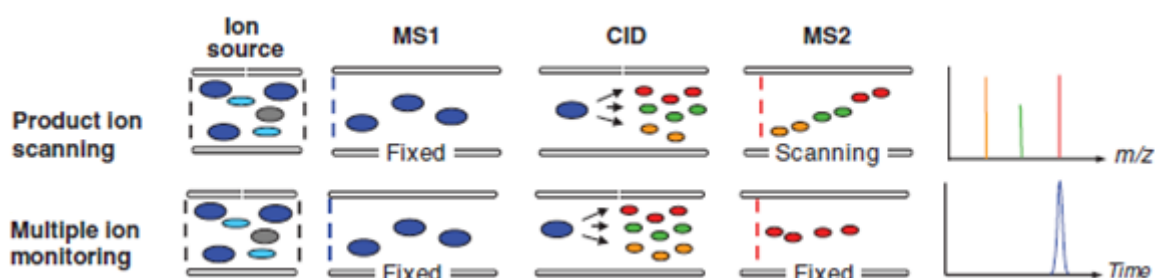


Figure 76: Conventional MSMS versus MRMs [161]. The figure illustrates Product Ion scanning and Multiple Ion Monitoring in the triple quadrupole.

The conventional MSMS performed on peptides in a sample will fragment the chosen precursor for analysis [161]. Usually this is the most intense precursor leading to the most abundant and intense precursors being analysed first which means the less abundant and less intense masses will be “masked” or missed. The MRM method fixes both quadrupole 1 and quadrupole 3 to target set precursor-fragment pairs allowing low abundant peptides to be detected. The reason for the conventional MSMS not detecting any chloro- or nitrotyrosine modifications in the clinical samples is because they are in low abundance. The MRM method is therefore more suited to the detection of low abundant modifications in complex samples.

## 4.7 Oxidative modification seen in healthy samples

As discussed before in the introduction, most individuals when they have reached a certain age will suffer from a thickening of the arterial wall and from a level of oxidative stress. Although we know the sources of the clinical samples; all male patients and for the controls all male healthy volunteers, there are many possible explanations for ClTyr and NiTyr modifications. If any of the individuals were smokers this would be an explanation of modification as it has been reported that the nitrogen oxides and/or their reaction products in the gas phase will convert tyrosine to nitrated and oxidised products<sup>[205]</sup>. The healthy volunteers may have also just recently been involved in physically strenuous activity. Increased aerobic metabolism during exercise is a potential source of oxidative stress, creating an imbalance between the oxidant and anti-oxidant levels<sup>[206]</sup>. In muscle the mitochondria are a potential source of reactive intermediates producing superoxide ( $O_2^{\cdot-}$ ), hydrogen peroxide ( $H_2O_2$ ), the hydroxyl radical ( $HO^{\cdot}$ ) and nitric oxide ( $NO^{\cdot}$ ) under aerobic activities. The benefits of regular exercise is well documented and although there is initial oxidative damage the individual will adapt to reduce overall oxidative stress by an upregulation of anti-oxidant enzymes and a reduced basal level of oxidants.

The MRM acquisition method although successfully detecting and indicating the targeted NiTyr and ClTyr modified peptides in some of the clinical samples do not correlate well with patients suffering from the symptoms of cardiovascular disease.

### 4.7.1 The initial development of atherosclerosis by the heme enzyme, myeloperoxidase (MPO)

The fatty streak is an inflammatory lesion consisting of monocyte derived macrophages and T-lymphocytes. The development of atherosclerosis begins with the oxidative damage initiated by the inflammatory cells on the arterial wall. The inflammatory cells such as monocytes, macrophages and neutrophils release oxidising enzymes such as the heme enzyme, myeloperoxidase (MPO). The myeloperoxidase enzyme catalyses the oxidation and modification of proteins and free 3-ClTyr and NiTyr have been seen elevated in the blood of atherosclerotic patients. The presence of 3-ClTyr and NiTyr in a system serve as specific markers for oxidative damage by MPO-activity. It is not atherosclerosis that triggers myocardial infarction but the precipitation by the rupture of

atherosclerotic plaque <sup>[207]</sup>. The oxidants (Reactive Oxygen Species [ROS] and Reactive Nitrogen Species [RNS]) play an important role in plaque rupture. Regions of the ruptured plaque were investigated by Hazell et al <sup>[208]</sup> using a specific anti body to detect for hypochlorous acid-modified proteins which would indicate an increase in damage to proteins by oxidative stress in these ruptured plaque areas.

#### **4.7.2 Development of atherosclerotic lesions**

It has been found that the initiation of atherosclerosis can start early in individuals. Almost every N. American child over 3years in age possesses a degree of fatty streaks <sup>[209]</sup>. The fatty streak is harmless but appears to be the initial atherosclerotic lesion. The research showed that juvenile fatty streaks vary characteristically at certain anatomical sites but can go on to be converted into a fibrous plaque and undergo changes directly causing arterial occlusion in the later stages in life when the disease becomes more progressive. There have been studies showing that 1 in 6 American teenagers already suffered from the pathological, thickening in the coronary arteries <sup>[210]</sup>. In a study of 262 male and females with an average age of  $33.4 \pm 13.2$  years, 51.9% of the individual studied were found to possess atherosclerotic lesions. Out of that group, 17% were under 20years of age and 85% were over 50years in age. Although the younger members of the study were prevalent to possessing atherosclerotic lesions it was only after the age of 40year that the individual began to suffer from the symptoms of atherosclerosis such as hypertension, angina (when the plaque narrows and then blocks the arteries), shortness of breath and arrhythmias (irregular heart beat). Another study demonstrating that atherosclerosis begins early in life is the investigation of the results following the autopsy of soldiers killed in the Korean and Vietnam wars. It was indicated that they too had suffered from atherosclerosis <sup>[211]</sup> although the individuals had not suffered from any atherosclerotic-complications that may have become more evident later in life. The Pathological Determinants of Atherosclerosis in Youth (PDAY) have also investigated young individuals (age range between 15-34years) that had passed away by causes unrelated to atherosclerosis (suicide, accidents or homicide for example) and found extensive lesions and not just fatty streaks in the aorta and right coronary artery in some individuals <sup>[212]</sup>.

The increased concentration of cholesterol and changes in its physical state accompanied with morphological progression of atherosclerotic lesions was evidence that atherosclerosis is a seamless process beginning in childhood or adolescence and culminating in rupture of a plaque, thrombosis and ischaemic necrosis of a target organ in adulthood <sup>[213]</sup>. It is important to monitor the development and progression of atherosclerosis as in the case of coronary arterial thromboses, it is reported, the underlying lesion does not produce critical arterial narrowing until weeks or months before myocardial infarction <sup>[214]</sup>.

#### 4.7.3 Challenges when choosing targeted modified peptides specific to disease

Choosing modified peptides to be targeted by the MRM method to diagnose cardiovascular disease is challenging. There can be many possible modifications for one peptide. The modified NiTyr peptide, Y<sup>1</sup>LY<sup>2</sup>EIAR can have either the modified Y1 or Y2 or both as discussed in 3.6.4. For the Y<sup>1</sup>LY<sup>2</sup>EIAR peptide the MRM only detected Y1 to be nitrotyrosine modified. When the MRM method was used to detect NiTyr modifications in chemically modified Human Serum Albumin and plasma samples by SIN-1 both the NiTyr and di-NiTyr (Y<sup>1</sup>LYEIAR + NiTyr and Y<sup>1</sup>LY<sup>2</sup>EIAR + 2NiTyr) modified peptides were detected. The Y<sup>1</sup>LYEIAR + ClTyr and Y<sup>1</sup>LY<sup>2</sup>EIAR + 2ClTyr modified peptides were not targeted for as they were not seen in the MSMS analysis of the HOCl chemically modified HSA and plasma samples.

The MRM acquisition method detected the targeted RHPDYSVLLLR peptide, both NiTyr modified and ClTyr modified, in both samples that were initially classified as “diseased” and “healthy” by our criteria.

The DVFLGMFLY<sup>1</sup>EY<sup>2</sup>AR targeted peptide is even more problematic to analyse accurately due to the number of modification sites present. As discussed in 3.9.2 both Y modification sites are unlikely to both be modified and the peptide was always observed with the methionine residue oxidized first as the methionine site is the initial site of oxidation. The di-chloro and di-nitrotyrosine modifications were not detected in clinical samples. The DVFLGMFLYEYAR + Ox(M) modification is not useful in the diagnosis or identification of diseased samples from healthy samples as the oxidation of methionine is non specific to

disease and can be caused by exposure to the air. There are two tyrosine sites for modification so possible modified peptides that were not targeted for are the methionine oxidation, NiTyr(Y1) + ClTyr(Y2) modified state DVFLGMFLY<sup>Ni</sup>EY<sup>Cl</sup>AR + Ox(M);NiTyr;ClTyr and the methionine oxidation, ClTyr(Y1) + NiTyr(Y2) modified state DVFLGMFLY<sup>Cl</sup>EY<sup>Ni</sup>AR + Ox(M);ClTyr;NiTyr . If these modified states of the peptide are present this would mean that the peptide is highly modified and is maybe unlikely considering the di-nitrotyrosine modified peptide, Y<sup>1</sup>LY<sup>2</sup>EIAR + 2NiTyr, was not identified.

The RHPYFYAPELLFFAK peptide was seen to be modified in clinical samples 3 and 8, both NiTyr and ClTyr modified states were seen and in sample 11 the peptide was only seen to be NiTyr modified. Again there is a possibility of more than the NiTyr(Y2) and ClTyr(Y2) modification states of the RHPY<sup>1</sup>FY<sup>2</sup>APELLFFAK peptide being present. The Y2 tyrosine is always seen to be modified first and even though it is not close to a methionine or lysine residue in the primary sequence it may be in close proximity in space by the secondary or tertiary sequence due to the folding of the albumin protein. In strongly oxidised conditions the RHPY<sup>1</sup>FY<sup>2</sup>APELLFFAK + NiTyr(Y1);ClTyr(Y2) and RHPY<sup>1</sup>FY<sup>2</sup>APELLFFAK + ClTyr(Y1);NiTyr(Y2) peptide may be present. Again this is unlikely as the Y<sup>1</sup>LY<sup>2</sup>EIAR + 2NiTyr targeted peptide was not detected.

In the clinical samples the Y<sup>Ni</sup>LY<sup>2</sup>EIAR + NiTyr peptide is seen but the Y<sup>Ni</sup>LY<sup>Ni</sup>EIAR + 2NiTyr is not. The Y2 residue or the second tyrosine may be modified by a chlorine atom and not NO<sub>2</sub>, giving the Y<sup>Ni</sup>LY<sup>Cl</sup>EIAR + NiTyr(Y1);ClTyr(Y2). This may be possible the Y<sup>Cl</sup>LY<sup>Ni</sup>EIAR + ClTyr(Y1);NiTyr(Y2) but not very probable under the oxidation conditions. These “hetero-modified peptides” were not targeted by the MRM acquisition method as MSMS data was collected from the analysis of individually SIN-1 or HOCl modified purified HSA and plasma so were obviously never seen.

#### 4.8 Conclusion and further work

The MRM acquisition method developed from the SIN-1 and HOCl chemically modified purified HSA and plasma samples successfully detected nitrotyrosine and chlorotyrosine modified peptides in clinical samples. Although the MRM method was successful in detecting the modified peptides these peptides and our criteria were unable to differentiate between healthy and diseased samples

and therefore failed as a diagnosis tool correctly identifying only 13 out of a total of 24 clinical samples. As discussed; from the fragmented nature of the data collected from the analysis, there may have been a problem in sampling during analysis. There needs to be more technical replicates of the analysis of the clinical samples.

#### **4.8.1 False Positives**

The transitions for the MRM acquisition method were chosen from observations made from the MSMS analysis of chemically modified purified human serum albumin and plasma samples. The Q3 masses for the MRM transitions were chosen due to their intensity and frequency seen in the MSMS analysis. To improve the MRM acquisition method the Q3 masses could also be chosen depending on the number or intensity of anomalous peaks they show in the chromatography run. The anomalous peaks in the XIC traces are not difficult to identify and are easily recognised by a single transition peaking in respect to the other two Q3 transitions. False positives caused by breakthrough can be confusing. Breakthrough is caused from another signal due to poor selection in Q1 and all the transitions are seen to peak at the same time. To identify which peak of the three commonly eluted transitions is the elution of the peptide targeted for the retention time when it is eluted can be used. The ClTyr/NiTyr modified peptides are seen later and the oxidation of a methionine in a peptide will be seen sooner in the chromatography gradient with respect to the unmodified peptide due to changes in polarity.

#### **4.8.2 Improving the MRM method to detect disease specific Ni- and ClTyr modifications**

Although elevated levels of ClTyr and NiTyr have been found in the plasma of diseased patients it is clear that the initial stages of atherosclerosis and therefore oxidative stress occur at a very young age. At a young age although suffering or possessing atherosclerotic lesions the individual is asymptomatic until the later stages in life. Modification of proteins by oxidative stress will therefore also occur at an early age as the fatty streak begins to develop.

##### **4.8.2.1 Patient Heterogeneity**

In this study patient heterogeneity is not taken into account and it is assumed that the individuals taking part in this study are homogeneous. There will be

differences between patients or between the “healthy” volunteers caused by the individual’s genetics, their behavioural profile that is their disease management skills which will be influenced by their habits; diet, smoking, exercise levels (as discussed by Kaplan et al <sup>[215]</sup>). These variables may effect factors such as the antioxidant levels in the individual and therefore the results of the the study.

# Chapter 5

---

Investigating the post-translational modification of the low density lipoprotein (LDL) protein moiety, apolipoprotein B-100 (Apo B100), caused by oxidative stress

## **5 Chapter – Investigating the post-translational modification of the low density lipoprotein (LDL) protein moiety, apolipoprotein B-100 (Apo B100), caused by oxidative stress**

The major target for oxidation is thought to be the intimal low-density lipoproteins. The “oxidation theory” for atherosclerosis implies that the lipid and/or protein oxidation products are responsible for the formation and development of lesions <sup>[216]</sup>. The study of LDL and its relevance to atherosclerosis has found that patients suffering from the disease possess elevated levels of LDL in the body and ox-LDL (LDL modified by oxidative stress) have also been found in atherosclerotic lesions <sup>[13;39;217;218]</sup>. The formation of lesions or the fatty streak on the arterial wall is formed by a series of events. The intimal accumulation of plasma lipoproteins and the increased expression of adhesion molecules on the endothelium at inflamed sites on the vessel wall lead to the margination of monocytes and their migration across the endothelium where they accumulate large intracellular deposits of lipoprotein derived cholesterol ergo producing the atherosclerotic lesion. As well as being the major target for oxidation, increased levels of LDL in the body is a known risk factor for atherosclerosis as the majority of the intracellular lipids accumulating in the macrophages beneath the endothelium is thought to be derived from LDL <sup>[219]</sup>. The formation or development of these lipid-laden macrophages or “foam cells” that form the fatty streak or early lesion is an early event in atherosclerosis. Normally the LDL-receptor pathway controls the cellular uptake of LDL particles in a controlled manner that does not allow macrophages to form foam cells (see 1.1.1). However when the LDL becomes modified to Ox-LDL this creates high-uptake forms of LDL leading to the high unspecific uptake of LDL into the endothelium leading to foam cell formation and the development of the fatty streak. Due to atherosclerosis occurring in individuals at an early age the modification of the circulating LDL particle may be another viable way to diagnose cardiovascular disease in patients.

The heme enzyme, myeloperoxidase (MPO), is expressed during inflammation and has been shown to play a role in the development and progression of

atherosclerosis. The enzyme forms the reactive species, HOCl and NO<sub>2</sub> which leads to the formation of chlorotyrosine and nitrotyrosine which are clinically significant and serve as markers for MPO activity<sup>[57]</sup>. The direct treatment of proteins with HOCl and NO<sub>2</sub> has already been reported to cause oxidative damage related to disease and levels of nitrotyrosine and chlorotyrosine have also both been detected in the fatty streak of atherosclerotic lesions in the arteries<sup>[155;160;160;7]</sup>.

## 5.1 Aims

In this chapter we aim to chemically oxidise native LDL by HOCl and SIN-1 and detect the oxidised modifications in the protein moiety, Apolipoprotein B100 using sensitive mass spectrometry techniques; the precursor scan and by MRM methods.

## 5.2 Materials and Methods

### 5.2.1 Preparation of LDL from Plasma

15ml plasma samples from a plasma pool were supplied by Corinne M. Spickett (Institute of Pharmacy and Biomedical sciences, University of Strathclyde, Glasgow). The plasma had been stored at -80°C for approximately 2years. To prepare the LDL the plasma was thawed in a water bath at 37°C before the plasma density was adjusted to 1.24g/ml by the addition of 0.3816g of KBr (potassium bromide) per ml of plasma by stirring thawed plasma in ice. The stirring of the plasma and KBr was gentle to avoid denaturing. An EDTA (ethylenediaminetetraacetic acid, 1g EDTA/L, d=1.0g/ml, pH 7.4) solution is deoxygenated in its bottle by bubbling oxygen-free nitrogen through it for a minimum period of 15 minutes. A long luer fitting needle with a blunt end was used to place 3.6ml of deoxygenated EDTA solution into a 5.1ml quick seal disposable plastic centrifuge tube. The density-adjusted plasma is then underlaid beneath the EDTA until the liquid comes to just below the bottom of the thin neck of the centrifuge tube. The tubes are balanced and if required were adjusted with small amounts of EDTA solution. The quick-seal centrifuge tubes were then sealed with a heat sealer before being placed in a Beckman VTi 90 rotor. The centrifuging of the samples was carried out at 60,000 rpm for 2 hours at 10°C in a Beckman XL-90 ultra centrifuge with acceleration and deceleration set to 9. After centrifugation the tubes containing the plasma were removed

using tweezers and handled carefully as not to disturb the lipoprotein bands. The LDL band is visualised as a darker band in the tube when viewed against a white background. To remove the LDL a small needle was inserted into the top of the tube by the neck and a second sterile guage needle (21G x 1½", 0.8mm x 40mm, BD Microlance™ 3) attached to a 5ml syringe was inserted just below the LDL band (about two-thirds of the way down the tube) and the needle was swept back and forth whilst sucking up the LDL. The vial where the LDL was to be collected was prepared by flushing through with nitrogen gas. The LDL was stored at 4 °C in the dark for up to two weeks. To avoid denaturing of the LDL de-salting was usually performed on the same day.

#### **5.2.1.1 Desalting of the LDL**

Desalting of the LDL preparation was performed by gel filtration to remove any traces of KBr and EDTA.

1ml of the LDL solution was removed from the vial using a sterile needle and a 1ml syringe and placed on the top of an Econopac column 10 DG column (Bio-Rad, Hemel Hempstead, Hertfordshire, UK) which had previously been equilibrated with 20ml of Tris 50mM, pH7 buffer. When the LDL solution had entered the column 2ml of tris buffer (pH7, 50mM) was added and allowed to elute. A further 1ml of tris buffer was added to the column and the eluent of the column (containing the LDL) was collected in an eppendorf tube for assaying.

#### **5.2.2 Assay of Cholesterol**

After desalting the LDL the cholesterol concentration was determined by the CHOL-PAD method using the cholesterol kit supplied by Boehringer-Mannheim (Mannheim, Germany). A factor of 3.16 was used to convert mg cholesterol/ml into mg LDL total mass/ml. The below was performed in duplicate;

10µl of LDL was mixed with 1ml CHOL-PAD reagent

10µl of the tris buffer was mixed with 1ml CHOL-PAD reagent as a blank

The above was allowed to react with the CHOL-PAD reagent for 10minutes before the absorbance of the LDL samples at 500nm against the blanks was read using a spectrophotometer. The LDL concentration was calculated as follows;

Total Cholesterol concentration in mg/dL = Average Abs<sub>500</sub> x 575

Divide by 100 to obtain cholesterol in mg/ml

Multiply by 3.16 gives the LDL concentration in mg/ml

A Bradford assay, kit supplied by Bio-rad, was also used to assay the protein concentration of the LDL sample. The Bio-rad protein assay is a dye-binding assay with a differential colour change depending on the protein concentration of a solution. The dye primarily binds to basic and aromatic acid residues. This protein assay will only give an approximation of Apo B-100 content, as the sample will not be a pure LDL sample and will contain contaminants from plasma like albumin.

Typical results were 5.56mg/ml cholesterol and 0.28mg/ml protein in the LDL solution.

### 5.2.3 Chemical *in vitro* modification of the LDL

The native LDL was chemically modified using varying concentrations of SIN-1 and HOCl. The samples with their oxidant are incubated at 37°C for 4hours.

The following Table 24 is an example of the chemical modification of the LDL by HOCl.

Table 24: LDL is modified with varying HOCl concentrations

Sample	Protein	HOCl	Tris Buffer
Unmodified LDL	100µl LDL (28µg)	X	100µl
30mM HOCl Modified LDL	100µl LDL (28µg)	40µl HOCl, 150ML	60µl
15mM HOCl Modified LDL	100µl LDL (28µg)	20µl HOCl, 150ML	80µl
3mM HOCl Modified LDL	100µl LDL (28µg)	40µl HOCl, 15ML	60µl
1.5mM HOCl Modified LDL	100µl LDL (28µg)	20µl HOCl, 15ML	80µl

From left to right; the first column is the HOCl concentration of which the LDL was modified. The second column is how much protein was modified and the third column is the HOCl added to the sample. The fourth column is how much tris buffer was added to the eppendorf to adjust the HOCl concentration.

“Simple Protein”, Lysozyme, was modified by varying concentrations of HOCl as a control Table 25.

**Lysozyme stock solution in Tris 50mM pH7 buffer = 1mg/ml**

**Table 25: Lysozyme is modified by varying concentrations of HOCl as a control**

Sample	Protein	HOCl	Tris Buffer
Unmodified Lysozyme	20µl Lysozyme (20µg)	X	180µl
30mM HOCl Modified Lysozyme	20µl Lysozyme (20µg)	40µl HOCl, 150ML	60µl
15mM HOCl Modified Lysozyme	20µl Lysozyme (20µg)	20µl HOCl, 150ML	80µl
3mM HOCl Modified Lysozyme	20µl Lysozyme (20µg)	40µl HOCl, 15ML	60µl
1.5mM HOCl Modified Lysozyme	20µl Lysozyme (20µg)	20µl HOCl, 15ML	80µl

From left to right; the first column is the HOCl concentration of which the LDL was modified. The second column is how much protein was modified and the third column is the HOCl added to the sample. The fourth column is how much tris buffer was added to the eppendorf to adjust the HOCl concentration.

The HOCl modified samples were then delipidated to prevent the blocking of the C<sub>18</sub> column during chromatography then trypsin digested.

#### **5.2.4 Trichloroacetic Acid (TCA) Delipidation**

The HOCl modified protein samples were dried down using a centrifugal evaporator (eppendorf concentrator 5301) before being TCA delipidated and trypsin digested. Samples were then made up to 60µl with dH<sub>2</sub>O before the addition of 9.3µl SDS 7.5% and 0.7µl DTT 1M to give 1% SDS and 10mM DTT. Samples were heated in a block at 95°C for 5minutes followed by the addition of 8µl 0.5M iodoacetamide, 50mM ammonium bicarbonate before shaking in the dark for 30minutes at room temperature. The TCA delipidation step was then as follows; 52 µl 50% TCA was added to give 20% TCA and the protein was allowed to precipitate on ice for a minimum of 15minutes. The sample to be delipidated was then spun down for 10minutes at 13K rpm and the supernatant was carefully removed. A second wash with 150µl 10% TCA followed, and the sample spun down as before and the supernatant removed. The protein pellet was washed three times with 250µl dH<sub>2</sub>O, spun down and the supernatant removed. The protein pellet underwent trypsin digestion overnight as before described in 2.4.1.2.

## 5.2.5 Mass Spectrometry methods

As described in section 2.4.1.4

### 5.2.5.1 Mascot parameters

The LDL and lysozyme samples separated on the LC (2.4.1.3) before being analysed by the conventional MSMS method on the Qtrap 2000 (*Applied Biosystems*, Warrington, UK). The MSMS data generated was then searched with Mascot, version 1.6b9. The Mascot parameters when searching the data were as follows; the enzyme was “Trypsin”, the fixed modifications were “Carbamidomethyl (C), the variable modifications were Chlorotyrosine (ClTyr (Y)) and Oxidation (M) and the mass values were monoisotopic. The peptide mass tolerance was  $\pm 2\text{Da}$ , the fragment mass tolerance was  $\pm 1\text{Da}$  and the maximum missed cleavages were set to 1.

## 5.2.6 Detecting ClTyr by Western Blotting

Running Gel

(5X) Protein Loading Buffer

• Glycerol - 1.6ml • 10% SDS - 1.6ml • 1M Tris pH 6.8 - 0.5ml • dH<sub>2</sub>O - 3.9ml •  $\beta$ -Mercaptoethanol - 0.4ml • Bromophenol Blue (BPB) - pinch

HiMark™ Pre-stained High Molecular Weight Protein Standard from Invitrogen  
NuPage - 9 protein bands range 30 - 460kDa

Tris-acetate Running Buffer 20X from Invitrogen NuPage - Diluted to 1X = 50ml in 1L

Samples ran in 3-8% Tris acetate gel *from* Invitrogen NuPage; V = 150V, mA = 50A  
t = 1hr

Semi-dry Blotting

*Transfer Buffer* - 1L - 3.02g Tris Base (from Sigma Aldrich), 14.4g glycine (from Sigma Aldrich), 200mL methanol and 800mL dH<sub>2</sub>O.

The gel was removed from the cassette and left immersed in transfer buffer to equilibrate the gel and prevent shrinkage for 15mins. Before blotting, the PDVF membrane was prepared by wetting with methanol for 15s followed by 2mins in water and a further 15mins in the transfer buffer. The filter paper was soaked in transfer buffer and cut to the same size as the gel to prevent uneven transfer.

### Probing for Cl-Tyr

The membrane was rewetted with methanol and a solution of dried milk powder 5% in 5ml 1xPBS (phosphate buffered saline) used to block was poured onto the membrane and shaken for an hour to prevent unspecific binding. 2x5min washes with PBS-T (1xPBS with 0.05%Tween) follows. The membrane was then incubated in 5ml with the ClTyr antibody (from Sigma Aldrich) at a 1:500 ratio in 1xPBS-T 5% dried milk solution and then agitated for an hour. 6x5min washes with PBS-T (1xPBS with 0.05%Tween) follows. The membrane was then incubated in 5ml with the secondary antibody, HRP(horse radish peroxidase) rabbit at a 1:500 ratio in 1xPBS-T 5%dried milk and agitated for an hour.

### Enhanced Chemiluminescence - kit from Thermo Scientific

Two solutions were used; Luminol Enhance solution and Peroxide solution.

Equal volumes of each were mixed in a universal tube. The membrane was placed in the resulting mixture for 1min. The membrane was then removed and wrapped in clingfilm ready for immediate exposure using the X-omat to develop the film.

## **5.3 Results and Discussion**

Native LDL was extracted from a plasma pool and was modified with varying concentrations of HOCl. As a control a simpler protein model, lysozyme was modified in parallel to test the HOCl modification protocol.

### **5.3.1 Analysis of HOCl modified LDL and lysozyme samples**

The native LDL and the simpler protein model, lysozyme, were modified using varying concentrations of HOCl. Both the 15mM HOCl modified LDL and lysozyme samples were analysed by conventional MSMS (see 2.4.1.4) on the Qtrap 2000 (*Applied Biosystems*, Warrington, UK) and the MSMS data was searched with

Mascot. The MSMS analysis of the 15mM HOCl modified LDL sample detected and identified to be the Apo B-100 protein as the top protein hit (Figure 77) with a score of 2202 (the significance threshold was set for 48) and sequence coverage of 24%. There were Apo B-100 peptides identified as methionine oxidised (Ox (M)) modification but no ClTyr modifications identified.

1. [APOB\\_HUMAN](#) Mass: 515241 Score: 2202 Queries matched: 82 emPAI: 0.56  
 Apolipoprotein B-100 precursor - Homo sapiens (Human)  
 Check to include this hit in error tolerant search or archive report

Query	Observed	Mr (expt)	Mr (calc)	Delta	Miss	Score	Expect	Rank	Peptide
<input checked="" type="checkbox"/> <a href="#">31</a>	621.1856	620.1783	620.3897	-0.2114	0	7	45	1	K.LTIFK.T
<input checked="" type="checkbox"/> <a href="#">34</a>	653.2563	652.2490	652.3656	-0.1166	0	6	50	4	R.LLDHR.V
<input checked="" type="checkbox"/> <a href="#">50</a>	774.2580	773.2507	773.5011	-0.2503	1	6	73	7	K.LTALTKK.Y
<input checked="" type="checkbox"/> <a href="#">57</a>	401.2207	800.4268	800.4796	-0.0528	0	37	0.062	1	K.FIIPSPK.R
<input checked="" type="checkbox"/> <a href="#">68</a>	435.6873	869.3600	869.4429	-0.0829	0	50	0.0021	1	K.HVAEAIK.E
<input checked="" type="checkbox"/> <a href="#">72</a>	456.2400	910.4654	911.5076	-1.0422	0	27	0.41	1	K.VEDIPLAR.I
<input checked="" type="checkbox"/> <a href="#">94</a>	508.2039	1014.3933	1014.5386	-0.1453	0	16	7.7	1	R.VSTAFVYTK.N
<input checked="" type="checkbox"/> <a href="#">100</a>	517.7748	1033.5350	1033.5192	0.0158	0	14	9.8	9	K.DNVFDGLVR.V
<input checked="" type="checkbox"/> <a href="#">101</a>	1039.4172	1038.4100	1038.6325	-0.2225	0	(15)	7	1	K.LAPGELTIIL.-
<input checked="" type="checkbox"/> <a href="#">102</a>	520.2555	1038.4964	1038.6325	-0.1360	0	30	0.26	1	K.LAPGELTIIL.-
<input checked="" type="checkbox"/> <a href="#">110</a>	533.7387	1065.4629	1065.5818	-0.1189	0	41	0.021	1	R.INDVLEHVK.H
<input checked="" type="checkbox"/> <a href="#">111</a>	538.7723	1075.5301	1073.6121	1.9180	0	33	0.14	1	K.NIILPVYDK.S
<input checked="" type="checkbox"/> <a href="#">112</a>	540.7189	1079.4232	1079.5472	-0.1240	0	41	0.019	1	K.GSTSHLVS.R.K
<input checked="" type="checkbox"/> <a href="#">116</a>	544.2602	1086.5058	1086.6033	-0.0975	1	40	0.029	1	K.DKIGVELTGR.T
<input checked="" type="checkbox"/> <a href="#">131</a>	576.2562	1150.4979	1150.5618	-0.0639	0	62	0.00016	1	K.LDFSSQADLR.N
<input checked="" type="checkbox"/> <a href="#">133</a>	578.7489	1155.4833	1155.6036	-0.1204	0	69	3.5e-05	1	K.SPAFTDLHLR.Y
<input checked="" type="checkbox"/> <a href="#">141</a>	588.7307	1175.4468	1175.5782	-0.1314	0	69	3.2e-05	1	K.GNVATEISTER.D
<input checked="" type="checkbox"/> <a href="#">150</a>	601.2475	1200.4804	1200.6462	-0.1658	0	58	0.00041	1	K.LTISEQNIQR.A
<input checked="" type="checkbox"/> <a href="#">170</a>	637.2660	1272.5174	1270.6768	1.8405	0	36	0.065	1	K.SVSLPQLDPASAK.I
<input checked="" type="checkbox"/> <a href="#">176</a>	644.2512	1286.4878	1285.7241	0.7637	0	45	0.0079	1	K.NTLELSNGVIVK.I
<input checked="" type="checkbox"/> <a href="#">181</a>	653.2563	1304.4981	1305.6466	-1.1485	0	(73)	1.3e-05	1	K.IISDYHQQFR.Y
<input checked="" type="checkbox"/> <a href="#">183</a>	654.4730	1306.9314	1305.6466	1.2848	0	82	1.4e-06	1	K.IISDYHQQFR.Y

Figure 77: A sample of Mascot search results for 15mM HOCl modified LDL. The above figure displays the first 20 peptides from the Mascot search on the analysis of the 15mM HOCl modified LDL sample by the Qtrap. There were many more peptide hits assigned but there are too many to be shown here.

The identification of Apo B100 as the top protein hit suggests that the LDL extraction protocol and the delipidation were successful. It is possible any ClTyr modifications on the Apo B-100 protein are in very low abundance and therefore were not detected by the conventional MSMS experiment.

### 5.3.1.1 Verification of the HOCl modification protocol

The detection and assignment of Apo B100 as a top protein hit verifies the LDL extraction and delipidation protocol. To verify the modification protocol, lysozyme, a simpler, smaller protein model was modified using the same method and analysed on the Qtrap and the mass spectrum data searched with Mascot as before. In the lysozyme sample ClTyr modifications were identified by Mascot. The NTDGSTYDYCILQIDSR + ClTyr peptide is an example of one of the peptides found to be ClTyr modified with an ion score of 82. The mass spectrum of the example ClTyr modified peptide identified displayed a near complete *y-ion*

series and the ClTyr fragment could be observed (Figure 78). The assignment and detection of ClTyr modifications in the 15mM HOCl modified lysozyme sample verifies the HOCl modification protocol. Lysozyme is a smaller (16kDa), simpler protein and has been found to be modified so in theory the Apo B-100 protein too should be ClTyr modified but in low abundance below the limit of detection.

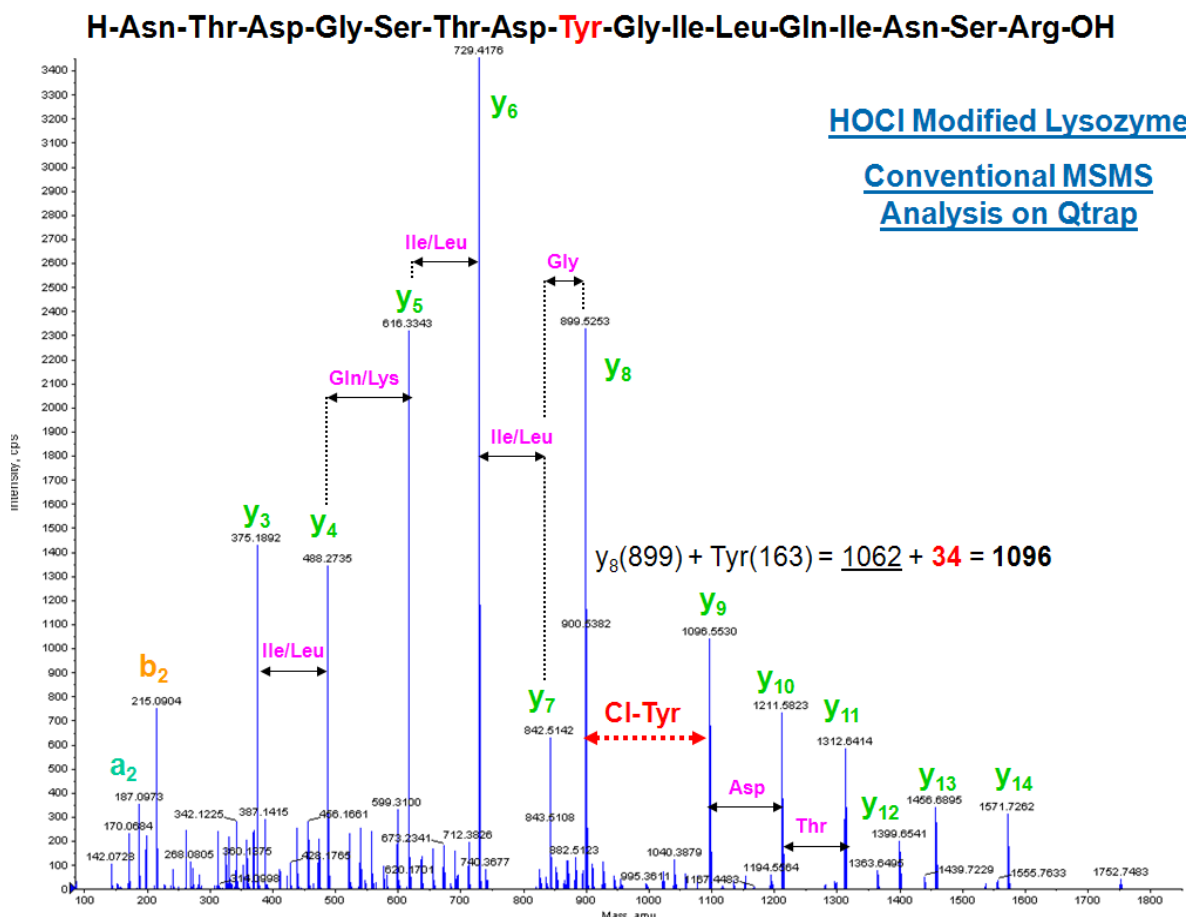


**Figure 78:** Mass spectrum of the NTDGSTYDYCILQDSR + ClTyr peptide. The above figure displays the mass spectrum data for the example NTDGSTYDYCILQDSR + ClTyr peptide detected in the 15mM HOCl modified lysozyme sample. A near complete *y-ion* series can be observed and the ClTyr fragment (*y9*) can be identified.

### 5.3.2 Detecting ClTyr in LDL

The LDL is a spherical particle consisting mainly of cholesteryl ester with a small amount of tri-glycerides. The LDL coat consists of phospholipids, free cholesterol and a large single protein, Apolipoprotein B-100 which “dips” in and out of lipid core [20]. The Apo B100 protein will then not only be able to interact with the lipids on the lipoprotein particle but also with the surrounding environment. In this experiment we modify the native LDL with the HOCl rather than delipidated

or digested LDL as this is “truer” to life. It may be possible that the lipids on the LDL particle may be being oxidised rather than the Apo B-100 protein.

Spickett et al reviews the reactions of lipids (unsaturated fatty acids and cholesterol) with either HOCl or HOCl generated by the MPO-hydrogen peroxide-chloride system <sup>[220]</sup>. In lipids, the major site of attack by HOCl is at the double bonds which are present in the unsaturated fatty acids and cholesterol which in turn leads to the formation of chlorohydrins and peroxidation. HOCl or HOCl generated by the MPO/H<sub>2</sub>O<sub>2</sub>/Cl<sup>-</sup> system can initiate lipid peroxidation both in lipoproteins and liposomes. It has also been found that HOCl-induced lipid peroxidation is pH dependant. An increase in pH values leads to an increase in lipid peroxidation products <sup>[221]</sup>.

The effect of HOCl on the LDL particle has been modelled by Malle et al <sup>[222]</sup> under the assumption that all sites of the LDL particle are equally accessible to modification. The absolute second order rate constants for the reaction of HOCl with the LDL components (substrate; amino acid residues, back bone amide etc.) were calculated. From this kinetic data the order of reactivity is seen to be modulated by the relative concentrations of each component present in the LDL. The rate constants were used to computer model the reaction between the LDL particle and HOCl to predict the extent of the reaction and the effects on the protein components versus the lipid double bonds versus the antioxidants (primarily the more abundant, fat-soluble, tocopherols) (Table 26). With a HOCl:LDL molar ratio below 50:1 the HOCl is predicated to be consumed exclusively by the protein. Above the 50:1 molar ratio it is predicated that the lipid and antioxidants are incorporated into the consumption of the HOCl although consumption of the HOCl is still predominantly by the protein. Reaction with antioxidants present in LDL (primarily tocopherols, as these species are much more abundant than other components) is predicted to be a minor reaction at all HOCl ratios.

Table 26: Computer-modelled predicted sites of HOCl activity on LDL [222].

HOCl:LDL molar ratio	Percentage of HOCl consumed by		
	Protein	Lipid	Antioxidants
1:1	100	0	0
25:1	100	0	0
50:1	100	0	0
100:1	99.6	0.4	0
200:1	97.5	2.4	0.1
400:1	94.2	5.5	0.3
800:1	86.4	12.5	1.1
1000:1	80.1	19.0	0.9
2000:1	66.5	33.0	0.5

The above displays the HOCl:LDL molar ratio and what substrate; protein, lipid and antioxidant, the HOCl is most predominantly consumed by.

Malle modelled the oxidations of the side-chains on the protein. Modelling the oxidation of protein is sometimes challenging due to the complex nature of the process. Methionine when reacted with HOCl *in vivo* can reversibly form sulfoxides or irreversibly form sulfones making oxidation difficult to measure. HOCl reactions with histidine and lysine will give unstable chloramines (RNCl) and di-chloroamines (RNCl<sub>2</sub> species) when in excess of HOCl. These species retain the oxidising equivalent of HOCl and can transfer Cl to other substrates regenerating the parent side-chain thus appearing unchanged and unaffected by oxidation. The effect of HOCl oxidation on tryptophan will form kynurenine and N-formylkynurenine via inter- and intramolecular, radical-mediated reactions and chlorotyrosine will be formed by either direct HOCl reaction or indirect HOCl reaction with chloramines. The side-chains; alanine, valine, leucine, isoleucine, proline and phenylalanine were found to be poorly reactive with HOCl.

This suggests that there should be ClTyr modifications on the Apo B100 protein on our *in vitro* HOCl modified LDL but due to their very low abundance detection is challenging. Modification of the lipids on the particle should not greatly affect the efficiency of Apo B100 protein modification by the HOCl reagent.

### 5.3.2.1 Detecting the ClTyr modification by Western Blotting

We visualised the Apo B100 protein in the unmodified LDL sample and LDL samples modified with varying HOCl concentrations by silver staining.

The protein in the LDL samples was separated on a gel by their size. To confirm the presence of the Apo B100 protein in the LDL samples a western blot was performed probing specifically for the Apo B100 protein (Figure 79). The molecular weight for the Apo B100 protein is 516kDa and the Apo B100 is observed at lower molecular weights indicated by the protein ladder suggesting degradation of the sample.

In other studies the atherosclerotic arterial intima and fatty streak have previously been probed with a western blot using the HOP-1 antibody for the detection of proteins oxidised by HOCl<sup>[155;208;217;223]</sup>. The antibody is highly specific for HOCl-modified proteins and does not cross-react with native proteins or those modified by other methods. Professor Ernst Malle (Karl-Franzens University, Graz, Austria) developed the HOP-1 by raising a mouse monoclonal antibody against HOCl-modified low-density lipoprotein (LDL). We attempted western blotting of the LDL chemically modified *in vitro* by HOCl using an anti-ClTyr antibody from Sigma. However this antibody was proved to bind non-specifically to the Apo B100 protein (Figure 80). Binding of the ClTyr antibody appeared to be to albumin as this protein is visualized approximately where albumin is expected (~67kDa) with respect to the protein ladder.

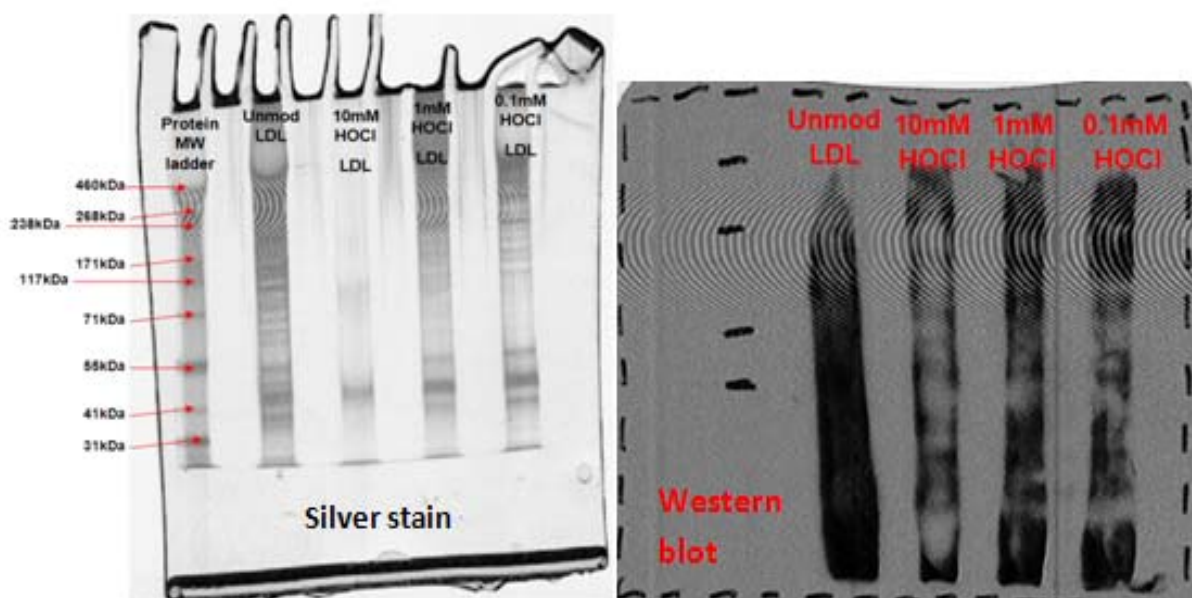


Figure 79: Silver stain and western blot of unmodified and HOCl modified LDL separated on a reducing SDS PAGE. The left hand side of the figure displays the silver stain of the LDL samples and the right hand side of the figure displays the western blot probing for the Apo B100 protein. Unmodified and various HOCl modified LDL samples were visualised in a gel separated by size. To confirm the Apo B100 protein in the LDL samples the protein was probed with an Apo B100 antibody.

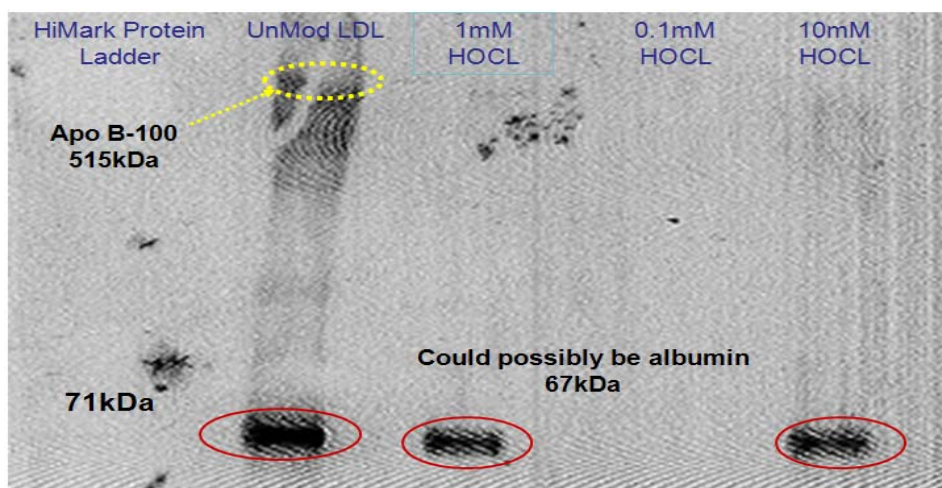


Figure 80: Western blot of unmodified LDL and 0.1mM, 1mM and 10mM HOCl modified LDL when probed for C1Tyr. From left to right in the first column is the protein ladder. The second lane is the unmodified LDL. Where the Apo B-100 appeared in the gel is ringed in yellow. The third column is the 1mM HOCl modified LDL sample, the fourth the 0.1mM HOCl modified LDL sample and the fifth lane the 10mM HOCl modified LDL sample. The C1Tyr antibody was found to bind non-specifically. Binding could possibly be to albumin (ringed in red) as the protein appears at the correct molecular weight.

### 5.3.3 An alternative oxidation product - Hydroxytryptophan

No ClTyr modifications were detected when searching the mass spectrometry data collected from the conventional MSMS analysis of the 15mM HOCl modified LDL sample by Mascot. It was hypothesised that although ClTyr modifications may be present but in very low abundance and are therefore not detected perhaps there are other oxidative modifications that can be detected.

Aromatic side chains (tyrosine, tryptophan, phenylalanine and histidine) are the major targets of free radical reaction [224, 225]. Aromatic rings are more susceptible to modification due to the high electron-density of the ring. Hydroxytryptophan is an example of a tryptophan oxidation products, first reported by Previero in 1967 [226-228]. Initially the tryptophan oxidation products were detected using characteristic electronic absorbance spectra. The first complete MS characterization of a protein from bovine lens,  $\alpha$ -crystallin, found oxidized Trp residues as a result of exposition to the oxidative Fenton insult which has been described (in 1.3). The occurrence of hydroxytryptophan, N-formylkynurenine, kynurenine, and 3OH-kynurenine in reaction products was ascertained by direct ESI measurements [229].

More recently however, oxidised tryptophan residues were reported to be present in cardiac mitochondrial proteins when analysed by ESI-MSMS [230]. This led to the conclusion that the Trp modifications could occur *in vivo* as a result of these proteins being subjected to a source of reactive oxygen species and indeed a result of oxidative stress.

The mass spectrometry data for the MSMS analysis of the 15mM HOCl modified LDL and lysozyme samples was searched again by Mascot as before (see 5.3.1) but the variable modifications now included hydroxytryptophan (HOTrp (W)). This modification has been identified as a potential marker for protein oxidation [231]. In the 15mM HOCl modified lysozyme sample the HOTrp modified CKGTDVQAWIR peptide was identified (Figure 81). From MSMS analysis it is unclear of the position of the HO-group on the tryptophan aromatic ring.



protein hit. The first analysis reported the Apo B100 to have a score of 114 and the significance threshold was 48. The sequence coverage reported for the Apo B100 protein in the first analysis was 1%. The second analysis of the 15mM HOCl LDL sample reported Apo B100 as the top protein hit with a score of 239 with 1% of the protein's sequence coverage being identified. Analysis of the 15mM HOCl modified LDL sample reported a good statistical score (above the significance threshold of 48) for the Apo B100 protein in the first and second analysis. Only a small percentage of the protein was identified by analysis (1% in the first analysis and 5% in the second analysis) so we are missing a lot of information. Loss of information may be due to the complexity of the sample; even though Apo B-100 is a single protein it is very large and when trypsin digested will generate many peptides for analysis.

1. <a href="#">APOB_HUMAN</a> Mass: 516666 Score: 114 Queries matched: 11									
Apolipoprotein B-100 precursor - Homo sapiens (Human)									
<input type="checkbox"/> Check to include this hit in error tolerant search or archive report									
Query	Observed	Mr(expt)	Mr(calc)	Delta	Miss	Score	Expect	Rank	Peptide
<input checked="" type="checkbox"/> <a href="#">29</a>	829.7700	1657.5254	1656.8682	0.6572	0	23	2.3	1	K.SVSDGIAALDLNAVANK.I
<input checked="" type="checkbox"/> <a href="#">32</a>	873.7700	1745.5254	1745.8988	-0.3734	0	26	1.1	1	K.IEGNLIFDPNNYLPK.E
<input checked="" type="checkbox"/> <a href="#">34</a>	924.5600	1847.1054	1846.8584	0.2470	0	36	0.12	1	R.EYSGTIASEANTYLNISK.S
<input checked="" type="checkbox"/> <a href="#">35</a>	936.4800	1870.9454	1870.9346	0.0108	0	38	0.12	1	K.LLLQMDSSATAYGSTVSK.R
<input checked="" type="checkbox"/> <a href="#">42</a>	1077.7500	2153.4854	2153.1256	0.3599	0	36	0.14	1	K.TTLTAPGFASADLIEIGLEGK.G
<input checked="" type="checkbox"/> <a href="#">45</a>	1119.6800	2237.3454	2237.1613	0.1841	0	32	0.33	1	K.AALTELSLGSAYQAMILGVDSK.N
<input checked="" type="checkbox"/> <a href="#">47</a>	1174.6500	2347.2854	2347.1763	0.1092	0	15	20	9	K.CSLLVLENELENAELGLSGASK.L
<input checked="" type="checkbox"/> <a href="#">53</a>	833.6900	2498.0482	2497.1609	0.8873	0	37	0.18	1	K.ADSVVDLLSYNVQSGGETTYDHK.N
<input checked="" type="checkbox"/> <a href="#">54</a>	837.1700	2508.4882	2508.0605	0.4277	1	15	18	5	R.DPSAEYEDGKFEGLQEWEGK.A + Oxidation (HW)
<input checked="" type="checkbox"/> <a href="#">60</a>	942.5000	2824.4782	2823.4290	1.0492	0	77	1.7e-05	1	R.LELELRPTGEIEQYSVSATYELQR.E
<input checked="" type="checkbox"/> <a href="#">68</a>	1139.9400	3416.7982	3415.9251	0.8730	1	43	0.05	1	R.TLADLTLLDSPIKVPLLSEPINIIDAEMR.D

**MASCOT search results for the first analysis of 15mM HOCl modified LDL**

1. <a href="#">APOB_HUMAN</a> Mass: 516666 Score: 239 Queries matched: 4									
Apolipoprotein B-100 precursor - Homo sapiens (Human)									
<input type="checkbox"/> Check to include this hit in error tolerant search or archive report									
Query	Observed	Mr(expt)	Mr(calc)	Delta	Miss	Score	Expect	Rank	Peptide
<input checked="" type="checkbox"/> <a href="#">7</a>	623.0000	1243.9854	1243.6448	0.3406	0	66	8.1e-05	1	K.IDDIWNLEVK.E
<input checked="" type="checkbox"/> <a href="#">9</a>	754.0000	1505.9854	1504.7733	1.2121	0	88	4.7e-07	1	R.IQGDIQSTSATNLRK.C
<input checked="" type="checkbox"/> <a href="#">11</a>	786.5000	1570.9854	1569.8549	1.1306	0	67	7.3e-05	1	R.TLQGIQIQMIGEVIR.K + Oxidation (M)
<input checked="" type="checkbox"/> <a href="#">12</a>	791.0000	1579.9854	1580.7868	-0.8014	0	43	0.017	1	K.AVSMPSFSLGSDVR.V + Oxidation (M)

**MASCOT search results for the second analysis of 15mM HOCl modified LDL**

Figure 82: The Mascot search results for the analysis of the 15mM HOCl LDL sample by the precursor scan. The above figure displays the Mascot search results for the analysis of the 15mM HOCl LDL sample.

### 5.3.5 Further work to investigate ClTyr modifications on the Apo B100 protein

Unfortunately our methods were not able to detect ClTyr on the Apo B100 protein. Further work should include the development of the analysis of the HOCl modified LDL samples by the precursor scan. The gas phase fractionation (GPF) technique should be applied to combat under sampling and sample variance which is a common problem in complex samples. This will target

smaller mass ranges (200amu with 20amu overlap) leading to data being collected for longer therefore increasing the sensitivity of the technique <sup>[162]</sup> (see also 2.5.8).

The precursor scan is a sensitive method for the detection of modifications in a sample where no prior information is known about the site of modification (see Chapter 2). An MRM method can be used to “mine” complex samples but we must first know about the modified peptides that are to be targeted before an acquisition program can be written to identify them.

#### **5.4 The detection of specific nitration sites on the Apo B100 protein**

The focus of the study is to identify modifications that are specific to atherosclerosis and develop techniques that may eventually be applied for the high throughput, early diagnosis of the disease. Both chloro and nitrotyrosine modifications can be caused by oxidative stress in atherosclerosis and ClTyr have been investigated previously in a model 9 protein mix sample, purified human serum albumin, plasma samples and clinical samples (see chapters 3, and 4).

Hamilton et al <sup>[233]</sup>, studied the nitrotyrosine modification sites of the Apo B100 protein after *in vitro* and *in vivo* modification. It has been widely discussed that oxidative modifications of LDL are required for the particle to possess inflammatory properties inherent to the initiation and progression of atherosclerosis <sup>[234-236]</sup>. This concept is strengthened by the observed elevated levels of post-translational modifications of the Apo B100 protein in atherosclerotic lesions <sup>[60]</sup>. The oxidised modified LDL particle consists of peroxidised lipids and the unfolded Apo B100 protein moiety. Hamilton’s study was focused to establish specific modification sites on the Apo B100 protein and to observe the conformational changes using LCMSMS (*ThermoFinnigan LCQ Deca XP Plus ion trap*) and circular dichroism (CD) respectively.

Hamilton modified the LDL *in vitro* after isolation of LDL from human plasma using 3-morpholino sydnonimine (SIN-1). Protein oxidation was determined in *in vivo* sub-fractions of LDL and in the *in vitro* SIN-1 chemically modified LDL by performing a western blot. The specific sites of nitration were verified by liquid chromatography tandem mass spectrometry. The peptides resulting from the

trypsin digested LDL<sup>-</sup> (modified LDL) and nLDL (native LDL) were separated using reverse phase chromatography and analysis was obtained by the ion trap mass spectrometer. Mass spectra data was acquired between 400-2000m/z using a Top Five method where the five most intense ions for the full scan were subjected to collision induced dissociation (CID). Peptide identification was achieved using Mascot version 1.9 and the spectra was searched against the NCBI database. Quantification of nitrated peptides was carried out by analysis of peak area nitration to peak area unmodified plus total peak area modified peptides (NO<sub>2</sub>-peptide/(NO<sub>2</sub>-peptide + unmodified peptide). To confirm those peptides assigned to be NO<sub>2</sub> modified by Mascot they were analysed against their *y-ion* and *b-ions* to ensure that the peptides were present and not false positives. The change in the protein's conformational structure caused by oxidative modification was a decrease in the  $\alpha$ -helical structure and an increase in  $\beta$ -structure components.

The results of Hamilton's study found that after separating native *in vivo* LDL (nLDL) and LDL<sup>-</sup> from total LDL (tLDL) using anion exchange chromatography, nitrotyrosine was only detected in the LDL<sup>-</sup> fraction but not in the nLDL or tLDL fractions when LDL nitration was assayed for by immunoreactivity to a nitrotyrosine antibody. LCMSMS analysis revealed specific modifications in the Apo B100 moiety (Table 27). Previously we have discussed chloro or nitrotyrosine modifications that have been identified by Mascot and then manually verifying the presence of the modified peptide by matching the mass spectrum against its *y-ion* series (see chapters 3, and 4). Hamilton also identified the ions in the mass spectrum generated by the analysis of the NiTyr modified peptides and matched the *y*- and *b-ion* series to it. The fully annotated mass spectrum for the modified peptides were available in the supplementary data (Figure 83). Ringed in red is the NiTyr fragment and boxed in blue is the NiTyr modification site. The mass spectrum and matched *y* and *b-ions* verify the NiTyr modified peptide and site in the apo B100 protein. Like Hamilton we have also manually confirmed our modifications in previous chapters to ensure true positives and avoid false positives.

Table 27: Specific oxidative sites identified in LDL [65].

LC/MS/MS analyses of LDL<sup>-</sup> Apo-B100 protein modifications

Secondary structure	Peptide	Modified AA	Sequence	Msc	Charge	XC	Δcn	Modification	% modified
α <sub>1</sub>	276–287	NO <sub>2</sub> -Tyr <sup>276</sup>	y <sup>7</sup> gmvaqvtqtk	51	2	2.8	0.4	nitrotyrosine	100 ± 0
α <sub>1</sub>	580–589	NO <sub>2</sub> -Trp <sup>581</sup>	IVQilpw <sup>581</sup> eqneqv	30	2	3.0	0.2	nitrotryptophan	49.8 ± 0.6
α <sub>1</sub>	580–589	HO-Trp <sup>583</sup>	IVQilpw <sup>583</sup> eqneqv	38	2	3.8	0.3	hydroxytryptophan	32.6 ± 1.9
α <sub>1</sub>	655–669	NO <sub>2</sub> -Tyr <sup>665</sup>	iegnlifdpnny <sup>665</sup> lpk	46	2	3.3	0.4	nitrotyrosine	18.3 ± 0.7
α <sub>1</sub>	718–732	NO <sub>2</sub> -Tyr <sup>720</sup>	aly <sup>720</sup> wavngqvpdgvs	49	2	2.4	0.1	nitrotyrosine	29.9 ± 0.07
β <sub>1</sub>	1101–115	SO <sub>2</sub> H-Cys <sup>1112</sup>	itevalmghisc <sup>1112</sup> dtk	84	2	4.9	0.5	cysteic acid	100 ± 0
α <sub>2</sub>	2523–2534	NO <sub>2</sub> -Tyr <sup>2524</sup>	my <sup>2524</sup> qmdiqelqr	36	2	3.0	0.3	nitrotyrosine	87.1 ± 0.2
β <sub>2</sub>	3137–3148	NO <sub>2</sub> -Tyr <sup>3139</sup>	lpy <sup>3139</sup> tiitpplk	30	2	1.9	0.5	nitrotyrosine	60.2 ± 0.2
β <sub>2</sub>	3292–3311	NO <sub>2</sub> -Tyr <sup>3295</sup>	vsv <sup>3295</sup> tliloslolvhvr	70	2	5.6	0.5	nitrotyrosine	80.4 ± 0.2
β <sub>2</sub>	3481–3497	NO <sub>2</sub> -Tyr <sup>3489</sup>	lsleslty <sup>3489</sup> fsiesstk	62	2	4.7	0.7	nitrotyrosine	27.1 ± 1.1
β <sub>2</sub>	3953–3973	HO-Phe <sup>3965</sup>	disaeyecdk <sup>3965</sup> egiqr	59	2	2.5	0.5	HO-phenylalanine	92.6 ± 0.9
α <sub>3</sub>	4133–4145	NO <sub>2</sub> -Tyr <sup>4141</sup>	aasgttgy <sup>4141</sup> qewk	46	2	2.7	0.1	nitrotyrosine	81.8 ± 0.1

Quantification of NO<sub>2</sub>-Y  
mmol NO<sub>2</sub>-Y/(mol Y)  
LDL<sup>-</sup> = 34.8 ± 1.0  
tLDL = 2.0 ± 0.2  
nLDL = 0.3 ± 0.1

The above table displays the specific sites of oxidative modification identified in the apo B100 protein moiety after the analysis of the *in vivo* LDL fraction by LCMSMS. Sites where the nitrotyrosine modification is identified are boxed in red. The peptide boxed in blue has the mass spectrum displayed in the following Figure 83.

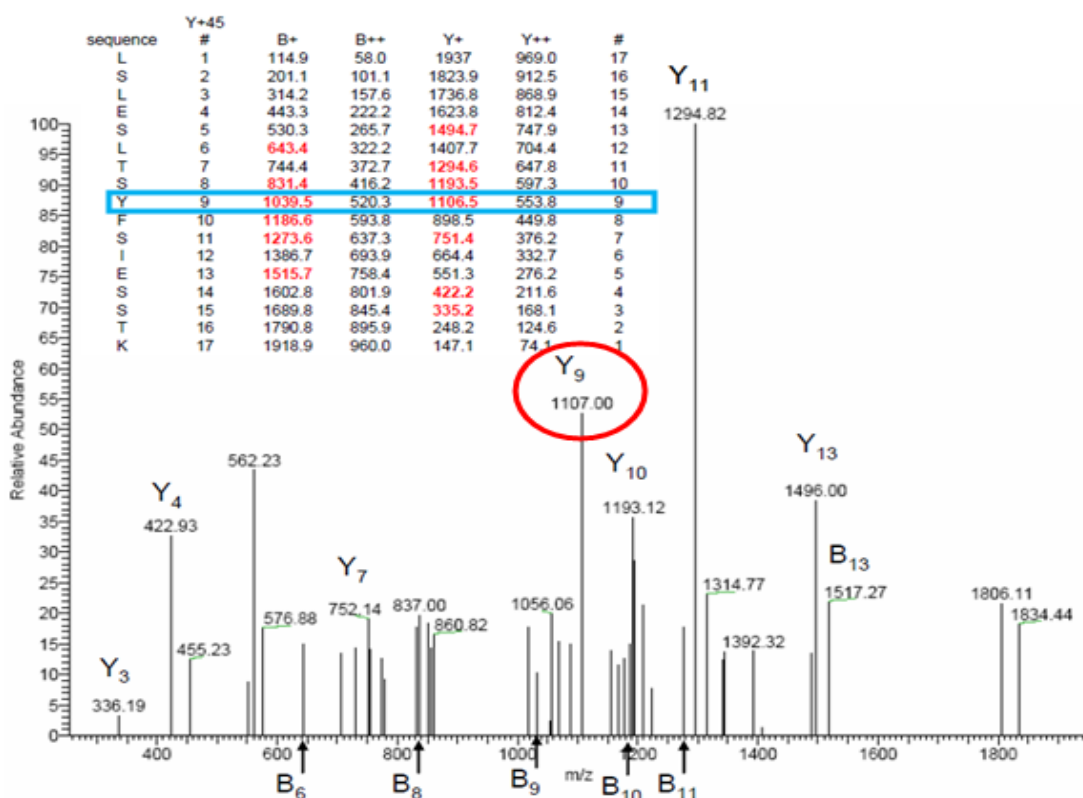


Figure 83: The fully annotated LSLESLSY<sup>Ni</sup>FSIESSTK nitrotyrosine modified peptide [65 - supplementary data]. The above figure displays an example of a fully annotated mass spectrum of one of the modified peptides identified on the apo B100 protein. The above mass spectrum concerns the LSLESLSY<sup>Ni</sup>FSIESSTK + NiTyr modified peptide.

### 5.4.1 Detecting nitrotyrosine modifications on the Apo B100 protein

Previously we have not been found to have detected ClTyr modifications of the Apo B100 protein by the precursor scan (see 5.3.4 ). The precursor scan has been found to be a sensitive and selective method for detecting modifications when there is no prior knowledge of the modifications <sup>[94;117-120;162;163]</sup>. We, however, were still unable to determine ClTyr sites on the Apo B100 protein although modification was indicated in a chemically modified 9 protein mix sample when the precursor scan was applied (Chapter 2).

We had prior knowledge about the modification sites when we analysed the clinical samples from the diseased and healthy volunteers in chapter 4 and were then able to write an MRM method to target for these. With Hamilton's work <sup>[233]</sup> we now have knowledge of the m/z's of which peptides in the apo B100 protein are nitrotyrosine modified and the fragmentation pattern (Q3 values) generated allowing for an MRM method to be written .

#### 5.4.1.1 NiTyr Modified peptides detected in *in vivo* and *in vitro* LDL samples

What was interesting with Hamilton's findings were the differences between the NiTyr sites detected when *in vivo* modified LDL was analysed and when *in vitro* LDL was analysed by the ion trap. Along with other modifications (NO<sub>2</sub>-Trp, HO-Trp and SO<sub>3</sub>-Cys) detected on the Apo B100 protein, eight peptides were found to be NiTyr modified in the *in vivo* samples. In the *in vitro* samples there were 7 peptides found to be NiTyr modified. The NiTyr modified peptides in the *in vitro* and *in vivo* LDL samples differed apart from two; IEGNLIFDPNNY<sup>Ni</sup>LPK and MY<sup>Ni</sup>QMDIQQELQR. The native LDL particle was modified *in vitro* meaning that the same sites available for modification are the same as for those when modified *in vivo*. The peptides identified to be NiTyr modified in the *in vivo* and *in vitro* samples therefore should be identical.

## 5.5 An MRM acquisition method

From the data provided from Hamilton's study <sup>[233]</sup> an MRM program was written to analyse our LDL that had been chemically modified by SIN-1. The most intense *y*-ions and *b*-ions seen in the mass spectra of each nitrotyrosine modified peptide in the spectra were used as the transitions. Precursor ions that were above 1500m/z or below 400m/z were omitted. On the Qtrap 2000 data is usually collected between 400 and 1500m/z as sensitivity decreases above

1500m/z and below 400m/z is usually singly charged ions unable to fragment or background noise. Fragments from the unmodified peptides that had been seen frequently in the MSMS analysis of the LDL samples on the Qtrap were used. Optimisation of the method was carried out by running the MRM method with a collisional energy of 25eV then 40eV as there were peptides that fragmented better when a collisional energy of 25eV was employed and others that required a higher collisional energy of 40eV to fragment (Table 28). The MRM acquisition method written from Hamilton's findings and mass spectrometry data was optimised and confirmatory fragments were chosen dependant on what had been seen in previous analysis of the LDL samples on our Qtrap 2000.

**Table 28: MRM acquisition method for the detection of the nitrotyrosine modification on the Apo B100 protein.**

Peptide	Modification	Q1	Q3 transitions	Optimal CE	Vivo/vitro/both
(K)YGMVAQVTQLK(L)	X 1Oxidation 1Nitro 1Oxidation	670.30315 678.30285 700.8016	Y8 = 888.519 Y7 = 817.4777 Y5=590.3508 Y8 = 888.519 Y7 = 817.4777 Y5=590.3508 Y8 = 888.38 Y7 = 817.50 Y5=590.46	25eV	in vivo
(K)IEGNLIFDPNNYLPK(E)	X 1Nitro	874.5004 896.99915	Y9 = 1107.5469 B4 = 414.1983 B2 = 243.1339 Y9 = 1152.32 B4 = 414.1983 B2 = 243.1339	25eV	in vivo AND in vitro
(K)ALYWVNGQVPDGVSK(V)	X 1Nitro	817.42785 839.9266	Y6 = 602.3114 Y4 = 390.2347 B3 = 348.1918 Y6 = 602.3114 Y4 = 390.2347 B3 = 393.2	25eV	in vivo
(R)MYQMDIQQLQR(Y)	X 1Oxidation 2Oxidation 1Nitro 1Oxidation 1Nitro 2Oxidation	792.41835 800.92 807.715(2+) 823.417 830.91645	Y5 = 673.3628 Y3 = 416.2616 Y1 = 175.1190 Y5 = 673.3628 Y3 = 416.2616 Y1 = 175.1190	40eV	in vivo AND in vitro
(R)VPSYTLILPSELPLVHVR(N)	X 1Nitro	748.73 763.6	Y7 = 817.5043 Y4 = 508.299 B4 = 447.2238 Y7 = 817.5043 Y4 = 508.299 B4 = 492.2	40eV	in vivo
(K)LSLESLSYFSIESSTK(G)	X 1Nitro	947.0554 969.55415	Y3 = 335.1952 Y4 = 422.2245 Y5 = 551.2671 Y3 = 335.2 Y4 = 422.2245 Y5 = 551.2671	40eV	in vivo
(K)AASGTTGTQEWK(D)	X 1Nitro	700.7483 723.24705	Y2 = 333.1921 Y7 = 911.4258 Y4 = 590.2933 Y2 = 333.1921 Y7 = 956.36 Y4 = 590.2933	40eV	in vivo
(K)EVYGFNPEGK(A)	X 1Nitro	570.26 592.75	Y4 = 430.2296 Y2 = 204.1343 Y7 = 748.3624 Y4 = 430.2296 Y2 = 204.1343 Y7 = 748.3624	40eV	in vitro
(K)YHWEHTGLTLR(E)	X 1Nitro	707.29415 729.79285	Y6 = 660.404 Y4 = 502.335 Y2 = 288.2030 Y6 = 660.404 Y4 = 502.335 Y2 = 288.2030	40eV	in vitro

The above displays (from left to right) the targeted peptide, the modification state targeted for, the confirmatory fragment masses, the optimal collisional energy used and if this peptide was seen in Hamilton's study from the analysis of LDL *in vitro* or *in vivo* samples. The fragment ions highlighted in yellow are confirmatory peptides.

### 5.5.1 Analysing SIN-1 modified LDL by the MRM acquisition method

The LDL samples were analysed in parallel using the MRM acquisition method and conventional MSMS. No NiTyr modifications should be seen in an unmodified LDL sample so the unmodified LDL was analysed using the MRM method as a control

or test for the MRM program. It is unlikely that any NiTyr modified peptides will be detected but they are still targeted for. The only unmodified peptides that were not seen (no common elution time for the three transitions) are boxed in the Table 29. These unmodified peptides were also not identified and observed in the conventional MSMS analysis of the LDL samples. There was confidence that the unmodified peptides targeted for and detected by the MRM acquisition method identified as there was a common elution time for the three transitions (Figure 84). The unmodified peptide is seen to be eluted at 42 minutes into the chromatography gradient with an intensity of <600cps. The peak ringed in blue at approximately 60 minutes is a false positive peak as only one transition out of the three is observed. The NiTyr modified state of the LSLESLTSYFSIESSTK peptide (969.5m/z) has not been identified in the unmodified control sample. There is no common elution time seen for all three transitions and the intensity of the signal is low, <18cps. No NiTyr modified states of the peptides targeted for were detected in the unmodified LDL sample.

Table 29: Unmodified peptides that were not detected using the MRM acquisition method during the analysis of the control unmodified LDL sample.

Peptide	Modification	Q1	Q3 transitions	Optimal CE	Vivo/vitro/both
(K)YGMVAQVTQLK(L)	X 1Oxidation 1Nitro 1Oxidation	670.30315 678.30285 700.8016	Y8 = 888.519 Y7 = 817.4777 Y5=590.3508 Y8 = 888.519 Y7 = 817.4777 Y5=590.3508 Y8 = 888.38 Y7 = 817.50 Y5=590.46	25eV	in vivo
(K)IEGNLIFDPNNYLK(E)	X 1Nitro	874.5004 896.99915	Y9 = 1107.5469 B4 = 414.1983 B2 = 243.1339 Y9 = 1152.32 B4 = 414.1983 B2 = 243.1339	25eV	in vivo AND in vitro
(K)ALYWVNGQVPDGVSK(V)	X 1Nitro	817.42785 839.9266	Y6 = 602.3114 Y4 = 390.2347 B3 = 348.1918 Y6 = 602.3114 Y4 = 390.2347 B3 = 393.2	25eV	in vivo
(R)MYQMDIQELQR(Y)	X 1Oxidation 2Oxidation 1Nitro 1Oxidation 1Nitro 2Oxidation	792.41835 800.92 807.715(2+) 823.417 830.91645	Y5 = 673.3628 Y3 = 416.2616 Y1 = 175.1190 Y5 = 673.3628 Y3 = 416.2616 Y1 = 175.1190	40eV	in vivo AND in vitro
(R)VPSTLULPSLELPVLHVPR(N)	X 1Nitro	748.73 763.6	Y7 = 817.5043 Y4 = 508.299 B4 = 447.2238 Y7 = 817.5043 Y4 = 508.299 B4 = 492.2	40eV	in vivo
(K)LSLESLTSYFSIESSTK(G)	X 1Nitro	947.0554 969.55415	Y3 = 335.1952 Y4 = 422.2245 Y5 = 551.2671 Y3 = 335.2 Y4 = 422.2245 Y5 = 551.2671	40eV	in vivo
(K)AASGTTGYQEWK(D)	X 1Nitro	700.7483 723.24705	Y2 = 333.1921 Y7 = 911.4258 Y4 = 590.2933 Y2 = 333.1921 Y7 = 956.36 Y4 = 590.2933	40eV	in vivo
(K)EVYGFNPEGK(A)	X 1Nitro	570.26 592.75	Y4 = 430.2296 Y2 = 204.1343 Y7 = 748.3624 Y4 = 430.2296 Y2 = 204.1343 Y7 = 748.3624	40eV	in vitro
(K)YHWEHTGLTLR(E)	X 1Nitro	707.29415 729.79285	Y6 = 660.404 Y4 = 502.335 Y2 = 288.2030 Y6 = 660.404 Y4 = 502.335 Y2 = 288.2030	40eV	in vitro

The table displays the peptides (boxed in purple) not identified in the unmodified control LDL sample.

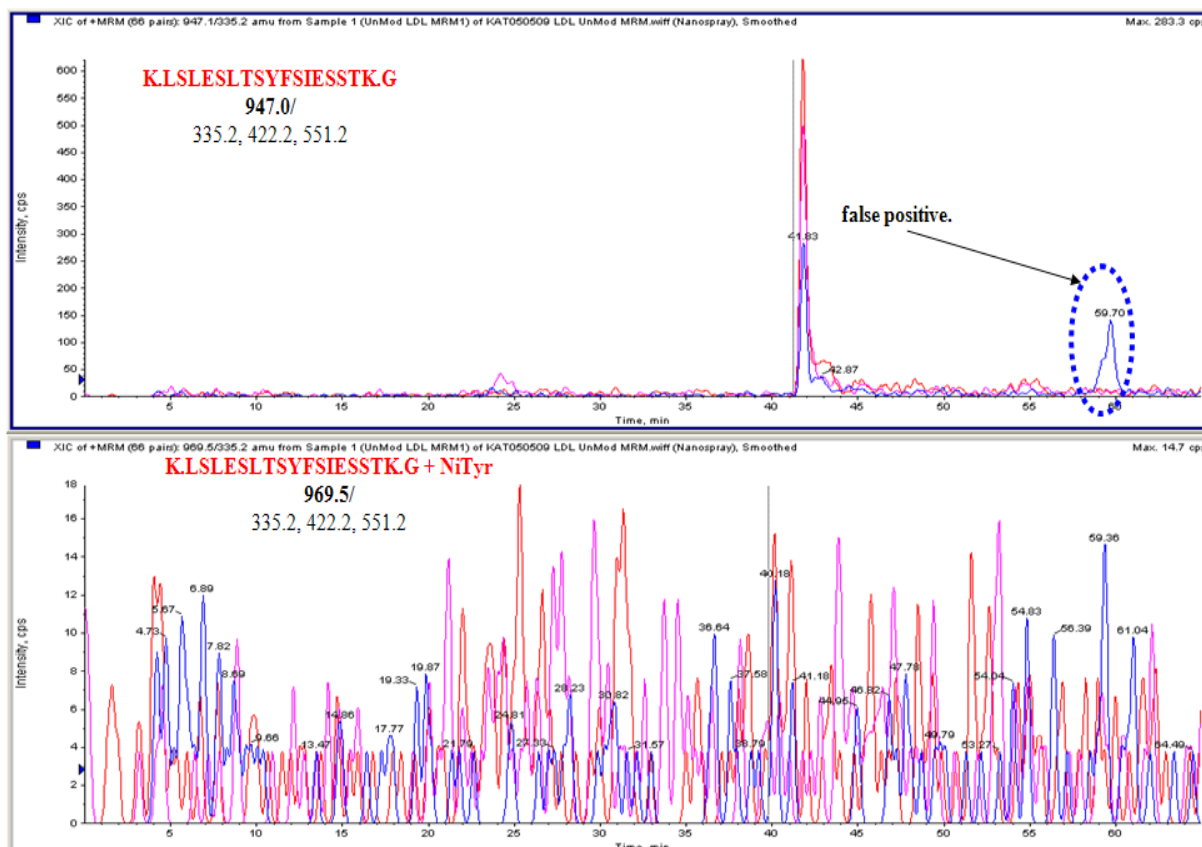


**Figure 84:** The detection of the targeted LSLESLTSYFSIESSTK peptide in the unmodified control LDL sample. The above figure displays an example of one of the unmodified peptides that are targeted for and seen in the MRM acquisition method when the unmodified control LDL sample was analysed. The top panel displays the XIC's for the unmodified peptide state (947.0 m/z) and the bottom panel displays the XIC's for the NiTyr modified state (969.5m/z) of the peptide. The unmodified LSLESLTSYFSIESSTK peptide was not seen in the conventional MSMS analysis of the control LDL sample.

#### 5.5.1.1 Detection of a targeted NiTyr modified peptide in a 1mM SIN-1 modified LDL sample

LDL samples that had been chemically modified *in vitro* with varying SIN-1 concentrations were analysed using the MRM acquisition method for the detection of NiTyr modifications on the Apo B100 protein and by conventional MSMS. The unmodified EYGFNPEGK peptide that was not detected in the unmodified LDL sample was observed in LDL samples modified with 1mM, 2.5mM and 10mM SIN-1. The peptide's NiTyr modified counter-part was also identified in these SIN-1 modified LDL samples (for example see Figure 85 and Figure 86). In the 10mM and 1mM SIN-1 modified LDL sample the unmodified peptide (top panel in both figures) is seen at 18 minutes into the chromatography gradient with an intensity of <845cps (10mM SIN-1 modified sample) and <5344cps (1mM SIN-1 modified sample). The peak seen at 44 minutes in both the 1mM and 10mM

modified SIN-1 sample is an anomalous peak where only one transition is seen at this point. The bottom panel in both figures displays the elution of the NiTyr modified peptide at 23 minutes into the chromatography gradient with an intensity of <497cps (10mM SIN-1 modified sample) and <180cps (1mM SIN-1 modified sample). The transitions common to both the unmodified and modified peptide; Q3=430.2, 204.1 and 748.3, are all seen to be eluted at a common retention time. There is increased confidence that the NiTyr modified peptide is identified in these samples as the elution time is to be expected with respect to the unmodified peptide. The addition of the NO<sub>2</sub> on the tyrosine will make the peptide less polar leading to the peptide appearing later in the chromatography gradient. Elution of peptides on the C<sub>18</sub> column is in order of polarity or hydrophobicity with the more polar or less hydrophobic peptides being eluted first.

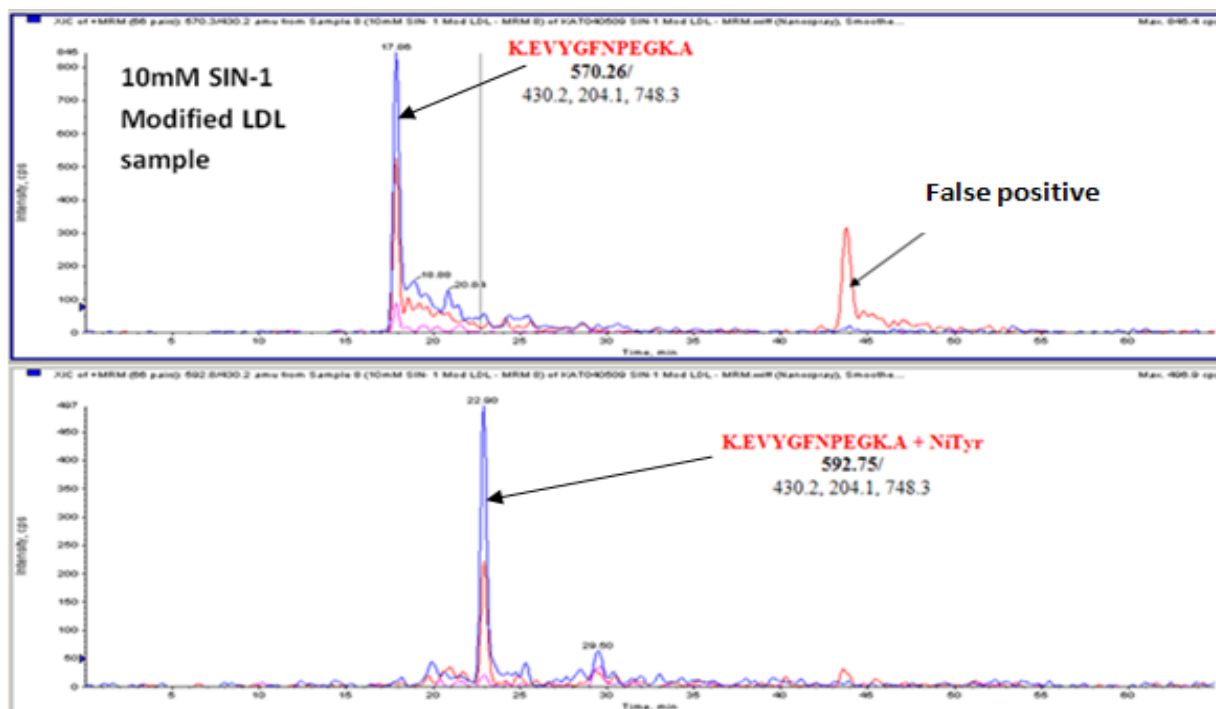


Figure 85: The EVYGFNPEGK + NiTyr modified peptide in a 10mM SIN-1 Modified LDL sample. The above figure displays the detection of the EVYGFNPEGK + NiTyr modified (bottom panel) and the unmodified (top panel) peptide.

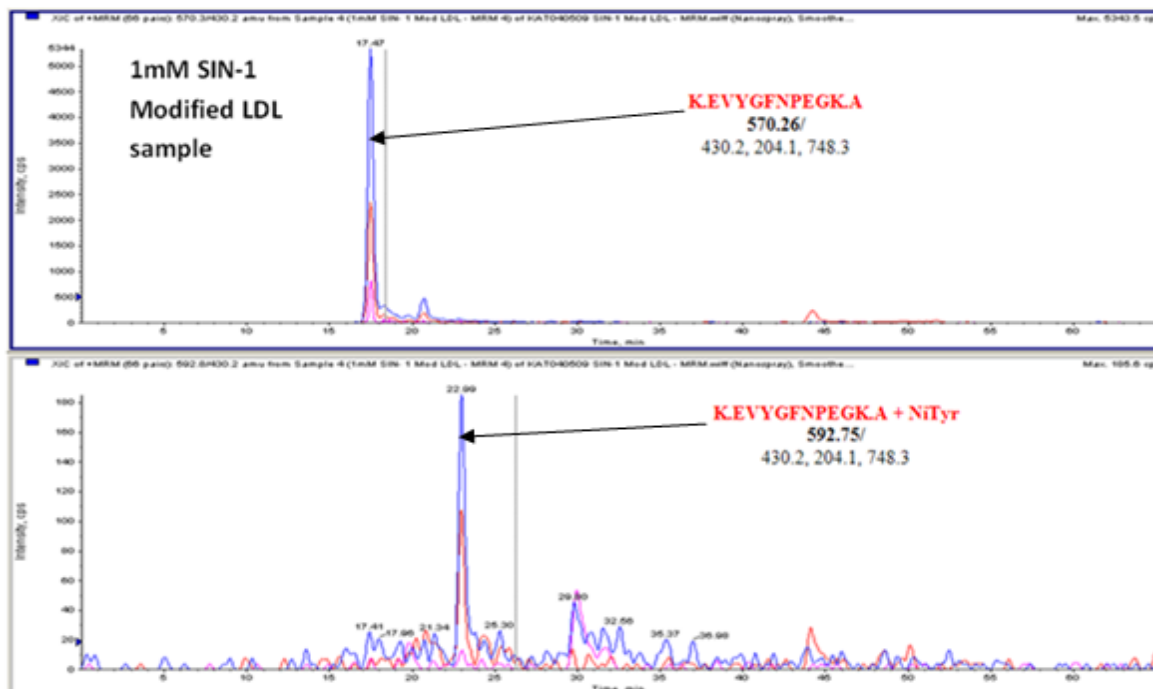


Figure 86: The EVYGFNPEGK + NiTyr peptide detected in a 1mM SIN-1 modified LDL sample. The above figure displays the EVYGFNPEGK + NiTyr peptide (bottom panel) detected in a 1mM SIN-1 modified LDL sample.

The results from the 1mM and 10mM modified LDL sample are only shown for example. The relative percentage modification for the peptide in the 1mM SIN-1 modified and 10mM SIN-1 modified LDL sample is calculated using intensities, assuming the ionisation efficiency of both the unmodified and modified peptide is equal using the equation 7 (3.4.1.1);

1mM SIN-1 Modified LDL Sample

$$(180/180 + 5344) \times 100 = \underline{3.25\%} \text{ (approximate percentage modification)}$$

10mM SIN-1 Modified LDL sample

$$(497/497 + 845) \times 100 = \underline{37.03\%} \text{ (approximate percentage modification)}$$

Assuming the ionisation energies are equal for the EVYGFNPEGK unmodified and NiTyr modified state, the relative percentage modification of this peptide is 3.25% in a 1mM SIN-1 modified LDL sample and 37.03% in a 10mM SIN-1 modified LDL sample. It should be noted that the EVYGFNPEGK peptide in its modified and unmodified state is seen more intensely in the 1mM SIN-1 modified sample (unmodified peptide intensity <5344cps) than in the 10mM SIN-1 modified sample

(unmodified peptide intensity <845cps). The higher concentration of SIN-1 may cause aggregation of the protein, decreasing the efficiency of the trypsin digestion and therefore affect the loading of the sample for analysis.

#### 5.5.1.2 The detection of other NiTyr modified peptides in SIN-1 modified LDL samples

The MYQMDIQQELQR peptide in comparison with other peptides targeted for in the MRM acquisition method is more difficult to analyse (Figure 87). A number of common elution times for the Q3 masses common to each modified state were seen in the analysis of the 1mM, 2.5mM and 10mM SIN-1 modified LDL samples. Oxidation of the methionine should increase the polarity of the peptide and it should therefore be seen sooner in the chromatography gradient with respect to the unmodified state. Nitration of the tyrosine should decrease the polarity of the peptide and it should then be seen later with respect to the unmodified peptide. The criteria for an assumed identification of an unmodified or modified peptide in a sample are the common elution of the three transitions with an elution time appropriate to the modification. If there is more than one common elution time to identify which peak is the targeted peptide we have to consider when it is expected to be seen based on its polarity.

In Figure 87 Panel A is the unmodified MYQMDIQQELQR peptide and there is a common elution time for the Q3=673.3, 416.2 and 175.1 masses. The first elution that could be the peptide is seen at 20minutes into the chromatography gradient with an intensity <500cps. The second possible elution of the unmodified peptide is seen at 30 minutes with an intensity of <1000cps. Panel B displays the Ox(M) modified state of the peptide with three possible elution times. The first is at 20 minutes with an intensity of <256cps, the second at 21.5 minutes with an intensity of <200cps and the third is seen at 25 minutes with an intensity of <200cps. Panel C displays the "Ox(M) modification state of the peptide. Unlike the other modification states there is only one elution time seen at 19 minutes with an intensity of <3599cps. Panel D displays the Ox(M);NiTyr modification state of the peptide. There are three possible elution times for this peptide. The first is seen at 20minutes with intensity <200cps, the second is seen at 47 minutes with an intensity of <300cps and the third is seen at 52 minutes with intensity <400cps. Panel D shows the 2Ox(M); Nityr modification state. There is a peak at 31 minutes with intensity >132cps. This is a false positive as

there is only one transition observed at this point. The 2Ox(M);NiTyr modification state is a very highly modified state and is unlikely to be seen when the LDL is modified by a 1mM SIN-1 concentration. There is a possible common elution of the three transitions for this modification state at 20 minutes, intensity <40cps. It is difficult to identify if this is a possible elution because of the low intensity.

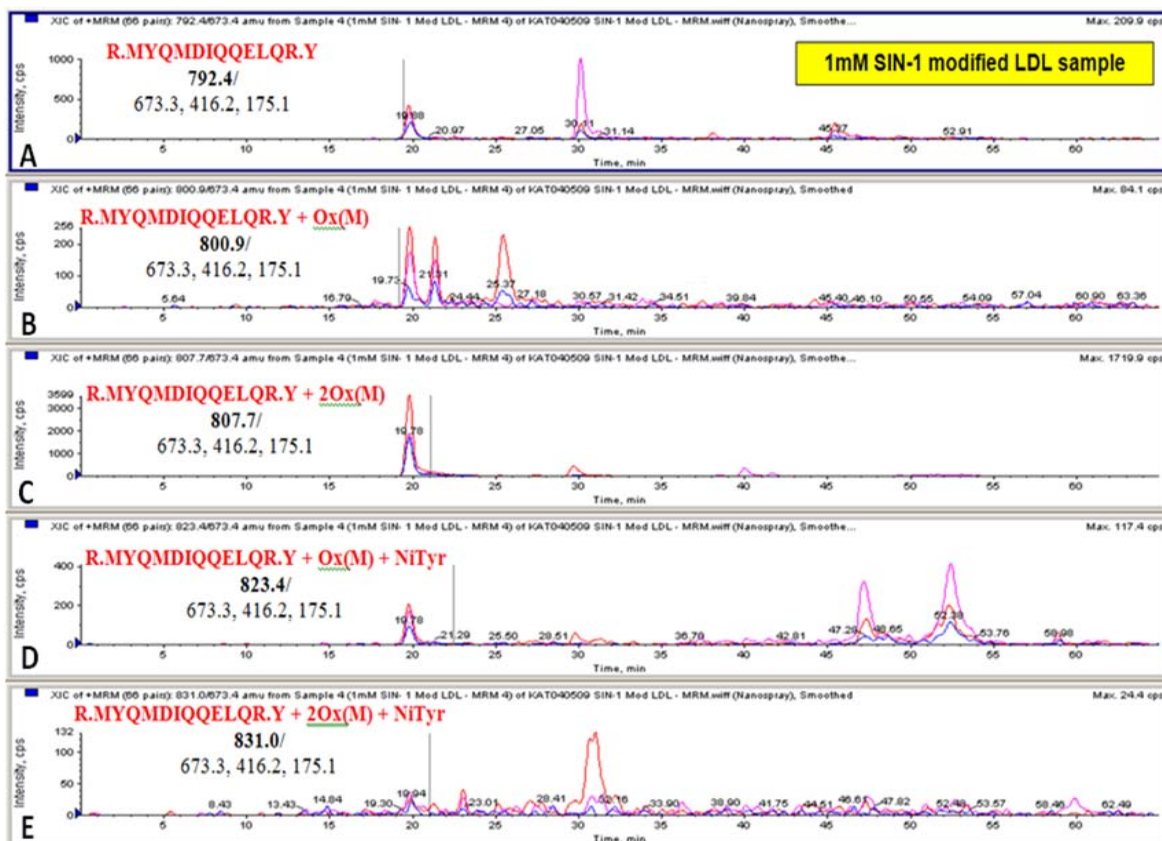


Figure 87: The MYQMDIQQLQR peptide’s modified states in a 1mM SIN-1 modified LDL sample. The figure displays the ambiguous elution times for the different modified states of the MYQMDIQQLQR peptide.

A possible explanation for the appearance of more than one elution time common to all three transitions being present for one modified state is break thorough. The resolution in Q1 is set to “low” for the MRM method and the Q3 masses are common to all modification states so selection at Q1 is not optimal.

For the MYQMDIQQLQR peptide and its modified states, blue and green arrows have been used to illustrate the “same” peak observed in different modification states (Figure 88). The Peak “1” denoted by the green arrow is seen in the unmodified peptide state (Panel A) and the 2Ox(M) + NiTyr state (Panel E, intensity <132cps). The 2Ox(M) + NiTyr state is a highly oxidised state so is

unlikely to be present at this intensity in a 1mM SIN-1 modified sample. It is likely that the peak labelled as “7” in the figure (panel E) is the breakthrough of signal caused by poor selection in Q1 from the peak labelled “1”. Peak “1” is therefore more likely to be the elution of the unmodified peptide.

Panel B displays three peaks. Peak “2” (seen at 26 minutes) is likely to be the Ox(M) modified state of the peptide as with respect to peak “1” (the unmodified peptide seen at 30 minutes) the elution time of this peptide in the chromatography gradient at a time expected.

The peak denoted by the blue arrows is observed in the unmodified (Panel A), Ox(M) (Panel B), 2Ox(M) (Panel C), Ox(M) + NiTyr (Panel D) and is suggested in low intensity (>40cps) in the 2Ox(M) + NiTyr (Panel E) peptide states. This peak is observed most strongly in the 2Ox(M) (with intensity >3599cps) and is the only elution peak common to all three transitions seen for this modified state. It is therefore likely that the peak labelled “4” is the elution of the 2Ox(M) modified peptide.

In Panel B, the Ox(M) modified state, peak “3” is seen (with intensity >200cps) and is suggested in low intensity (>30cps) in the 2Ox(M) + NiTyr modified state (peak “8”, panel E). The elution time of peak “3” and “8” (approximately 23 minutes) satisfies the 2Ox(M) + NiTyr modified state with respect to the 2Ox(M) modified state (seen to be eluted at 20 minutes- peak “4”) and the Ox(M) modified state (peak “1”, seen to be eluted at approximately 26 minutes into the chromatography gradient. As discussed previously the oxidation of the methionine will increase the polarity of the peptide leading to an earlier elution time and the addition of a NO<sub>2</sub> group onto the tyrosine will lead to a decrease in polarity and therefore a longer retention time. Peak “3” is therefore likely to be break through from the 2Ox(M) + NiTyr modified peptide which is likely to be peak “8”.

There is some uncertainty with peak “5” and “6” observed in Panel D (elution time approximately 47 minutes and 57 minutes respectively). Peak “5” has two clear transitions Q3=416.2 and 175.1 present and peak “6” shows the elution of all three transitions states. Both or either may be a breakthrough signal from another targeted peptide or one may be the Ox(M);NiTyr modification state of this peptide.

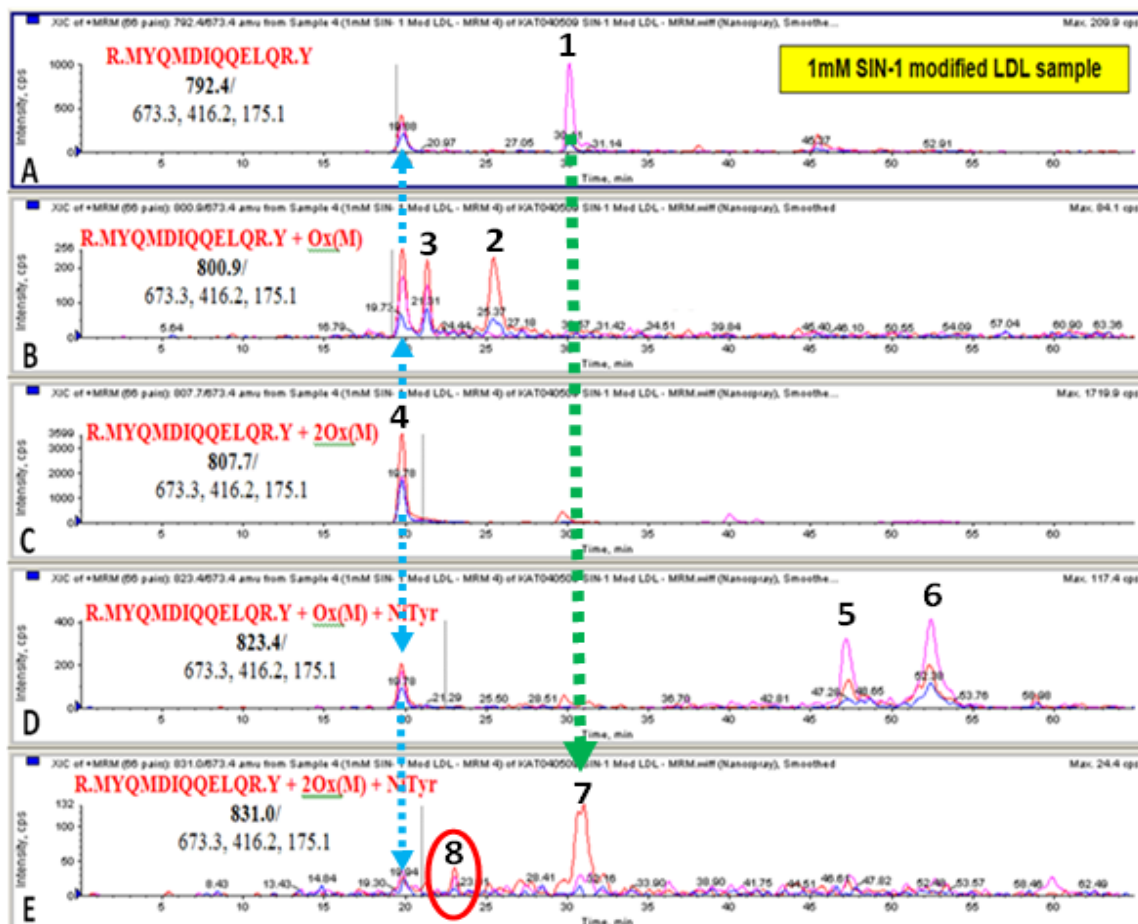


Figure 88: An explanation for the common elution of the three transitions for one modified peptide state. Peak 1 is likely to be the unmodified peptide, peak 2 is likely to be the Ox(M) modified peptide, peak 4 is likely to be the 2Ox(M) modified peptide and peak 8 is likely to be the 2Ox(M) + NiTyr peptide. Peaks 3 and 7 are likely to be breakthrough signal. Peaks 5 and 6 may both be breakthrough signal from another peptide (not shown in the figure) or may be the Ox(M);NiTyr modified state.

To confirm and identify the expected retention time for the unmodified and modified peptide states of the MYQMDIQQLQR peptide a targeted MSMS experiment should be performed (see 4.4.3.2 and 4.4.3.5).

### 5.5.1.3 Another example of “break-through” in the detection of NiTyr modifications in the LDL samples - The ALYWVNGQVPDGVSK peptide

The MRM method for the detection of NiTyr modifications on the Apo B100 protein required more analysis than what was needed in the previous MRM experiments (Chapter 3) due to the amount of breakthrough signal observed. The ALYWVNGQVPDGVSK peptide was seen to be the NiTyr modified in the 10mM SIN-1 modified LDL sample but not in the 1mM or 2.5mM SIN-1 modified LDL samples (Figure 89). The unmodified peptide is seen as a split-peak beginning to

be eluted at 27 minutes during the chromatography gradient with an intensity <math><5996\text{cps}</math>. The “split-peak” is unlikely to be due to poor chromatography of the peptide as the split-peak nature is observed in both the modified and unmodified peptide states and other peptides targeted for by the MRM do not display a “split”. The peaks suggests the identification of the presence of the unmodified and modified peptide in the 10mM SIN-1 modified LDL sample as all three common transitions; 602.3, 390.2 and 348.2 are eluted at the same time. The bottom panel displaying the NiTyr modified peptide displays two peaks, one seen at 27 minutes into the chromatography gradient with an intensity of <math><110\text{cps}</math> and one at 32 minutes with an intensity of <math><177\text{cps}</math> (ringed in green). The peak seen at 27 minutes is also observed in the 1mM and 2.5mM SIN-1 modified LDL samples but the one seen at 32 minutes (ringed in green) is not. The peak seen at 27 minutes is likely to be breakthrough signal from the unmodified peptide as it is observed at the same time as the unmodified peptide is seen to elute. The peak ringed in green is therefore likely to be the NiTyr modified peptide. The three Q3 masses for the NiTyr modified state of this peptide (Q3=602.3, 390.2 and 393.2) are all eluted at the same time and is observed at the expected time in the gradient. The Q3=393.2 is the  $b_3$ -ion for the NiTyr modified peptide. The  $b_3$ -ion is targeted for in the unmodified peptide (Q3 = 348.2) but the 393.2 mass is a confirmatory NiTyr fragment (highlighted in blue).

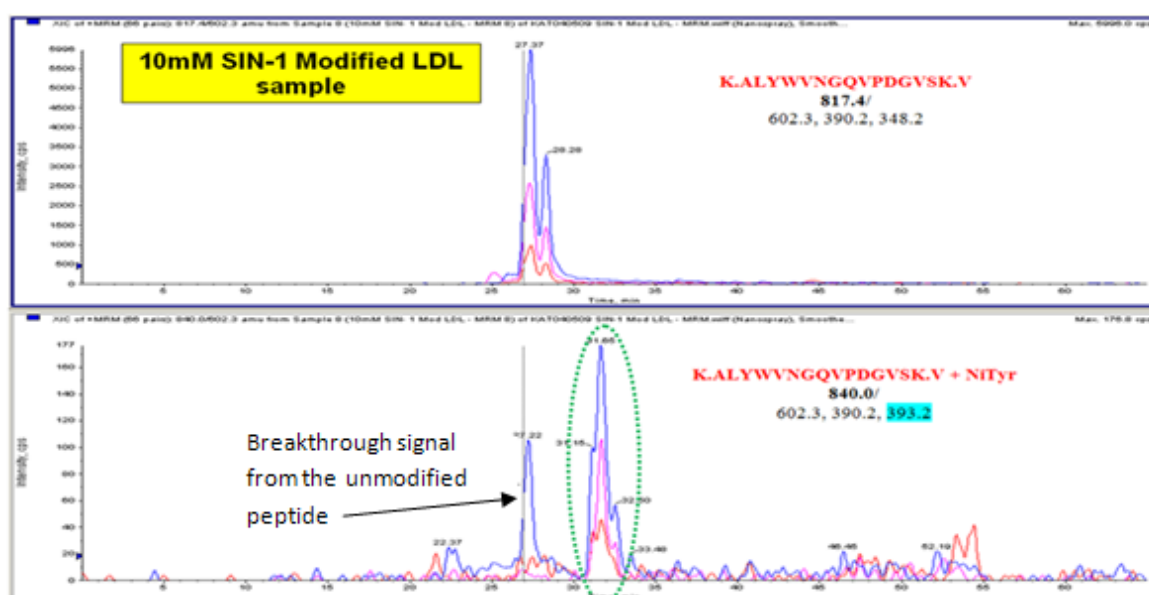


Figure 89: The above figure displays the XIC's for the unmodified ALYWVNGQVPDGVSK peptide (top panel - 817.4m/z) and the NiTyr modified state (bottom panel - 840.0m/z).

### 5.5.2 Critical evaluation of the MRM acquisition method

Likely break-through caused by poor selection in Q1 was a bigger problem in the MRM acquisition method for the detection of NiTyr modification on the Apo B100 protein than in the detection of ClTyr and NiTyr modifications on the albumin protein in plasma (see Chapters 3 and 4). False positive peaks of one transition is not as initially confusing as more than one peak displaying the common elution of the all three Q3 masses being observed for one modified state of a peptide (see 5.5.1.2). The problem of break-through did not arise in the analysis of the clinical plasma samples perhaps due to the abundance of albumin in plasma (50-75% of proteins) and the complexity and size of the Apo B100 protein. Break through may have become more apparent during the analysis of LDL as although extracted from plasma the amphipathic nature of the Apo B100 protein means that it is complex in comparison to lysozyme, purified proteins and abundant albumin in the plasma samples.

The MRM acquisition method written for the detection of ClTyr and NiTyr modifications on albumin was written using MSMS observations seen during conventional MSMS analysis on the Qtrap 2000. The MRM acquisition method written for the detection of NiTyr modifications on the Apo B100 protein was written from the mass spectrometry data collected on an ion-trap (*ThermoFinnigan LCQ Deca XP Plus ion trap*) to be used to write a program for a triple-quadrupole mass spectrometer (Qtrap 2000, *Applied Biosystems*, Warrington, UK).

In Hamilton's study there were a number of NiTyr modification sites detected in *in vivo* samples and a number of NiTyr modification sites detected in *in vitro* SIN-1 modified samples (see 5.4.1.1). In our analysis we indicated the detection of NiTyr modification sites only reported in *in vivo* samples in Hamilton's study in our *in vitro* samples modified with varying concentrations of SIN-1. Perhaps there are even more NiTyr sites *in vitro* and *in vivo* and these were not identified by Hamilton as he applied a "Top Five" method of analysis. The Top Five method analyses the precursor masses in order of their abundance, the most intensely seen first. Less abundant, low intensity masses will then be missed or masked by the more abundant masses. It is possible that Hamilton missed the lower abundant modified peptides and that the NiTyr modifications found in *in vivo* samples are also found in *in vitro* modified LDL samples and vice

versa. Due to the conformation of the Apo B100's protein some tyrosines will be more susceptible to modification than others depending on neighbouring amino acids both sequentially in the secondary structure and those spatially in the tertiary structure. It would therefore be expected for there to be a higher abundance of some modified peptides than others in a sample.

## **5.6 Conclusion and Further work on the Detection of NiTyr modifications on the Apo B100 protein**

The MRM method identified and suggested NiTyr modification on the Apo B100 protein. The modifications detected by the MRM method were not detected by conventional MSMS or by the precursor scan.

Further work on the MRM method should include a targeted MSMS to confirm the presence of the NiTyr modified peptides in the SIN-1 modified LDL samples. From the targeted analysis we would be able to confirm if detection of the NiTyr modified peptide had been successful and note where in the chromatography the targeted peptide was observed. The MRM method for targeting modified NiTyr Apo B-100 peptides should also be applied to the clinical samples (analysed in section 4.4.1) to see if there is a correlation between those NiTyr modifications targeted in diseased and healthy samples.

## 6 General Discussion

The main aim of this research was to develop techniques for the detection and identification of nitro- and chlorotyrosine modifications in protein samples. Nitro- and chlorotyrosine are known markers for inflammatory disease [50;54;166;167;207;237] and elevated levels of these oxidative markers have been found in the blood of atherosclerotic patients [57;238]. It is important for the mass spectrometry techniques to be sensitive as post translational modifications are low in abundance. Ideally these methods developed for the detection of post translational modifications may be applied to clinical samples to classify cardiovascular disease.

### 6.1 A summary of the findings from this study

A precursor scan may be used as a sensitive and selective method in comparison to a conventional MSMS experiment alone for the detection of chlorotyrosine modifications when there is no prior knowledge of the modification sites. In chapter 2 the precursor scan was employed to detect ClTyr modifications in 9 protein mix samples. The gas phase fractionation experiment (scanning smaller mass ranges) was then used and although sample consumption was increased this method was found to detect more ClTyr modifications in a HOCl modified 9 protein mix sample than the precursor alone (scanning a larger mass range). The precursor scan is ideal when there is no prior knowledge of a sample and chlorotyrosine modified peptides were identified here in a 9 protein mix model.

A multiple reaction monitoring (MRM) method is a sensitive and selective method for targeting nitro- and chlorotyrosine modifications in proteins. The MRM method requires prior knowledge about the modification site and was used to identify modified peptides in human serum albumin and plasma samples in chapter 3. An MRM method was developed to target nitro- and chlorotyrosine modifications in chemically in vitro modified human serum albumin and plasma samples.

The MRM method developed can be employed to indicate the presence of nitro- and chlorotyrosine modifications in clinical samples as seen in chapter 4. The targeted modified peptides were detected but unfortunately these modified

peptides alone could not be used to classify diseased from healthy patients and volunteers.

The MRM mass spectrometry technique was also employed to detect nitrotyrosine modification of the LDL's protein moiety, Apo B100, in *in vitro* SIN-1 modified LDL samples in chapter 5.

When discussing the methods developed and used in this study of post translational modifications it is important to be aware of their limitations as well their benefits.

## **6.2 The limitations and advantages**

### **6.2.1 The precursor scan**

In chapter 2 the precursor scan was used to increase identification of ClTyr modifications in *in vitro* HOCl modified 9 protein mix samples with respect to a conventional MSMS analysis. I found that the precursor scan detected and identified more ClTyr modifications than the MSMS method. More technical replicates of this experiment are required as there was variation between which modifications were identified by each method. This was also the case when the gas phase fractionation (GPF) experiment was employed. The GPF experiment was found to detect more ClTyr modifications when narrower mass ranges were scanned using 200amu ranges (400\_600, 600\_800 and 800\_1000amu) in comparison to 600amu ranges (400\_1000amu). Even narrower mass scans (100amu ranges) with a 20amu overlap (400\_510, 490\_610, 690\_710amu...) were then investigated with the GPF experiment and by sacrificing more sample detected a greater number of ClTyr modifications. The variation observed was that some modified peptides were seen in a less sensitive scan (between the 400\_600amu range) but not in more sensitive scans (between the 400\_510 and 490\_610amu ranges). The experiment needs further repetition to collate a list of the modified peptides seen by each scan.

### **6.2.2 The MRM method – developing and applying a targeted approach for the classification of disease in clinical samples**

The MRM method in chapter 4 was written from using observations from the conventional MSMS method of the analysis of *in vitro* modified SIN-1 and HOCl modified human serum albumin and plasma from chapter 3. The three peptides

seen to be ClTyr modified were also seen to be NiTyr modified with the exception of one peptide (YLYEIAR + NiTyr). This was explained by the susceptibility of a tyrosine residue to modification with respect to the neighbouring side chains. Three transitions were employed for the identification of a peptide. To calculate the relative percentage modification the unmodified peptide was also targeted for identification. Using three transitions decreased the number of false positives.

MIDAS will write an MRM method automatically by performing an in-silico digest with the user-specified protease, generating and calculating theoretical MRM precursor masses; their transitions and optimal collisional energy. I found that as MIDAS only chose one transition for each peptide, analysis by an MRM method written by MIDAS and not MSMS observations produced a lot of false positives.

From the analysis of the *in vitro* modified protein sample anomalous peaking of transitions was sometimes observed but this was not mistaken to be the targeted peptide as not all three transitions were seen to be eluted at the same time. It may be likely, especially in a complex sample that a precursor (Q1) and fragment (Q3) may be isobaric to the targeted peptide. It is less likely that there will be a precursor with three fragments (Q3) isobaric to the targeted peptide. False positives were seen in the form of “break-through”. In an MRM experiment there was sometimes some confusion as to which peak with the commonly eluted three transitions was the targeted peptide. It is impossible for a peptide with a certain polarity to be eluted at two different times during the chromatography gradient. The retention time is therefore important in the identification of the targeted peptides in the MRM method. When a peptide becomes NiTyr or ClTyr modified the peptide will become less polar meaning the retention time is later. If a peptide becomes methionine oxidised the polarity is increased and the peptide will be eluted earlier with respect to the unmodified peptide. When a peptide is methionine oxidised and a tyrosine is modified by a Cl- or NO<sub>2</sub> group the polarity and therefore elution time of the peptide will remain relatively similar with respect to the unmodified peptide. Break-through is caused by poor selectivity in the first quadrupole (Q1). Q1 selects the precursor mass to be fragmented but the resolution is set to low. The three (Q3) transition masses are where possible common to all modified states of the peptide. If in Q1 two

precursors close in mass are selected the signal from another modified state will be “break-through” and be observed.

The MRM method successfully detected modification in the clinical samples which was confirmed by a targeted MSMS experiment and the data collected was searched by Mascot. We failed to classify the diseased from healthy clinical samples. This does not mean that our modified peptides cannot be used to classify disease but it does mean that they are not enough to classify disease. The MRM method employed only targeted for four peptides and their modified states. These peptides and the modified states were based on the MSMS analysis of the SIN-1 and HOCl modified samples. More important or at least NiTyr and/or ClTyr modified peptides key to the classification of disease may have been in very low abundance therefore not observed during MSMS analysis. The detection of modification in healthy samples can be explained by the variation of causes of NiTyr and ClTyr. These modified tyrosines are caused by oxidative stress in a response to inflammation. The healthy volunteers may have been smokers or had just taken part in physical activity <sup>[205;206]</sup>. In order to combat this the sample population could be increased to allow for healthy samples to be modified by these environmental factors.

It is known from other studies (discussed in 4.7) that the onset of atherosclerosis can happen at a very early age and the individual is asymptomatic for years before developing symptoms at a later stage in life <sup>[209-213]</sup>. In order to overcome the problem of modified peptides unspecific to disease more modified peptides or indeed a combination of modified peptides may be required to identify diseased samples. It may be possible that employing modified Apo B-100 peptides would be more successful for the diagnosis of diseased samples (as discussed in chapter 5) as increased levels of LDL are related to the development of atherosclerosis.

### **6.2.3 The MRM method and precursor scan – NiTyr detection in the Apo B100 protein**

The LDL was modified *in vitro* with HOCl in parallel with a simpler protein, lysozyme. The precursor scan identified and suggested ClTyr modification in the lysozyme protein. The precursor scan however, failed to detect any ClTyr modified peptides in the LDL protein moiety Apo B100. Even though the

precursor scan is a sensitive and selective mass spectrometry method the ClTyr modifications are extremely low in abundance and were not detected during analysis. The Qtrap 4000 is more sensitive for precursor ion scanning and multiple reaction monitoring in comparison to the Qtrap 2000 used throughout this study due to the bigger trapping abilities and faster scan times<sup>[239]</sup>. Perhaps if this analysis was performed on the Qtrap 4000 instead of the Qtrap 2000, ClTyr modifications would have been identified.

The MRM method for the detection of NiTyr in Apo B-100 was written from the observations made from the work carried out by Hamilton et al <sup>[233]</sup>. Hamilton performed the study of in vivo and in vitro modified LDL samples on the LCMSMS (ThermoFinnigan LCQ Deca XP Plus ion trap). The Q3 fragments were chosen depending on their intensity seen in the mass spectrum. The MRM method written was able to identify NiTyr modifications on the Apo B100 protein in LDL samples. Some targeted MSMS was required to confirm the identification of the post translational modifications and there were a lot of incidences of break-through signal and anomalous peaks seen in the MRM analysis of the LDL samples. The MRM method was performed on the Qtrap but the MSMS observations used were taken from the LCQ which is a different machine. If the MRM method had been written from MSMS observations on the Qtrap the MRM method may have been more optimal.

In conclusion to this general discussion I have detected post translational modifications by a precursor scan and by MRM methods in purified proteins and biological and clinical samples. Precursor scans are useful when there is no prior sample knowledge but MRM is more selective when targeting known peptides as both Q1 and Q3 are fixed.

## Reference List

1. Venter JC, Adams MD, Myers EW, Li PW, Mural RJ, Sutton GG *et al.* The sequence of the human genome. *Science* 2001;**291**:1304-+.
2. Plebani M. Proteomics: The next revolution in laboratory medicine? *Clinica Chimica Acta* 2005;**357**:113-22.
3. Pennington SR, Wilkins MR, Hochstrasser DF, Dunn MJ. Proteome analysis: From protein characterization to biological function. *Trends in Cell Biology* 1997;**7**:168-73.
4. Wilkins MR, Gasteiger E, Tonella L, Ou K, Tyler M, Sanchez JC *et al.* Protein identification with N and C-terminal sequence tags in proteome projects. *Journal of Molecular Biology* 1998;**278**:599-608.
5. Thom TJ. International Mortality from Heart-Disease - Rates and Trends. *International Journal of Epidemiology* 1989;**18**:S20-S28.
6. G.Pasterkamp, .E.Falk. Atherosclerotic Plaque Rupture: an Overview. *journal of clinical basic cardiology* 2000;**3**:81-6.
7. Madamanchi NR, Vendrov A, Runge MS. Oxidative stress and vascular disease. *Arteriosclerosis Thrombosis and Vascular Biology* 2005;**25**:29-38.
8. Jonasson L, Holm J, Skalli O, Bondjers G, Hansson GK. Regional Accumulations of T-Cells, Macrophages, and Smooth-Muscle Cells in the Human Atherosclerotic Plaque. *Arteriosclerosis* 1986;**6**:131-8.
9. Guyton JR, .Klemp KF. Development of the lipid-rich core in human atherosclerosis. *Arteriosclerosis Thrombosis and Vascular Biology* 1996;**16**:4-11.
10. Restrepo C, .Tracy RE. Variations in Human Aortic Fatty Streaks Among Geographic Locations. *Atherosclerosis* 1975;**21**:179-93.
11. Katz SS, Shipley GG, Small DM. Physical-Chemistry of Lipids of Human Atherosclerotic Lesions - Demonstration of A Lesion Intermediate Between Fatty Streaks and Advanced Plaques. *Journal of Clinical Investigation* 1976;**58**:200-11.
12. Howard C. Hydrolysis of cholesteryl linoleate by a high-speed supernatant preparation. *Biochimica et Biophysica Acta* 1966;**125**:623-6.
13. Ylaherttua S, Palinski W, Rosenfeld ME, Parthasarathy S, Carew TE, Butler S *et al.* Evidence for the Presence of Oxidatively Modified Low-Density Lipoprotein in Atherosclerotic Lesions of Rabbit and Man. *Journal of Clinical Investigation* 1989;**84**:1086-95.

14. Daugherty A, Dunn JL, Rateri DL, Heinecke JW. Myeloperoxidase, A Catalyst for Lipoprotein Oxidation, Is Expressed in Human Atherosclerotic Lesions. *Journal of Clinical Investigation* 1994;**94**:437-44.
15. Guyton JR, Klemp KF. Transitional Features in Human Atherosclerosis - Intimal Thickening, Cholesterol Clefts, and Cell Loss in Human Aortic Fatty Streaks. *American Journal of Pathology* 1993;**143**:1444-57.
16. Krisko A, Etchebest C. Theoretical model of human apolipoprotein B100 tertiary structure. *Proteins-Structure Function and Bioinformatics* 2007;**66**:342-58.
17. Steinberg D. Lipoproteins and Atherosclerosis - A Look Back and A Look Ahead. *Arteriosclerosis* 1983;**3**:283-301.
18. Hoff HF, Whitaker TE, Oneil J. Oxidation of Low-Density-Lipoprotein Leads to Particle Aggregation and Altered Macrophage Recognition. *Journal of Biological Chemistry* 1992;**267**:602-9.
19. Hoff HF, Whitaker TE, Oneil J. Oxidation of Low-Density-Lipoprotein Leads to Particle Aggregation and Altered Macrophage Recognition. *Journal of Biological Chemistry* 1992;**267**:602-9.
20. Segrest JP, Jones MK, De Loof H, Dashti N. Structure of apolipoprotein B-100 in low density lipoproteins. *Journal of Lipid Research* 2001;**42**:1346-67.
21. Kingsbury K, Bondy G. Understanding the Essentials of Blood Lipid Metabolism. *Progress in Cardiovascular Nursing* 2007;**18**:13-8.
22. Yang. Structure of ApoB-100 of Human Low-Density Lipoproteins. *Atherosclerosis* 1989;**9**:96-108.
23. Yang et al. Structure and conformational Analysis of Lipid Associating Peptides of ApoB-100 produced by Trypsinolysis. *J. Protein Chem.* 1989;**8**:689-99.
24. Gordon S, Clarke S, Greaves D, Doyle A. Molecular Immunobiology of Macrophages - Recent Progress. *Current Opinion in Immunology* 1995;**7**:24-33.
25. Li AC, Glass CK. The macrophage foam cell as a target for therapeutic intervention. *Nature Medicine* 2002;**8**:1235-42.
26. Podrez EA, Poliakov E, Shen ZZ, Zhang RL, Deng YJ, Sun MJ *et al.* A novel family of atherogenic oxidized phospholipids promotes macrophage foam cell formation via the scavenger receptor CD36 and is enriched in atherosclerotic lesions. *Journal of Biological Chemistry* 2002;**277**:38517-23.
27. Yoshida H, Kondratenko N, Green S, Steinberg D, Quehenberger O. Identification of the lectin-like receptor for oxidized low-density lipoprotein in human macrophages and its potential role as a scavenger receptor. *Biochemical Journal* 1998;**334**:9-13.

28. Morel DW, Dicorleto PE, Chisolm GM. Endothelial and Smooth-Muscle Cells Alter Low-Density Lipoprotein In Vitro by Free-Radical Oxidation. *Arteriosclerosis* 1984;**4**:357-64.
29. Fayad ZA, Fuster V. Clinical imaging of the high-risk or vulnerable atherosclerotic plaque. *Circulation Research* 2001;**89**:305-16.
30. Falk E. Pathogenesis of atherosclerosis. *Journal of the American College of Cardiology* 2006;**47**:C7-C12.
31. Jennette JC, Xiao H, Falk RJ. Pathogenesis of vascular inflammation by anti-neutrophil cytoplasmic antibodies. *Journal of the American Society of Nephrology* 2006;**17**:1235-42.
32. Ehara S, Kobayashi Y, Yoshiyama M, Shimada K, Shimada Y, Fukuda D *et al.* Spotty calcification typifies the culprit plaque in patients with acute myocardial infarction - An intravascular ultrasound study. *Circulation* 2004;**110**:3424-9.
33. Ursini F, Davies KJA, Maiorino M, Parasassi T, Sevanian A. Atherosclerosis: another protein misfolding disease? *Trends in Molecular Medicine* 2002;**8**:370-4.
34. Millar JS, Lichtenstein AH, Cuchel M, Dolnikowski GG, Hachey DL, Cohn JS *et al.* Impact of Age on the Metabolism of Vldl, Idl, and Ldl Apolipoprotein B-100 in Men. *Journal of Lipid Research* 1995;**36**:1155-67.
35. Asztalos BF, Schaefer EJ. HDL in atherosclerosis: actor or bystander? *Atherosclerosis Supplements* 2003;**4**:21-9.
36. Assmann G, Gotto AM. HDL cholesterol and protective factors in atherosclerosis. *Circulation* 2004;**109**:8-14.
37. Smith LC, Pownall HJ, Gotto AM. Plasma Lipoproteins - Structure and Metabolism. *Annual Review of Biochemistry* 1978;**47**:751-77.
38. Kinnunen PKJ, Jackson RL, Smith LC, Gotto AM, Sparrow JT. Activation of Lipoprotein-Lipase by Native and Synthetic Fragments of Human-Plasma Apolipoprotein C-ii. *Proceedings of the National Academy of Sciences of the United States of America* 1977;**74**:4848-51.
39. Young SG, Parthasarathy S. Why Are Low-Density Lipoproteins Atherogenic. *Western Journal of Medicine* 1994;**160**:153-64.
40. Wilson JM, Walton B. Lesions and lipids and radicals - O my! *Texas Heart Institute Journal* 2004;**31**:118-26.
41. Mathews, Van Holden, Ahern. 3rd Edition Biology. X 2010.
42. Anderson RGW. The caveolae membrane system. *Annual Review of Biochemistry* 1998;**67**:199-225.
43. Anderson RGW. The caveolae membrane system. *Annual Review of Biochemistry* 1998;**67**:199-225.

44. van der Velde AE, Groen AK. Shifting gears: liver SR-BI drives reverse cholesterol transport in macrophages. *Journal of Clinical Investigation* 2005;115:2699-701.
45. Out R, Hoekstra M, Meurs I, de Vos P, Kuiper J, Van Eck M *et al.* Total body ABCG1 expression protects against early atherosclerotic lesion development in mice. *Arteriosclerosis Thrombosis and Vascular Biology* 2007;27:594-9.
46. Oram JF, Heinecke JW. ATP-binding cassette transporter A1: A cell cholesterol exporter that protects against cardiovascular disease. *Physiological Reviews* 2005;85:1343-72.
47. Ohashi R, Mu H, Wang X, Yao Q, Chen C. Reverse cholesterol transport and cholesterol efflux in atherosclerosis. *Qjm-An International Journal of Medicine* 2005;98:845-56.
48. Suer S, Ulutin T, Sonmez H, Kokoglu E, Ucisik N, Bayram C *et al.* Plasma Lp(a) and t-PA-PAI-1 complex levels in coronary heart disease. *Thrombosis Research* 1996;83:77-85.
49. Droge W. Free radicals in the physiological control of cell function. *Physiological Reviews* 2002;82:47-95.
50. Blokhina O, Virolainen E, Fagerstedt KV. Antioxidants, oxidative damage and oxygen deprivation stress: a review. *Annals of Botany* 2003;91:179-94.
51. Hawkins CL, Davies MJ. Hypochlorite-induced damage to proteins: formation of nitrogen-centred radicals from lysine residues and their role in protein fragmentation. *Biochemical Journal* 1998;332:617-25.
52. Davies JMS, Horwitz DA, Davies KJA. Potential Roles of Hypochlorous Acid and N-Chloroamines in Collagen Breakdown by Phagocytic-Cells in Synovitis. *Free Radical Biology and Medicine* 1993;15:637-43.
53. Hazell LJ, Stocker R. Oxidation of Low-Density-Lipoprotein with Hypochlorite Causes Transformation of the Lipoprotein Into A High-Uptake Form for Macrophages. *Biochemical Journal* 1993;290:165-72.
54. Hawkins CL, Pattison DI, Davies MJ. Hypochlorite-induced oxidation of amino acids, peptides and proteins. *Amino Acids* 2003;25:259-74.
55. Heinecke JW. Mechanisms of oxidative damage by myeloperoxidase in atherosclerosis and other inflammatory disorders. *Journal of Laboratory and Clinical Medicine* 1999;133:321-5.
56. Himmelfarb J, McMenamin ME, Loseto G, Heinecke JW. Myeloperoxidase-catalyzed 3-chlorotyrosine formation in dialysis patients. *Free Radical Biology and Medicine* 2001;31:1163-9.
57. Mohiuddin I, Chai H, Lin PH, Lumsden AB, Yao QZ, Chen CY. Nitrotyrosine and chlorotyrosine: Clinical significance and biological functions in the vascular system. *Journal of Surgical Research* 2006;133:143-9.

58. Souza JM, Peluffo G, Radi R. Protein tyrosine nitration - Functional alteration or just a biomarker? *Free Radical Biology and Medicine* 2008;**45**:357-66.
59. Shishehbor MH, Aviles RJ, Brennan ML, Fu XM, Goormastic M, Pearce GL *et al.* Association of nitrotyrosine levels with cardiovascular disease and modulation by statin therapy. *Jama-Journal of the American Medical Association* 2003;**289**:1675-80.
60. Leeuwenburgh C, Hardy MM, Hazen SL, Wagner P, Ohishi S, Steinbrecher UP *et al.* Reactive nitrogen intermediates promote low density lipoprotein oxidation in human atherosclerotic intima. *Journal of Biological Chemistry* 1997;**272**:1433-6.
61. Podrez EA, Schmitt D, Hoff HF, Hazen SL. Myeloperoxidase-generated reactive nitrogen species convert LDL into an atherogenic form in vitro. *Journal of Clinical Investigation* 1999;**103**:1547-60.
62. Davies MJ, Fu SL, Wang HJ, Dean RT. Stable markers of oxidant damage to proteins and their application in the study of human disease. *Free Radical Biology and Medicine* 1999;**27**:1151-63.
63. Kinlay S, Egidio J. Inflammatory biomarkers in stable atherosclerosis. *American Journal of Cardiology* 2006;**98**:2P-8P.
64. Plebani M. Proteomics: The next revolution in laboratory medicine? *Clinica Chimica Acta* 2005;**357**:113-22.
65. Hamilton RT, Asatryan L, Nilsen OT, Isas JM, Gallaher TK, Sawamura T *et al.* LDL protein nitration: Implication for LDL protein unfolding. *Archives of Biochemistry and Biophysics* 2008;**479**:1-14.
66. Anderson NL, Anderson NG. The human plasma proteome - History, character, and diagnostic prospects. *Molecular & Cellular Proteomics* 2002;**1**:845-67.
67. Hansson O, Zetterberg H, Buchhave P, Londos E, Blennow K, Minthon L. Association between CSF biomarkers and incipient Alzheimer's disease in patients with mild cognitive impairment: a follow-up study. (vol 5, pg 228, 2006). *Lancet Neurology* 2006;**5**:293.
68. Craig-Schapiro R, Fagan AM, Holtzman DM. Biomarkers of Alzheimer's disease. *Neurobiology of Disease* 2009;**35**:128-40.
69. de Seny D, Fillet M, Meuwis MA, Geurts P, Lutteri L, Ribbens C *et al.* Discovery of new rheumatoid arthritis biomarkers using the surface-enhanced laser desorption/ionization time-of-flight mass spectrometry ProteinChip approach. *Arthritis and Rheumatism* 2005;**52**:3801-12.
70. Vasan RS. Biomarkers of cardiovascular disease - Molecular basis and practical considerations. *Circulation* 2006;**113**:2335-62.
71. Shin HJ, Markey MK. A machine learning perspective on the development of clinical decision support systems utilizing mass spectra of blood samples. *Journal of Biomedical Informatics* 2006;**39**:227-48.

72. Kavallaris M, Marshall GM. Proteomics and disease: opportunities and challenges. *Medical Journal of Australia* 2005; **182**:575-9.
73. Frank R, Hargreaves R. Clinical biomarkers in drug discovery and development. *Nature Reviews Drug Discovery* 2003; **2**:566-80.
74. Shishehbor MH, Aviles RJ, Brennan ML, Fu XM, Goormastic M, Pearce GL *et al*. Association of nitrotyrosine levels with cardiovascular disease and modulation by statin therapy. *Jama-Journal of the American Medical Association* 2003; **289**:1675-80.
75. Tsimikas S. Oxidative biomarkers in the diagnosis and prognosis of cardiovascular disease. *American Journal of Cardiology* 2006; **98**:9P-17P.
76. Sever PS, Dahlof B, Poulter NR, Wedel H, Beevers G, Caulfield M *et al*. Prevention of coronary and stroke events with atorvastatin in hypertensive patients who have average or lower-than-average cholesterol concentrations, in the Anglo-Scandinavian Cardiac Outcomes Trial - Lipid lowering arm (ASCOT-LLA): A multicentre randomised controlled trial. *Drugs* 2004; **64**:43-60.
77. Hansson GK, Robertson AKL, Soderberg-Naucler C. Inflammation and atherosclerosis. *Annual Review of Pathology-Mechanisms of Disease* 2006; **1**:297-329.
78. Solassol J, Marin P, Demette E, Rouanet P, Bockaert J, Maudelonde T *et al*. Proteomic detection of prostate-specific antigen using a serum fractionation procedure: potential implication for new low-abundance cancer biomarkers detection. *Analytical Biochemistry* 2005; **338**:26-31.
79. Seam N, Gonzales DA, Kern SJ, Hortin GL, Hoehn GT, Suffredini AF. Quality control of serum albumin, depletion for proteomic analysis. *Clinical Chemistry* 2007; **53**:1915-20.
80. Towbin H, Staehelin T, Gordon J. Electrophoretic Transfer of Proteins from Polyacrylamide Gels to Nitrocellulose Sheets - Procedure and Some Applications. *Proceedings of the National Academy of Sciences of the United States of America* 1979; **76**:4350-4.
81. Burnette W. Western Blotting: Remembrance of Past Things. *Protein Blotting and Detection: Methods and Protocols* 2009;5-8.
82. Khan J, Brennan DM, Bradley N, Gao BR, Bruckdorfer R, Jacobs M. 3-nitrotyrosine in the proteins of human plasma determined by an ELISA method. *Biochemical Journal* 1998; **330**:795-801.
83. Spickett CM, Pitt AR. Protein oxidation: role in signalling and detection by mass spectrometry. *Amino Acids* 2010.
84. Niall HD. Automated Edman degradation: the protein sequenator. *Methods Enzymol* 1973; **27**:942-1010.
85. Stolowitz ML. Chemical protein sequencing and amino acid analysis. *Current Opinion in Biotechnology* 1993; **4**:9-13.
86. Hanash S. Disease proteomics. *Nature* 2003; **422**:226-32.

87. Hunt DF, Henderson RA, Shabanowitz J, Sakaguchi K, Michel H, Sevilir N *et al.* Characterization of Peptides Bound to the Class-I Mhc Molecule Hla-A2.1 by Mass-Spectrometry. *Science* 1992;**255**:1261-3.
88. Yates JR, McCormack AL, Link AJ, Schieltz D, Eng J, Hays L. Future prospects for the analysis of complex biological systems using micro-column liquid chromatography electrospray tandem mass spectrometry. *Analyst* 1996;**121**:R65-R76.
89. Douglas DJ, Frank AJ, Mao DM. Linear ion traps in mass spectrometry. *Mass Spectrometry Reviews* 2005;**24**:1-29.
90. Paul W, Steinwedel H. \*Ein Neues Massenspektrometer Ohne Magnetfeld. *Zeitschrift fur Naturforschung Section A-A Journal of Physical Sciences* 1953;**8**:448-50.
91. Campbell JM, Collings BA, Douglas DJ. A new linear ion trap time-of-flight system with tandem mass spectrometry capabilities. *Rapid Communications in Mass Spectrometry* 1998;**12**:1463-74.
92. Hager JW. A new linear ion trap mass spectrometer. *Rapid Communications in Mass Spectrometry* 2002;**16**:512-26.
93. Hager JW, Le Blanc JCY. Product ion scanning using a Q-q-Q(linear ion trap) (Q TRAP (TM)) mass spectrometer. *Rapid Communications in Mass Spectrometry* 2003;**17**:1056-64.
94. Hopfgartner G, Varesio E, Tschappat V, Grivet C, Bourgogne E, Leuthold LA. Triple quadrupole linear ion trap mass spectrometer for the analysis of small molecules and macromolecules. *Journal of Mass Spectrometry* 2004;**39**:845-55.
95. Collings BA, Campbell JM, Mao DM, Douglas DJ. A combined linear ion trap time-of-flight system with improved performance and MS<sub>n</sub> capabilities. *Rapid Communications in Mass Spectrometry* 2001;**15**:1777-95.
96. Steen H, Mann M. The ABC's (and XYZ's) of peptide sequencing. *Nature Reviews Molecular Cell Biology* 2004;**5**:699-711.
97. Fenn JB, Mann M, Meng CK, Wong SF, Whitehouse CM. Electrospray Ionization for Mass-Spectrometry of Large Biomolecules. *Science* 1989;**246**:64-71.
98. Sen AK, Darabi J, Knapp DR, Liu J. Modeling and characterization of a carbon fiber emitter for electrospray ionization. *Journal of Micromechanics and Microengineering* 2006;**16**:620-30.
99. Dole M, Mack LL, Hines RL. Molecular Beams of Macroions. *Journal of Chemical Physics* 1968;**49**:2240-&.
100. Clegg GA, Dole M. Molecular Beams of Macroions .3. Zein and Polyvinylpyrrolidone. *Biopolymers* 1971;**10**:821-&.
101. Fenn JB, Mann M, Meng CK, Wong SF, Whitehouse CM. Electrospray Ionization for Mass-Spectrometry of Large Biomolecules. *Science* 1989;**246**:64-71.

102. Li KY, Tu HH, Ray AK. Charge limits on droplets during evaporation. *Langmuir* 2005;21:3786-94.
103. Wilm M, Mann M. Analytical properties of the nanoelectrospray ion source. *Analytical Chemistry* 1996;68:1-8.
104. Juraschek R, Dulcks T, Karas M. Nanoelectrospray - More than just a minimized-flow electrospray ionization source. *Journal of the American Society for Mass Spectrometry* 1999;10:300-8.
105. Abian J, Oosterkamp AJ, Gelpi E. Comparison of conventional, narrow-bore and capillary liquid chromatography mass spectrometry for electrospray ionization mass spectrometry: Practical considerations. *Journal of Mass Spectrometry* 1999;34:244-54.
106. Sobott F, Watt SJ, Smith J, Edelman MJ, Kramer HB, Kessler BM. Comparison of CID versus ETD based MS/MS fragmentation for the analysis of protein ubiquitination. *J Am Soc Mass Spectrom* 2009;20:1652-9.
107. Sadygov RG, Cociorva D, Yates JR. Large-scale database searching using tandem mass spectra: Looking up the answer in the back of the book. *Nature Methods* 2004;1:195-202.
108. Syka JEP, Coon JJ, Schroeder MJ, Shabanowitz J, Hunt DF. Peptide and protein sequence analysis by electron transfer dissociation mass spectrometry. *Proceedings of the National Academy of Sciences of the United States of America* 2004;101:9528-33.
109. Mikesh LM, Ueberheide B, Chi A, Coon JJ, Syka JEP, Shabanowitz J *et al.* The utility of ETD mass spectrometry in proteomic analysis. *Biochimica et Biophysica Acta-Proteins and Proteomics* 2006;1764:1811-22.
110. Thompson MS, Cui WD, Reilly JP. Fragmentation of singly charged peptide ions by photodissociation at  $\lambda=157$  nm. *Angewandte Chemie-International Edition* 2004;43:4791-4.
111. Lammert SA, Cooks RG. Surface-Induced Dissociation of Molecular-Ions in A Quadrupole Ion Trap Mass-Spectrometer. *Journal of the American Society for Mass Spectrometry* 1991;2:487-91.
112. Schey KL, Durkin DA, Thornburg KR. Design and Performance of An In-Line Surface-Induced Dissociation Device in A 4-Sector Mass-Spectrometer. *Journal of the American Society for Mass Spectrometry* 1995;6:257-63.
113. Galhena AS, Dagan S, Jones CM, Beardsley RL, Wysocki VN. Surface-induced dissociation of peptides and protein complexes in a quadrupole/Time-of-Flight mass spectrometer. *Analytical Chemistry* 2008;80:1425-36.
114. Aebersold R, Mann M. Mass spectrometry-based proteomics. *Nature* 2003;422:198-207.
115. Mann M, Kelleher NL. Precision proteomics: The case for high resolution and high mass accuracy. *Proceedings of the National Academy of Sciences of the United States of America* 2008;105:18132-8.

116. Pappin P. A Statistical Model of Proteolytic Digestion. *Current Biology* 1993;**3**:327-32.
117. Niggeweg R, Kocher T, Gentzel M, Buscaino A, Taipale M, Akhtar A *et al.* A general precursor ion-like scanning mode on quadrupole-TOF instruments compatible with chromatographic separation. *Proteomics* 2006;**6**:41-53.
118. Krutchinsky AN, Cohen H, Chait BT. A novel high-capacity ion trap-quadrupole tandem mass spectrometer. *International Journal of Mass Spectrometry* 2007;**268**:93-105.
119. Hager JW, Le Blanc JCY. High-performance liquid chromatography-tandem mass spectrometry with a new quadrupole/linear ion trap instrument. *Journal of Chromatography A* 2003;**1020**:3-9.
120. Le Blanc JCY, Hager JW, Ilisiu AMP, Hunter C, Zhong F, Chu I. Unique scanning capabilities of a new hybrid linear ion trap mass spectrometer (Q TRAP) used for high sensitivity proteomics applications. *Proteomics* 2003;**3**:859-69.
121. Krutchinsky AN, Cohen H, Chait BT. A novel high-capacity ion trap-quadrupole tandem mass spectrometer. *International Journal of Mass Spectrometry* 2007;**268**:93-105.
122. Mann M, Ong SE, Gronborg M, Steen H, Jensen ON, Pandey A. Analysis of protein phosphorylation using mass spectrometry: deciphering the phosphoproteome. *Trends in Biotechnology* 2002;**20**:261-8.
123. Williamson BL, Marchese J, Morrice NA. Automated identification and quantification of protein phosphorylation sites by LC/MS on a hybrid triple quadrupole linear ion trap mass spectrometer. *Molecular & Cellular Proteomics* 2006;**5**:337-46.
124. Barford D, Das AK, Egloff MP. The structure and mechanism of protein phosphatases: Insights into catalysis and regulation. *Annual Review of Biophysics and Biomolecular Structure* 1998;**27**:133-64.
125. Chang C, Stewart RC. The two-component system - Regulation of diverse signaling pathways in prokaryotes and eukaryotes. *Plant Physiology* 1998;**117**:723-31.
126. Steen H, Kuster B, Fernandez M, Pandey A, Mann M. Detection of tyrosine phosphorylated peptides by precursor ion scanning quadrupole TOF mass spectrometry in positive ion mode. *Analytical Chemistry* 2001;**73**:1440-8.
127. Cirulli C, Chiappetta G, Marino G, Mauri P, Amoresano A. Identification of free phosphopeptides in different biological fluids by a mass spectrometry approach. *Analytical and Bioanalytical Chemistry* 2008;**392**:147-59.
128. Steen H, Mann M. A new derivatization strategy for the analysis of phosphopeptides by precursor ion scanning in positive ion mode. *Journal of the American Society for Mass Spectrometry* 2002;**13**:996-1003.
129. Steen H, Kuster B, Fernandez M, Pandey A, Mann M. Detection of tyrosine phosphorylated peptides by precursor ion scanning quadrupole TOF mass spectrometry in positive ion mode. *Analytical Chemistry* 2001;**73**:1440-8.

130. Maltby D, Burlingame A. Identification of posttranslational modifications of peptides using a hybrid triple quadrupole linear ion trap mass spectrometer. *Molecular & Cellular Proteomics* 2003;2:S18.
131. Loyet KM, Stults JT, Arnott D. Mass spectrometric contributions to the practice of phosphorylation site mapping through 2003 - A literature review. *Molecular & Cellular Proteomics* 2005;4:235-45.
132. Witze ES, Old WM, Resing KA, Ahn NG. Mapping protein post-translational modifications with mass spectrometry. *Nature Methods* 2007;4:798-806.
133. Louris JN, Wright LG, Cooks RG, Schoen AE. New Scan Modes Accessed with A Hybrid Mass-Spectrometer. *Analytical Chemistry* 1985;57:2918-24.
134. McLachlin DT, Chait BT. Analysis of phosphorylated proteins and peptides by mass spectrometry. *Current Opinion in Chemical Biology* 2001;5:591-602.
135. Cox DM, Zhong F, Du M, Duchoslav E, Sakuma T, McDermott JC. Multiple reaction monitoring as a method for identifying protein posttranslational modifications. *J Biomol Tech* 2005;16:83-90.
136. Matar KM. Quantification of levetiracetam in human plasma by liquid chromatography-tandem mass spectrometry: Application to therapeutic drug monitoring. *Journal of Pharmaceutical and Biomedical Analysis* 2008;48:822-8.
137. Kato Y, Dozaki N, Nakamura T, Kitamoto N, Yoshida A, Naito M *et al.* Quantification of Modified Tyrosines in Healthy and Diabetic Human Urine using Liquid Chromatography/Tandem Mass Spectrometry. *Journal of Clinical Biochemistry and Nutrition* 2009;44:67-78.
138. Winnik WM, Kitchin KT. Measurement of oxidative stress parameters using liquid chromatography-tandem mass spectroscopy (LC-MS/MS). *Toxicology and Applied Pharmacology* 2008;233:100-6.
139. Yang X, Lazar IM. MRM screening/biomarker discovery with linear ion trap MS: a library of human cancer-specific peptides. *Bmc Cancer* 2009;9.
140. Kato Y, Dozaki N, Nakamura T, Kitamoto N, Yoshida A, Naito M *et al.* Quantification of Modified Tyrosines in Healthy and Diabetic Human Urine using Liquid Chromatography/Tandem Mass Spectrometry. *Journal of Clinical Biochemistry and Nutrition* 2009;44:67-78.
141. Rifai N, Gillette MA, Carr SA. Protein biomarker discovery and validation: the long and uncertain path to clinical utility. *Nature Biotechnology* 2006;24:971-83.
142. Ptolemy AS, Lee R, Britz-McKibbin P. Strategies for comprehensive analysis of amino acid biomarkers of oxidative stress. *Amino Acids* 2007;33:3-18.
143. Morrow JD. Quantification of isoprostanes as indices of oxidant stress and the risk of atherosclerosis in humans. *Arteriosclerosis Thrombosis and Vascular Biology* 2005;25:279-86.

144. Unwin RD, Griffiths JR, Leverentz MK, Grallert A, Hagan IM, Whetton AD. Multiple reaction monitoring to identify sites of protein phosphorylation with high sensitivity. *Molecular & Cellular Proteomics* 2005;4:1134-44.
145. Unwin RD, Griffiths JR, Whetton AD. A sensitive mass spectrometric method for hypothesis-driven detection of peptide post-translational modifications: multiple reaction monitoring-initiated detection and sequencing (MIDAS). *Nature Protocols* 2009;4:870-7.
146. Mollah S, Wertz IE, Phung Q, Arnott D, Dixit VM, Lill JR. Targeted mass spectrometric strategy for global mapping of ubiquitination on proteins. *Rapid Communications in Mass Spectrometry* 2007;21:3357-64.
147. Boutilier K, Ross M, Podtelejnikov AV, Orsi C, Taylor R, Taylor P *et al.* Comparison of different search engines using validated MS/MS test datasets. *Analytica Chimica Acta* 2005;534:11-20.
148. Pedrioli PGA, Eng JK, Hubley R, Vogelzang M, Deutsch EW, Raught B *et al.* A common open representation of mass spectrometry data and its application to proteomics research. *Nature Biotechnology* 2004;22:1459-66.
149. Eng JK, McCormack AL, Yates JR. An Approach to Correlate Tandem Mass-Spectral Data of Peptides with Amino-Acid-Sequences in A Protein Database. *Journal of the American Society for Mass Spectrometry* 1994;5:976-89.
150. Weatherly DB, Atwood JA, Minning TA, Cavola C, Tarleton RL, Orlando R. A heuristic method for assigning a false-discovery rate for protein identifications from mascot database search results. *Molecular & Cellular Proteomics* 2005;4:762-72.
151. Perkins DN, Pappin DJC, Creasy DM, Cottrell JS. Probability-based protein identification by searching sequence databases using mass spectrometry data. *Electrophoresis* 1999;20:3551-67.
152. Pearson WR. Comparison of Methods for Searching Protein-Sequence Databases. *Protein Science* 1995;4:1145-60.
153. Pappin DJC, Hojrup P, Bleasby AJ. Rapid Identification of Proteins by Peptide-Mass Fingerprinting. *Current Biology* 1993;3:327-32.
154. Anderson MM, Hazen SL, Hsu FF, Heinecke JW. Human neutrophils employ the myeloperoxidase-hydrogen peroxide-chloride system to convert hydroxy-amino acids into glycolaldehyde, 2-hydroxypropanal, and acrolein - A mechanism for the generation of highly reactive alpha-hydroxy and alpha,beta-unsaturated aldehydes by phagocytes at sites of inflammation. *Journal of Clinical Investigation* 1997;99:424-32.
155. Hazen SL, Heinecke JW. 3-chlorotyrosine, a specific marker of myeloperoxidase-catalyzed oxidation, is markedly elevated in low density lipoprotein isolated from human atherosclerotic intima. *Journal of Clinical Investigation* 1997;99:2075-81.

156. Winterbourn CC, Kettle AJ. Biomarkers of myeloperoxidase-derived hypochlorous acid. *Free Radical Biology and Medicine* 2000;**29**:403-9.
157. Hawkins CL, Davies MJ. Hypochlorite-induced damage to DNA, RNA, and polynucleotides: Formation of chloramines and nitrogen-centered radicals. *Chemical Research in Toxicology* 2002;**15**:83-92.
158. Kettle AJ. Neutrophils convert tyrosyl residues in albumin to chlorotyrosine. *Febs Letters* 1996;**379**:103-6.
159. Spickett CM. Chlorinated lipids and fatty acids: An emerging role in pathology. *Pharmacology & Therapeutics* 2007;**115**:400-9.
160. Podrez EA, Abu-Soud HM, Hazen SL. Myeloperoxidase-generated oxidants and atherosclerosis. *Free Radical Biology and Medicine* 2000;**28**:1717-25.
161. Domon B, Aebersold R. Review - Mass spectrometry and protein analysis. *Science* 2006;**312**:212-7.
162. Chalmers MJ, Gaskell SJ. Advances in mass spectrometry for proteome analysis. *Current Opinion in Biotechnology* 2000;**11**:384-90.
163. Carr SA, Huddleston MJ, Annan RS. Selective detection and sequencing of phosphopeptides at the femtomole level by mass spectrometry. *Analytical Biochemistry* 1996;**239**:180-92.
164. Johnson JV, Yost RA, Kelley PE, Bradford DC. Tandem-In-Space and Tandem-In-Time Mass-Spectrometry - Triple Quadrupoles and Quadrupole Ion Traps. *Analytical Chemistry* 1990;**62**:2162-72.
165. Winter J, Ilbert M, Graf PCF, Ozcelik D, Jakob U. Bleach Activates a Redox-Regulated Chaperone by Oxidative Protein Unfolding. *Cell* 2008;**135**:691-701.
166. Chapman ALP, Senthilmohan R, Winterbourn CC, Kettle AJ. Comparison of mono- and dichlorinated tyrosines with carbonyls for detection of hypochlorous acid modified proteins. *Archives of Biochemistry and Biophysics* 2000;**377**:95-100.
167. Drabik G, Naskalski JW. Chlorination of N-acetyltyrosine with HOCl, chloramines, and myeloperoxidase-hydrogen peroxide-chloride system. *Acta Biochimica Polonica* 2001;**48**:271-5.
168. Garza S, Moini M. Analysis of complex protein mixtures with improved sequence coverage using (CE-MS/MS)(n). *Analytical Chemistry* 2006;**78**:7309-16.
169. Scherl A, Shaffer SA, Taylor GK, Kulasekara HD, Miller SI, Goodlett DR. Genome-specific gas-phase fractionation strategy for improved shotgun proteomic profiling of proteotypic peptides. *Analytical Chemistry* 2008;**80**:1182-91.
170. Spahr CS, Davis MT, McGinley MD, Robinson JH, Bures EJ, Beierle J *et al.* Towards defining the urinary proteome using liquid chromatography-tandem mass spectrometry I. Profiling an unfractionated tryptic digest. *Proteomics* 2001;**1**:93-107.

171. Yi EC, Marelli M, Lee H, Purvine SO, Aebersold R, Aitchison JD *et al.* Approaching complete peroxisome characterization by gas-phase fractionation. *Electrophoresis* 2002;**23**:3205-16.
172. Sugio S, Kashima A, Mochizuki S, Noda M, Kobayashi K. Crystal structure of human serum albumin at 2.5 angstrom resolution. *Protein Engineering* 1999;**12**:439-46.
173. Anderson NL. The roles of multiple proteomic platforms in a pipeline for new diagnostics. *Molecular & Cellular Proteomics* 2005;**4**:1441-4.
174. Pieper R, Su Q, Gatlin CL, Huang ST, Anderson NL, Steiner S. Multi-component immunoaffinity subtraction chromatography: An innovative step towards a comprehensive survey of the human plasma proteome. *Proteomics* 2003;**3**:422-32.
175. Pieper R, Gatlin CL, Makusky AJ, Russo PS, Schatz CR, Miller SS *et al.* The human serum proteome: Display of nearly 3700 chromatographically separated protein spots on two-dimensional electrophoresis gels and identification of 325 distinct proteins. *Proteomics* 2003;**3**:1345-64.
176. Rose K, Bougueleret L, Baussant T, Bohm G, Botti P, Colinge J *et al.* Industrial-scale proteomics: From liters of plasma to chemically synthesized proteins. *Proteomics* 2004;**4**:2125-50.
177. BioAnalyst. Simultaneous quantitative screening and qualitative confirmation of 300 pesticides using the new 3200 Qtrap LC/MS/MS System. *114AP38-01* 2010.
178. Lange V, Picotti P, Domon B, Aebersold R. Selected reaction monitoring for quantitative proteomics: a tutorial. *Molecular Systems Biology* 2008;**4**.
179. Houde D, Kauppinen P, Mhatre R, Lyubarskaya Y. Determination of protein oxidation by mass spectrometry and method transfer to quality control. *Journal of Chromatography A* 2006;**1123**:189-98.
180. Hamilton RT, Asatryan L, Nilsen OT, Isas JM, Gallaher TK, Sawamura T *et al.* LDL protein nitration: Implication for LDL protein unfolding. *Archives of Biochemistry and Biophysics* 2008;**479**:1-14.
181. Torres-Rasgado E, Fouret G, Carbonneau MA, Leger CL. Peroxynitrite mild nitration of albumin and LDL-albumin complex naturally present in plasma and tyrosine nitration rate-albumin impairs LDL nitration. *Free Radical Research* 2007;**41**:367-75.
182. Dickhout JG, Hossain GS, Pozza LM, Zhou J, Lhotak S, Austin RC. Peroxynitrite causes endoplasmic reticulum stress and apoptosis in human vascular endothelium - Implications in atherogenesis. *Arteriosclerosis Thrombosis and Vascular Biology* 2005;**25**:2623-9.
183. Yamaguchi Y, Kagota S, Haginaka J, Kunitomo M. Nitrotyrosine content in LDL modified with aqueous extracts of cigarette smoke. *Japanese Journal of Pharmacology* 2001;**85**:101P.

184. Yamagucki Y, Kagota S, Haginaka J, Kunitomo M. Peroxynitrite-generating species: Good candidate oxidants in aqueous extracts of cigarette smoke. *Japanese Journal of Pharmacology* 2000;**82**:78-81.
185. Bergt C, Fu XY, Huq NP, Kao J, Heinecke JW. Lysine residues direct the chlorination of tyrosines in YXXK motifs of apolipoprotein A-I when hypochlorous acid oxidizes high density lipoprotein. *Journal of Biological Chemistry* 2004;**279**:7856-66.
186. Zhang H, Zielonka J, Sikora A, Joseph J, Xu YK, Kalyanaraman B. The effect of neighboring methionine residue on tyrosine nitration and oxidation in peptides treated with MPO, H<sub>2</sub>O<sub>2</sub>, and NO<sub>2</sub><sup>-</sup> or peroxynitrite and bicarbonate: Role of intramolecular electron transfer mechanism? *Archives of Biochemistry and Biophysics* 2009;**484**:134-45.
187. Zhang H, Xu YK, Joseph J, Kalyanaraman B. Intramolecular electron transfer between tyrosyl radical and cysteine residue inhibits tyrosine nitration and induces thiyl radical formation in model peptides treated with myeloperoxidase, H<sub>2</sub>O<sub>2</sub>, and NO<sub>2</sub><sup>-</sup> - EPR spin trapping studies. *Journal of Biological Chemistry* 2005;**280**:40684-98.
188. Shishehbor MH, Aviles RJ, Brennan ML, Fu XM, Goormastic M, Pearce GL *et al.* Association of nitrotyrosine levels with cardiovascular disease and modulation by statin therapy. *Jama-Journal of the American Medical Association* 2003;**289**:1675-80.
189. Zou J, Wu D, Xiao D, Qi D, Liu L, Ding L *et al.* A sensitive LC-ESI-MS-MS method for the determination of huperzine A in human plasma: method and clinical applications. *Chromatographia* 2009;**69**:453-8.
190. Rashed MS. Clinical applications of tandem mass spectrometry: ten years of diagnosis and screening for inherited metabolic diseases. *Journal of Chromatography B-Analytical Technologies in the Biomedical and Life Sciences* 2001;**758**:27-48.
191. Hager JW, Le Blanc JCY. Product ion scanning using a Q-q-Q(linear ion trap) (Q TRAP (TM)) mass spectrometer. *Rapid Communications in Mass Spectrometry* 2003;**17**:1056-64.
192. Wilm M, Neubauer G, Mann M. Parent ion scans of unseparated peptide mixtures. *Analytical Chemistry* 1996;**68**:527-33.
193. Hung CW, Schlosser A, Wei JH, Lehmann WD. Collision-induced reporter fragmentations for identification of covalently modified peptides. *Analytical and Bioanalytical Chemistry* 2007;**389**:1003-16.
194. Salek M, Lehmann WD. Neutral loss of amino acid residues from protonated peptides in collision-induced dissociation generates N- or C-terminal sequence ladders. *Journal of Mass Spectrometry* 2003;**38**:1143-9.
195. Hager JW, Le Blanc JCY. High-performance liquid chromatography-tandem mass spectrometry with a new quadrupole/linear ion trap instrument. *Journal of Chromatography A* 2003;**1020**:3-9.

196. Anderson L. Candidate-based proteomics in the search for biomarkers of cardiovascular disease. *Journal of Physiology-London* 2005;**563**:23-60.
197. Caldwell RL, Caprioli RM. Tissue profiling by mass spectrometry - A review of methodology and applications. *Molecular & Cellular Proteomics* 2005;**4**:394-401.
198. Pitt JJ, Eggington M, Kahler SG. Comprehensive screening of urine samples for inborn errors of metabolism by electrospray tandem mass spectrometry. *Clinical Chemistry* 2002;**48**:1970-80.
199. Anderson L, Hunter CL. Quantitative mass spectrometric multiple reaction monitoring assays for major plasma proteins. *Molecular & Cellular Proteomics* 2006;**5**:573-88.
200. Yang X, Lazar IM. MRM screening/biomarker discovery with linear ion trap MS: a library of human cancer-specific peptides. *Bmc Cancer* 2009;**9**.
201. Bagnato C, Thumar J, Mayya V, Hwang SI, Zebroski H, Claffey KP *et al*. Proteomics analysis of human coronary atherosclerotic plaque - A feasibility study of direct tissue proteomics by liquid chromatography and tandem mass spectrometry. *Molecular & Cellular Proteomics* 2007;**6**:1088-102.
202. Kim HK, Kim JE, Chung J, Lee DS, Han KS, Park S *et al*. Plasma level of stromal derived factor-1 (SDF-1) is increased in disseminated intravascular coagulation patients who have poor outcomes: In vitro effect of SDF-1 on coagulopathy. *Thrombosis Research* 2007;**120**:559-66.
203. Zheng H, Dai T, Zhou BQ, Zhu JH, Huang H, Wang M *et al*. SDF-1 alpha/CXCR4 decreases endothelial progenitor cells apoptosis under serum deprivation by PI3K/Akt/eNOS pathway. *Atherosclerosis* 2008;**201**:36-42.
204. Abi-Younes S, Sauty A, Mach F, Sukhova GK, Libby P, Luster AD. The stromal cell-derived factor-1 chemokine is a potent platelet agonist highly expressed in atherosclerotic plaques. *Circulation Research* 2000;**86**:131-8.
205. Eiserich JP, Vossen V, Oneill CA, Halliwell B, Cross CE, Vandervliet A. Molecular Mechanisms of Damage by Excess Nitrogen-Oxides - Nitration of Tyrosine by Gas-Phase Cigarette-Smoke. *Febs Letters* 1994;**353**:53-6.
206. Leeuwenburgh C, Heinecke JW. Oxidative stress and antioxidants in exercise. *Current Medicinal Chemistry* 2001;**8**:829-38.
207. Ross R. Mechanisms of disease - Atherosclerosis - An inflammatory disease. *New England Journal of Medicine* 1999;**340**:115-26.
208. Hazell LJ, Baerenthaler G, Stocker R. Correlation between intima-to-media ratio, apolipoprotein B-100, myeloperoxidase, and hypochlorite-oxidized proteins in human atherosclerosis. *Free Radical Biology and Medicine* 2001;**31**:1254-62.
209. McGill HC, McMahan CA, Herderick EE, Malcom GT, Tracy RE, Strong JP *et al*. Origin of atherosclerosis in childhood and adolescence. *American Journal of Clinical Nutrition* 2000;**72**:1307S-15S.

210. Tuzcu EM, Kapadia SR, Tutar E, Ziada KM, Hobbs RE, McCarthy PM *et al.* High prevalence of coronary atherosclerosis in asymptomatic teenagers and young adults - Evidence from intravascular ultrasound. *Circulation* 2001;**103**:2705-10.
211. Libby P. Inflammation and cardiovascular disease mechanisms. *American Journal of Clinical Nutrition* 2006;**83**:456S-60S.
212. McGill HC, McMahan CA, Tracy RE, Oalmann MC, Cornhill JF, Herderick EE *et al.* Relation of a postmortem renal index of hypertension to atherosclerosis and coronary artery size in young men and women. *Arteriosclerosis Thrombosis and Vascular Biology* 1998;**18**:1108-18.
213. Malcom GT, McMahan CA, McGill HC, Herderick EE, Tracy RE, Troxclair DA *et al.* Associations of arterial tissue lipids with coronary heart disease risk factors in young people. *Atherosclerosis* 2009;**203**:515-21.
214. Hackett D, Davies G, Maseri A. Preexisting Coronary Stenoses in Patients with 1st Myocardial-Infarction Are Not Necessarily Severe. *European Heart Journal* 1988;**9**:1317-23.
215. Kaplan S, Billimeck J, Sorkin D. Who can respond to treatment? Identifying patient characteristics related to heterogeneity of treatment effects. *Medical Care* 2010;**48**:S9-S16.
216. Jessup W, Krithairides L, Stocker R. Lipid oxidation in atherogenesis: an overview. *Biochemical Society Transactions* 2004;**32**:134-8.
217. Avogaro P, Bon GB, Cazzolato G. Presence of A Modified Low-Density Lipoprotein in Humans. *Arteriosclerosis* 1988;**8**:79-87.
218. Witztum JL, Steinberg D. Role of Oxidized Low-Density-Lipoprotein in Atherogenesis. *Journal of Clinical Investigation* 1991;**88**:1785-92.
219. Hazell LJ, Vandenberg JJM, Stocker R. Oxidation of Low-Density-Lipoprotein by Hypochlorite Causes Aggregation That Is Mediated by Modification of Lysine Residues Rather Than Lipid Oxidation. *Biochemical Journal* 1994;**302**:297-304.
220. Spickett CM, Jerlich A, Panasenکو OM, Arnhold J, Pitt AR, Stelmaszynska T *et al.* The reactions of hypochlorous acid, the reactive oxygen species produced by myeloperoxidase, with lipids. *Acta Biochimica Polonica* 2000;**47**:889-99.
221. Panasenکو OM, Arnhold J, Sergienko VI. The effect of pH on hypochlorite-induced peroxidation of phospholipid liposomes. *Biofizika* 1998;**43**:463-9.
222. Malle E, Marsche G, Arnhold J, Davies MJ. Modification of low-density lipoprotein by myeloperoxidase-derived oxidants and reagent hypochlorous acid. *Biochimica et Biophysica Acta-Molecular and Cell Biology of Lipids* 2006;**1761**:392-415.
223. Jerlich A, Fritz G, Kharrazi H, Hammel M, Tschabuschnig S, Glatter O *et al.* Comparison of HOCl traps with myeloperoxidase inhibitors in prevention of low density lipoprotein oxidation. *Biochimica et Biophysica Acta-Protein Structure and Molecular Enzymology* 2000;**1481**:109-18.

224. Grune T, Reinheckel T, Davies KJA. Degradation of oxidized proteins in mammalian cells. *Faseb Journal* 1997;11:526-34.
225. Vandervliet A, Oneill CA, Halliwell B, Cross CE, Kaur H. Aromatic Hydroxylation and Nitration of Phenylalanine and Tyrosine by Peroxynitrite - Evidence for Hydroxyl Radical Production from Peroxynitrite. *Febs Letters* 1994;339:89-92.
226. Previero A, Colettip MA, Jolles P. Localization of Non-Essential Tryptophan Residues for Biological Activity of Lysozyme. *Journal of Molecular Biology* 1967;24:261-&.
227. Previero A, Colettip MA, Axelrudc C. Prevention of Cleavage Next to Tryptophan Residues During Oxidative Splitting by N-Bromosuccinimide of Tyrosyl Peptide Bonds in Proteins. *Archives of Biochemistry and Biophysics* 1967;122:434-&.
228. Previero A, Colettip MA, Cavadore JC. A Reversible Chemical Modification of Tryptophan Residue. *Biochimica et Biophysica Acta* 1967;147:453-&.
229. Finley EL, Dillon J, Crouch RK, Schey KL. Identification of tryptophan oxidation products in bovine alpha-crystallin. *Protein Science* 1998;7:2391-7.
230. Taylor SW, Fahy E, Murray J, Capaldi RA, Ghosh SS. Oxidative post-translational modification of tryptophan residues in cardiac mitochondrial proteins. *Journal of Biological Chemistry* 2003;278:19587-90.
231. Dalle-Donne I, Scaloni A, Giustarini D, Cavarra E, Tell G, Lungarella G *et al.* Proteins as biomarkers of oxidative/nitrosative stress in diseases: The contribution of redox proteomics. *Mass Spectrometry Reviews* 2005;24:55-99.
232. Kapiotis S, Jirovetz L, Hermann M, Laggner H, Exner M, Esterbauer H *et al.* Products of the reaction of HOCl with tryptophan protect LDL from atherogenic modification. *Biochimie* 2006;88:785-91.
233. Hamilton RT, Asatryan L, Nilsen OT, Isas JM, Gallaher TK, Sawamura T *et al.* LDL protein nitration: Implication for LDL protein unfolding. *Archives of Biochemistry and Biophysics* 2008;479:1-14.
234. Asatryan L, Hamilton RT, Isas JM, Hwang J, Kayed R, Sevanian A. LDL phospholipid hydrolysis produces modified electronegative particles with an unfolded apoB-100 protein. *Journal of Lipid Research* 2005;46:115-22.
235. Dorweiler B, Torzewski M, Dahm M, Ochsenhirt V, Lehr HA, Lackner KJ *et al.* A novel in vitro model for the study of plaque development in atherosclerosis. *Thrombosis and Haemostasis* 2006;95:182-9.
236. Torzewski M, Lackner KJ. Initiation and progression of atherosclerosis - enzymatic or oxidative modification of low-density lipoprotein? *Clinical Chemistry and Laboratory Medicine* 2006;44:1389-94.
237. Kang JI, Neidigh JW. Hypochlorous acid damages histone proteins forming 3-chlorotyrosine and 3,5-dichlorotyrosine. *Chemical Research in Toxicology* 2008;21:1028-38.

238. Cheng ML, Chen CM, Gu PW, Ho HY, Chiu DTY. Elevated levels of myeloperoxidase, white blood cell count and 3-chlorotyrosine in Taiwanese patients with acute myocardial infarction. *Clinical Biochemistry* 2008;41:554-60.
239. Using Mass spectrometry for drug metabolism studies. *Google books* 2010;Chapter 10.